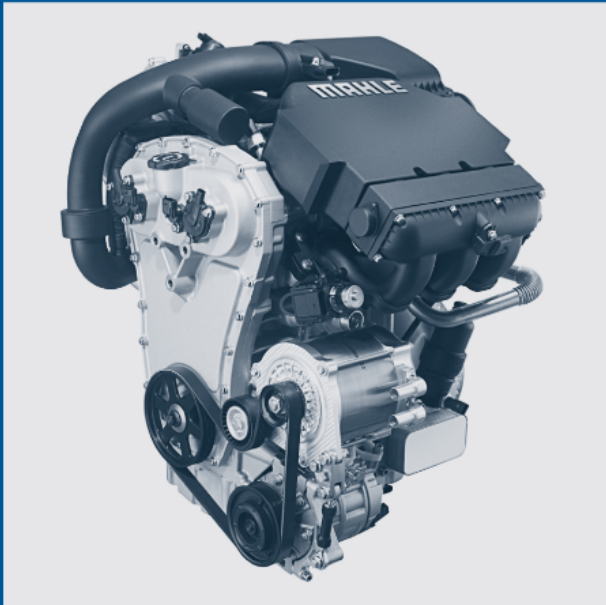


WOODHEAD PUBLISHING
IN MECHANICAL ENGINEERING

Advanced direct injection combustion engine technologies and development

Volume 1: Gasoline and gas engines

Edited by Hua Zhao



MAHLE
Powertrain



WP

Advanced direct injection combustion engine technologies and development

Related titles:

The science and technology of materials in automotive engines
(ISBN 978-1-85573-742-6)

This authoritative book provides an introductory text on the science and technology of materials used in automotive engines. It focuses on reciprocating engines, both four and two-stroke, with particular emphasis on their characteristics and the types of materials used in their construction. The book considers the engine in terms of each specific part: the cylinder, piston, camshaft, valves, crankshaft, connecting rod and catalytic converter. The materials used in automotive engines are required to fulfil a multitude of functions. It is a subtle balance between material properties, essential design and high performance characteristics. The intention here is to describe the metallurgy, surface modification, wear resistance, and chemical composition of these materials. It also includes supplementary notes that support the core text.

HCCI and CAI engines for the automotive industry
(ISBN 978-1-84569-128-8)

HCCI/CAI has emerged as one of the most promising engine technologies with the potential to combine fuel efficiency and improved emissions performance. Despite the considerable advantages, its operational range is rather limited and controlling the combustion (timing of ignition and rate of energy release) is still an area of on-going research. However, commercial applications are close to reality. This book reviews the key international research on optimising its use, including gasoline HCCI/CAI engines, diesel HCCI engines, HCCI/CAI engines with alternative fuels, and advanced modelling and experimental techniques.

Tribology and dynamics of engine and powertrain: Fundamentals, applications and future trends
(ISBN 978-1-84569-361-9)

Tribology is one element of many interacting within a vehicle engine and powertrain. In adopting a detailed, theoretical, component approach to solving tribological problems, the minutiae can be overwhelmingly complex and practical solutions become elusive and uneconomic. The system perspective generally adopted in industry, however, can lead to shortcuts and oversimplifications, industrial projects are subject to *ad hoc* trial and error, and subsequent 'fire-fighting' activity is required. This book seeks to bridge this divide, using a multi-physics approach to provide sufficient fundamental grounding and understanding of both detailed and approximate analyses – thereby making 'first time right' design solutions possible. Tribological issues and solutions in piston systems, valve train systems, engine bearings and drivetrain systems are addressed. New developments in materials, micro-engineering, nano-technology and MEMS are also included.

Details of these and other Woodhead Publishing books can be obtained by:

- visiting our web site at www.woodheadpublishing.com
- contacting Customer Services (e-mail: sales@woodheadpublishing.com;
fax: +44 (0) 1223 893694; tel.: +44 (0) 1223 891358 ext.130; address: Woodhead Publishing Limited, Abington Hall, Granta Park, Great Abington, Cambridge CB21 6AH, UK)

If you would like to receive information on forthcoming titles, please send your address details to: Francis Dodds (address, tel. and fax as above; e-mail: francis.dodds@woodheadpublishing.com). Please confirm which subject areas you are interested in.

Advanced direct injection combustion engine technologies and development

Volume 1: Gasoline and gas engines

Edited by

Hua Zhao

MAHLE

Powertrain



CRC Press

Boca Raton Boston New York Washington, DC

WOODHEAD PUBLISHING LIMITED

Oxford Cambridge New Delhi

Published by Woodhead Publishing Limited, Abington Hall, Granta Park,
Great Abington, Cambridge CB21 6AH, UK
www.woodheadpublishing.com

Woodhead Publishing India Private Limited, G-2, Vardaan House, 7/28 Ansari Road, Daryaganj,
New Delhi – 110002, India
www.woodheadpublishingindia.com

Published in North America by CRC Press LLC, 6000 Broken Sound Parkway, NW, Suite 300,
Boca Raton, FL 33487, USA

First published 2010, Woodhead Publishing Limited and CRC Press LLC
© 2010, Woodhead Publishing Limited; Ch 3 © J.W.G. Turner and R.J. Pearson
The authors have asserted their moral rights.

This book contains information obtained from authentic and highly regarded sources. Reprinted material is quoted with permission, and sources are indicated. Reasonable efforts have been made to publish reliable data and information, but the authors and the publishers cannot assume responsibility for the validity of all materials. Neither the authors nor the publishers, nor anyone else associated with this publication, shall be liable for any loss, damage or liability directly or indirectly caused or alleged to be caused by this book.

Neither this book nor any part may be reproduced or transmitted in any form or by any means, electronic or mechanical, including photocopying, microfilming and recording, or by any information storage or retrieval system, without permission in writing from Woodhead Publishing Limited.

The consent of Woodhead Publishing Limited does not extend to copying for general distribution, for promotion, for creating new works, or for resale. Specific permission must be obtained in writing from Woodhead Publishing Limited for such copying.

Trademark notice: Product or corporate names may be trademarks or registered trademarks, and are used only for identification and explanation, without intent to infringe.

British Library Cataloguing in Publication Data
A catalogue record for this book is available from the British Library.

Library of Congress Cataloging in Publication Data
A catalog record for this book is available from the Library of Congress.

Woodhead Publishing ISBN 978-1-84569-389-3 (book)
Woodhead Publishing ISBN 978-1-84569-732-7 (e-book)
CRC Press ISBN 978-1-4398-0208-3
CRC Press order number: N10046

The publishers' policy is to use permanent paper from mills that operate a sustainable forestry policy, and which has been manufactured from pulp which is processed using acid-free and elemental chlorine-free practices. Furthermore, the publishers ensure that the text paper and cover board used have met acceptable environmental accreditation standards.

Typeset by Replika Press Pvt Ltd, India
Printed by TJ International Limited, Padstow, Cornwall, UK

Contents

<i>Contributor contact details</i>	<i>ix</i>
<i>Preface</i>	<i>xi</i>
1 Overview of gasoline direct injection engines <i>H. Zhao, Brunel University, UK</i>	1
1.1 Introduction	1
1.2 Overview of direct injection gasoline engines	2
1.3 Potential and technologies for high-efficiency direct injection (DI) gasoline engine	5
1.4 High-pressure fuel injection system	11
1.5 Exhaust emissions and aftertreatment devices	14
1.6 Summary	17
1.7 References	18
2 Stratified-charge combustion in direct injection gasoline engines <i>U. Spicher and T. Heidenreich, Universität Karlsruhe (TH), Germany</i>	20
2.1 Introduction	20
2.2 Thermodynamic and combustion process	21
2.3 Production engines with stratified gasoline direct injection (GDI)	36
2.4 Future trends	42
2.5 References	43
3 The turbocharged direct injection spark-ignition engine <i>J. W. G. Turner and R. J. Pearson, Lotus Engineering, UK</i>	45
3.1 Introduction	45
3.2 Historical background: turbocharging for high specific output	46
3.3 Problems and challenges associated with turbocharging the spark-ignition (SI) engine	51

vi	Contents	
3.4	Advantages of combining direct injection and turbocharging in spark-ignition (SI) engines	65
3.5	Challenges of applying direct injection to a turbocharged spark-ignition (SI) engine	74
3.6	Future trends and possibilities	75
3.7	Summary	83
3.8	References	84
4	The lean boost combustion system for improved fuel economy <i>T. Lake, J. Stokes, R. Osborne, R. Murphy and M. Keenan, Ricardo UK Ltd, UK</i>	91
4.1	Pressures on the gasoline engine	91
4.2	Downsizing strategies	93
4.3	The lean-boost direct injection (LBDI) concept	93
4.4	Exhaust emissions control: drive-cycle emissions	99
4.5	Exhaust emissions control: off-cycle emissions	99
4.6	Selective catalytic reduction (SCR) NO _x control as an alternative to lean NO _x trap (LNT)	101
4.7	Conclusions	103
4.8	Future trends	104
5	Exhaust gas recirculation boosted direct injection gasoline engines <i>A. Cairns, H. Blaxill and N. Fraser, MAHLE Powertrain Ltd, UK</i>	105
5.1	Introduction	105
5.2	Fundamentals of wide-open-throttle exhaust gas recirculation (WOT- EGR) operation	108
5.3	Exhaust gas recirculation (EGR) circuit design	115
5.4	Exhaust gas recirculation (EGR) operating maps	124
5.5	In-vehicle requirements	127
5.6	Future trends	130
5.7	References	131
6	Direct injection gasoline engines with autoignition combustion <i>H. Zhao, Brunel University, UK</i>	133
6.1	Introduction	133
6.2	Principle of autoignition combustion in the gasoline engine	135
6.3	Approaches to autoignition combustion operation in gasoline engines	137

6.4	Operation and control of direct injection gasoline engines with autoignition combustion	146
6.5	Development of practical gasoline engines with autoignition and spark-ignition (SI) combustion	158
6.6	Future trends	161
6.7	References	163
7	Design and optimization of gasoline direct injection engines using computational fluid dynamics <i>J. Yi, Ford Research and Advanced Engineering, Research and Innovation Center, USA</i>	166
7.1	Introduction	166
7.2	Direct injection spark-ignition (DISI) injector technologies	169
7.3	Homogeneous-charge direct injection (DI) system design and optimization	173
7.4	Stratified-charge direct injection (DI) combustion system design and optimization	189
7.5	Turbo-charged or super-charged direct injection (DI) combustion system design and optimization	192
7.6	Future trends	194
7.7	References and further reading	196
8	Direct injection natural gas engines <i>D. Zhang, Westport Innovations Inc., Canada</i>	199
8.1	Introduction	199
8.2	Technologies	200
8.3	Potential applications	221
8.4	Strengths and weaknesses	222
8.5	Future trends	225
8.6	Sources of further information and advice	227
8.7	References	228
9	Biofuels for spark-ignition engines <i>J. D. Pagliuso, University of São Paulo, Brazil and M. E. S. Martins, Sygma Motors, Brazil</i>	229
9.1	Introduction	229
9.2	Types and sources of biofuels	231
9.3	Performance	237
9.4	Emissions	246
9.5	Operation	253
9.6	Conclusions	255
9.7	References	256

viii	Contents	
10	Optical diagnostics for direct injection gasoline engine research and development <i>V. Sick, The University of Michigan, USA</i>	260
10.1	Need for and merit of optical diagnostics	260
10.2	Applications of optical diagnostics	262
10.3	Future trends	278
10.4	Conclusions	279
10.5	References	279
	<i>Index</i>	287

Contributor contact details

(* = main contact)

Chapter 1

Professor Hua Zhao
Brunel University
West London
Uxbridge UB8 3PH
UK

Email: hua.zhao@brunel.ac.uk

Chapter 2

Professor Dr Ulrich Spicher* and
Thomas Heidenreich
Institut für Kolbenmaschinen
Universität Karlsruhe (TH)
PO box 6980
76128 Karlsruhe
Germany

Email: ulrich.spicher@ifkm.uni-karlsruhe.de; thomas.heidenreich@ifkm.uni-karlsruhe.de

Chapter 3

James W. G. Turner* and Dr
Richard. J. Pearson
Lotus Engineering
Hethel
Norwich
Norfolk NR18 4EZ
UK

E-mail: JTurner@lotuscars.co.uk;
RPearson@lotuscars.co.uk

Chapter 4

Dr Tim Lake,* J. Stokes, R.
Osborne, R. Murphy and M.
Keenan
Ricardo UK Ltd
UK

Email: Tim.lake@ricardo.com

Chapter 5

Dr Alasdair Cairns*, Hugh Blaxill
and Neil Fraser
MAHLE Powertrain Ltd
Northampton
UK

E-mail: alasdair.cairns@gb.mahle.com

Chapter 6

Professor Hua Zhao
Brunel University
West London
Uxbridge UB8 3PH
UK

Email: hua.zhao@brunel.ac.uk

Mario Eduardo Santos Martins
Sygma Motors
Avenida Cassiano Ricardo, 1306/S2
Jardim Alvorada, 12240-540
São José dos Campos, SP
Brazil

Email: mario@sygma.com.br

Chapter 7

Dr Jianwen Yi
Ford Research and Advanced
Engineering Research and
Innovation Center
Room 3622, MD 2629
2101 Village Road
Dearborn MI 48121
USA

Email: jyil@ford.com

Chapter 10

Professor Volker Sick
2023 W. E. Lay Automotive
Laboratory
Department of Mechanical
Engineering
The University of Michigan
1231 Beal Avenue
Ann Arbor MI 48109-2133
USA

E-mail: vsick@umich.edu

Chapter 8

Dr DeHong Zhang
Westport Innovations Inc.
1691 West 75th Avenue
Vancouver BC V6P 6P2
Canada

Email: dzhang@westport.com

Chapter 9

Prof. Josmar D. Pagliuso*
University of São Paulo
Av. Trabalhador São Carlense 400,
13566-590
São Carlos, SP
Brazil

Email: josmar@sc.usp.br

Preface

Over the last decade, significant progress has been made in the development of direct injection internal combustion engines. It may have been by coincidence that direct injection technology was developed and applied almost simultaneously to spark ignition (SI) gasoline engines and light-duty diesel engines in the mid-1990s, but the direct injection technology had been adopted in both engines for the same reason – to increase the efficiency of internal combustion (IC) engines for automotive applications while improving their performance. However, the route to growth and market penetration has proved more haphazard in the case of direct injection SI engines, owing to relatively high cost, lower than expected gains in fuel economy and full load performance, their complexity and the requirement for a lean NO_x aftertreatment system. In comparison, the high-speed direct injection (HSDI) diesel engine has achieved remarkable commercial success due to its excellent fuel economy and good performance characteristics.

With heightened concern over the greenhouse gas effect, imminent CO₂ emission targets in Europe and Japan, and new fleet vehicle fuel consumption requirements in the US, direct injection gasoline engines are staging a comeback, mainly through downsized boosted operations in the short term and stratified charge and/or controlled autoignited combustion in the medium term. In the meantime, HSDI and heavy-duty (HD) diesel engines are facing the challenge of meeting ever more stringent emission legislation across the globe, but without deteriorating fuel economy. It is therefore timely that the state of the art with respect to current direct injection combustion engines and their development needs should be presented and discussed in a single book so that researchers and practising engineers can ‘stand on the shoulders of giants’ in developing future high-efficiency and low-emission combustion engines. One particular strength of this book is its wide-ranging but balanced coverage of the fundamental understanding and applied technologies involved in DI combustion engines and the complementary contributions by both practising engineers and academic researchers.

This book is divided into two volumes, the first dealing with gasoline and gas engines, and the second discussing diesel engines. In Volume 1,

following an overview of the history and principles of high-efficiency direct injection gasoline engines, approaches to achieving better fuel economy from such engines are presented. These include a discussion on stratified charge combustion for part-load operations in Chapter 2, downsized engines through turbocharging in Chapter 3, lean-boost and exhaust gas recirculation (EGR) boost for further engine downsizing in Chapters 4 and 5, and autoignition combustion for simultaneous reduction in NO and fuel consumption in Chapter 6. Chapter 7 illustrates the use of computational fluid dynamics (CFD) in the design and optimisation of direct injection gasoline engines. Chapter 8 reviews direct injection compressed natural gas (CNG) engines that have been developed for commercial vehicles. Chapter 9 has been written to reflect the experience of the world's most successful bio-fuel market in Brazil. Finally Chapter 10 provides an up-to-date summary of advanced optical techniques and their applications to the development of gasoline engines.

Volume 2 starts with a survey of HSDI diesel engines developed over the last decade, which sets the scene for the following chapters. Chapter 2 provides an overview of state-of-the-art fuel injection systems for light-duty diesel engines. The fundamentals of mixture formation, combustion and emissions from HSDI diesel engines are presented in Chapter 3. This is complemented by a detailed discussion on the effect of multiple injections on diesel combustion and emissions in Chapter 4. Air management and turbocharging technologies are crucial to the diesel engine's performance and emissions, and they are the subject of Chapter 5. Chapter 6 presents and discusses some advanced concepts for future light-duty HSDI diesel engines. With the incorporation of a more sophisticated fuel injection system, turbocharging, EGR, and regenerative and active aftertreatment systems in modern diesel engines, Chapter 7 introduces the concept and example of a model-based control and engine management approach to illustrate how such a complex system can be controlled and optimised.

In the second part of volume 2, following an overview of current heavy-duty diesel engines in Chapter 8, the evolution and development in the fuel injection system for heavy-duty diesel engines is described in Chapter 9. Chapter 10 gives an excellent presentation on the turbocharging technologies for heavy-duty diesel engines by one of the major turbocharger manufacturers. Chapter 11 presents results of a series of experimental and CFD studies carried out on a single-cylinder heavy-duty diesel engine using multiple injections and combustion chamber designs. Part II concludes with a detailed description of the systematic process in the design of heavy-duty diesel engines in Chapter 12.

Part III of Volume 2 discusses exhaust emission abatement, diesel combustion diagnostics and modelling. Fuel reforming is an interesting topic in that it offers the potential to generate on-board hydrogen for not only better combustion but also the opportunity for improving the performance

of aftertreatment systems, which is the topic of Chapter 13. Aftertreatment systems are now an integral part of a diesel powertrain system. Chapters 14 and 15 provide a summary of current practice and future development needs in light-duty and heavy-duty diesel engine aftertreatment systems.

Advanced modelling and in-cylinder optical techniques have made significant contributions to the research and development of direct injection gasoline and diesel engines. Chapter 16 provides an up-to-date summary of advanced optical techniques and their applications to the development of direct injection gasoline and diesel engines. Chapter 17 presents the latest research results of low-temperature diesel combustion through the application of advanced in-cylinder optical diagnostics. Finally, the latest developments in the CFD modelling of internal combustion engines are described in Chapter 18.

This book has been made possible by the dedication of contributing authors to complete their work to the agreed publication schedule, for which I am grateful. In particular, I would like to express my gratitude to the authors who had to endure the extracurricular activities imposed on them. I would also like to thank Sheril Leich and Diana Gill (née Leusenrink) of Woodhead Publishing for commissioning the project and their professional support in preparing this book. Finally, I would like to thank my wife and daughter, who put up with my absence during homework and playtimes.

*Professor Hua Zhao
School of Engineering and Design
Brunel University West London
UK*



SUPERIOR DOWNSIZING

OUR COMPETENCE FOR YOUR SUCCESS

Turbocharged engines, in conjunction with innovative technologies, provide the optimum solution for improved fuel economy and lower emissions. Our downsizing engine with a displacement of 1.2 liters, which we developed as a technology demonstrator, offers the performance of a conventional engine twice the size. More importantly, it reduces fuel consumption, and consequently CO₂ emissions by up to 30 percent. Our numerous high-performance projects and systems contribute to this achievement. As a result of this extensive systems expertise, MAHLE is the leading development partner for the international automotive and engine industry. www.mahle-powertrain.com
Contact: daren.mottershead@gb.mahle.com

MAHLE
Powertrain

Overview of gasoline direct injection engines

H. ZHAO, Brunel University, UK

Abstract: This chapter begins with a brief description of the history of direct injection gasoline engines. Having identified the areas of improvement for fuel economy and performance, technological approaches to high-efficiency and high-performance direct injection gasoline engines are presented and linked to other chapters of the book. This is followed by an overview of recent developments in the high-pressure gasoline fuel injector. Pollutant formation and emissions pertinent to direct injection gasoline engines are highlighted and the relevant lean-NO_x aftertreatment systems are described.

Key words: direct injection, stratified charge, lean-burn combustion, homogeneous charge compression ignition (HCCI), controlled auto-ignition (CAI).

1.1 Introduction

The combination of high specific power with refinement at relatively low cost has made the gasoline engine the dominant power plant for passenger vehicles since the invention of motor vehicles. However, pressure to reduce carbon dioxide emissions and fuel consumption has increased emphasis on the development of more efficient gasoline engines. This is exemplified by the recently proposed EU regulations on fleet average CO₂ emissions of 130 g/km by 2015. Over the last decade the reduction in fleet average CO₂ emission in Europe has been achieved mainly through the rapid market penetration of high speed direct injection diesel engines, which now accounts for more than 50% of new cars sold in Western Europe. However, the intrinsic nature of the refinery process of crude oil dictates the mandatory production and usage of gasoline fuels. In addition, diesel engines require higher injection pressure and more complicated and expensive aftertreatment devices to meet future emission legislations. Therefore, it is very important to develop more efficient gasoline engines that can compete with direct injection diesel engines, with higher specific power output, simpler aftertreatment devices and relatively lower cost fuel injection systems. Direct injection (DI) gasoline engines have the potential to realise the higher specific power output and improved fuel economy by virtue of their ability to minimise knocking combustion at full load operations and reduce pumping losses at part load conditions. The high volatility of gasoline fuel dispenses with the use of very high pressure fuel injection for fuel preparation. Combustion of the premixed fuel and air

mixture, in particular the burning of the stoichiometric mixture, allows simpler, less expensive and more effective aftertreatment devices to be used.

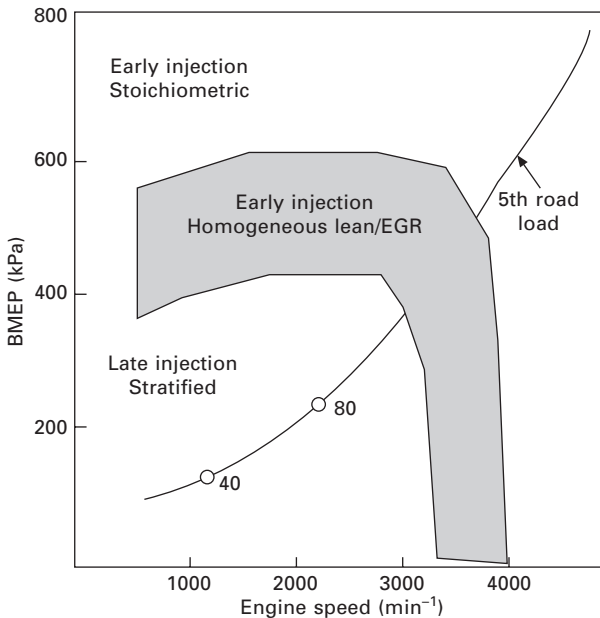
This chapter begins with a brief overview of the history of direct injection gasoline engines. It then presents the potential benefits of direct injection for gasoline engines. This is followed by an overview of the technical approaches to realise such benefits in practice. The recent development of direct injection fuel injectors is then presented. Finally, the exhaust emissions and specific aftertreatment system for DI gasoline engines will be discussed.

1.2 Overview of direct injection gasoline engines

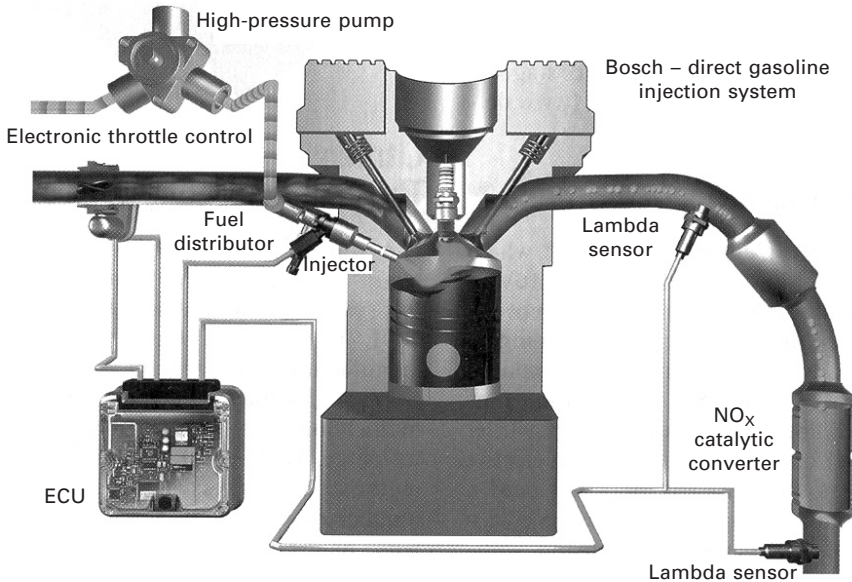
Direct injection for gasoline engines is not a new idea. Much work was carried out during the 1930s to develop a new generation of aircraft piston engines for military applications in the form of a two-stroke direct injection sleeve valve engine (Rolls-Royce Crecy) with a specific power of 165 kW/litre and less than 225 g/kWh specific fuel consumption. Contrary to what has been reported by the press or claimed by some automotive manufacturers, the honour of being the first to apply a direct injection system to automotive applications belongs to Goliath and Gutbrod in 1952. Both the Goliath GP700 E and the Gutbrod Superior 600 were propelled by two-cylinder two-stroke gasoline engines equipped with the direct fuel injection system manufactured by Bosch. They were a few years before the well-known Mercedes-Benz 300SL, though the Benz engine was the first four-stroke direct injection gasoline engine in production. The Bosch fuel injectors were placed into the bores on the cylinder wall used by the original spark plugs, which were relocated to the cylinder head. The use of direct injection in this era was mainly aimed at increasing the vehicle's performance through the charging cooling effect of direct fuel injection.

During the 1970s, a brief flurry of activity was reported into the research and development of direct injection gasoline engines. The best known case was the 'ProCo' (programmed combustion) system developed by the Ford Motor Company, which was implemented in a V8 engine and tested on 100 Crown Victoria cars (Scussei *et al.*, 1978). The system utilised later injection and a bowl-in-piston combustion chamber to achieve the stratified charge combustion and hence unthrottled operation throughout most of the engine's operating range. The project was soon cancelled due to the extremely high cost and inflexibility of the fuel injection system. The mechanical pump-line-nozzle fuel injection system dictated the use of late fuel injection timing even at full load, resulting in smoke-limited combustion at air to fuel ratios richer than 20:1. In addition, the NO_x emissions could not meet the EPA limit. The availability of the three-way catalytic converter proved to be a more cost-effective solution in an era when the exhaust emission legislation was being introduced.

The fundamental limitations of the earlier work on DI gasoline engines were circumvented in the 1990s when direct fuel injection systems, initially developed for two-stroke gasoline engines, found their first commercial success in four-stroke engines. In 1996, the first modern gasoline direct injection automotive engine was introduced in the Japanese market by Mitsubishi Motors as Galant/Legnum’s 1.8 L straight-4, which was subsequently marketed in Europe in 1997 in the Mitsubishi Carisma (Iwamoto *et al.*, 1997). By 2001, over one million GDI engines in four families were manufactured by Mitsubishi in both straight-t and V6 versions. Almost at the same time, DI gasoline engines were introduced to the Japanese and European markets by Toyota (Harada *et al.*, 1997). These engines were designed to operate in the stratified charge spark ignition combustion mode at part load and low to medium speed operations and in the homogeneous charge spark ignition combustion mode at high load and high speed operations, as shown in Fig. 1.1. Most other European and Japanese car manufacturers followed suit and produced their own DI gasoline engines or took licences from Mitsubishi. Figure 1.2 shows the main features of a typical DI gasoline engine: an in-cylinder injector supplied with high-pressure gasoline fuel from a common rail and cam-driven high-pressure pump, sophisticated intake ports and combustion chamber, and dedicated exhaust aftertreatment devices.



1.1 DI gasoline engine operating modes. BMEP is brake mean effective pressure (see Section 1.3).



1.2 A typical DI gasoline engine.

However, fuel efficiency experienced in real-world driving conditions was less than claimed. The introduction of tighter emission legislation mandates the use of expensive, bulky and less efficient lean-burn NO_x aftertreatment for stratified lean-burn operations. As a result, DI gasoline engines after 2001 have been designed to operate only in the homogeneous charge mode. They are tuned and marketed for their high performance. Among them, Toyota's 2GR-FSE V6 uses a combination of in-cylinder direct injection and port injection (Ikoma *et al.*, 2006). It uses two injectors per cylinder, a traditional port injector and a new dual fan-shaped spray injector nozzle. Direct injection is used to obtain additional maximum power output. A combination of port injection and direct injection is utilised to provide smooth operation with a stoichiometric mixture at part load conditions in the absence of large-scale charge motion.

VW and the Audi group have been the most aggressive in adopting direct injection technologies in their gasoline engines, under the trademark of FSI (although this stands for fuel stratified injection, the current engines are not stratified). They are now leading a new wave of production of turbocharged DI gasoline engines, including the two-stage charged TSI 1.4 litre DI gasoline engine with a mechanical supercharger and a turbocharger, which produces an impressive 90 kW/litre power density. This represents the arrival of a new era in gasoline engine downsizing, which involves the substitution of a naturally aspirated engine by a smaller displacement volume but turbocharged engine. Several manufacturers have announced their planned introduction

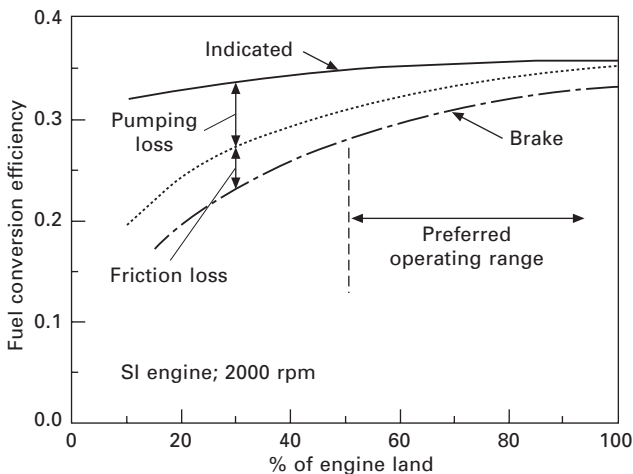
of boosted DI gasoline engines in the line-up of their next generation of vehicles (e.g., the Ford Eco-Boost engine in Europe).

With the newly developed second-generation high-precision injection system, BMW has led the way by reintroducing stratified lean-burn combustion operation in the updated straight six-cylinder 3.0 litre gasoline engine in 2007 (Schwarz *et al.*, 2006). This engine surpasses many others with a wider envelope of lean-burn time, increasing overall efficiency. The gasoline engines for the new BMW 3-series in 2009 will all be equipped with the most advanced piezo-electric actuated direct injection system.

1.3 Potential and technologies for high-efficiency direct injection (DI) gasoline engine

The overview of DI gasoline engines in the previous section illustrates the efforts that have been devoted to the development of gasoline engines with direct injection over the last 50 years. The questions to be asked are: what are the drives for developing such engines for automotive applications? and what would be the real benefits to be gained from direct injection in the gasoline engine? In this section, the areas of improvement in gasoline engines and the technical approaches needed to achieve such improvements are first outlined. The potential of direct injection and its synergy with other technologies to achieve substantial fuel economy benefits will be presented.

Figure 1.3 shows the three main areas of improvement that can be achieved in gasoline engines over a typical driving cycle. The expansion ratio of a current gasoline engine is normally limited to 10:1 or lower by knocking



1.3 Gasoline engine fuel economy analysis.

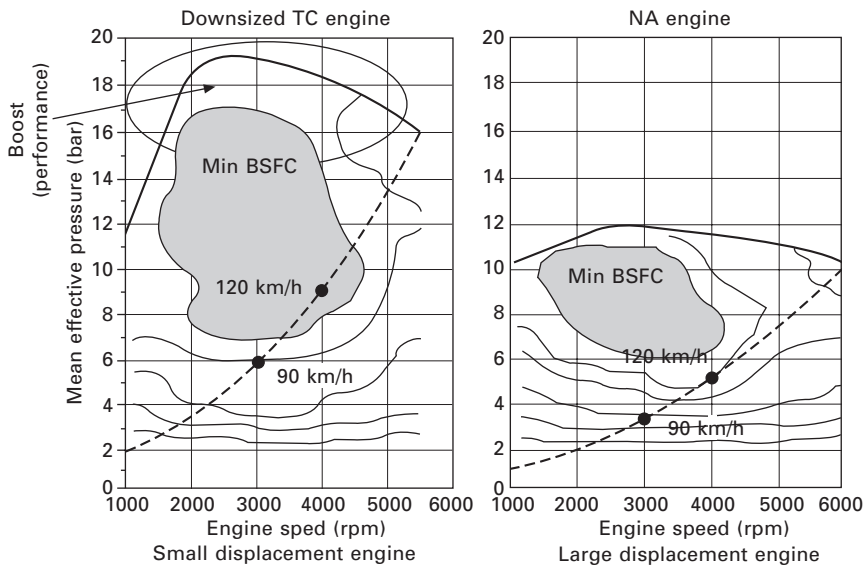
combustion. An increase in the expansion ratio from 10 to 14 can reduce the specific fuel consumption by 10%. The expansion ratio of a reciprocating combustion engine is basically determined by its geometric compression ratio. Since knocking combustion occurs at full load operations, engines can be made to operate at a higher compression ratio at part load conditions and at a reduced compression ratio at full load by designing them to be capable of variable compression ratios. Unfortunately, owing to the additional complexity and cost as well as performance issues, no variable compression ratio engines are currently in production, though this is an active area of research and development. In addition to altering the geometric compression ratio, the actual compression and expansion ratios can be altered through the retarded or early closing of the intake valves. The retarded closing of the intake valves, commonly associated with the Atkinson cycle, delays the start of the compression process and hence reduces the peak compression temperature while the expansion ratio is kept constant. The earlier closing of the intake valves before the bottom dead centre in the intake stroke can also lead to a reduction in pressure and temperature at the start of the compression process, hence lowering the compression temperature. This process is often referred as the Miller cycle. Either Atkinson or Miller cycle operation allows the engine to operate at a higher geometric compression ratio and hence a greater expansion ratio. Such engines would require pressure charging to compensate for the loss in the trapped air mass due to changes in intake valve timings in order to maintain their full load performance.

The use of high octane fuel is another effective way to allow the gasoline engine to operate with higher compression ratios, such as alcohol fuels. Since knocking combustion is most sensitive to the compression temperature of the fuel/air mixture, it can be minimised by reducing the charge temperature in the cylinder. Direct injection of liquid fuel in the cylinder permits the fuel evaporation to take heat from the surrounding air and causes the air temperature to drop. At full load conditions, the charge cooling effect is large enough to allow the engine's geometric compression ratio to be increased by a couple of ratios without causing knocking combustion. The charge cooling effect is particularly noticeable if alcohol fuels are used in direct injection gasoline engines.

Frictional loss can be reduced by adopting low friction mechanical devices, improved surface treatment and lubrication management. As the rubbing loss is proportional to the surface area, a smaller displacement engine will suffer less friction. In addition, smaller displacement engines reduce the weight and installation requirements for a lighter and safer vehicle. However, the most important attribute of replacing a large engine with a smaller displacement one is its potential for significant fuel economy benefit by shifting the engine operation from the least efficient part load operation conditions to wide open throttle operations. This is commonly referred to as engine downsizing. As

shown in Fig. 1.4, pumping loss due to the partly closed throttle valve is the largest factor contributing to the inefficiencies at part load operations, which increases with decreasing load. Through downsizing, the smaller engine will be operated more often at higher load and wide open throttle conditions, as shown in Fig. 1.4, avoiding the less efficient part load conditions. However, the downsized engine needs to be boosted to meet the maximum power and maximum torque requirement. The maximum pressure charging of spark ignition gasoline engines is, however, limited by knocking combustion. With the charge cooling effect of direct injection, higher boost pressure can be employed without the risk of knocking combustion to allow a naturally aspirated engine to be replaced with a smaller boosted engine. Chapter 3 discusses in more detail the potential and the challenges of boosted direct injection gasoline engines.

In order to explore the full potential of engine downsizing, it would be desirable to maximise the specific power and torque output of the downsized engine, measured by its maximum brake mean effective pressure (BMEP) value, through increasing the boost pressure. Under such highly boosted operations, the maximum low speed torque is limited by knocking combustion. In addition, maximum high speed power is principally restrained by the high exhaust gas temperature that will lead to damage to the turbine components in the turbocharger unit. Traditionally, over-fuelling has been used to suppress



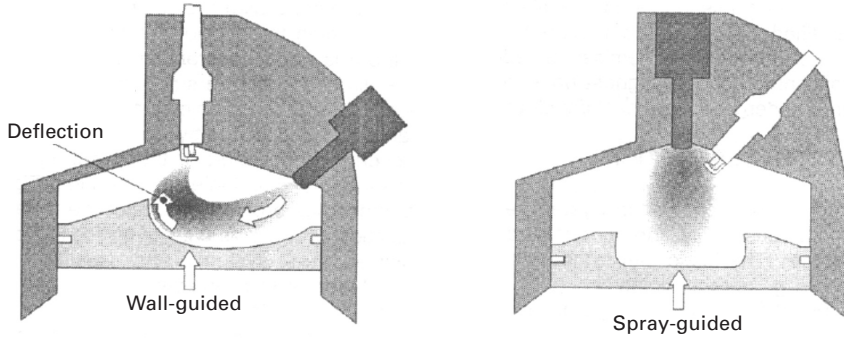
1.4 Principle of engine downsizing. A small engine allows higher efficiency part load operation, due to lower pumping losses and less frictional losses.

knocking combustion and lower the exhaust gas temperature, which can lead to a significant increase in fuel consumption. Since hot residual gas has been found to promote the auto-ignition reactions and hence knocking combustion at full load conditions, the residual gas fraction should be minimised. This may be realised by over-scavenging the cylinder content with pressurised air through the intake valves during the valve overlap period near intake TDC. In a conventional port fuel injection engine, the over-scavenging process will force both the residual gas and some of the intake air and fuel mixture into the exhaust system, causing high fuel consumption and emissions. With direct injection, over-scavenging can be carried out without fuel being sent to the exhaust, as fuel injection takes place after the overlap period. However, in order to obtain a scavenging air flow from the intake side of the engine to the exhaust side, it is mandatory that during valve overlap, the instantaneous intake pressure is larger than the exhaust pressure, which can be achieved at low speed and full load operations. The over-scavenging effect may be further enhanced by an optimised exhaust system that achieves lower exhaust back-pressure during the valve overlap period, for example through grouping the exhaust ports to a twin scroll charger to avoid any impairing interaction between the exhaust streams from other cylinders.

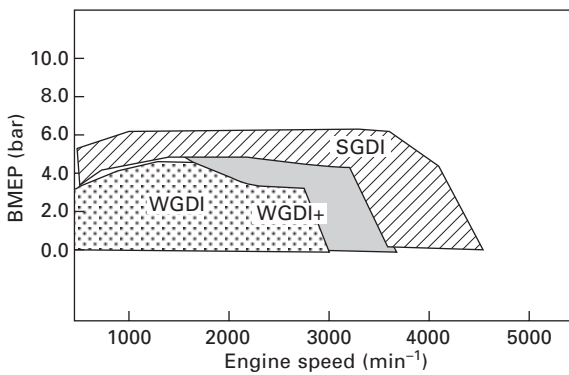
Recently, two other technical approaches have been developed to overcome knocking combustion. The first method is the use of lean-boosted direct injection technology, which is the subject of Chapter 4. The second approach is the EGR-boosted direct injection that is discussed in Chapter 5. Both technologies can extend the knocking combustion limit and the maximum BMEP value of homogeneous stoichiometric turbocharged direct injection gasoline engines.

While the engine downsizing approach forces the engine to operate more in the higher efficiency regions of the engine, the pumping loss at part load is still present. Until recently, lean-burn combustion technology has been researched and developed to minimise the pumping loss of a gasoline engine, by allowing the engine to operate with wider open throttle with excess air. Owing to the lean-burn limit of the propagating flame front, the air to fuel ratio in the flame front region is typically limited to less than 20:1 for gasoline. Direct injection technology can extend the overall in-cylinder air to fuel ratio to 100:1 by stratified charge combustion, where the near-stoichiometric mixture is located near the spark plug, while the excess air is mainly distributed in the rest of the combustion chamber.

There are two basic approaches to stratified charge combustion: the wall-guided and spray-guided systems, as shown in Fig. 1.5. The wall-guided combustion system relies heavily on the presence of strong large-scale in-cylinder motion and the unfavourable shape of the piston geometry, both contributing to a deterioration in full load performance and increased wall heat losses. In addition, the wall-guided system causes unavoidable wall



1.5 Stratified charge combustion systems.



1.6 Comparison of performance of spray-guided (SGDI) and wall-guided (WGDI) combustion systems.

wetting by the fuel, resulting in excessive HC and soot emissions. The stratified charge operation is limited to a small speed and load region. In the spray-guided system, the spark plug and injector are positioned centrally. The charge motion and the piston geometry are of less importance for stratified mixture formation. As a result, the full load performance and part load stratified charge operation can be optimised at the same time. Figure 1.6 compares the stratified charge operation range with a first-generation wall-guided combustion system with a solenoid-actuated swirl injector and that obtained with a spray-guided combustion system using a solenoid-actuated multi-hole injector (Wirth *et al.*, 2004). Further discussion of stratified charge combustion systems will be given in Chapter 2.

Over the last several years, an alternative combustion, controlled auto-ignition (CAI), often known as homogeneous charge compression ignition (HCCI), has been researched and employed to overcome the flammability limit associated with the propagating flame front. As will be discussed in

Chapter 7, auto-ignition combustion of a premixed and diluted mixture allows combustion to take place with excess air or high exhaust gas concentration at lower combustion temperature. Such combustion takes place with a wide open throttle and hence there is little pumping loss due to the partially closed throttle. As a result, simultaneous reductions in fuel consumption and exhaust emissions have been achieved (Zhao, 2007). Compared to stratified charge lean-burn combustion, this combustion technology represents a step change in both engine performance and control characteristics. As will be shown in Chapter 7, direct injection technology allows single and multiple injection strategies to be adopted to obtain closed-loop control over such a combustion process as well as an extended operational range of controlled auto-ignition combustion.

Another potential benefit of direct injection is its ability to realise fast and efficient engine stop and start operation. Currently, the engine in a vehicle is kept running at idle when the vehicle is at a standstill so that the driver can immediately pull away subsequently. In a typical urban driving cycle, the fuel consumption during the idling periods can account for more than 10% of the total fuel consumption. It is therefore desirable to have the engine shut off when the vehicle is stopped. But the engine must be able to restart immediately when the driver wishes to pull away. In addition the energy required for restart should be considered. For a conventional port fuel injection gasoline engine, it takes several engine cycles for the engine to restart and its fuel consumption for one restart is estimated to correspond to that required to idle the engine for about 5 seconds. With direct injection, the duration and fuel consumption for restart can be significantly reduced due to the short cranking through the rapid restart of combustion of directly injected fuel. The instant restart of combustion is achieved through the direct injection of fuel into the cylinder that is operating in the compression stroke (Ueda *et al.*, 2001). The piston position that is used to determine the cylinder in the compression stroke can be detected by crank angle sensors. In the Smart Idling Stop System developed by Mazda (Mazda, 2008) for a four-cylinder engine, a small amount of fuel is injected into the cylinder whose piston is part-way through its compression stroke, and ignites it, causing the engine to run slightly in reverse. The system then injects fuel into the cylinder that has begun to undergo compression owing to the engine's reverse operation. The ignition and combustion of the latterly injected fuel cause greater expansion which drives the engine in the forward direction, thereby starting the engine. For this to work, the compression-stroke piston and expansion-stroke piston must be stopped at positions that create the right balance of air volumes. Consequently, the Smart Idling Stop System effects precise control over the piston positions during engine shutdown. It is claimed that this system is capable of restarting the engine more quickly and quietly than a conventional idle stop and start system. The fuel consumption for restart

of the direct injection idle stop system corresponds only to that required to idle the engine for a fraction of one second. This system enables the engine to be restarted in just 0.35 seconds, roughly half the time of a conventional electric motor idling stop system.

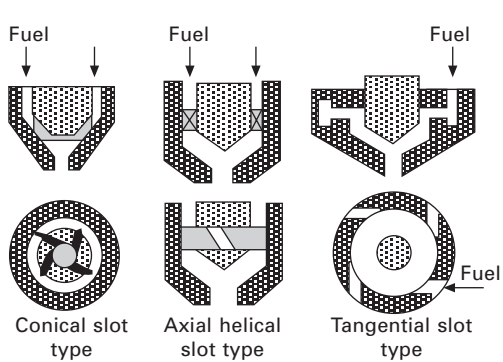
1.4 High-pressure fuel injection system

The fuel injection system is a key component of the DI gasoline engine. It should have the capability of providing both late injection for stratified charge combustion at part load and early injection during the intake stroke for homogeneous charge combustion at high load operations. The homogeneous charge operation requires a well-atomised and evenly dispersed fuel spray with early injection at low in-cylinder pressure. For stratified charge operation, a well-atomised but compact and repeatable spray pattern is desirable to achieve rapid mixture formation and controlled stratification.

The key technology enabler for the modern DI gasoline engine is the development of electronically controlled fuel injection systems. Until the 1990s, mechanical pump–line–nozzle fuel injection systems had been used with fixed injection timings and single injection. Initially developed for two-stroke direct injection gasoline engines, the solenoid-actuated electronic high-pressure fuel injector became available in the late 1980s and was soon adopted for the development of four-stroke direct injection gasoline engines. As shown in Fig. 1.2, the high-pressure fuel system for direct injection gasoline engines comprises a high-pressure pump driven directly by one of the camshafts, which supplies the pressurised fuel to a common rail mounted in the cylinder head, and high-pressure electronic fuel injectors.

The first generation of modern DI gasoline engines are designed with a wall-guided combustion system. The high-pressure solenoid injectors are mostly of swirl-type design, as shown in Fig. 1.7, which features an inwardly opening pintle and a single exit orifice (e.g. Hentschel *et al.*, 1999). The liquid emerges from the single discharge orifice as an annular sheet that spreads radially outwards to form a hollow-cone spray. However, the spray pattern from such an inward-opening swirl injector undergoes significant changes with the injection pressure, the ambient pressure or density, and the injector operating temperature. At the designed injection pressure (between 50 and 100 bar) and elevated ambient density during the late injection of the stratified charge operation, collapse of the hollow-cone spray will occur, forming a narrow spray envelope with an increased spray penetration. As a result, the structure of spray from the swirl injector changes substantially over the operational range of the in-cylinder density and fuel rail pressure, leading to significant difficulty in the optimisation of stratified charge operations over a wide range of part load conditions.

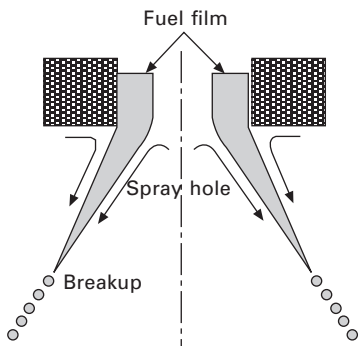
One of the major limitations of first-generation DI gasoline engines with



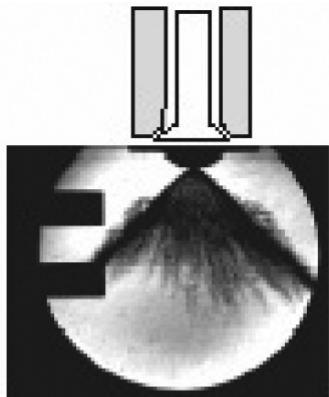
Conical slot type

Axial helical slot type

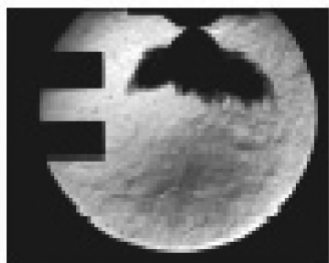
Tangential slot type



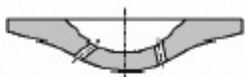
(a) Swirl injector



A-nozzle



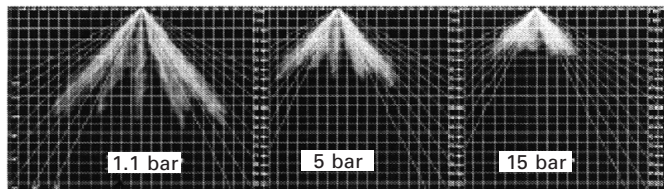
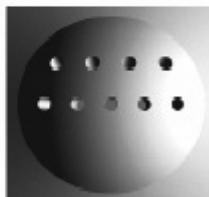
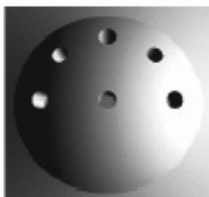
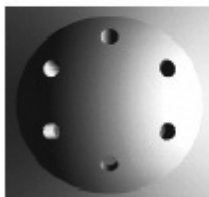
(b) Outward-opening injector



Cone

Crescent

Fan



(c) Multi-hole injector

1.7 Direct injection gasoline injectors in production.

wall-guided combustion systems is the requirement for strong in-cylinder charge motion, such as tumble or swirl. Either a high tumble intake port or a helical port is required to produce the charge motion, which often leads to reduced volumetric efficiency and hence lower full-torque performance. In order to reduce the reliance on a variable flow-control system, a high-pressure slit-type injector was used in the Toyota second-generation DI gasoline engine (Keanda *et al.*, 2000). The slit-type injector has a single rectangular orifice and its slit is positioned to produce a fan-shaped spray either on-axis or off-axis. The ratio of the length and width of the rectangular slit can be adjusted to generate a range of nominal fan included angles. Employment of the slit-type injector was reported to provide both an improved torque curve and a wider range of stratified charge operations.

In order to achieve a spray-guided stratified charged combustion system at part load and improve the full load performance of the direct injection gasoline engine, the solenoid-actuated multi-hole nozzle injector and piezo-electrically actuated injector have been developed and put into mass production vehicles. A major advantage of the multi-hole injectors is that any spatial fuel distribution pattern can be produced in principle by the number of holes, including the angle or angles of the spray pattern, on or offset from the injector axis. A portfolio of multi-hole injectors can therefore be designed to suit the combustion system optimisation needed, as shown in Fig. 1.7. However, as pressure atomisation is the only mechanism to generate the fuel droplets, a relatively higher injection pressure (*c.* 150 Mpa) is normally employed to produce good-quality atomisation. In addition, the small nozzle hole diameter and the higher charge temperature of spark ignition combustion increase the tendency for the injector hole to become blocked by soot deposits. The injector should therefore be placed in a region where the injector could be well cooled to below 130°C to prevent the formation of a soot deposit.

The outward-opening injector, as shown in Fig. 1.7, in comparison can effectively eliminate blocking of the injector nozzle by soot through its outward opening pintle. Moreover, the initial liquid sheet thickness of the spray is directly controlled by the pintle stroke. As a result, the outwardly opening injector allows the spray angle, penetration and droplet size to be controlled.

Piezo-electric actuation utilises the rapid dimensional change in certain ceramics when subject to an electric field. The rapid opening and closing times allow a significant reduction in the minimum opening period and more fuel injection taking place at full pintle lift. The variation in the opening characteristics from actuation to actuation is also superior with the piezo actuator. The ability to operate with much shorter injection duration with repeatable actuation dynamics and fuel quantity leads to a substantial improvement in the dynamic range and the working flow rate of the injector. The extended dynamic range and greater flow rate are pre-requisite for the

development of boosted DI gasoline engines and engines that can operate with both alcohol and gasoline fuels. Moreover, the fast piezo-electric actuated injector allows multiple injections per cycle to be utilised.

Table 1.1 summarises the main characteristics of the three main types of injectors as discussed above. Both solenoid-actuated multi-hole injectors and piezo-electric actuated outward-opening injectors are now in series production with high-pressure pumps supplying the fuel pressure up to 20 Mpa (Stach *et al.*, 2007; Achleitner *et al.*, 2007).

1.5 Exhaust emissions and aftertreatment devices

Unburned hydrocarbons (HC), carbon monoxide (CO) and nitrogen oxides (NO_x) have been targeted by the legislation regulating gasoline engine emissions up to now. However, new emission legislation, such as EURO V, stipulates a limit on the particulate emissions from gasoline engines as well.

Under homogeneous charge operation, the direct injection gasoline engine exhibits similar emission characteristics to that of the port fuel injection engine. The major difference lies in the part load stratified charged operation. In the case of direct injection stratified charge operation, the flame is subject to quenching in the extra lean region at the outer boundary of the stratified charge, resulting in a significant amount of unburned fuel mass in the cylinder. Over-rich regions near the piston due to wall wetting by the fuel spray also contribute to the unburned fuel left in the cylinder. Furthermore, an over-rich mixture in the inadequately prepared stratified charge region will not only contribute to additional unburned HC mass in the cylinder but can also lead to the formation of soot particles and subsequent particulate emissions. The presence of liquid fuel is another source of hydrocarbon and soot emissions from stratified charge operation. Finally, the lower in-cylinder temperature associated with the overall lean-burn operation reduces the

Table 1.1 Comparison of three types of DI gasoline injectors

Characteristics	Multi-hole injector	Piezo outward opening injector	Swirl/inward opening injector
Flexibility of spray pattern	++	+	+
Inclined spray axis	+	-	+
Atomisation quality at 10 MPa	-	+	+
Spray shape dependence on back-pressure	++	++	-
Homogeneous mixture preparation with early injection	-	++	+
Flow rate and dynamic range	-	++	-
Multiple injection	+	++	+
Robustness against fouling	-	++	+

post-flame oxidation effect more than that of homogeneous stoichiometric combustion. The overall unburned HC and soot/particulate emissions at part load stratified charge operation with direct injection are typically several times higher than those from homogeneous operations.

However, HC emissions during cold start can be significantly reduced with direct injection. For example, split in-cylinder injection allows spark timing to be further retarded to produce a higher exhaust gas temperature for faster catalyst light-off. This is in addition to the removal of wall wetting on the intake port and the associated over-enrichment with direct in-cylinder injection. As a result, DI gasoline engines can reach stable operation within the first few cycles when starting from cold whereas the PFI engine typically require more than 10 cycles to reach stable operation.

NO_x emissions from part load stratified charge operation are higher than that from the homogeneous charge operation at the same load. Although the peak cycle cylinder average temperature is reduced due to the overall lean-burn charge, combustion temperature in the stratified charge remains high and becomes higher than the homogeneous charge as combustion takes place at elevated pressure without throttle operation. Furthermore, NO_x emission increases with advanced combustion timing, which is sometimes necessary to achieve stable stratified charge combustion by catching the near-stoichiometric mixture formed soon after the end of injection. Exhaust gas recirculation (EGR) is effective in reducing in-cylinder NO_x formation by lowering the peak combustion temperature and acting as a diluent. However, a larger amount of EGR is required to reduce NO_x emissions, since the exhaust gas of a lean-burn mixture contains less CO_2 and water vapour.

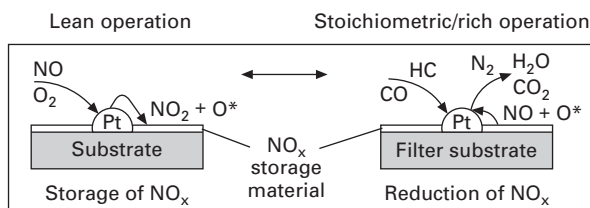
Whilst the higher HC and CO emissions of stratified charge operation with direct injection can be accommodated by a more effective three-way catalyst, an additional aftertreatment system must be employed to reduce the level of exhaust NO_x emission to meet the current emission legislation. In fact, the successful market penetration of DI gasoline engines with stratified charge lean-burn operation is strongly dependent on the cost-effective lean- NO_x aftertreatment technologies. It is not possible to meet the scheduled emission legislations without such devices.

Two types of lean- NO_x aftertreatment systems have been implemented in production engines. The De NO_x catalyst or lean- NO_x catalyst utilises unburned hydrocarbons as the reduction agent to chemically reduce NO emissions. Maximum conversion efficiency of 30–50% occurs in a relatively narrow working temperature window of 180–300°C. In addition, the high HC/NO ratio requirement of the catalytic reactions means that it cannot be used downstream of a closed coupled catalyst that is necessary to cope with the hydrocarbon emissions during the cold start phase. Hence, this type of catalyst has little potential for the stratified DI gasoline engine to meet current and future emission standards.

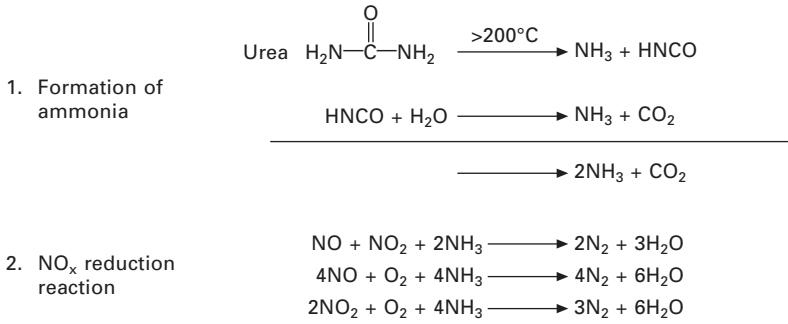
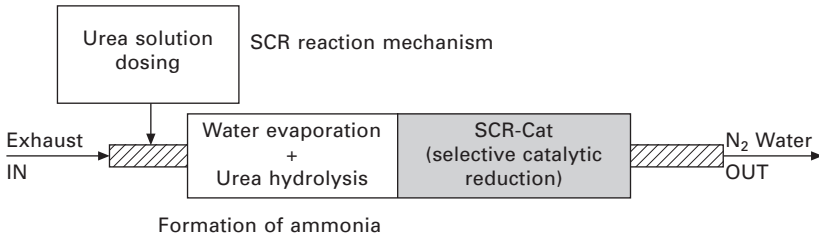
In the NO_x trap or NO_x storage catalyst (Ikeda *et al.*, 1999), as shown in Fig. 1.8, during the lean operation, the precious metal component of the catalyst converts NO and O_2 to NO_2 , which is then absorbed by the storage medium M as thermally stable nitrates. As the storage level of NO increases, regeneration is activated by a brief enrichment phase, during which a slightly rich mixture is burned to increase the exhaust temperature to cause the nitrate to decompose to NO_2 . This is accomplished by the nitrogen oxides reacting with the HC , CO and H_2 from the rich combustion to produce H_2O , CO_2 and H_2 in a similar way to the conventional three-way catalyst. Compared to the DeNO_x catalyst, the temperature window is much wider (in the range of $200\text{--}550^\circ\text{C}$) and the conversion efficiency can be more than 90%. The NO_x trap is also compatible with the closed coupled three-way catalyst setup for cold start emission control. However, regeneration by rich operation calls for complicated control, increased fuel consumption and particulate emissions. It is also sensitive to sulphur poisoning, hence requiring very low sulphur lubricants and gasoline fuels. Good thermal management of the catalyst temperature, particularly at high load operations, is necessary for its durability and stability. All these requirements mandate the use of additional sensors and OBD diagnostics to ensure its proper operation.

Selective catalytic reduction (SCR) by ammonia through liquid urea injection has been developed and used in production diesel commercial vehicles in Europe. In such a SCR system, as shown in Fig. 1.9, liquid urea is atomised into the hydrolysis catalyst at the front and reacts with water to form ammonia and carbon dioxide. The ammonia then reacts with NO_x in the exhaust to form nitrogen in the actual SCR catalyst. An oxidation catalyst at the rear is used to oxidise any ammonia that has slipped through the SCR catalyst.

The major advantages of SCR technology are its low sensitivity to fuel sulphur content, its high conversion efficiency in the region of 90%, and little fuel economy penalty (bearing in mind the additional cost and energy associated with the additives). It is self-contained and can be manufactured as an add-on system independent of the powertrain system. However, such a system would require separate urea storage and delivery, and a closed-loop control system on-board as well as the widespread availability of urea.



1.8 Principle of the lean- NO_x trap.



1.9 Schematic of the urea-based SCR NO_x aftertreatment.

Last but not least is the particulate matter (PM) emissions from the DI gasoline engine. Up to now, gasoline engines have been exempt from the requirement to meet the particulate emissions that diesel engines are subject to, due to their extremely low level of particulate emissions (about 1% of that of diesel engines). This is changing with the new EU V light duty emission legislation, which for the first time includes PM limits for all light duty vehicles. This adds particular challenges to the DI gasoline engine, which produces typically 10 times the particle numbers of the PFI gasoline engine. Furthermore, the stratified charge mode is found to emit 10 to 40 times more particles than the homogeneous charge operation, yet another obstacle for the introduction of stratified charge DI gasoline engines into the market. The reduction of particulate emissions is an important research area. A better understanding of the underlying processes of particulate formation for both homogeneous and stratified charge operation is necessary to achieve significant reductions in their emissions.

1.6 Summary

Direct injection represents the ultimate step in the evolutionary path of a gasoline fuel supply system. Its potential in improving engine performance and fuel economy has long been recognised and actively researched for several decades. Whilst earlier attempts were focused on high engine output

using direct injection, it was not until the mid-1990s that the fuel economy benefit was demonstrated in production vehicles. Such improvements in fuel economy have been realised by the practical implementation of stratified lean-burn operations through technological advancement in the electronic fuel injection equipment and control system, and scientific revelation of in-cylinder flow, fuel spray and their interactions (Zhao *et al.*, 2002).

However, the ever more stringent emission legislation, the variation in fuel quality, and the additional cost of lean-burn aftertreatment have hindered the market penetration of stratified lean-burn combustion technologies. The current focus of the automotive industry is the development of high-performance boosted gasoline engines through homogeneous charge operation. The fuel economy benefit is to be gained through engine downsizing. In addition, the introduction of more advanced valve actuation systems, turbo or/and supercharging, and in-cylinder pressure sensing provides the opportunity for the utilisation of premixed and diluted low temperature combustion, including CAI/HCCI combustion, to achieve simultaneous reductions in CO₂ emissions and pollutant emissions.

1.7 References

- Achleitner E., Baecker H. and Funaioli A.E., Direct injection systems for Otto engines, SAE Paper 2007-01-1416, 2007.
- Harada J. *et al.*, Development of a direct injection gasoline engine, SAE Paper 970540, 1997.
- Hentschel W. *et al.*, Investigation of spray formation of DI gasoline hollow-cone injectors inside a pressure chamber and a glass ring engine by multiple optical techniques, SAE Paper 1999-01-3660, 1999.
- Ikeda Y. *et al.*, Development of NO_x storage reduction 3-way catalyst for D-4 engines, SAE Paper 1999-01-1279, 1999.
- Ikoma T., Abe A., Sonoda Y., Suzuki H., Suzuki Y. and Basaki M., Development of V-6 3.5 litre engine adopting new direct injection system, SAE Paper 2006-01-1259, 2006.
- Iwamoto Y., Noma K., Nakayama O., Yamauchi T. and Ando H., Development of gasoline direct injection engines, SAE Paper 970541, 1997.
- Keanda *et al.*, Application of a new combustion concept to direct-injection gasoline engine, SAE paper 2000-01-053, 2000.
- Mazda press release, <http://www.mazda.com/publicity/release/2008/200809/080909a.html>, 2008.
- Schwarz C., Schunemann E., Durst B., Fischer J. and Witt A., Potential of the spray-guided BMW DI combustion system, SAE Paper 2006-01-1265, 2006.
- Scussei A. *et al.*, The Ford PROCo engine update, SAE Paper 780699, 1978.
- Stach T., Schlerfer J. and Borbach M., New generation multi-hole fuel injector for direct injection SI engines – optimisation of spray characteristics by means of adapted injector layout and multiple injection, SAE Paper 2007-01-1404, 2007.
- Ueda K. *et al.*, Idling stop system coupled with quick start features of gasoline direct injection, SAE Paper 2001-01-0545, 2001.

- Wirth M. *et al.*, A cost optimised spray guided direct injection system for improved fuel economy, IMechE Fuel Economy and Engine Downsizing Seminar, 2004.
- Zhao F., Harrington D. and Lai D., *Automotive Gasoline Direct-Injection Engines*, SAE International, 2002.
- Zhao H. (ed.), *HCCI and CAI Engines for the Automotive Industry*, Woodhead Publishing, Cambridge, 2007.

Stratified-charge combustion in direct injection gasoline engines

U. SPICHER and T. HEIDENREICH,
Universität Karlsruhe (TH), Germany

Abstract: Direct injection gasoline engines promise the highest potential to minimise fuel consumption. The first gasoline direct injection engines of the ‘second generation’ with spray-guided combustion systems were introduced to the market in 2006. These engines are able to operate in lean operation mode throughout a wide operating range. Fuel savings of 10–20% can be achieved compared to conventional gasoline engines with port fuel injection. In this chapter, the thermodynamic aspects of gasoline direct injection are explained and the various combustion processes are described and compared. This is followed by an overview of engines with gasoline direct injection together with an indication of where future developments are leading.

Key words: spark ignition direct injection engine (SIDI), wall-guided, air-guided, spray-guided, gasoline direct injection engine (GDI).

2.1 Introduction

In gasoline engines, direct injection is regarded as the most promising technology to minimise fuel consumption. Although the first modern gasoline engines with direct fuel injection and common-rail injection systems were already on the market in the 1990s, the level of acceptance amongst customers for these engines was very low in comparison with diesel engines with direct injection. One reason for this was that these engines did not entirely fulfil customers’ expectations with regards to fuel economy. One of the factors contributing to this problem was that these engines were designed as wall- or air-guided combustion systems, and as such, they could only operate in lean-burn, stratified charge mode within a comparatively small engine operating range. In reality, these engines were not capable of achieving the desired fuel consumption savings on the road (Fröhlich *et al.*, 2003; Wirth *et al.*, 2003). This restriction in the engine operation map for stratified-charge operation, along with the complex exhaust aftertreatment required as a result of the lean operation mode, led a number of automobile manufacturers to develop direct injected engines that employed stoichiometric, homogeneous mixtures. Although this gave rise to a number of benefits due to the direct introduction of fuel into the combustion chamber, the full potential for fuel consumption reduction was still not achieved (Schnittger *et al.*, 2003). With these stoichiometric combustion systems, it was also possible to

retain conventional exhaust aftertreatment using three-way catalytic converters.

The implementation of standard spray-guided combustion systems has recently become possible as a result of intensive research and development work combined with further advances in fuel injection technology. The first gasoline direct injection engines of the ‘second generation’ (as spray-guided systems are often referred to) were introduced to the market by BMW and Mercedes-Benz in 2006. It was possible to operate these engines with globally lean equivalence ratios throughout a wide operating range, i.e. in lean operation mode, and also achieve fuel savings between roughly 10% and 20% when compared to conventional gasoline engines with port fuel injection and stoichiometric operation in everyday driving situations (Wirth *et al.*, 2003; Lückert *et al.*, 2005). Further reductions in fuel consumption are anticipated as a result of a combination of the above with supercharging strategies and downsizing measures.

In the following section, the thermodynamic aspects of gasoline direct injection are explained and the various combustion processes are described and compared. This is followed by an overview of engines with gasoline direct injection together with an indication of where future developments are leading.

2.2 Thermodynamic and combustion process

Nowadays, modern diesel engines are equipped with direct fuel injection and most of these are supported by forced induction, which means that they can achieve a favourable level of fuel consumption. Modern gasoline engines, on the other hand, are still mainly of a conventional type in which the mixture is prepared externally, i.e. via port fuel injection; they are manufactured for stoichiometric operation, and their load is controlled via the intake throttle. The conventional gasoline engine therefore presents considerable disadvantages in terms of its efficiency and therefore also fuel consumption, particularly during part-load operation. With gasoline engines, a reduction in throttling loss during the charge cycle presents considerable potential for reductions in fuel consumption and therefore conservation of natural resources. In addition to the use of variable valve timing to reduce charge cycle losses, renewed efforts have been made since the mid-1990s towards achieving throttle-free operations in gasoline engines by injecting fuel directly into the combustion chamber. The efficiency of direct fuel injection and stratified-charge operations is further enhanced by using lean mixtures.

The benefits of direct fuel injection in gasoline engines in terms of efficiency can be demonstrated by considering the Otto cycle (constant-volume process) – the assumed ideal process for a gasoline engine. In the constant-volume process, isentropic compression is followed by combustion at

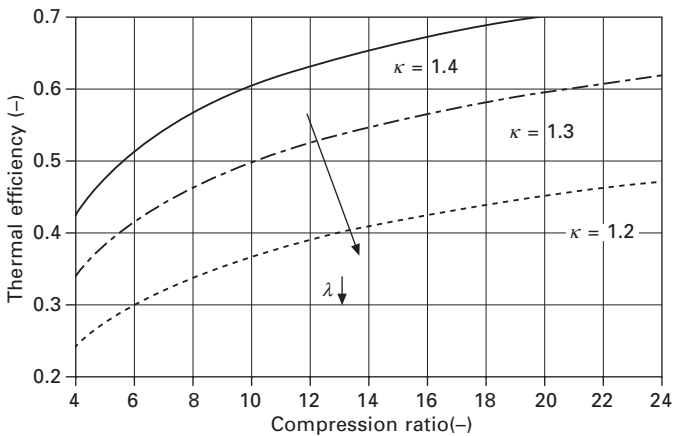
constant volume at top dead centre. This is followed by isentropic expansion and then exhaust with constant-volume heat rejection. In simplified form, with the assumption of ideal gas as a working fluid, the thermal efficiency of the constant-volume process follows this equation (Heywood, 1988):

$$\eta_{f,i} = 1 - \frac{1}{r_c^{\kappa-1}}$$

Assuming a closed, loss-free process without fuel conversion, the efficiency is only affected by the compression ratio r_c of the engine and the isentropic exponent κ . The highest possible efficiency is therefore produced by a high compression ratio and a large isentropic exponent, which in turn depends on the mixture composition and temperature.

With direct fuel injection, sensible enthalpy is decreased in the combustion chamber due to the vaporisation of fuel and the associated evaporative cooling. This decreases the temperature at the end of compression, which means that these engines are less prone to knock than engines with port fuel injection. The improved knock resistance can be used to increase the compression to between roughly 1.5 and 2 units, which reduces fuel consumption by approximately 3%.

The greatest increase in efficiency is achieved by the implementation of unthrottled operation with lean charge stratification. A high isentropic exponent (κ) is achieved by maximising the leanness of the mixture. The leaner the mixture that can be successfully used to operate the engine, the closer the isentropic exponent will be to its maximum value of 1.4 (that of pure air). In the case of direct injection, thermal efficiency can be increased by influencing two decisive variables: the compression ratio and the isentropic exponent (see Fig. 2.1).



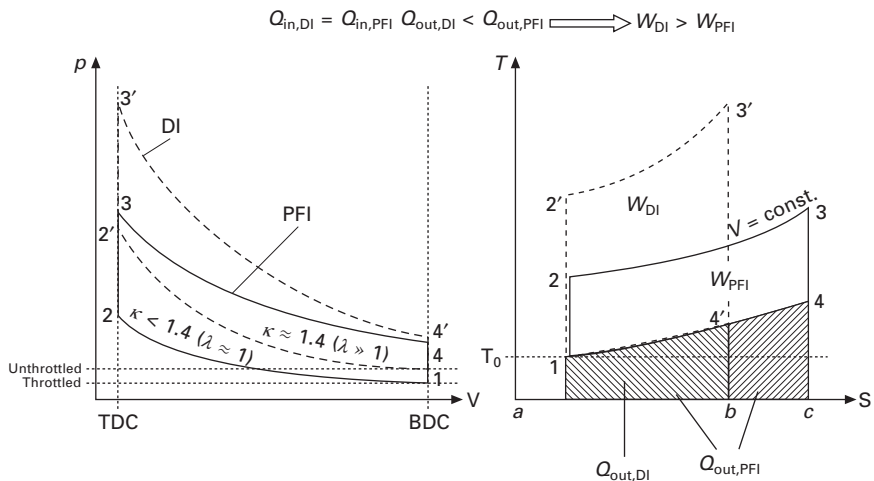
2.1 Thermal efficiency of the constant-volume process.

The differences in efficiency between port fuel injection and direct injection can also be seen in the $p-V$ and $T-S$ diagram (see Fig. 2.2). To make the comparison easier, the compression ratio has been kept constant for both cases in the illustration below. Compression starts from a low intake pressure in throttled, part-load operation in the case of port fuel injection, as opposed to direct injection where the starting point is more or less at ambient pressure. Assuming that the same quantity of heat is delivered in both processes, the areas in the $T-S$ diagram show that the quantity of heat rejected during the exhaust process is less for the unthrottled cycle and the efficiency is therefore higher.

In a real engine, the advantages of gasoline direct injection in terms of efficiency are due to the following:

- The unthrottled load control reduces pumping losses during part-load operation.
- The extremely lean mixtures have higher isentropic exponents and therefore higher thermal efficiencies.
- Lean mixtures burn at lower temperatures than stoichiometric mixtures.
- The internal cooling as a result of fuel vaporisation decreases the tendency to knock; this can be used to increase the compression ratio, which increases the efficiency.

In principle, direct injection in gasoline engines can be implemented using two different operating modes/strategies: homogeneous operation and

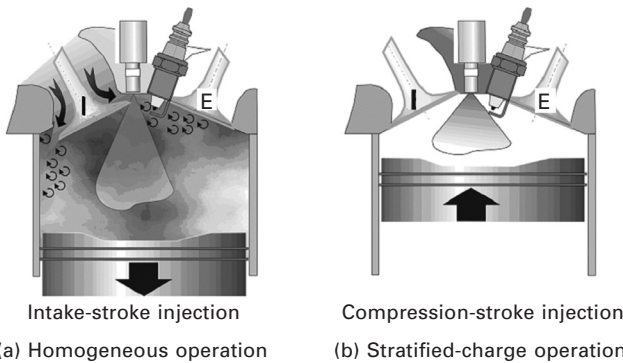


2.2 Constant-volume processes for port fuel injection (PFI) and direct injection (DI).

stratified-charge operation (Fig. 2.3). In the higher load range, an engine in which fuel injection occurs during the intake stroke and which therefore has a homogeneous mixture composition is operated in a similar way to a gasoline engine with external mixture preparation (see Fig. 2.3a). The fuel is then injected into the combustion chamber during the intake process on the downward stroke of the piston, similarly to the fuel-injection system in gasoline engines where the mixture is prepared externally (port fuel injection). This produces a largely homogeneous mixture distribution in the compression phase that follows, accompanied by a more or less uniform air ratio throughout the entire combustion chamber at the point of ignition.

During part-load operation, the advantages of unthrottled operation can be realised via operation with charge stratification. To achieve unthrottled part-load operation with a homogeneous mixture in the combustion chamber, the mixture present at the spark plug would be leaner than the lean ignition limit. To ensure that an ignitable combustible mixture is always present near the spark plug at the point of ignition, the fuel–air mixture must be stratified in the combustion chamber through appropriate preparation of the mixture.

During stratified-charge operation, a gasoline engine with direct injection should ideally be operated with the throttle valve fully open. The load is then regulated purely by the quantity of fuel injected (mixture quality regulation), as is the case with a diesel engine. During this process, the fuel is injected directly into the combustion chamber immediately before ignition occurs during the upward stroke of the piston. This operation is therefore also referred to as compression-stroke injection (see Fig. 2.3b). An ignitable mixture cloud forms in the centre of the combustion chamber, surrounded by air that is not required for combustion. Stratified charging therefore takes place in the combustion chamber and the heat losses at the wall of the combustion chamber that occur during subsequent combustion are reduced by this layer



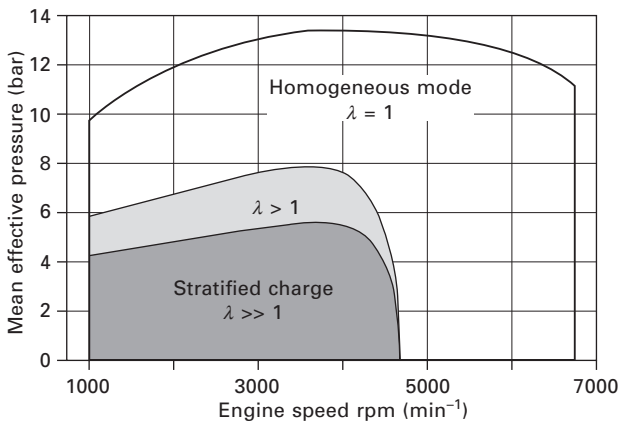
2.3 Operating modes for gasoline direct injection engines.

of insulating air. Therefore, when viewed as a whole, the engine is indeed operating globally lean of stoichiometric, whereby large air ratio gradients form in the combustion chamber.

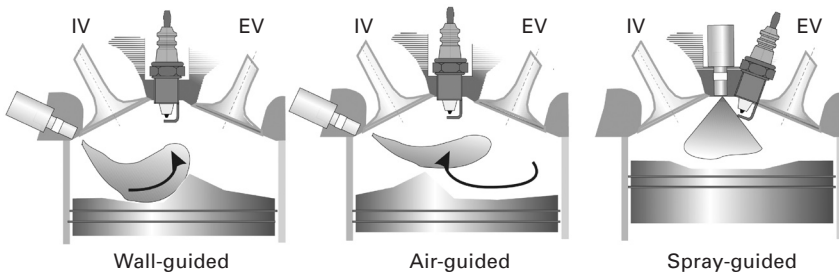
Figure 2.4 shows the range of the operating modes for gasoline direct injection engines in the engine operation map. The mixture preparation, mixture transportation to the spark plug, and reliable ignition of extremely lean mixtures are important preconditions for successful charge stratification (Wirth *et al.*, 2003; Waltner *et al.*, 2006). As a basic rule, three different combustion concepts for the implementation of mixture preparation and fuel guidance can be identified in the case of gasoline direct injection (see Fig. 2.5).

2.2.1 Wall-guided combustion systems

The majority of first-generation engines with stratified-charge operation were designed with wall-guided combustion systems, in which the mixture



2.4 Operating modes in the engine operation map.



2.5 Wall-, air- and spray-guided combustion concepts (Fischer, 2004).

is prepared and transported to the spark plug via a wall in the combustion chamber. In most cases, the piston is shaped in such a way that the spray from the fuel injector is directed to the spark plug via the piston crown bowl. The mixture transportation during this process is normally supported by a swirl or tumble flow operation. As the injection jet is directed straight at the piston, this combustion procedure results in increased fuel deposits and emissions of unburned hydrocarbons. As the injection timing is linked to the piston position, it is therefore dependent on engine speed. Furthermore, desirable and stable in-cylinder flow patterns also depend on the engine speed; it is difficult to coordinate the injection and ignition timings across a wide engine speed/load range. In practice, it was not possible to realise the theoretical potential of gasoline direct injection for reducing fuel consumption in the case of wall-guided combustion operation for the following reasons:

- As mixture transport is linked to the piston position, it is difficult to properly coordinate the injection and ignition timing over a wide engine operating range.
- The tumble or swirl ports required to produce the desired intake flow adversely influence the charge at higher loads.
- Fuel is deposited on cylinder walls and the piston. A pronounced film may form on the wall, not only during cold starts and when the engine is warming up, but also during normal engine operation. Incomplete combustion causes soot formation and deposits at these locations. Deposits that accumulate cannot be fully burned off because of the low combustion temperatures encountered during partial load operation. These porous residues absorb fuel that is sprayed onto them during subsequent injection. The emission of combustible hydrocarbons increases as a consequence.
- Fuel enters the squish gap. It is necessary to inject more fuel during the transition from low- to medium-part load. This means that it is necessary to advance the fuel injection time to achieve the optimum ignition timing in terms of efficiency. However, it is possible that the injected fuel will spill over the edge of the crown bowl and penetrate the squish gap. In this case, since the fuel is not fully consumed, the emission of unburned hydrocarbons is greater.
- There are increased mechanical losses. Due to the special shape of the piston, it is larger and heavier than a conventional piston, which means the mechanical losses are greater.

2.2.2 Air-guided combustion systems

In contrast to wall-guided systems, air-guided combustion systems aim to reduce the hydrocarbon emissions that are a by-product of wall-guided systems by preventing the fuel from coming into contact with the walls of

the combustion chamber. This ideally eliminates fuel deposits on the wall of the combustion chamber. The aim in this case is to utilise charge movement to effectively mix the fuel and intake air. The charge movement can also be supported by appropriately shaped piston crowns. The success of this method therefore depends on the directional orientation of the injection jet and on the generation of a specific charge movement. It is particularly important to ensure that the specific charge movement is sustained far into the compression phase in order to ensure transport of the mixture up to the spark plug. The swirl or tumble flow required to perform this operation reduces volumetric efficiency and therefore adversely affects performance.

Wall-guided operations also use highly distinctive air flows to direct the mixture which means that, in reality, clear differentiation of combustion systems is not practical. These systems can therefore be referred to as wall/air-guided combustion systems or first-generation gasoline direct injection.

2.2.3 Spray-guided combustion systems

An important feature of spray-guided combustion systems is the physical proximity of the spark plug to the fuel injector. It must be ensured, through optimum positioning of the spark plug in relation to the injection plume, that an ignitable mixture is present at the spark plug at the point of ignition for a wide range of operating conditions. Decisive factors in this case are the characteristics of the fuel injector. The injector must produce a spray pattern that is as robust and repeatable as possible, even when subjected to changes in back pressure or flow conditions. Furthermore, the system must ensure that extremely lean mixtures with steep stratification gradients at the edges of the fuel spray can be reliably ignited.

Owing to the special features of the spray-guided combustion system, particular attention must be paid to the following points:

- Coking at the spray nozzle. Coking may occur at the spray nozzle due to low combustion temperatures during part load operation and idling. These may have negative effects on the spray profile.
- Tolerances in the spray pattern. The spray pattern may change as a result of operating conditions or manufacturing tolerances and have undesirable effects on combustion performance.
- Coking at the spark plug. Low combustion temperatures during partial load operation and when idling can lead to coking at the spark plug and, as a consequence, misfiring.
- Thermal shock at the spark plug. If liquid fuel comes into contact with the hot spark plug, it cools the spark plug rapidly, therefore subjecting it to an extremely high thermal load.
- Effect of fuel injection time. As fuel injection and ignition are closely linked, fuel is injected at a thermodynamically favourable time shortly

before ignition at top dead centre (TDC). Very little time is therefore available to prepare the mixture.

- Effect of engine speed. High or low engine speeds change the speed of the intake air flow and the relative speeds of the cylinder charge and injected fuel spray. This affects mixture preparation and may interfere with air stratification in the area around the spark plug.

Owing to the problems mentioned above, a number of requirements must be satisfied in order to fully exploit the potential of a spray-guided combustion system in terms of its theoretical efficiency (Kemmler *et al.*, 2002; Hübner *et al.*, 2003):

- The spray quality of the fuel injector must be high and as reproducible as possible over all relevant engine speed and load ranges. This is the only way to achieve complete combustion with low carbon monoxide and unburned hydrocarbon emissions.
- The mixture preparation must also be optimised at retarded fuel injection times in order to achieve a thermodynamically favourable combustion process.
- To minimise hydrocarbon emissions, the geometry of the combustion chamber and spray pattern must be such that contact between liquid fuel and the combustion chamber is as low as possible.
- The mixture composition at the spark plug can be selectively modified in order to maximise the stability of combustion performance using a highly flexible injection system capable of multiple injections within a cycle.
- The sensitivity of the fuel injector to contamination must be as low as possible, and it must demonstrate considerable long-term stability in terms of the spray characteristic.
- High injection pressures reduce the mixture preparation time, which is important when fuel injection is retarded for the purposes of optimising the course of combustion. Faster evaporation of smaller fuel droplets can reduce particle emissions.
- A robust, efficient and variable ignition system that satisfies the special requirements of spray-guided operation must be employed. The spark plug should have the highest possible resistance to wear and should also be resistant to thermal shock.

In addition to the known thermodynamic benefits of direct injection, such as reduced pumping losses, the effect of modified calorific gas properties, lower temperature as a result of the internal evaporation of fuel, etc., spray-guided combustion systems also provide additional benefits in terms of efficiency. When compared with wall/air-guided systems, fuel wetting on the pistons or combustion chamber walls is reduced to the point where it is essentially eliminated. This reduces the emissions of unburned hydrocarbons. Improved

primary atomisation of the fuel spray and a more compact mixture cloud leads to faster and more comprehensive fuel conversion, which further reinforces the similarities between this process and the constant-volume process.

Direct-injected engines are less sensitive to knock due to the evaporation of fuel in the combustion chamber (internal cooling). The allowed increase in compression ratio improves the thermal efficiency of the engine throughout the entire operating range. Additionally, the higher final compression pressure also has a positive effect on the ignition of the mixture.

With wall/air-guided combustion systems, the swirl and/or tumble flow necessary to transport the mixture to the spark plug reduces the volumetric efficiency and therefore has disadvantages in terms of performance. In principle, this restriction does not apply to spray-guided systems; in this case the inlet ports can be designed as filling channels to optimise the full-load performance. As no specific charge movement is required for transportation of the mixture to the spark plug for spray-guided systems, the charge movement can be specified so that the turbulence in the combustion chamber supports the flame propagation and therefore comprehensive and rapid burn-out of the mixture.

Spray-guided systems can also benefit from efficient mixture preparation and a centrally located fuel injector and spark plug. This ensures favourable conditions that affect the efficiency of the combustion process and also unburned hydrocarbon emissions.

The positive effect on the dynamic engine response characteristics is a further consequence of direct fuel injection and unthrottled operation. When a sudden change from part-load operation to full-load operation occurs as the throttle is opened in a conventional quantity-regulated engine, the air intake system must initially be filled and a higher air intake pressure must be allowed to build up. With direct fuel injection and unthrottled stratified-charge operation, the full air intake pressure is nearly always present and the torque response is much faster.

The advantages of spray-guided combustion systems mean that stratified-charge operation can be designed not only to optimise low pollutant emissions and low fuel consumption; considerable advantages over conventional engines with port fuel injection or first-generation direct fuel injection also exist.

The intake port wall film that forms and enriches the mixture during rapid load shifts with port fuel injection is eliminated. In addition, gasoline direct injection also presents the opportunity of using special operating modes, such as stratified starting or homogeneous lean-burn operation mode.

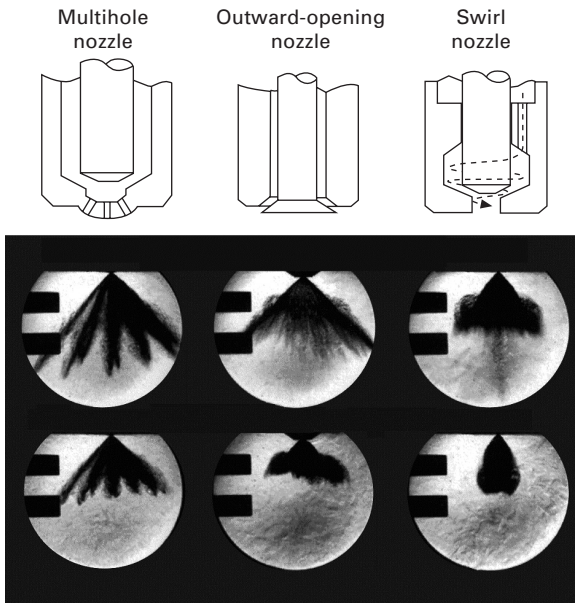
Comparison of nozzle types

The three standard types of nozzles used nowadays in fuel injectors for gasoline direct injection are shown in Fig. 2.6. The nozzles can be differentiated

from one another by the means by which they open and close. The outward-opening nozzle (A-nozzle) exposes the nozzle cross-section when the valve opens and generates the self-forming spray via the cone. The multihole nozzle and the swirl nozzle are both inward-opening concepts (I-nozzles). The multihole nozzle is well known in diesel engines. An upstream swirl generator is used in conjunction with the swirl nozzle to prepare the mixture. A comparison of the spray profiles for the three different nozzle types at the same point after fuel injection starts is also shown in Fig. 2.6.

The swirl nozzle exhibits very good atomisation quality and high spray flexibility. It also has a relatively low sensitivity to contamination as well as mechanical and thermal interference. It is relatively affordable since it is produced in high quantities. The spray of this fuel injector forms a hollow cone, the angle of which is largely determined by the pressure in the combustion chamber. This is a major disadvantage in regard to spray-guided combustion systems, as it influences the position of the spray in relation to the spark plug. This concept is currently favoured by most developers and manufacturers for purely homogeneous gasoline direct injection and for stratified charging operations with wall-guided mixture preparation.

Sharply defined injection jets are a characteristic of the multihole nozzle. Because of the inadequate atomisation quality of the multihole nozzle, it is only possible to establish a partially homogeneous mixture in the combustion chamber with the injection jet shape, even when using a variety



2.6 Nozzle types and their spray profiles (Wirth *et al.*, 2003).

of configurations. Enriched mixture zones containing excess fuel are directly adjacent to lean mixture zones containing insufficient fuel. As a consequence, once an injection jet is ignited – the origin of ignition is determined by the position of the spark plug – the flame front in the combustion chamber does not progress uniformly. Rather, it spreads at varying speeds: the flame front accelerates in enriched zones of individual injection jets, but slows down in lean zones between the injection jets. The number of injector holes therefore significantly influences the operating characteristics of the engine. A hole pattern that results in effective fuel distribution and constant flame spread between the various injection jets produces the best engine operating characteristics. The lean-burn capability of the engine can be improved by increasing the number of nozzle holes and also by reducing the individual flow areas. However, the number of holes is currently limited due to an increasing tendency towards coking. The spray penetrates further with multihole valves than with A-nozzles. This can lead to excessive wetting of the piston during retarded fuel injection operations, thus increasing hydrocarbon and soot emissions (Warnecke, *et al.*, 2006).

When compared to the swirl injector, the outward-opening nozzle (A-nozzle) has the distinct advantage of being able to produce a uniform hollow cone without generating a pre-spray. The spray angle is more or less unaffected by the back pressure in this case. Using this injector type in conjunction with a piezo control, it is possible to inject several times at extremely short intervals. Furthermore, using this type of control system, it is possible to control droplet size and injection mass separately, which makes it far superior to the conventional solenoid-actuated system. With spray-guided combustion systems, the spark plug can be positioned in the recirculation area and also at the boundary of the fuel jet produced by the A-nozzle. The A-nozzle is an attractive choice for spray-guided systems due to the low sensitivity of its spray profile.

Mixture preparation can be optimised through multiple fuel injections. The stratification of the fuel–air mixture can be improved by injecting the fuel two or more times in succession. The ignition and burnout characteristics can be stabilised by optimising the fuel injection times in relation to the time of ignition. This can be achieved if fuel that previously evaporated during the first injection in the recirculation zone of the injection jet is present at the ignition location at the time of ignition. The ignition of the entire mixture and subsequent burnout can be supported by the second injection. Faster ignition leads to a shorter combustion time and increased efficiency.

Thermodynamic analysis

The thermodynamic advantages of gasoline direct injection can be clearly demonstrated by analysing the losses using a part-load operating point as an

example (Fig. 2.7). The positive influence of real gas is particularly noticeable in the case of direct injection. The increased isentropic exponent results in considerable advantages over engines with premixed intake. When compared to throttled engines with port fuel injection, direct fuel injection also reduces the pumping losses considerably. In terms of efficiency, the benefits of direct injection outweigh the disadvantages such as losses due to incomplete and thermodynamically unfavourable combustion due to lean peripheral areas.

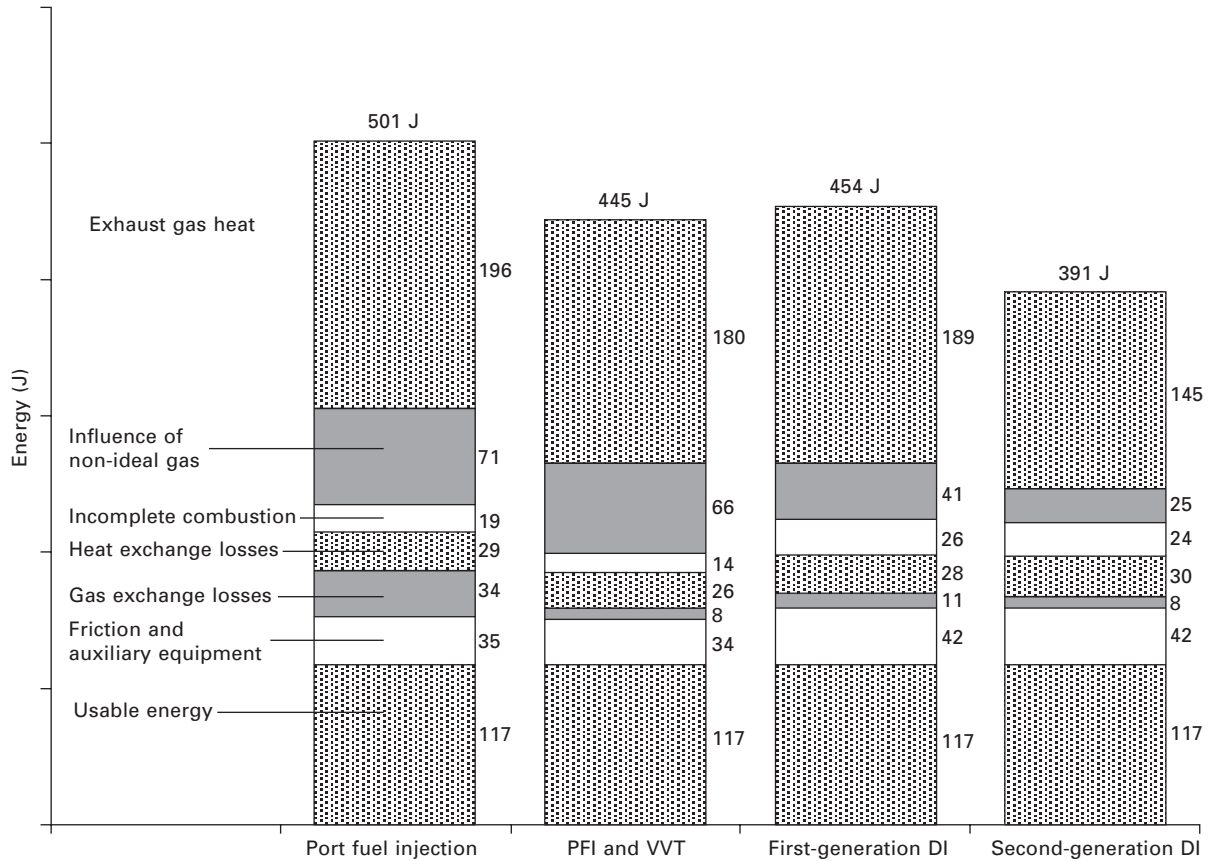
The combustion process for direct-injected engines is normally characterised by a 50% mass fraction burn point that is too early (Fig. 2.8). Assuming the presence of enriched mixture zones around the ignition location, the combustion process accelerates rapidly at the start of combustion. As soon as the flame reaches the lean peripheral areas, combustion slows down and burnout decelerates. This process therefore departs from the thermodynamic ideal of the constant-volume process, and the efficiency decreases. The deceleration of lean mixture burnout that occurs in spray-guided combustion systems can be countered by increasing turbulence in the combustion chamber using well-directed charge movement.

In the case of direct injection, the compression end temperatures rise due to the high charge and high compression ratio. As the wall heat flux occurs in higher concentrations around top dead centre, the wall heat losses are higher compared to a stoichiometrically operated engine with port fuel injection even though the average temperatures of the combustion chamber are lower with direct injection. Gasoline direct injection has further disadvantages due to higher friction and the increased amount of energy required to drive the high-pressure fuel pump.

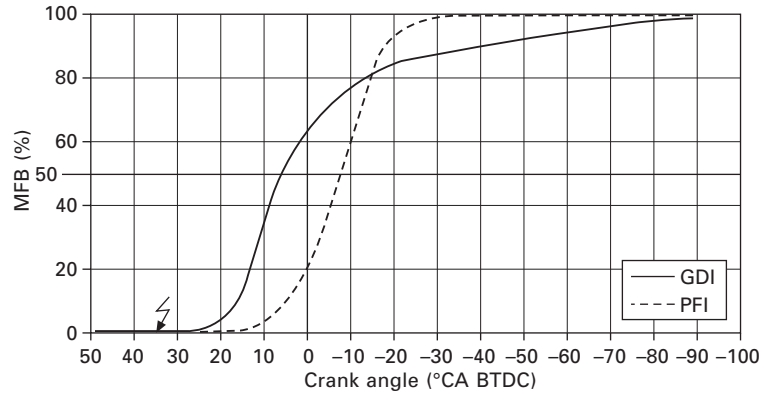
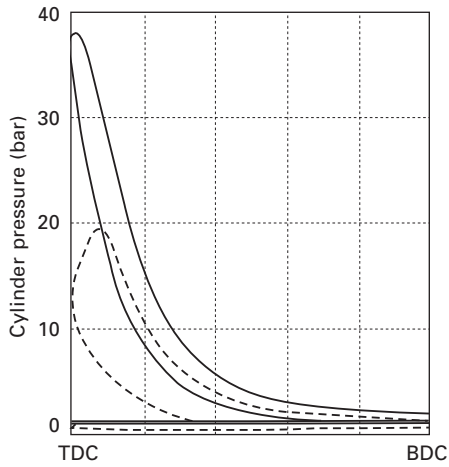
To fully exploit the potential of direct injection, the operating range in which the engine can run with a stratified charge must be maximised. The stratified charge range can only be extended to include higher loads to a limited extent, particularly due to particulate emissions that largely depend on the characteristics of the injection system, the sizes of the droplets, and evaporation properties of the fuel spray. It was possible to expand the stratified charging range of second-generation engines with spray-guided combustion systems considerably when compared with first-generation gasoline direct injection engines. This was made possible due to further developments in fuel injection technology, including increased injection pressures, use of outward-opening nozzles with piezo actuators, and multiple injection capability. The increased stratified charge range means that it is possible to drive economically at speeds above 150 km/h with lean stratified charge operation (see Fig. 2.9).

Fuel consumption

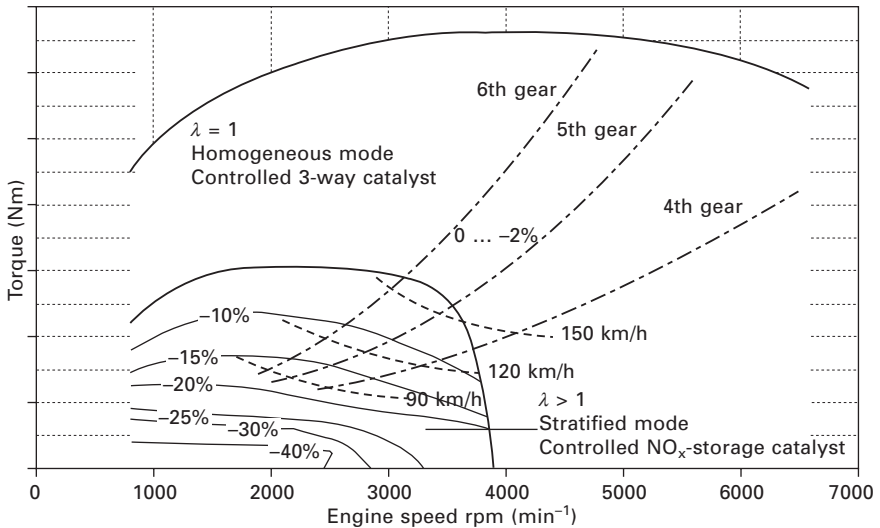
In terms of fuel consumption, engines with first-generation gasoline direct injection were claimed to achieve a reduction in fuel consumption of roughly



2.7 Analysis of losses for port fuel injection (PFI), VVT, first- and second-generation GDI (Lückert *et al.*, 2004).



2.8 Combustion process: comparison of port fuel injection (PFI) vs. gasoline direct injection (GDI) (Krämer, 1998) (Waltner *et al.*, 2006).



2.9 Engine operating map, stratified charge ranges with driving resistance curves and fuel reduction.

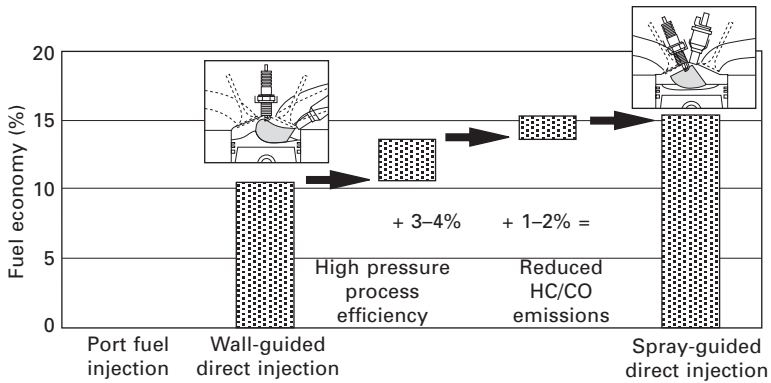
40% when running at idle as opposed to conventional engines with port fuel injection. A reduction in fuel consumption of roughly 15% was achieved with lean stratified charge operation at part-load operating points. As the lean stratified charge range was limited to low engine speeds and loads, it was not possible to turn this potential into perceptible fuel savings for customers.

It only became possible to operate these engines through the New European Driving Cycle (NEDC) predominantly with lean stratified-charge operation (i.e. with low fuel consumption) following the transition to second-generation gasoline direct injection with spray-guided systems. Once the engine has warmed up, it is only necessary to interrupt the lean stratified-charge operation during the regeneration phases of the nitrogen oxide storage catalyst.

The increased efficiency and optimised performance of spray-guided combustion systems mean that the corresponding fuel consumption is around 4–6% less than for wall-guided systems (Fig. 2.10). In terms of fuel consumption, customers have benefited from more extensive use of the stratified charge operation with second-generation gasoline direct injection.

Exhaust gas treatment

Exhaust gas treatment has a major influence on fuel consumption. Stringent regulations apply in relation to exhaust gas treatment with gasoline direct injection systems. It must be ensured that catalytic converters also reach their activation temperature at low exhaust gas temperatures, particularly



2.10 Fuel economy of first- and second-generation direct injection compared to port fuel injection engines (Wirth *et al.*, 2003).

during part-load operation. Selective exhaust manifold heating strategies can be implemented by means of flexible multiple injection, thus effectively reducing hydrocarbon emissions during cold starts.

Gasoline direct injection is characterised by a variety of air–fuel ratios, ranging from extremely lean mixtures (part load) in stratified charge operation to rich mixtures (full load). During lean-burn operation, combustible hydrocarbons and carbon monoxide are readily oxidised due to the high proportion of oxygen.

On the other hand, NO_x adsorber catalysts (De- NO_x catalysts; also called NO_x storage catalysts) must be used to reduce the nitrogen oxide produced during lean-burn operation ($\lambda > 1$). As the NO_x storage capacity of these catalysts is limited, the engine must be briefly operated with rich mixtures ($\lambda < 1$) during regeneration phases. During regeneration, stored NO_x is released and reduced to N_2 . As the engine is operated with a rich mixture during regeneration phases, fuel consumption is increased. To further increase efficiency, it is necessary to optimise the combustion and exhaust gas aftertreatment systems so that additional fuel consumption as a result of aftertreatment is minimised. In order to be able to reduce nitrogen oxide efficiently, the De NO_x -Cat must have reached its minimum operating temperature. As sulphur in the fuel contaminates the storage converter, engines with this exhaust gas treatment system cannot be used in countries where fuel of the necessary quality does not exist.

2.3 Production engines with stratified gasoline direct injection (GDI)

This section provides an overview of a selection of standard first- and second-generation gasoline direct injection engines.

2.3.1 First-generation gasoline direct injection engines

One of the first examples of the modern generation of engines with gasoline direct injection was the GDI engine (Gasoline Direct Injection) unveiled by Mitsubishi at the International Motor Show IAA 1995 in Frankfurt. It was launched on to the Japanese market in 1996 and the European market in 1997. The Mitsubishi engine employs a wall-guided combustion system in which the fuel is directed through a special piston crown bowl to the spark plug, supported by what is referred to as a reverse tumble flow. The exhaust aftertreatment is performed by a selective, continuously operating reduction catalytic converter with an iridium coating. This catalytic converter has been combined with a conventional three-way catalytic converter to form what is referred to as a tandem catalytic converter. Owing to its low thermal resistance, this catalytic converter is mounted on the underbody. However, a NO_x conversion rate of only 60% is achieved using a catalytic converter that operates according to this principle.

Technical data for Mitsubishi GDI (1997)

Engine displacement:	1.8 litres
Power:	90 kW(122 HP) at 5500 rpm
Number of cylinders:	4 (16 valves)
Fuel consumption:	approx. 8.5–9 litres per 100 km

In 2000, Volkswagen launched the first engine with gasoline direct injection (referred to as FSI or Fuel Stratified Injection) for the VW Lupo onto the market (Winterkorn *et al.*, 2000). This was a further development of the EA111 engine with port fuel injection, 1.4 litre cylinder capacity and 74 kW power. It was possible to increase the power to 77 kW with gasoline direct injection. In this case, the FSI operation is wall-guided and air-supported. The piston has a fuel bowl on the inlet side and a flow recess on the outlet side that redirects the air in the required direction. The inlet ports are designed as filling channels but the lower duct cross-section can be sealed off using a flow flap to produce a strong tumble flow that assists the mixture preparation. The high pressure fuel injector has a spray cone angle of 70° and an inclination angle of 20° and is positioned below the inlet ports. The spark plug is positioned centrally as is the case with the basic engine.

Through the cooling effect of the evaporating fuel, it was possible to raise the compression ratio from 10.5:1 to 12:1. The benefit in terms of fuel consumption as a result of increased compression ratio was roughly 2.3%. The engine is operated essentially unthrottled in stratified-charge mode ($p_{\text{intake}} > 900$ mbar) and therefore achieves an air–fuel ratio of between 1.8 and 3. The benefits in terms of fuel consumption during lean stratified-charge operation

depend on the operating point and are 10% in the medium part-load range and up to 44% when running in idle, according to VW specifications.

The intensive charge movement of the FSI engine also results in extremely favourable EGR compatibility. Therefore, in the homogeneous mode, an EGR rate of up to 25% can be employed without producing a significant increase in hydrocarbon emissions. This results in additional fuel savings.

Although, at the time of its launch, the Lupo FSI was compliant with Euro III legislation, the engine also met the more stringent Euro IV values. A low-volume pre-catalytic converter with a three-way catalyst section was subsequently installed near the engine, combined with a NO_x storage converter installed on the underbody. VW was the first vehicle manufacturer in the world to use a NO_x sensor downstream of the NO_x catalytic converter to optimise nitrogen oxide conversion.

Technical data for engine installed in VW Lupo FSI

Engine displacement:	1390 cm ³
Number of cylinders:	4
Compression ratio:	12:1
Power:	77 kW (105 HP) at 6200 rpm
Torque:	130 Nm at 4250 rpm
Camshaft adjustment:	inlet camshaft with 40° adjustment range
Internal flow of cylinder:	switchable tumble flap system

FSI engines were subsequently offered with different cylinder capacities (1.6 l, 2.0 l, 3.2 l) in other VW models (Golf, Passat). However, today's FSI engines are still only driven in homogeneous mode and use of the stratified-charge operation is completely avoided, as is the case with all turbocharged FSI engines.

In 2002, Audi also launched an engine with gasoline direct injection with the designation FSI. In contrast to the VW version, however, the four-valve aluminium cylinder head and piston geometry was fully reworked, as an air-guided combustion system was used in this case. A strong tumble flow is generated via an infinitely variable charge movement flap and redirected by the piston crown bowl in such a way that the injected fuel is transported by the air flow to the spark plug. Fuel is delivered to the high-pressure valves by a Bosch HDP2-type high-pressure pump with controlled delivery, according to requirements. To avoid contact with the piston crown, the fuel is injected into the combustion chamber at a shallow angle of 22.5°.

The engine has two catalytic converters for exhaust gas aftertreatment. In addition to the three-way catalytic converter installed near the engine, an additional NO_x storage converter is installed on the underbody. This is equipped with a NO_x sensor at the catalyst outlet, as is the case with the

VW engine. The storage converter is controlled by both the engine operating map and the converter temperature.

Technical data for Audi 2.0 FSI engine

Design:	4-cylinder in-line engine with gasoline direct injection
Engine displacement:	1984 cm ³
Bore × stroke:	82.5 mm × 92.8 mm
Valves per cylinder:	4
Camshafts:	2
Power:	110 kW (150 HP) at 6000 rpm
Maximum torque:	200 Nm between 3250 and 4250 rpm
Emission level:	Euro 4
CO ₂ emission:	170 g/km

2.3.2 Second-generation gasoline direct injection engines

Mercedes-Benz and BMW were the first manufacturers to bring second-generation engines with gasoline direct injection, i.e. with spray-guided combustion systems and stratified charging, onto the market in 2006 and 2007. The M272 DE 35 engine has been supplied by Mercedes-Benz in the CLS 350 CGI (Charged Gasoline Injection) since the end of June 2006 (Lückert *et al.*, 2006). This is a V6 engine with a 3.5 litre displacement volume, four-valve technology with two camshafts per cylinder bank, and piezo injectors with outward-opening nozzles (A-nozzles), positioned centrally in the cylinder head. The spark plug has been slightly displaced from the centre position in the direction of the exhaust valves, and tilted so that the electrodes are positioned at the edge of the injected fuel plume. Fuel is introduced to the combustion chamber using up to three individual fuel injection sequences at a pressure of up to 200 bar. A quantity-controlled three-piston high-pressure pump is used to generate the pressure. Higher stratification rates are possible with spray-guided gasoline direct injection, which means that these engines are potentially more economical to run than engines with first-generation gasoline direct injection.

A double-flow external exhaust gas recirculation system helps reduce NO_x emissions. Two close-coupled three-way catalytic converters ensure that the light-off temperature during cold starts is quickly attained throughout the exhaust gas system, which has a double-flow configuration throughout. The downstream NO_x storage converters are mounted on the underbody to protect them against excessively high temperatures. They have an active temperature window of 250–500°C. To enable precise regulation of the NO_x catalytic

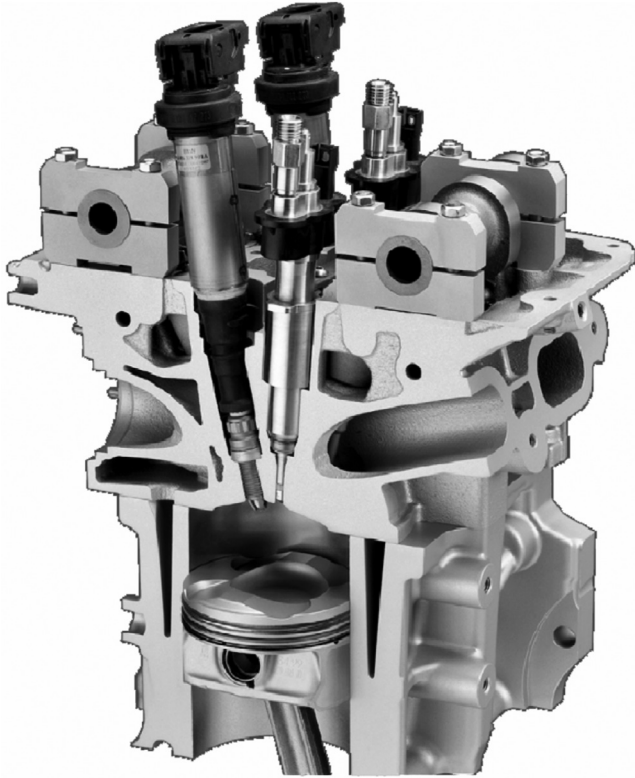
converters, a temperature sensor is installed upstream of the converter and a NO_x sensor is installed downstream of each converter. The latter serves to ensure that the NO_x values remain within the limits throughout the entire service life of the vehicle.

In the case of spray-guided systems, it has been possible to considerably extend the engine operating range in which charge stratification takes place when compared to first-generation combustion systems. The CLS 350 CGI can therefore be driven at speeds of more than 120 km/h in stratified charge mode. Two-figure reductions in fuel consumption can be achieved in large sections of the engine operating map. Compared to versions with port fuel injection, engines with gasoline direct injection in the New European Driving Cycle achieve a 10% reduction in fuel consumption. Furthermore, the power output of this engine is 15 kW higher and the torque is 15 Nm higher than for the V6 port-injected gasoline engine.

Technical data for Mercedes-Benz CLS 350 CGI

Cylinder layout/number:	V6
Included cylinder-bank angle:	90°
Stroke × bore:	86 mm × 92.9 mm
Stroke–bore ratio	0.926
Engine displacement:	3498 cm ³
Valves per cylinder:	4
Compression ratio:	12.2:1
Power:	215 kW (292 HP) at 6400 rpm
Torque:	365 Nm at 3000–5100 rpm
Spec. fuel consumption at best point:	240 g/kWh
Fuel consumption at 2000 rpm, 2 bar:	290 g/kWh (port fuel injection: 360 g/kWh)

In 2007, BMW launched new engines with spray-guided gasoline direct injection (Schwarz *et al.*, 2006), starting with the new 3 Series Convertible. A model with an inline six-cylinder engine, twin-turbo charging and High Precision Injection (HPI) was introduced; it was operated homogeneously. Additionally, two naturally aspirated versions of the engine with stratified-charge operation were also introduced. These engines all have an identical injection system, the same as the homogeneously operated turbocharged engine. A number of four-cylinder engines with gasoline direct injection and stratified-charge operation are now used as standard by BMW in various vehicle models. These engines are characterised by a centrally positioned injector with a spark plug directly adjacent to it (Fig. 2.11). The injector used is an outward-opening piezo injector with an oil-damped thermal compensator. This technology has known benefits such as a low coking tendency and an extremely short injector switching time of 200 µs that makes full and partial



2.11 Cylinder head BMW (source: BMW).

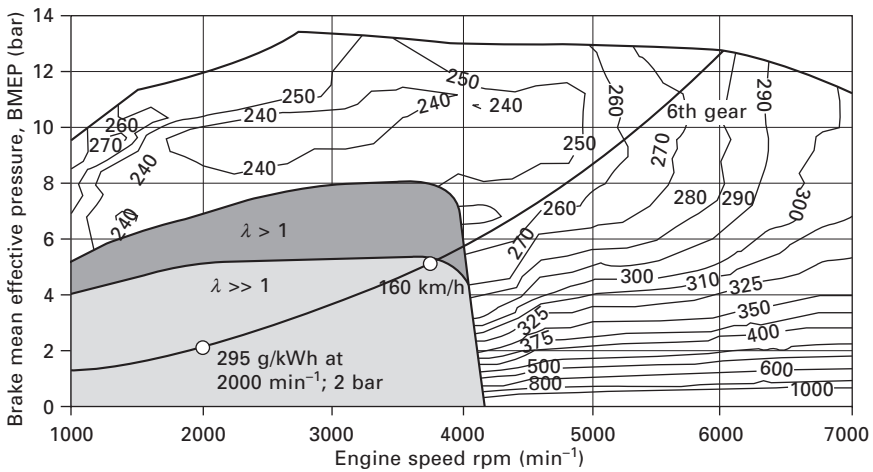
strokes, in addition to multiple injection operations, possible. A three-cylinder axial-piston pump with integrated delivery control valve with a combined pressure and delivery control function compresses the fuel up to a maximum pressure of 200 bar. The fuel arrives at the injectors via short separate lines and a common rail with integrated pressure sensor. Specifications for these spray-guided BMW engines can be seen in Table 2.1.

The stratified charge range of an engine with gasoline direct injection and spray-guided combustion system is shown in Fig. 2.12. The fuel consumption of the engine is favourable when operated using a lean mixture throughout a wide load and engine speed range. The best point shows an effective specific consumption of approximately 240 g/kWh.

Fuel consumption is reduced by approximately 13% to 295 g/kWh when compared with an equivalent engine with Valvetronic variable valve timing that already performs extremely favourably. This underscores the potential of gasoline direct injection with spray-guided systems for achieving reductions in fuel consumption and increases in efficiency.

Table 2.1 Technical data for second-generation direct injection BMW engines

Type	6 cylinder in-line (R6)	6 cylinder in-line (R6)	6 cylinder in-line (R6)	4 cylinder in-line (R4)	4 cylinder in-line (R4)
Stroke (mm)	88	88	78.7	90	90
Bore (mm)	85	85	82	84	84
Cylinder capacity (l)	2.996	2.996	2.497	1.995	1.995
Compression ratio	12 : 1	12 : 1	12 : 1	12 : 1	12 : 1
Space between cylinders (mm)	91	91	91	91	91
Valves per cylinder:	4	4	4	4	4
Pollutant class	EU4	EU4	EU4	EU4	EU4
Power (kW), (HP) at engine speed (rpm)	200 (272) 6700	160 (218) 6100	140 (190) 6100	125 (170) 6700	105 (143) 6000
Torque (Nm) at engine speed (rpm)	320 2750–3000	270 2400–4200	240 3500–5000	210 4250	190 4250–4500



2.12 Stratified-charge range of BMW engine with gasoline direct injection and spray-guided combustion system (Missy et al., 2007).

2.4 Future trends

Future developments in the area of combustion engines will concentrate on further reductions in fuel consumption and pollutant emissions. Gasoline direct injection technology will play a significant role in achieving this. The first engines with spray-guided combustion systems were launched in 2006. It can be assumed that in the next few years, other manufacturers will follow by producing engines with second-generation direct injection systems. Gasoline direct injection with turbocharging is an ideal combination for

increasing the efficiency of the engines. Several manufacturers have already combined homogeneously operated engines with forced induction and direct injection and have also created attractive downsizing concepts. These kinds of engines offer good road performance comparable with engines with higher displacements and achieve favourable fuel consumption. The CO₂ emissions of modern engines with gasoline direct injection or a downsizing concept already compare favourably with diesel engines. The combination of stratified direct injection with supercharging represents the biggest potential for reduction in fuel consumption, as this enables the stratified charge range to be extended further, thus providing benefits in terms of fuel consumption.

Exhaust emissions legislation in Europe is becoming increasingly stringent and the introduction of limiting values for particle emissions of gasoline engines with lean-burn stratified operation is now envisaged. This means that in future, the avoidance and aftertreatment of soot emissions will also be a relevant issue for gasoline engines. Owing to the costs and complexity of particulate filters, measures leading to the reduction of soot formation inside the engine will be of primary interest. The mixture preparation process has a significant effect on the formation of soot. To avoid soot, it must be ensured that the amount of liquid fuel present at the point of ignition is as small as possible, and/or that no liquid fuel comes into contact with the flame as it expands. Fast evaporation of the fuel is advantageous, as there is only a very short time available during stratified-charge operation for preparation of the mixture. Improved fuel atomisation avoids locally over-rich zones and reduces the risk of soot formation. Fuel atomisation can be influenced by increasing the injection pressure. Injection pressures of up to 200 bar are used at present in engines with second-generation direct injection, and if this value were exceeded in the future, it would lead to improvements in the mixture preparation process.

2.5 References

- Fischer J (2004), 'Einfluss variabler Einlassströmung auf zyklische Schwankungen bei Benzin-Direkteinspritzung', Dissertation, Universität Karlsruhe (TH), Germany
- Fröhlich K *et al.* (2003), 'Potenziale zukünftiger Verbrauchstechnologien', 24th Vienna Engine Symposium 2003
- Heywood J B (1988), *Internal Combustion Engine Fundamentals*, McGraw-Hill, New York
- Hübner W *et al.* (2003), 'Methodeneinsatz bei der Entwicklung eines weiterführenden DI-Brennverfahren', conference 'Direkteinspritzung im Ottomotor IV', published by Expert Verlag, Renningen, Germany
- Kemmler R *et al.* (2002), 'Thermodynamischer Vergleich ottomotorischer Brennverfahren unter dem Fokus minimalen Kraftstoffverbrauchs', 11th Aachen Colloquium for Vehicle and Engine Technology 2002
- Krämer, S (1998), 'Untersuchung zur Gemischbildung, Entflammung und Verbrennung

beim Ottomotor mit Benzin-Direkteinspritzung', Dissertation, Universität Karlsruhe (TH), VDI Verlag, Düsseldorf, Germany

Lückert P *et al.* (2004), 'Weiterentwicklung der Benzin-Direkteinspritzung bei Mercedes Benz', 13th Aachen Colloquium for Vehicle and Engine Technology, 2004.

Lückert P *et al.* (2005), 'Kunden- und zukunftsorientierte Technologie am Ottomotor – heute und morgen', 26th International Vienna Engine Symposium 2005

Lückert P *et al.* (2006), 'Der neue V6-Ottomotor mit Direkteinspritzung von Mercedes-Benz', *MTZ*, No. 11, Vieweg, Wiesbaden, Germany

Missy S. *et al.* (2007), 'Brennverfahrensentwicklung am Beispiel der neuen BMW Sechs- und Vierzylinder Ottomotoren mit High Precision Injection und Schichtbrennverfahren', conference 'Direkteinspritzung im Ottomotor IV', published by Expert Verlag, Renningen, Germany

Schnittger W *et al.* (2003), '2.2 Direct Ecotec – Neuer Ottomotor mit Direkteinspritzung von Opel', *MTZ*, No. 12, pp. 1010–1019

Schwarz C *et al.* (2006), 'Potentials of the spray-guided BMW DI combustion system', SAE Paper 2006-01-1265

Waltner A *et al.* (2006), 'Die Zukunftstechnologie des Ottomotors: strahlgeführte Direkteinspritzung mit Piezo-Injektor', 27th International Vienna Engine Symposium 2006

Warnecke V *et al.* (2006), 'Entwicklungsstand des Siemens VDO Piezo-Einspritzsystems für strahlgeführte Brennverfahren', 27th Vienna Engine Symposium 2006

Winterkorn M *et al.* (2000), 'Der Lupo FSI von Volkswagen', *ATZ*, No. 10, Vieweg, Wiesbaden, Germany

Wirth M *et al.* (2003), 'Die nächste Generation der Benzin-Direkteinspritzung – gesteigertes Verbrauchspotenzial bei optimierten Systemkosten', 12th Aachen Colloquium for Vehicle and Engine Technology 2003

The turbocharged direct injection spark-ignition engine

J. W. G. TURNER and R. J. PEARSON,
Lotus Engineering, UK

Abstract: This chapter discusses the concept of turbocharging the spark-ignition engine both within the historical context of increasing performance and in the modern one of its application for fuel consumption and CO₂ reduction. The advantages and drawbacks of turbocharging are discussed against the use of external fuel delivery, and then the mechanisms by which in-cylinder direct fuel injection addresses most of the disadvantages are described. The chapter concludes with a section discussing some future trends and possibilities for the technology, including its synergy with some of the alternative fuels currently being proposed (principally the alcohols), with cooled exhaust gas recirculation EGR for knock suppression and also with some new engine architecture developments.

Key words: spark-ignition engines, turbocharging, direct injection, knocking combustion, CO₂ reduction.

3.1 Introduction

Turbocharging the automotive spark-ignition (SI) engine is a technology which has traditionally been used to increase the performance range of engine families to provide a more powerful option within existing engine architectures and vehicle platforms. In more recent years, however, the technology has also become synonymous with fuel consumption improvement with the advent of engine ‘downsizing’. In this case, an engine in turbocharged form is conceived and designed from the outset, rather than being a development of an existing unit. This is one of the main thrusts in the current endeavour to increase engine efficiency and reduce carbon dioxide emissions.

Downsizing the SI engine is an attempt to reduce pumping losses by fitting a smaller-swept-volume engine than is normally the case for a given power output and recovering the loss in full-load performance by employing a pressure charging system, which usually comprises at least one turbocharger stage. This means that, for any given road load, the throttle is wider open and the irreversible losses incurred in the gas-exchange phase of the 4-stroke cycle are consequently reduced. The widespread adoption of the approach stems from the fact that the automotive industry remains committed to the 4-stroke Otto cycle and reducing the amount of throttling loss the cycle

suffers is the primary aim of many technologies currently being developed for application worldwide [1] since its attractiveness is not compromised by gasoline fuel specification and the requirements for emissions compliance. As a consequence of its cost-effectiveness compared with other fuel economy technologies, downsizing is becoming a major developmental avenue for the automotive industry in general.

This chapter will briefly review the history of turbocharging in automotive SI engines before discussing the purpose of turbocharging and the problems inherent in the concept which must be overcome in the development of the technology. It will then discuss the advantages of combining direct fuel injection (DI) with turbocharging and how this technology combination mitigates nearly all of those difficulties while offering many new opportunities. Some of the remaining challenges will be outlined and the possibility for further system optimization discussed against a background of engine architecture developments and other SI engine technologies. Finally, a projection of future trends is made.

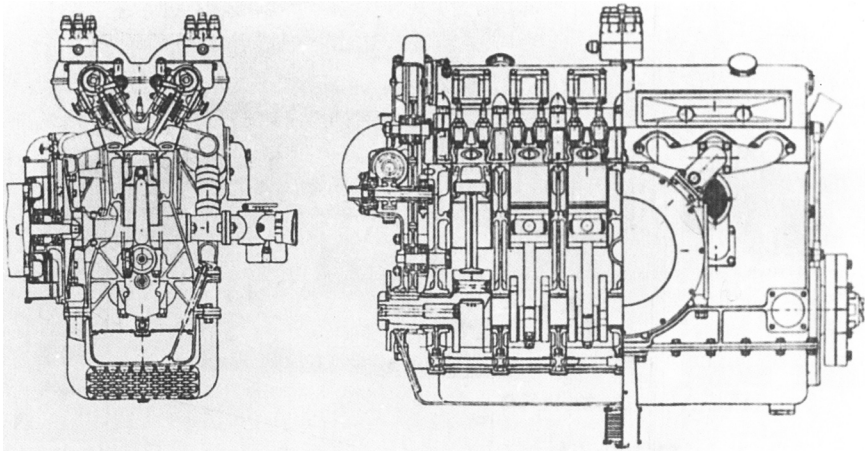
3.2 Historical background: turbocharging for high specific output

The amount of power an SI engine can produce is directly proportional to the amount of charge it can consume. Hence an engine with a larger swept volume, or one operating at higher rotational speed, will generate more power than a smaller or slower one. Similarly, pressurizing the intake charge ('pressure charging') in order to increase its density was recognized as a means of increasing the specific power output from the very first days of the internal combustion engine. Gottlieb Daimler was granted a German patent in 1885 for a supercharger applied to an internal combustion engine [2] and Louis Renault patented a supercharger based on a centrifugal air pump feeding the mouth of a carburettor in 1902 [3]. In 1907 Lee Chadwick developed a supercharged engine receiving compressed air from a single-stage centrifugal compressor driven via a belt from the engine flywheel and by 1908 had progressed to using a three-stage supercharger in a racing car in which he won a major hill-climb event [3]. In the background, a Swiss engineer, Alfred Buchi, realized that, rather than using the brake power of the engine to drive the compressor, it could be coupled via a shaft to a turbine powered by the exhaust gas, utilizing exhaust gas enthalpy that would ordinarily be lost. Buchi obtained a patent for the concept in 1905 [4] but the technology was not immediately adopted by his employer, Sulzer Brothers.

The increase in engine specific power output obtained from pressure-charging was attractive in early aerospace applications as a means of increasing wing loading and aircraft performance, shortening take-off distance and increasing operational altitude ceiling prior to the advent of the gas turbine [5]. The

Royal Aircraft Factory (later renamed the Royal Aircraft Establishment, or R.A.E.) began development of aero-engine supercharging in 1915 and, during 1918–25, began experiments with turbocharging (or turbo-supercharging¹) [6]. Although the R.A.E. terminated the development of turbocharged aero engines to concentrate on supercharging after this period, mainly due to bearing failures and the lack of affordable high-temperature alloys for the turbine wheels, in 1923 the first application of turbocharging in a car occurred when the aero engine designer and racing car driver Major Frank Halford equipped a 1.5 litre in-line 6-cylinder engine of his own design with a purpose-built turbocharger [7].

Halford's engine, as shown in Fig. 3.1, being intended for racing, was specifically designed for high performance, incorporating double overhead camshafts, inclined valves and twin-spark ignition, adopted from his experience of aircraft engines. The engine also benefited from Halford's knowledge of the development of high-octane fuel. The subject of synergies between engine architecture and turbocharging will be returned to later in this chapter, but it



3.1 Turbocharged racing car engine developed by Major Frank Halford in 1923. Note the adoption of double overhead camshafts and twin spark plugs and the separation of the manifolds for each set of three cylinders. The use of an underslung intercooler can also be discerned. Source: Taylor [7]; (courtesy Douglas R. Taylor and The Rolls-Royce Heritage Trust).

¹ Originally the term 'turbo-supercharging' was used to denote a particular embodiment of supercharging in which the compressor power is obtained from an exhaust-driven turbine. The term has become shortened to 'turbocharging', whilst 'supercharging' is generally understood to imply that the compressor is mechanically driven from the engine crankshaft.

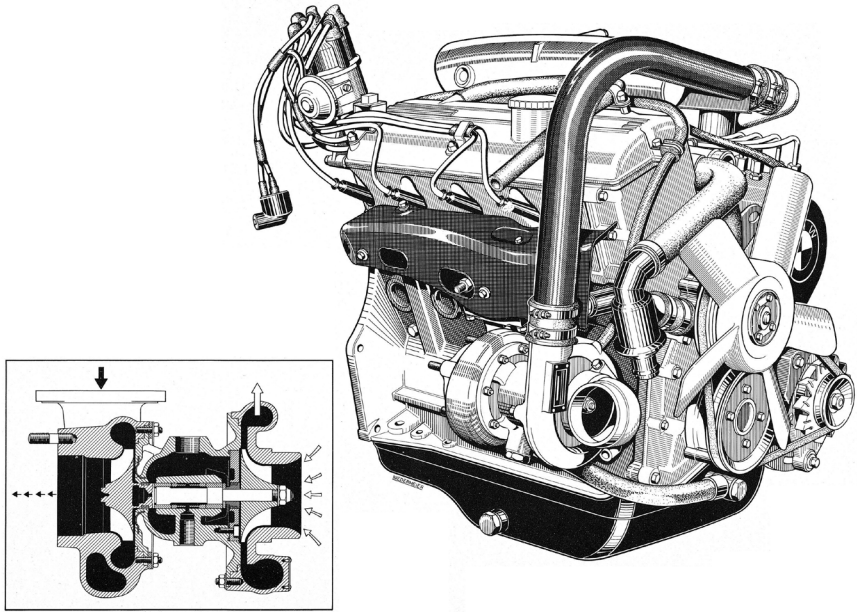
is remarkable that many of the features we now associate with turbocharged engines and their fuels were adopted in the so-called 'Halford Special' engine over 85 years ago.

The Halford Special engine, understandably, initially suffered from under-development of the turbocharger which was eventually replaced in this application by a Roots-type supercharger.² Although both Bristol and Rolls-Royce worked on developmental early turbocharged engines around the 1920s, their production aircraft engines were supercharged. Mercedes built the first supercharged production vehicles during this decade. Production turbocharger applications were first seen in diesel engines powering ships in 1925 [8] and in the 1930s turbochargers with axial turbines were used in marine, rail and large stationary applications and the first production aero engines appeared in a version of the Allison V-1710 in 1938.

Although trucks with turbocharged diesel engines started to appear in the 1950s, and Fred Agabashian took pole position at the Indianapolis 500 race in a car fitted with a 6.6 litre turbocharged Cummins diesel engine in 1952 [3], it was not until 1962 that the production car with a turbocharged engine appeared in the form of the Oldsmobile Cutlass Jetfire, closely followed by the Chevrolet Corvair Monza Spyder. These vehicles were fitted with turbocharged 3.5 litre V8 and 2.7 litre flat-6 gasoline engines respectively but production of the engines was abandoned after only a few years. Offenhauser turbocharged engines appeared at Indianapolis 500 in 1966 and won the race in 1968 [3]. Following this, BMW and Porsche were inspired to start developing their own turbocharged racing engines, culminating in the 1100 bhp Porsche 917s of 1973.

Following this racing background the resurgence in turbocharged automotive engines was led by BMW in 1973 with the 2002 Turbo (see Fig. 3.2), followed by Porsche with the 911 Turbo in 1974. Some of these early engines exhibited significant levels of 'turbo lag' (i.e. a significant delay in the demand for air at the throttle pedal and it being delivered to the engine by the charging system). This phenomenon was largely due to the fact that many of these early engines employed a 'floating' turbocharger. In such a turbocharger the turbine is sized to provide sufficient power to drive the compressor at maximum air flow conditions only, and there was no way of providing excess power to increase the boost pressure above the floating level at lower mass flows. This issue was, in large part, addressed by the invention by Saab of the 'wastegate', which is a controlled bypass around the turbine to allow some exhaust gas enthalpy to be intentionally 'wasted', so permitting the aerodynamic contraction of the turbine to enable

² The Roots 'blower' or supercharger was originally patented in 1860 by Philander and Frances Roots as a machine to help ventilate mine shafts.



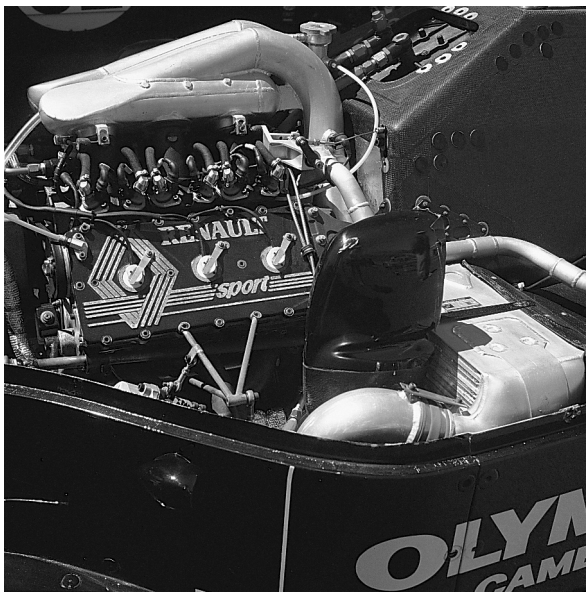
3.2 BMW 2002 tii turbo engine with floating (non-wastegated) turbocharger (courtesy BMW AG).

it to be made to provide a higher expansion ratio at lower mass flow rates. A significant reduction in the inertia of the turbine, which contributes the most significant portion of the assembly inertia, is also possible and the combined effects allow the engine to be brought on boost with much less delay [9]. The disadvantage of adopting this technology is that the turbine stage then provides a higher back-pressure on the cylinders at high engine power, which inhibits scavenging and increases pumping losses (both to the detriment of fuel consumption). However, the driveability improvements were considered worthwhile, and the wastegated turbocharger has become nearly universal. This subject will be returned to later. With the provision of adequate driveability, the application of turbocharging became more widespread with manufacturers such as Alfa Romeo, Audi, Buick, Ford, Lotus, Maserati (with the first 'bi-turbo'), Mazda, Mitsubishi, Nissan, Pontiac, Renault, Toyota and Volvo becoming associated with it in the late 1970s and early 1980s [10]. The first automotive turbodiesel was introduced in 1978 with the Mercedes-Benz 300SD and today virtually all automotive diesel engines are turbocharged.

This plethora of automotive applications was in part catalysed by the beginning of the 'turbo era' in Formula 1, which was led by Renault introducing their 1.5 litre turbocharged V6 to compete with 3.0 litre naturally

aspirated engines [11]. An application of the Renault Formula 1 turbocharged engine, fitted to a Lotus 97T, is shown in Fig. 3.3. The inherent advantage of turbocharging in low-exhaust back-pressure applications such as racing cars and aircraft – that the absence of a full exhaust system means that the pre-turbine pressure is low – could then be fully exploited and very rapidly nearly all of the Formula 1 grid turned to turbocharging. Driveability again became an issue because of the sheer levels of boost pressure being applied: in excess of 4 bar boost pressure above ambient was not uncommon [11]. This in turn led to the research and development of mitigating technologies including compound charging [12], which has only just begun to be applied to road vehicles [13]. Turbocharged rally cars followed from the introduction of the technology in the wider automotive field and Audi, with the Quattro, were the first to enter a turbocharged car in the FIA world championship. They were soon followed by Peugeot, Lancia and others.

With the banning of turbocharging in Formula 1 for the 1989 season there was a general retreat from the technology for automotive applications, largely because it was associated with driveability and fuel consumption issues (arising from the need to use an exhaust system with proper silencing and latterly exhaust gas catalysis). While modern ‘torque-based’ engine management systems and supporting technologies such as camshaft phasing devices have permitted the successful development of downsized port fuel injected (PFI) engines with excellent driveability, it is with the advent of



3.3 Renault turbocharged V6 Formula 1 engine fitted to a Lotus 97T racing car (courtesy William Taylor/Coterie Press Ltd).

direct injection that turbocharging has truly become a fuel consumption improvement technology.

3.3 Problems and challenges associated with turbocharging the spark-ignition (SI) engine

In this section the particular problems associated with turbocharging port fuel injected (PFI) SI engines versus their naturally aspirated (NA) counterparts are discussed as a backdrop to the synergy of the technology with direct fuel injection, which will be discussed later in the chapter. The problems fall into several different categories, chief amongst which are considered to be:

- Mechanical loading
- Thermal loading
- Turbocharger lag
- Knock and abnormal combustion
- Emissions.

This section will discuss these issues with particular reference to the current engine downsizing trend.

3.3.1 Mechanical loading

A good, naturally aspirated road engine will develop a maximum brake mean effective pressure (BMEP) in the region of 12–13 bar.³ Exceptional engines such as the BMW 3.25 litre in-line 6-cylinder from the E46 M3 produce up to 14 bar BMEP. Some motorcycle engines and true racing engines with low gas exchange pressure losses and heavily optimised gas dynamics may achieve higher levels [14].

Peak cylinder pressure for road-going turbocharged engines will be in the region of 75–85 bar. This peak pressure clearly has to be contained by the engine structure with a safety factor such that the integrity of the engine is maintained over its design life. Principally this demands that the scantlings of the engine be of sufficient section to contain the forces developed in the combustion chamber, which are a product of pressure and surface area. Piston area therefore affects bearing loads and the loads applied to the cylinder head bolts, whose function it is to resist the cylinder head lifting off the cylinder block and consequent loss of pressure in the combustion chamber.

³ BMEP is defined to be the pressure which, if applied over a single stroke of the engine cycle, produces work equivalent to that of the entire cycle. As a consequence of this, for the same swept volume, a 2-stroke engine only has to operate at half the BMEP of a 4-stroke engine to generate the same torque.

The skull of the combustion chamber also has to be sufficiently stiff to resist deformation, which can permit valve seat leakage and consequent burning-through of the valves.⁴

Because of the increase in cylinder loading in a pressure-charged engine all of these components need to be optimized. Turbocharging a road engine can result in BMEP levels in excess of 20 bar [15, 16], and in the region of 30 bar is being discussed as a future possibility by some researchers [17, 18], with further complementary measures (such as cooled exhaust gas recirculation, (EGR) being developed to achieve this level of output, which will be discussed in more detail in later chapters. (Note that in the era of turbocharged engines in Formula 1, BMEP levels in excess of 55 bar were produced [19].)

Turbocharging an existing naturally aspirated engine usually requires specification changes to bearings, cylinder block and head castings, cylinder head bolts, etc., and the cylinder head gasket may also be strengthened (usually with the addition of more layers in the modern multi-layer steel type). Connecting rods, pistons and crankshaft may undergo significant modification, particularly (in the case of pistons and rods) to provide a reduction in compression ratio, the reasons for which will be returned to in Section 3.3.4. Valves may be dimensionally changed if their deflection becomes problematic. Any strengthening of the combustion chamber skull by thickening it provides a barrier to rapid warm-up, and so must be balanced against material specification changes. The top land of the piston often has to be increased in height due to increases in both mechanical and thermal loading, and this can effect emissions (as discussed later in Section 3.3.5). High thermal loadings provide their own unique challenges, as discussed in the next section. Although these seem fairly sweeping changes, it must be remembered that there are still cost benefits to the manufacturer, because a turbocharged variant of an existing engine design can usually be developed relatively cheaply and built on existing production lines, which is unlikely to be the case were a different engine design to be newly developed to provide the same power output in any given vehicle.

3.3.2 Thermal loading

The increase in thermal load due to operating an engine under boosted conditions is primarily a result of the increase in charge mass flow rate

⁴The general architecture described in this chapter will relate to poppet-valve reciprocating engines. This is because, although it is accepted that other types of 4-stroke SI engine such as sleeve-valve and Wankel engines have been successfully developed, the poppet-valve engine is nearly completely universal in the light-duty automotive field.

through the engine. The combustion of this increased charge mass directly transfers more heat to the engine structure which must then be removed by the oil and cooling systems. Furthermore, the reduced compression – and hence expansion – ratio and retarded combustion phasing also result in considerably more heat energy being left in the exhaust gas at the end of the expansion phase.

The charging system itself contributes to an increase in thermal load. Work carried out in the compression of the charge air increases its temperature, a situation which is normally addressed in the interests of combustion efficiency and enabling increased charge density for a given boost pressure by the provision of an aftercooler (also known as an inter- or chargecooler⁵). This is returned to in Section 3.3.4 below. Nevertheless, since the charge air cannot be cooled to atmospheric conditions in such a device, the intake air must necessarily be at a higher temperature than that in an equivalently powerful, naturally aspirated engine. The heat rejected by the intercooler itself also has to be accommodated by the vehicle cooling pack, which in turn might re-balance the radiator thermal load.

The increased back-pressure created by the turbine in providing the expansion ratio to create the power to drive the compressor also increases the heat flux into the coolant and the engine structure in general. Pre-turbine temperatures are now approaching 1050°C in SI turbocharged engines, meaning that conventional uncooled exhaust manifolds conduct a significant amount of heat back into the cylinder head via their studs and gaskets. Any increase in exhaust back-pressure (EBP) in the vehicle exhaust system as a result of packaging, exhaust gas after-treatment or silencing will create a compounding effect; this can be further exacerbated by its effect on combustion (again, see below).

Under running conditions, the turbocharger is mainly cooled by the oil flowing through it, which also raises the thermal load on the lubrication sub-system. (Water-cooled bearing housings are universal on SI engine turbochargers, but the main reason for their provision is to ‘thermosyphon’ coolant through the bearing housing on engine shutdown to remove bearing heat and prevent cracking of the oil retained in the bearing itself.) Furthermore, the oil also performs an important function in cooling the piston, which may necessitate the provision of oil squirt jets targeting the underside of the piston crown.

All of these increases in thermal load need to be taken into account, and their effect on the mechanical strength of the engine considered as well. For this reason it is desirable to conduct full coupled thermal and physical

⁵ Strictly the term intercooling refers to cooling between compression stages in aerospace propulsion, but the distinction is not normally drawn in automotive applications.

models of turbocharged engine conversions, particularly with regard to main bearing panels, cylinder head integrity and cylinder block distortion.

3.3.3 Turbocharger lag

The delay in response between a demand for a load change and it being delivered can be very noticeable in turbocharged engines and is referred to as turbocharger lag (or more commonly ‘turbo lag’). It is a function of many factors and is being addressed in a number of ways.

Any discussion of turbo lag needs to be conducted in the context of what occurs in both naturally aspirated and supercharged engines. In a naturally aspirated engine with conventional throttle placement, i.e. upstream of the plenum entry, a load step has to increase the density of the air in the plenum to close to that of the ambient via filling it with fresh air, and the volume of the plenum consequently effects the driveability of the engine. In engines with fixed valve timing and significant valve overlap, the plenum will contain a high proportion of exhaust gas at part load due to the low pressure level relative to the exhaust system, and a load step may therefore cause a slight stumble. This being the case, it is not unusual to instead specify smaller throttles in the intake port of each cylinder to minimize the throttled volume and so alleviate the exhaust gas carryover effect. This is common in high-performance engines.

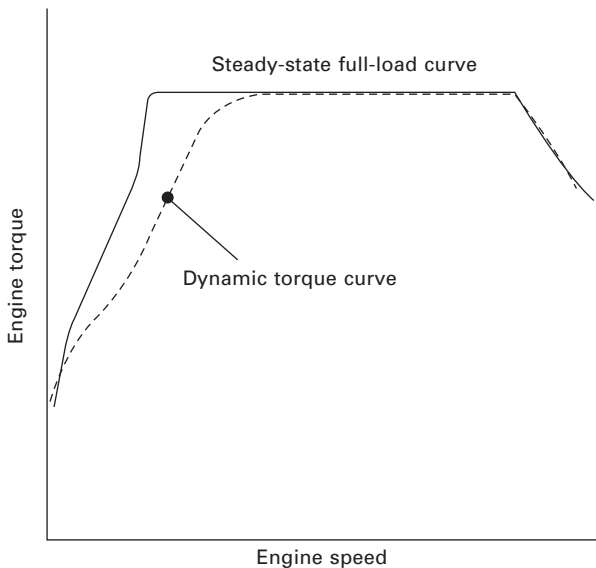
Supercharged engines also suffer lag. In a typical positive-displacement supercharger application (such as a Roots- or Lysholm-type) the throttle is conventionally upstream of the supercharger. This means that a load step has to provide enough air to pressurize the entire intake system volume (including the intercooler) before the change in engine load is sensed. Furthermore, in the case of high boost supercharging, such a load step demands a significant instantaneous input in work into the supercharger, which is taken from the crankshaft. Hence, a stumble can manifest itself in such engines, too, which can be increased if the supercharger is clutched (and bypassed) and possesses significant inertia (compounded by the gearing of the supercharger relative to the crankshaft).

The turbocharged engine suffers from lag due to various elements of the above and to additional factors. Its general throttling is similar to that of the naturally aspirated engine insofar as throttling at the plenum entry and downstream of the compressor outlet is the norm (although port throttles might equally well be used). This mismatch in the supply and demand of boost pressure is possible compared with a supercharged engine because the turbocharger shaft is independent of the crankshaft, and hence its pressure ratio and mass flow can vary because there is no mechanical link between the two. There is therefore an initial response to a load step which is the basic naturally aspirated response of the engine (modified by the restriction

of the extra components in the intake system such as any intercooler fitted). Once this naturally aspirated level has been reached the lag is a result of the aerodynamic characteristics of the compressor and turbine (and how they interact with the positive-displacement reciprocating engine and its valve timing) and the inertia of the turbocharger wheel assembly, which is dominated by that of the turbine wheel (or exducer).

Figure 3.4 indicates the difference between the full-load steady-state torque curve and the torque generated transiently as a vehicle is launched. At very low engine speeds a low level of boost is produced and the performance is essentially that of a naturally aspirated (NA) engine operating at part-load. When the throttle is opened the engine very quickly reaches the full-load NA level. The two curves then diverge as the dynamics of the charging system prevent the engine from reaching the steady-state curve. Because the engine is wastegated the two curves converge again because the steady-state curve is artificially capped.

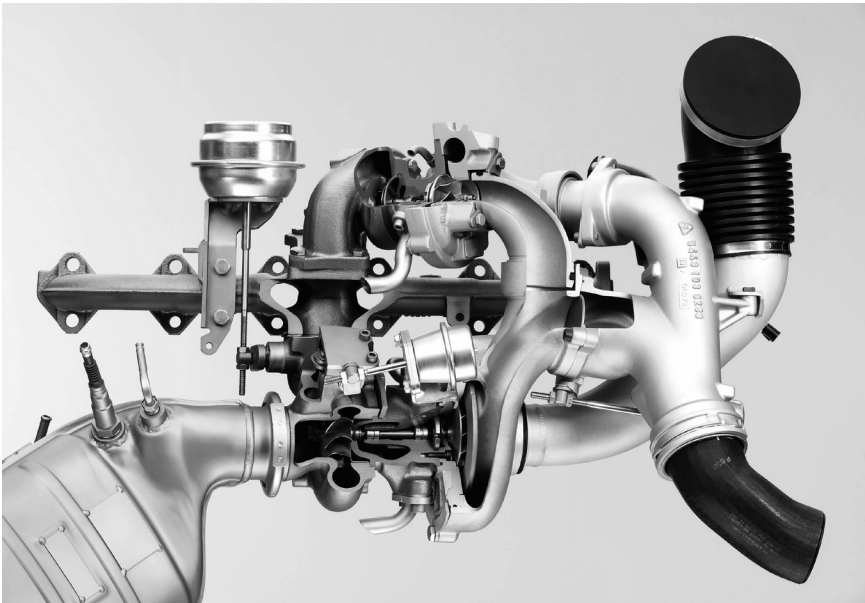
Consequently, there is some advantage in not specifying an engine with a requirement for a very high boost pressure to be provided by a single compression stage, and this pragmatic approach is one means of mitigating turbo lag [16]. If, however, high pressure ratios are required, compound charging becomes more attractive. In a compound-charged engine, at least two distinct compressor stages work in a complementary manner to provide sufficient air to the engine across its full speed and load range. These systems usually take the form of a turbocharger coupled with (a) a positive



3.4 Turbocharged engine transient and steady-state torque curves.

displacement compressor [13, 15], (b) an aerodynamic compressor [12] or (c) another turbocharger compressor. This last configuration can have the compressors configured in either sequential [18] or parallel [20] configurations. The ‘regulated two-stage’ approach was successfully demonstrated by Volvo in a methanol-burning engine in 1990 [21] and has more recently been successfully developed for production diesel engines [22, 23], whereas to date in SI engines the parallel configuration has most commonly been used in production [20]. The BMW diesel configuration is shown in Fig. 3.5. In any road-biased systems the aim is to provide improved driveability with better high-speed fuel consumption by rematching of the turbine stage as a consequence of the reduced need for it to provide all the driveability necessary [15]. Thus, the supercharger, or small ‘high-pressure’ turbocharger, provides the boost at low engine speeds, and a larger than usual, lower expansion ratio turbine drives the main compressor, providing the bulk of the boost at higher engine speeds and loads. Given its success in light-duty diesel production applications, it is expected that the regulated two-stage approach will be adopted for production gasoline engines at some point in the future.

In a historical context, the driveability of single-stage turbocharged engines has improved significantly over the years through a combination of engine control system development, the application of torque-based engine control, and improved understanding of the gas dynamics of all the devices in the charge



3.5 BMW ‘regulated 2-stage’ turbocharging system from the BMW 535d. (courtesy: BMW AG).

air path as well as the significant improvement in turbocharger technology. Over the same period of time, naturally aspirated engine performance has been improving due to widespread adoption of camshaft phasing devices. Such devices can also be applied to turbocharged engines and used to shift the operating point in the compressor map and so increase mass flow (with its beneficial effect on turbine work).

A further important operational benefit of using camshaft phasing devices is that the valve overlap can be reduced at part load, thereby minimizing the amount of trapped residual gas in the cylinder. The overlap can be increased as the boost pressure builds up, so that the engine scavenging and turbine mass flow rate benefit from the positive pressure differential across the engine, cooling the combustion chamber surfaces directly. However, with port fuel injection this would result in significantly increased amounts of unburned charge flowing into the exhaust manifold with its consequent combustion and overheating of exhaust system components. Hence camshaft phasing has not been applied as readily to turbocharged engines. With the advent of direct injection systems, however, there is now a means to prevent the introduction of fuel into the air until after the exhaust valve has closed and hence to provide a means to influence engine operation by compressor map shifting and to improve driveability further. The benefits of this will be returned to in Section 3.4 below.

3.3.4 Knock and abnormal combustion

Engine knock is the unintentional autoignition of the last part of the charge before the conventional flame front can consume it [24]. The autoignition results in pressure waves traversing the combustion chamber at very high speed, which excite the engine structure and create the characteristic sound which gives knock its name [25]. It is important to note that knock is the destructive manifestation of autoignition, and that it is possible to have autoignition occurring without destructive knock, as is the case in homogeneous charge compression ignition (HCCI) combustion systems. In conventional spark-ignited combustion, non-destructive autoignition can occur particularly in the case of side-valve engines and engines with large volumes of end gas such as the cooperative fuels research (CFR) fuels rating engine [26], but in the case of modern four-valve engines the maximum rate of energy release is usually such that knock is destructive, despite the minimization of end-gas volume in four-valve engines compared to older configurations.

As well as the mechanical overloading, knock results in an increase in heat transfer to the structure and consequent reduction in exhaust temperature. Piston surfaces and rings can suffer disproportionately due to the impact of pressure waves on the surface (which can lead to the plastic limit of the piston material being exceeded) and shock-induced ignition of charge in the

top ring land [27, 28]. If left unchecked it can destroy an engine in a matter of a few cycles.

Consequently, knock has been acknowledged to be a significant limit to engine performance since the dawn of the internal combustion engine [29]. Ricardo was the first to postulate the process by which knock occurs [30], providing a description of the process which still holds today, and which, with the benefit of many years' subsequent investigation, can be described as follows. Following ignition by the passage of the spark across the spark plug electrodes, there is a brief delay during which a flame kernel forms. Providing fluid motion does not extinguish the flame, once the temperature of the flame kernel reaches a critical point, rapid inflammation of the rest of the mixture begins and proceeds by the spreading of a deflagrating flame away from the spark plug. The time taken for the flame to break out of the kernel and into the bulk of the mixture is subject to cyclic irregularity and is one of the reasons why the first 5% of the mass fraction burned (MFB) is often disregarded in analysis of combustion statistics – indeed, 10–90% MFB is usually taken as an indicator of combustion duration (with 90% as the upper limit due to the related difficulty of establishing when all of the charge has been consumed).

Combustion of the charge within the flame front causes the gases behind it to heat up and consequently expand, both accelerating the flame front's passage in spatial terms and compressing the unburned gas ahead of the flame. This 'end gas' is also heated by radiation and so, due to both processes, increases in temperature and pressure before the flame reaches it. Whilst these processes are occurring, the end gas rejects some of its heat energy to the engine structure [31], which also influences the temperature and pressure histories that it undergoes.

The end gas temperature and pressure histories (which are also modified by piston motion and surface temperature effects) cause the occurrence of low-temperature chemistry in the fuel as a form of pre-flame reaction. This can assist in facilitating the passage of the flame but equally, as it is being heated by all of the events occurring in the chamber, the end gas will autoignite if and when the Livengood–Wu integral equation

$$\int \frac{1}{\tau} dt = 1 \quad 3.1$$

is satisfied [32]. The parameter τ in this case is the Livengood–Wu induction time representing the autoignition delay time at the instantaneous temperature and pressure of the mixture, and is defined by an Arrhenius rate equation of the form

$$\tau = Ap^{-n} \exp\left[\frac{B}{T}\right] \quad 3.2$$

where A , n and B are constants which vary for different fuels at different conditions in different engines. If the combustion is completed before equation 3.1 is satisfied then autoignition is avoided. If autoignition occurs and if in-cylinder conditions are correct, a flame front can then traverse the remaining end gas at 10–20 times the normal flame speed, in turn causing molecular vibration and bulk excitation of the engine structure [27, 33, 34].

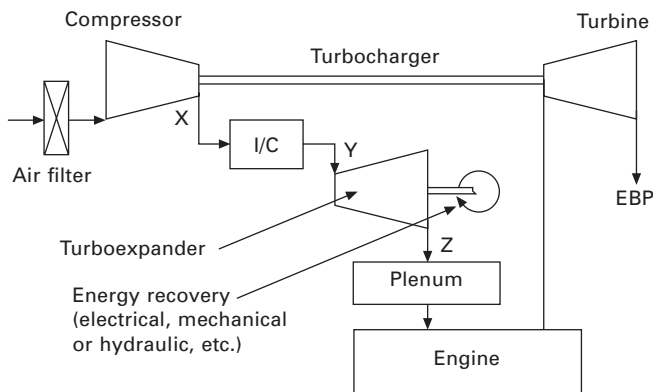
The local temperature gradient which can be promoted as a result of exothermic centres (arising either from the surface or from within the charge itself due to pockets of hot retained burned gas) is important with respect to the severity of the autoignition event if it occurs [35–37]. Up to five different types of flame propagation have been identified [37], but in general if the thermal gradient in the end gas is high (>100 K/mm) a deflagrating flame ensues, if it is low (<1.25 K/mm) a thermal explosion occurs, and if it is of a medium value (~ 12.5 K/mm) then there is a developing detonation. The thermal explosion case is that which is actually aimed for in homogeneous charge compression ignition (HCCI) engines, since it implies a softer autoignition than a knock event; however the processes involved in knock and HCCI, while related, are different. In SI combustion, the developing detonation case is that which leads to destructive knock [38], which will occur only if sufficient end gas has not been consumed by the flame front. Given that the flame front cannot consume the exothermic centres before they reach autoignition, the higher the proportion of charge in the end gas involved in the autoignition event, the more severe the knock amplitude and the more likely the danger of structural damage [38]. The margin for control also reduces as the amount of charge involved in the knock event increases [38].

From the foregoing it is apparent that, unless the flame front can consume any exothermic centres, thermal energy input to the charge is extremely important with regard to the likelihood and severity of any knock event as it controls the evolution of the autoignition integral. When operating on any given fuel, the turbocharged SI engine is at an immediate disadvantage in comparison to its naturally aspirated counterpart for several reasons: all of the thermal issues discussed in Section 3.3.2 affect end gas temperature, and the increase in pressure due to the boost applied affects the temperature and pressure histories too. It must also be remembered in the context of knock in general that the high trapped mass (and therefore heat released per cycle) in a turbocharged engine at full load increases the severity of any knock event significantly over that which would occur in a naturally aspirated engine of the same swept volume.

As a consequence of the above, the knock limit is lower in pressure-charged engines than in naturally aspirated ones, so that often the compression ratio of the engine needs to be reduced and the engine needs to be operated with retarded ignition timing or under ‘over-fuelled’ conditions (to make

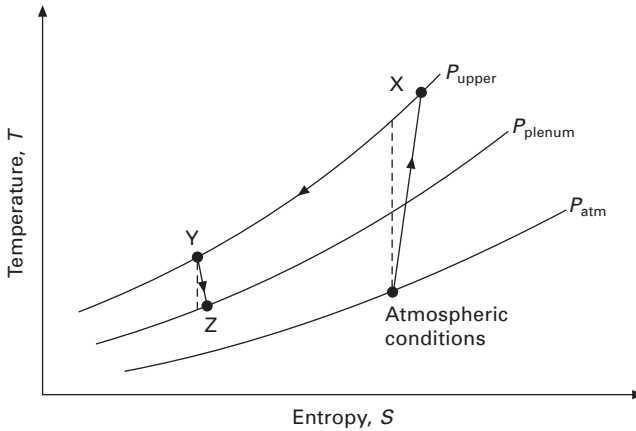
combustion less efficient and hence to cause less end gas heating to occur).⁶ Under conditions of adverse pressure gradient across the valves, when the pressure at the exhaust valves during the valve overlap period exceeds that at the intake valves, a reduction in compression ratio necessarily increases the mass of residual gas in the chamber. This then causes the knock limit to contract further, both because of any active species present and because of the thermal effect (both global and local if the residual gases are not well mixed, causing the hot spot effects discussed above). Various technologies have been investigated to mitigate this effect in PFI turbocharged engines, including turboexpansion [39–42] and the use of a divided exhaust period [43].

Turboexpansion seeks to use over-compression of the charge air to drive an intake expander which further removes heat energy from the charge, and so to provide a cooler charge to the engine. Between the compressor and expander stages charge-air cooling occurs at the elevated pressure condition. The combined process has the potential to provide a given charge-air density at a lower temperature than that of a conventional intercooling process alone. A schematic of the charge-air cycle is shown in Figs 3.6 and 3.7; this cycle is a form of air refrigeration and has also been used for aircraft air-conditioning systems. Turner *et al.* [40] found that, in a newly specified and designed test engine [44], the combustion benefits of turboexpansion were difficult

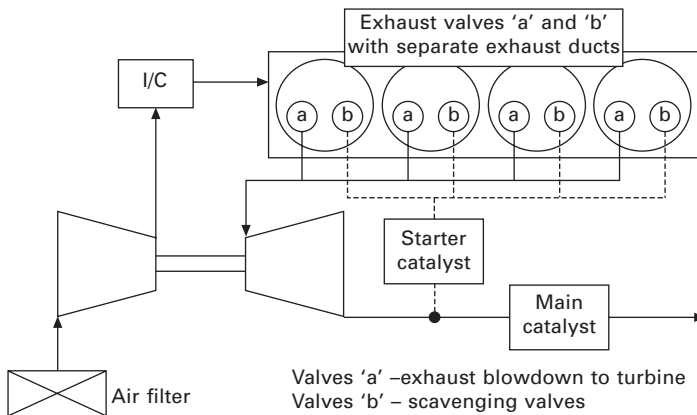


3.6 Schematic of one possible turboexpansion system for a turbocharged engine. I/C = charge-air intercooler; EBP = exhaust back pressure; X, Y and Z refer to states in the temperature–entropy diagram shown in Fig. 3.7.

⁶ While over-fuelling is also sometimes used to reduce gas temperatures to control component temperatures, retarding the ignition works counter to this aim with regard to components in the exhaust gas path.



3.7 Temperature–entropy diagram for the turboexpansion charging system shown schematically in Fig. 3.6.



3.8 Schematic of divided exhaust period system for turbocharged engines. I/C = charge-air intercooler. Adapted from Moller *et al.* [43].

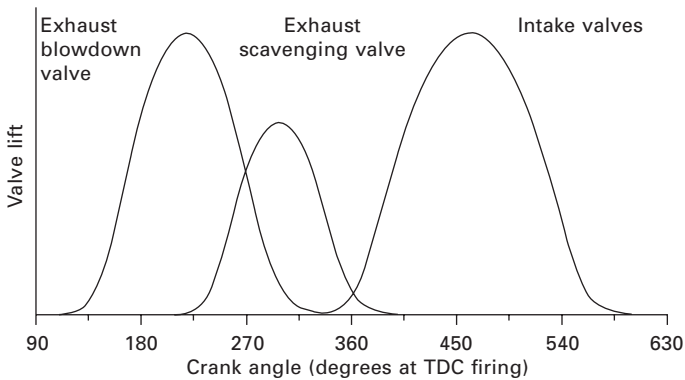
to realize because of the interactions between the different components in the charging system (further investigated by Taitt *et al.* [41]), though more fundamental combustion research is ongoing to assess its attractiveness.

The concept of ‘divided exhaust period’ (see the schematic shown in Fig. 3.8) divides the flow from the two exhaust valves in an engine and sends the first ‘blowdown’ pulse from the cylinder directly to the turbocharger turbine through a dedicated exhaust valve (‘a’ in Fig. 3.8) before closing that valve early and opening the second exhaust valve (‘b’) to perform final scavenging at an elevated pressure differential from intake to exhaust during the overlap period [43]. As a consequence of this, both of the staggered exhaust valve

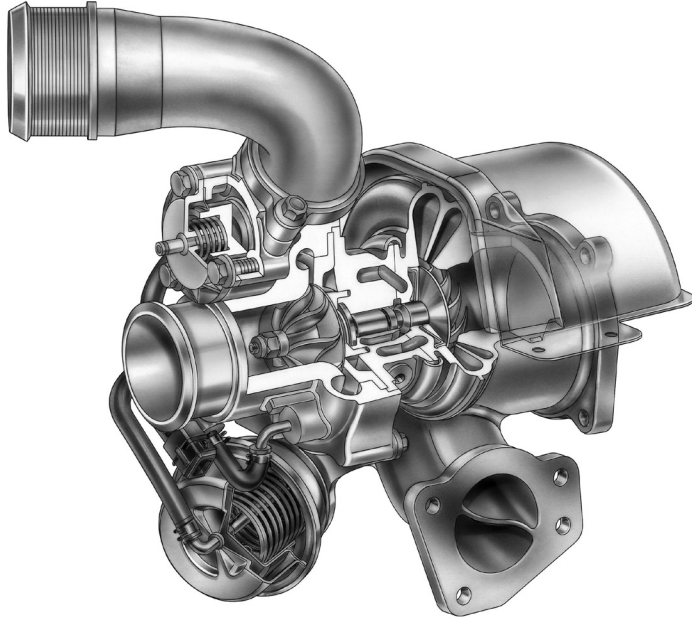
events are less than 180° long, and there is no pulse interaction between the cylinders, though the amount of valve time–area available to flow the burnt gas from the cylinder is necessarily reduced. An additional benefit is that the high pre-turbine pressure caused by using a small turbine would not have a detrimental effect on the scavenging efficiency of the engine, because the cylinder is not exposed to this pressure in the valve overlap period. Consequently it is possible to achieve a positive pressure gradient across the cylinder during the valve overlap period higher up in the engine speed range. By fitting a valve deactivation system to the blowdown valves, the turbine can be bypassed at startup and a starter catalyst used to improve emissions performance (see next section). An illustration of the valve events used in this concept is shown in Fig. 3.9.

A more pragmatic solution to exhaust pulse interaction in many pressure-charged engines is to divide the exhaust system itself and to use two separate entries to the turbocharger turbine. For example, in a 4-cylinder engine with a firing order of 1-3-4-2, if cylinders 1 and 4 are paired together separately to 2 and 3, the blowdown pulses are separated from the next cylinder in the firing order. An example of a pulse-divided turbocharger is shown in Fig. 3.10 and the general concept is shown in Fig. 3.11. The concept was discussed by Groff *et al.* [45], although Andriesse *et al.* [46] presented a slightly contradictory view, stating that with a 4-into-1 manifold connected to a single turbine housing, oxidation of carbon monoxide in the exhaust system before the turbine adds to the enthalpy available to drive it. This subject will be returned to in Section 3.4.3, and the general subject of architecture and turbocharged engines in Section 3.6.

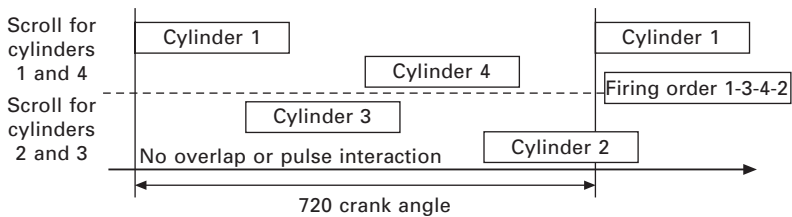
In conventional turbocharged engines employing no technology specifically to mitigate the thermal and chemical issues of residuals trapped in the gas



3.9 Representation of valve events used in the divided exhaust period system for turbocharged engines. Adapted from Moller *et al.* [43].



3.10 Pulse-divided turbocharger: note dividing wall cast into housing to maintain separation of exhaust gases through the volute and up to turbine wheel entry (courtesy General Motors).



3.11 Concept of pulse division in turbocharged engines (even-firing 4-cylinder configuration).

exchange process, retarding the ignition is often employed and is a very powerful control on knock. This approach results in a later-phased combustion event which changes the phase of combustion heat release versus piston position and reduces work output. Importantly it also results in an increase in gas temperature at the exhaust valve opening point and thus increases the thermal input to the engine structure. Overfuelling is also sometimes applied to counter knock and to control component temperatures, both in the combustion chamber and of components in the exhaust bath. Reducing compression ratio is another palliative which works by decreasing the

combustion efficiency to reduce the heat release rate. However, when these approaches are considered together, a destructive spiral ensues, which is at the heart of why PFI turbocharged engines historically have worse fuel consumption than naturally aspirated ones.

To illustrate one way out of this spiral, consider a turbocharged PFI racing engine versus its road-going cousin. In the racing engine, assume that the exhaust back-pressure can be removed significantly because the presence of the turbine provides nearly all of the silencing required for racing, and that a racing catalyst (with low cell density and hence pressure loss) is used. In this case the product of turbine expansion ratio and overall exhaust system back-pressure is significantly lower than in the road-going unit. As a consequence, for a given limiting temperature, either the boost or the compression ratio could be increased, and the ignition timing perhaps advanced, lowering the temperature at exhaust valve opening, and in turn permitting less fuel enrichment to be used to the benefit of fuel consumption and power output. This example is laid out in order to show how a significant improvement in one area of the engine–turbocharger system leads to a significant rebalancing of the whole, and the concept will be returned to in the discussion of the benefits of direct injection in SI turbocharged engines in Section 3.4 below.

3.3.5 Impact of turbocharging on pollutant emissions

The addition of a charging system and consequent respecification of the engine can have both positive and negative effects on its emissions performance. Of immediate interest following startup from cold is the thermal inertia of the exhaust manifold and turbocharger system, since this removes heat energy from the exhaust gas before it reaches the catalyst and hence can adversely affect catalyst light-off (i.e., the point at which meaningful conversion of pollutants takes place). However, in a downsized engine which must necessarily work at higher BMEPs in the drive cycle, the unit heat energy in the exhaust gas stream will necessarily be higher.

Unburned hydrocarbon (UHC) emissions are known to increase with increasing crevice volumes, particularly the top compression ring. Higher cylinder pressures and increased top ring-land volume lead to a greater mass of UHC being trapped, the partially combusted products of which then flow back into the cylinder gas as expansion occurs and thence into the exhaust; this also occurs for oxides of nitrogen (NO_x) [47]. At higher loads this can be a problem because nitric oxide (NO) is known to adversely affect the knock limit [48, 49]. In mitigation of these issues must be set the fact that downsizing (and, if applicable, reducing the number of cylinders) can obviously reduce the total crevice volume. The reduced compression ratio common in turbocharged engines, while reducing the mass of UHC forced

into the crevice volumes, also reduces combustion efficiency and this can increase carbon monoxide output, particularly at light load. On the beneficial side, the reduced temperatures associated with the reduced compression ratio also reduce the likelihood of NO_x formation.

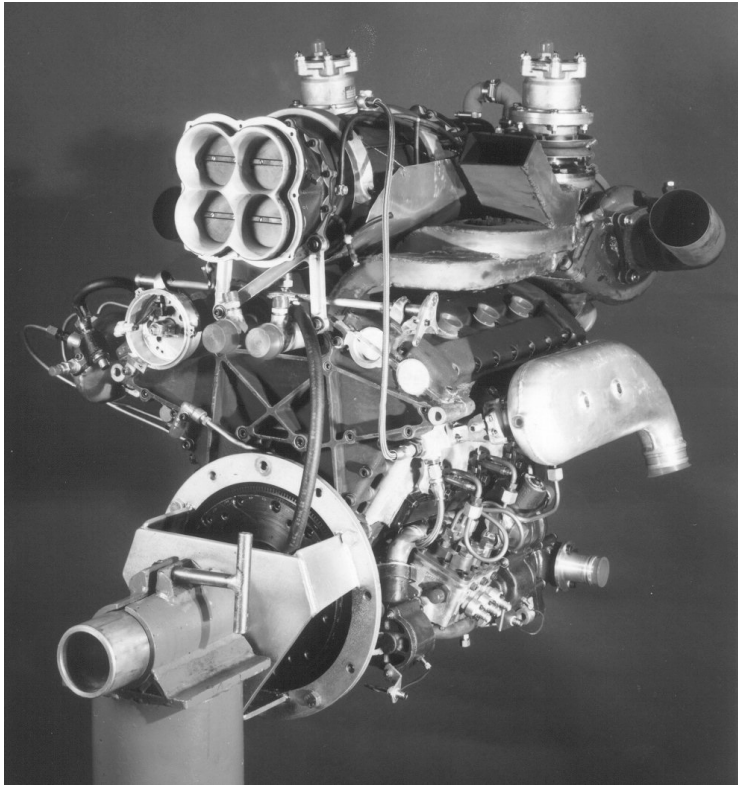
The conclusion to be drawn from this is that emissions from the engine combustion system are affected in different ways by turbocharging. However, the major impact is due to the thermal inertia of the exhaust manifold and hence any means which can improve emissions output and/or speed up the catalyst light-off point will be of particular benefit in turbocharged engines. This will be returned to in Section 3.4.5.

Having set out the major problems and challenges surrounding turbocharging the SI engine, and how these are further affected if the intention is to downsize a vehicle engine in the interest of fuel economy, the remainder of this chapter will be concerned with the combination of turbocharging technology with direct injection in SI engines. In particular the benefits that direct injection brings to such engines will be illustrated with reference to the disadvantages of turbocharging PFI engines outlined above.

3.4 Advantages of combining direct injection and turbocharging in spark-ignition (SI) engines

The combination of direct fuel injection and turbocharging in spark-ignition engines is not a new one. The direct injection Daimler-Benz DB601 inverted-V12 aero engine was used for tests with a turbocharger system in place of its more normal supercharger during the period 1939–45 [50]. At least one such direct injection Formula 1 engine was built and developed during the so-called ‘Turbo Era’ of the 1980s [12], as illustrated in Fig. 3.12. However, these early examples had, by necessity, to operate with bespoke injection equipment and, for mass-production automotive engine applications, it would take both the involvement of the ‘Tier-1’ suppliers to the industry and the development of the necessary electronic control systems to make the concept of direct injection a reality in road cars.

The early application of direct injection (DI) in road engines was targeted at achieving a stratified air–fuel mixture at part load to reduce fuel consumption primarily to de-throttle the engine by operating it lean [51]. However, the injection equipment available to developers of these so-called ‘first generation’ DI engines operated at relatively low fuel pressures, with consequent limitations on injection timing due to the limited fuel flow rates available. The nozzle systems were also at an early stage of development, with ‘pressure-swirl’ configurations being the norm. This, coupled with the reconfiguration of the engine to provide the reverse tumble found to be necessary to achieve the required fuel–air distribution and mixing, and coupled with the NO_x control issues associated with lean operation [24],



3.12 Turbocharged direct injection engine with compound charging built to Formula 1 regulations in the mid-1980s (courtesy Lotus Engineering).

meant that these early ‘wall-guided’ stratified combustion systems never fulfilled their desired potential and hence did not significantly penetrate the market; indeed, Mitsubishi was the only manufacturer to offer such engines for general sale, and they have now been withdrawn from the market.

The next development was ‘air-guided’ systems, typified by the VW/Audi Group’s FSI system (also considered to be of the first generation of direct injection combustion systems) [52]. Here, a more conventionally configured side intake port was utilized with the injector positioned underneath it. Tumble control was provided by a horizontally split intake port fitted with an engine control unit (ECU) controlled ‘tumble flap’ in the lower portion; closing this flap reduced flow area and increased the charge tumble motion in the cylinder. The system provided for much better fuel spray control in the cylinder and an improvement in the stratified benefit afforded by direct injection, and eschewed some of the problems of the high hydrocarbon levels experienced with the earlier wall-guided systems caused by the necessarily

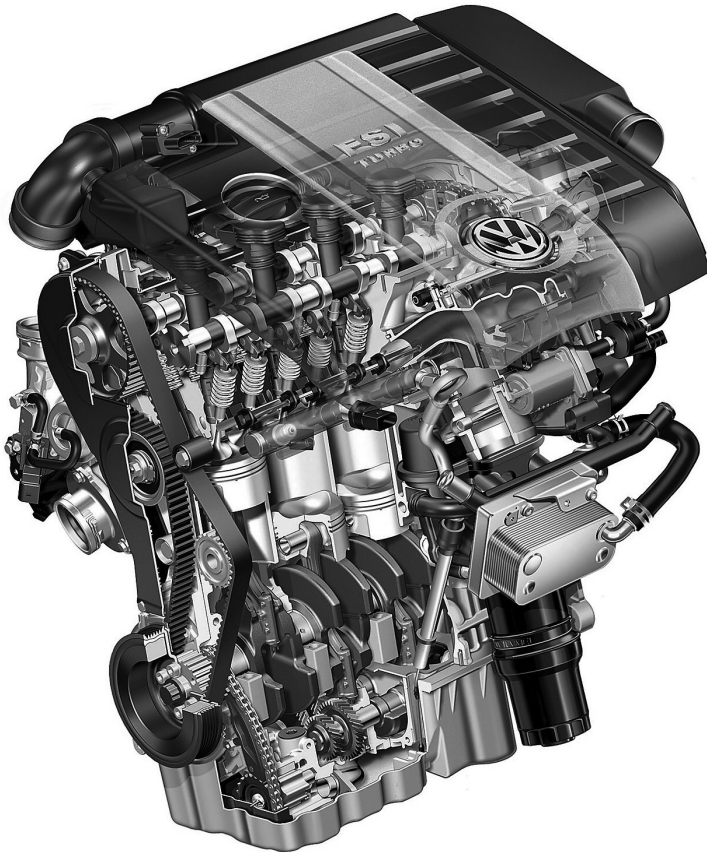
high degree of fuel impaction on the combustion chamber walls. A significant part of the benefit was to be found at cold engine startup; the fact that at this condition the catalyst was unlit (and so therefore could perform no feed gas conversion) permitted development of late-injection and late-ignition strategies which produced more heat at exhaust valve opening (EVO) and a consequent reduction in catalyst light-off time.

Having realized a more beneficial stratified DI combustion in the air-guided type, several manufacturers began marketing such engines. However, general NO_x control was always problematic, leading to complex calibration strategies, and with the enactment of ever more stringent exhaust emissions legislation such stratified engines began to be taken out of production. In their place engine downsizing was developed as a pragmatic means of circumventing throttling loss while at the same time permitting the use of cost-effective and robust three-way catalysis for exhaust emissions control. However, due to the investment in production equipment already made for the underport injector position and the extensive knowledge of the air and fuel interaction with this combustion system architecture, this layout has come to be seen as the norm. The subject of injector placement, and new 'second generation' DI configurations with the injector positioned more centrally and close to the spark plug, will be returned to in Section 3.6.

In the context of DI engines, further engine downsizing was made possible by realization of the synergies between DI and turbocharging in early studies [53–55], and an illustration of the first production turbocharged direct injection spark-ignition (DISI) engine employing this combination, from VW-Audi, is shown in Fig. 3.13. This engine also employs variable tumble flaps for manipulation of in-cylinder air flow. The remainder of this section will discuss these synergies with reference to the particular problems associated with turbocharging the SI engine already outlined in Section 3.3.

3.4.1 Effect of direct injection on mechanical loading of turbocharged engines

The overall effect on mechanical loading in turbocharged engines if all of the advantages afforded by combination with direct injection are taken advantage of is to increase it. This is because the BMEP of the engine can be increased markedly due to the effective increase in knock resistance afforded by the direct injection of the fuel into the cylinder due to its evaporative effect and also because (at low speeds in particular) the introduction of fuel can be delayed until after the exhaust valves are shut. This, in combination with camshaft phasing devices on both intake and exhaust (a dual, continuously variable camshaft phasing or 'DCVCP' system), permits positive 'over-scavenging' or 'flushing' of the combustion chamber to force burnt gases out. Both of these phenomena will be discussed in more detail in Section 3.4.4



3.13 VW-Audi 2.0 litre T-FSI engine, the first production spark-ignition engine combining turbocharging and direct fuel injection. Note under-port injector positioning and variable tumble flaps in the intake ports (courtesy Volkswagen-Audi Group).

and are mentioned here solely to illustrate that the degree of downsizing that can be obtained in turbocharged DISI engines is significantly increased over their PFI counterparts.

The consequence of this is greater cylinder loading across the engine speed range, and in a turbocharged DISI engine measures must be taken to ensure that the base engine can operate reliably at higher BMEP and cylinder pressures. As a consequence of the significant gearing between DI and turbocharging (together with variable camshaft phasing devices) several researchers report the ability to operate engines at 30–35 bar BMEP levels, significantly above that achieved with current PFI engines [17, 18]. The use of alcohol fuels in such engines also promises to permit operation at high boost levels and optimized spark advance, which suggests that ability to

withstand peak cylinder pressures in the region of 120 bar or higher will be necessary [56]. At present, the spark retardation necessary when operating such engines on gasoline ensures that these very high levels of cylinder pressure cannot be achieved in practice, but with future engine technology and fuel development they may be approached even when operating on relatively low-octane regular gasoline. As a consequence, the structure has to be upgraded to be sufficiently robust, although, since light-duty diesel engines operate at pressures in excess of 180 bar, this is unlikely to be an insurmountable challenge.

3.4.2 Effect of direct injection on thermal loading of turbocharged engines

The combination of direct injection and turbocharging has contradictory effects on the engine in terms of its thermal loading. Firstly, the thermal load can be expected to increase in proportion to the increase in BMEP, as is the case for all engines. Since this is not unique to the technology combination, it will not be considered further here. Secondly, however, the use of DI can have a significant mitigating effect on thermal load, due to a variety of factors.

The evaporative effect of the fuel tends to improve the knock limit, which permits better phasing of the combustion event and the possibility of increasing the compression ratio [57]. Both of these effects in turn mean that the burned gas temperature at EVO is significantly reduced relative to a turbocharged PFI engine of similar rating, which in turn reduces turbine inlet temperature and so also reduces the requirement to overfuel the engine for component protection. Hence there is a significant improvement in fuel consumption at both low load (because of the increase in compression ratio) and high load (because of the reduction in the requirement for over-fuelling).

Furthermore, at high load at low to medium speeds, there is the ability to phase the valve timing to permit excess fresh air to scavenge the cylinder. This is made possible by the fact that the plenum pressure is higher than the pre-turbine pressure before the boost crossover point (i.e., the point at which pre-turbine pressure exceeds plenum pressure), permitting greater amounts of valve overlap because fuel introduction can be delayed until after exhaust valve closure. In this way, there is no means for unburned fuel to pass directly into the exhaust system to directly combust there and cause excessive thermal issues. Increasing valve overlap under these conditions therefore means that the air flow through the engine increases, in turn shifting the compressor operating point away from the surge line at low speeds and usually to a more efficient area in its operating map by increasing its air flow rate. This has important benefits for knock control in the engine, since the increased air flow through it also helps to cool the combustion chamber

directly (see Section 3.4.4). Further benefits of compressor map shifting are discussed in later sections.

3.4.3 Effect of direct injection on turbo lag

Very early in the application of direct fuel injection to SI turbocharged engines, it was noted that compressor map shifting, made possible by the use of camshaft phasing devices to increase overlap and hence scavenge air flow (enabled by the delay of introduction of fuel until after exhaust valve closing (EVC), permitted by the use of DI), leads to significant benefits in driveability through a reduction of turbo lag [58]. In the first instance, compressor map shifting implies a higher rotational speed for the turbocharger shaft at the start point, meaning that less energy is required to reach the new operating point demanded by a load step. For a sudden load step, the valve overlap is shut down and gradually opens up as boost comes in; as the valve overlap is increased there is a greater airflow, which causes the turbocharger to rotate at a faster speed and hence operate at a higher pressure ratio, meaning that the time taken to reach new conditions of boost and speed is reduced. In the valve overlap period the increase in fresh air mass flow also permits some secondary oxidation of any CO in the exhaust manifold (oxidation of CO is a relatively slow reaction [59]), which also provides more turbine work. Exhaust camshaft phasing itself (if such a device is fitted) can also be used to advance EVO and provide greater enthalpy to the turbine to drive it.

It should also be mentioned that, if an increase in BMEP is *not* the principal aim of applying DI to a turbocharged engine, there are benefits through reducing the boost level necessary to achieve the same engine load. A lower boost pressure is required due to the increased knock limit and improved combustion phasing (see next section) and also because the steady-state, naturally aspirated torque can be expected to increase due to an increase in compression ratio and volumetric efficiency under these conditions, again because of the reduction of charge temperature due to evaporation of the fuel in-cylinder. Estimates for the improvements due to this over PFI vary, but a figure in the region of 5–6% improvement in steady-state, naturally aspirated torque is reasonable [60, 61]. A lower boost requirement and increased naturally aspirated torque both imply an improved throttle response.

3.4.4 Effect of direct injection on knock and abnormal combustion

As was outlined in Section 3.3.4, knock is a major limitation in the performance of any pressure-charged engine. Many potential means of addressing the problem have been investigated, including approaches based on engine architecture already discussed [39–43] and some targeting manipulation

of the combustion process directly. These include applying cooled EGR at full load [62–66] and excess air [67, 68], the former of which appears to show the greatest potential from a knock-suppression viewpoint [69, 70]. Many of these combustion-based approaches will be discussed directly in later chapters, but from a historical perspective it is interesting to note that several were investigated by Ricardo in early experiments and reported on in 1924 [71], for much of which a dedicated pressure-charged research engine was employed, and also that the effect of the specific heat capacity of any diluent was understood through the early development of supercharged aero engines [72].

However, the use of DI is in itself extremely beneficial in terms of knock suppression in turbocharged engines. This is because of the ability to target fuel introduction into the combustion chamber such that most of its heat of vaporization is removed from charge air and not from the engine structure itself. This has the effect of cooling the charge to a greater extent than can be achieved with PFI, so altering the pressure and temperature histories of the end gases to extend their induction time so that equation 3.1 is less likely to be satisfied during the time available for combustion. This concept bears some similarity to that of turboexpansion [39–42].

Gasoline, however, has a relatively low heat of vaporization (approximately 300 MJ/kg [73], depending on its exact composition) but the effect is still marked. Alcohol fuels promise even greater benefits in direct injection SI engines [74], which can be expected to be greater still in the case of pressure-charged units. Bromberg and Cohn [75] have performed calculations which clearly show the effective increase in octane index that can be expected due to DI of ethanol and methanol, both of which have a significantly higher heat of vaporization than gasoline (at 910 and 1160 MJ/kg, respectively [73]). These calculations suggest that DI of a very small volume percentage of alcohol (less than 20% of the total fuel volume) introduced at inlet valve closing (IVC) can increase the knock resistance of a low-octane gasoline introduced via the intake ports markedly in a turbocharged DI engine. From this, one can see that even when operating a DISI turbocharged engine on gasoline, a significant effect on the knock limit can be expected.

There is a secondary effect in conditions of high load and low engine speed due to the fact that the introduction of fuel can be delayed until post-IVC. As already discussed in Section 3.4.3, in these conditions increasing the valve overlap will have an effect of increasing air mass flow through the engine and will shift the compressor operating point to a more efficient point. This can only practically be supported by DI for reasons already discussed, but the effect on combustion is significant: the greater mass of air flowing through the combustion chamber during overlap (which has been heated less due to the improved adiabatic efficiency of the compressor at the rematched operating point) will (a) scavenge the hot residual gases from the chamber

(where the pressure differentials between the intake and exhaust ports permit) and (b) internally cool the combustion chamber and valves. Both of these benefit the knock resistance of the engine and permit the increase in low-speed torque reported for turbocharged DISI engines [58], before the effect of evaporation and the octane rating of fuels is considered.

The magnitude of the effect of the heat of vaporization of a fuel is influenced by architectural considerations. In order to make the best use of the heat of vaporization, it is very important to achieve mixing of the fuel and the charge air that is as good and rapid as possible. This leads to the adoption of high tumble intake ports in DI engines in which the injectors are positioned under the intake port. However, as discussed above, this injector position is something of a historical peculiarity, since it was originally developed for 'air-guided' stratified combustion systems, permitting ready manipulation of the tumble ratio by a tumble flap at low mass air flow [52]. In one recent homogeneous charge engine employing downsizing as the primary route to fuel economy, the tumble flap has been deleted [76], although the underport injector position is not as readily changed since production lines have already been laid down for this configuration. For best air–fuel mixing, however, a central injector position, close to the spark plug, automatically aligns the injection nozzle and its spray in the high-velocity air stream at the top of the intake port. Such an injector position, while utilized extensively for stratified operation in spray-guided lean-burn combustion systems which presently employ piezo injectors [77, 78], has been employed in second-generation homogeneous turbocharged combustion systems [79], and has been demonstrated to provide combustion advantages with solenoid injectors rather than piezo-activated ones [16]. At least one other research engine with this injector positioning and specifically targeting downsizing has been shown [80]. Lückert and co-workers [77] also point out that injection pressure is very important with respect to vaporization of the fuel, and this is an area of continual parallel development with injection pressures for non-piezo injectors increasing above 120 bar.

Coltman and co-workers [16] present a turbocharged DISI engine in which operation at stoichiometric air–fuel ratio ($\lambda = 1$) is possible to >4500 rpm at up to 20.5 bar BMEP, with a maximum enrichment to $\lambda = 0.9$ at maximum power. In this particular engine, many factors contribute to this (including the adoption of a water-cooled exhaust manifold integrated into the cylinder head), but maximizing the latent effect is undoubtedly an important factor. This has been achieved with close spacing of the solenoid injector to the spark plug and a process of optimization of the orientation of the six injection sprays by utilizing a newly developed injector targeting code. The effect of engine architecture on DISI turbocharged engines will be returned to in Section 3.6.

3.4.5 Effect of direct injection on the pollutant emissions of turbocharged SI engines

Direct fuel injection has led to important improvements in the emissions performance of turbocharged engines. As discussed in Section 3.3.5, in normal operation turbocharged engines offer advantages in terms of engine-out hydrocarbons and NO_x due to the usually lower compression ratio that they have to employ for knock-control reasons, but slightly worse CO due to the resulting lower maximum temperatures achieved in the combustion process. Conversely, at higher loads lower temperatures could be considered an advantage due to the potential for reduced dissociation. During a cold start, however, the emissions performance will be dominated by the thermal inertia of both the exhaust manifold and turbine stage, since these delay catalyst light-off, which can mean that emissions limits can be approached, as already discussed.

By adopting direct injection, however, things have been improved significantly. So-called ‘split injection’ strategies have been developed that permit a lean homogeneous main charge to be reliably ignited with acceptable combustion stability by a stratified-rich fuel cloud around the spark plug even at extremely retarded ignition timings (in the region of $20\text{--}30^\circ$ after top dead centre) [58]. This in turn ensures that fuel consumption is minimized during the pre-catalyst light-off phase, while providing the hottest possible gas at the point of EVO by delaying the combustion event. This means that respectively the mass of unconverted noxious emissions passing to the catalyst is minimized and the temperature of the gas is maximized, both of which improve emissions performance. Consequently, the thermal inertia of the turbine is overcome. As soon as the catalyst is lit the engine reverts to stoichiometric operation.

The strategy requires some injector targeting and piston bowl development to be carried out, but this can be optimized to the startup condition and does not compromise the combustion chamber to the same degree as would be necessary were wide-range stratified operation the aim. The capability to increase the compression ratio due to the extension of the knock limit at full load will affect the emissions performance to a degree, but overall the impact of DI on turbocharged SI engines is extremely positive [57]. Further note should be taken of the benefit of high-pressure starts where, because of the higher temperatures generated, vaporization is improved over that possible in PFI engines, and automated start procedures can be expected to draw upon this possibility to a greater extent in the future, particularly in so-called ‘flex-fuel’ vehicles where high proportions of alcohol may be present.

3.5 Challenges of applying direct injection to a turbocharged spark-ignition (SI) engine

There are some additional engineering challenges involved in the process of applying direct injection to SI engines, some of which affect the turbocharged engine more than its naturally aspirated counterpart.

Engine control becomes more problematic since the time available between the addition of fuel, the preparation of the mixture and the ignition decreases significantly when moving from PFI to direct injection. The problem is amplified again if stratification is to be employed, since spray-guided engines can demand split-injection strategies up to high part-load, with the ignition event occurring within the final injection event [77, 78]. Such an approach is also necessary at cold start during a split-injection catalyst heating strategy on a homogeneous engine, although the low engine speeds make the cycle time longer and the temporal challenge is somewhat reduced.

It follows that, in general, engine speed is more of a limitation on the performance of DI engines than on that of naturally aspirated ones. In addition to the control aspect, the instantaneous flow rate of the injectors must be much higher in DI engines; in theory a PFI engine can make use of a full 720° of crankshaft rotation to inject its fuel mass into the charge air, whereas in a DI engine this might be reduced to 120° at most. Hence the required injector flow rate could be more than six times higher, and if the engine is turbocharged and requires a significant degree of over-fuelling at full load for component protection this will exacerbate the problem further. Consequently, in a turbocharged DISI engine the absolute static flow rate could be very high indeed, which then presents problems with idle fuel control due to the large dynamic range required of the injectors. This problem is amplified in engines targeting high BMEP and aggressive downsizing, since the idle fuel quantity can be expected to reduce (or the strategy is not working). Note that idle-stop will not eradicate this problem since, if electric air conditioning is not used, the engine will still have to operate at idle under some conditions.

Strategies to reduce high-load fuel enrichment are therefore important not only from the viewpoint of high-load fuel consumption but also because they reduce the required injector dynamic range (or ‘turn-down ratio’). Strategies such as cooled EGR and excess air can both help to achieve this aim, but the use of a water-cooled exhaust manifold (integrated into the cylinder head or otherwise) also has a similar effect. There are therefore important potential synergies with control system implementation afforded by these technologies.

Clearly, the control system needs to become more complicated as wastegate and recirculation valves (for by-passing the compressor) are added to the turbocharger to improve driveability. A two-stage charging system will also

add complexity, regardless of its configuration. If fitted, a cooled EGR system will require controlling – both bypass and dead volume cut-off valves may be needed [66]. Since it became available, knock sensing has always been important in the successful application of pressure charging and new methods of achieving this will be developed; ion-sensing has been in production in turbocharged engines for some time [81], and ultimately one might expect to see production of in-cylinder pressure transducers (to date, this has only been done in a lean-burn PFI engine, and then only in one cylinder [82]). Increase of fuel system pressure (to the benefit of static flow rate and vaporization) will require more powerful injector drivers, regardless of whether a solenoid or a piezo injector is used.

All of these upgrades to the control system can be expected to drive its cost up, which is a major future challenge for this type of engine. Nevertheless, this type of engine does offer the opportunity to significantly improve fuel economy and reduce CO₂ emissions while continuing to employ simple and robust three-way catalysis (as long as general stratified operation is not the aim). This is a significant benefit since NO_x adsorption catalysts are obviously not required, and the significant extra control system complexity associated with NO_x trap regeneration is avoided. As a consequence of this trade-off, and the cost-benefit which turbocharged DISI engines continue to enjoy over their compression–ignition counterparts, the penetration of this type of engine into the marketplace can be expected to continue, allied to new and emerging technologies intended to further improve their efficiency or reduce their cost, some of which are discussed in later chapters of this book.

3.6 Future trends and possibilities

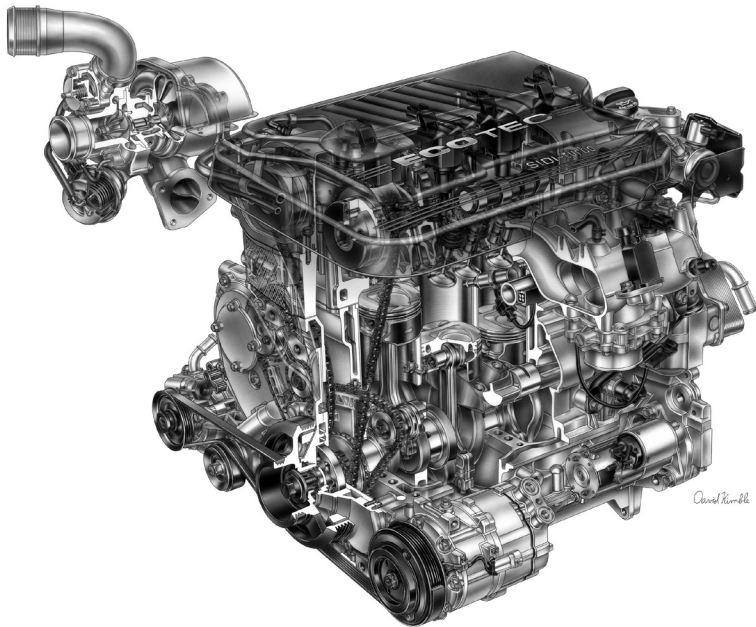
Very few current turbocharged engines were designed from a clean sheet of paper exclusively as downsized units. Most are evolutions of engine families originally conceived as naturally aspirated power units, and so do not exhibit solutions targeted specifically at an optimum pressure-charged configuration.

An immediate example of this is the question of how many cylinders should be grouped together in a turbocharged engine. For refinement and performance, a great many automotive engines have four cylinders. While this is in many ways a good solution for naturally aspirated engines, in turbocharged engines with short primary runner lengths it does lead to undesirable exhaust interactions. This is due to the fact that as one cylinder begins its exhaust phase that of another cylinder is coming to an end, and with elevated pre-turbine pressure this can cause significant amounts of residual burnt gas to be forced into and trapped in the combustion chamber of the next cylinder. This was discussed in Section 3.3.4. Szengel *et al.* [76]

discussed the specific use of exhaust periods less than 180° long to remove such pulse-interaction from a 4-cylinder downsized engine, and presented the effect on the torque curve as a result of this restriction of time–area. The use of intake and exhaust camshaft phasing devices also helps in mitigating this problem. An example of a production engine adopting these technologies is shown in Fig. 3.14, the General Motors ‘LNF’, a 2.0 litre engine, which was developed from a world engine family, itself always intended to include higher technology levels.

The use of divided turbine housings as a means of reducing the problem of adverse exhaust system gas dynamics was also discussed briefly in Section 3.3.4. Indeed, the use of direct fuel injection can be thought of as a strong enabling technology for the use of twin-entry turbine housings, since their beneficial effects in supporting the provision of a higher intake than exhaust pressure during the valve overlap period (even when the mean pressure level in the exhaust manifold exceeds that in the intake manifold) can only be fully exploited in an engine which can inject fuel into the charge air after the exhaust valve has closed.

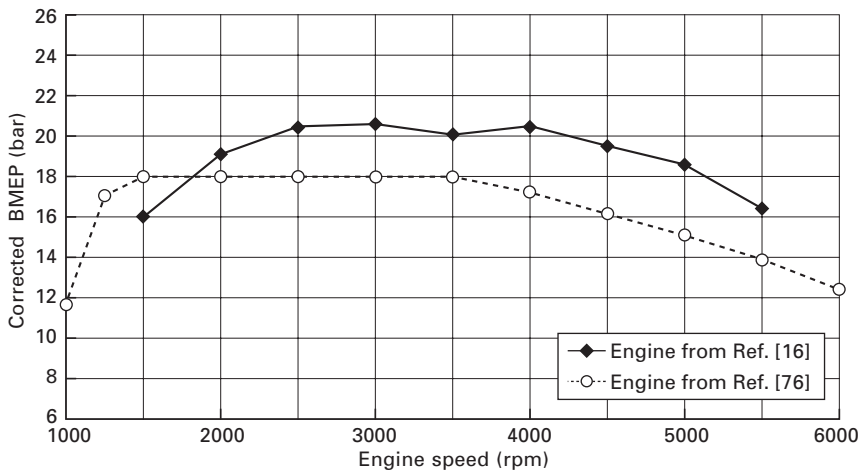
A very pragmatic solution to the problem, which entirely removes the conundrum of whether to pulse-divide an exhaust manifold or not, is to use



3.14 General Motors ‘LNF’ 2.0 litre 4-cylinder DISI engine employing dual continuously variable camshaft phasing and pulse-divided exhaust manifold (courtesy General Motors).

even-firing 3-cylinder groups in turbocharged engines. With such groupings, the maximum permissible exhaust period before inhibition of scavenging occurs is 240° long, which is exactly of the order of normal road car exhaust valve event durations. This is discussed by Cottman *et al.* [16], and a comparison of BMEP curves between the DISI engines described in References [16] and [76] is shown in Fig. 3.15. While Coltman *et al.* [16] state that the charging system is not fully optimized for low-speed torque, the difference in width of the effective BMEP curves is readily apparent. Also, the simple expedient of using three cylinders removes the need to employ a divided exhaust period approach as discussed by Moller *et al.* [43], which effectively reduces the total exhaust time–area in a manner similar to that described by Szengel *et al.* [76]. Because of these advantages, the 3-cylinder group also readily lends itself to the application of exhaust manifolds integrated with the engine structure (see below).

The benefit of achieving improved cylinder scavenging in the low- and mid-speed range by adopting a 3-cylinder engine configuration rather than using a divided turbine housing with a 4-cylinder architecture gives strong potential to reduce cost through the cheaper, and more durable,⁷ turbine housing, in addition to the reduced parts count. This benefit is compounded

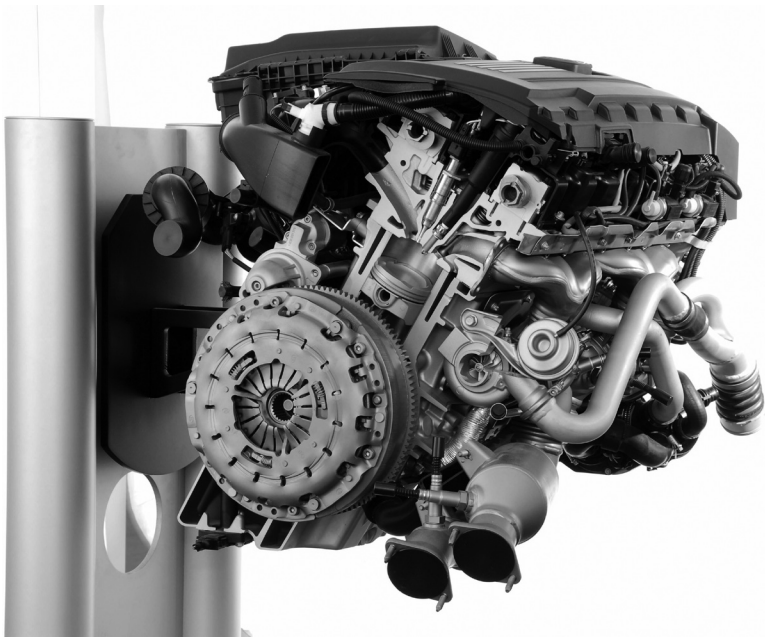


3.15 Effect of exhaust period on BMEP curves of two downsized DI engines of similar displacement with single-stage turbocharging. 1.5 litre 3-cylinder engine from Reference [16] compared to 1.4 litre 4-cylinder engine from Reference [76].

⁷ The ‘tongue’ of a meridionally divided turbine casing suffers severe thermal stress since it cannot easily be cooled.

if an integrated exhaust manifold is used. Divided entry turbine housings cause partial admission losses [83] which reduce the turbine efficiency and this can be a disadvantage outside the area where its superior pulse operation dominates. Thus, use of a single-entry turbine housing gives superior turbine efficiency at higher engine speeds when the mean expansion ratio across the device is high. An example of a BMW in-line 6-cylinder engine employing two groups of three cylinders, central piezo injection and twin camshaft phasing devices is shown in Fig. 3.16. Note that this BMW engine also employs an unusual manifold technology in that the header pipes are welded to the turbine housings, and not a bolted joint as is the norm, unless a combined housing and manifold casting is used.

It must also be remembered that the use of fewer cylinders for any given engine displacement (and especially in downsized applications) has important ramifications for architectural considerations in engines which have to package injection equipment into the combustion chamber. Compared to a 4-cylinder engine, a 3-cylinder engine is likely to have a significantly larger bore which will ease the packaging challenge of incorporating spark plug, valves and



3.16 BMW 3-litre in-line 6-cylinder twin-turbocharged engine with close-spaced piezo direct injection and twin camshaft phasing devices. This engine is arranged such that each group of three cylinders feeds one turbocharger in order to achieve pulse-division in the exhaust manifolds (courtesy BMW AG).

injector in the combustion chamber of the cylinder head. This is especially important for second-generation DI engines with the injector close-spaced to the spark plug. This is described by Cottman *et al.* [16], and comparison of this engine with that in Reference [18] shows the freedom afforded to the engine designer when employing a bigger bore. Reducing the number of cylinders is therefore likely to be very important should BMEP levels be increased to those described in References [17] and [18]. Even without such extreme developments in BMEP, it should be remembered that the larger the valves, the lower the pressure drop across them for a given air mass flow rate, and so the boost pressure can be reduced for any target BMEP, leading to a further reduction in fuel consumption and an improvement in driveability.

The engine described by Coltman *et al.* [16] also employs an exhaust manifold integrated into the cylinder head and cooled by the engine coolant, which is shown in Fig. 3.17. This so-called ‘integrated exhaust

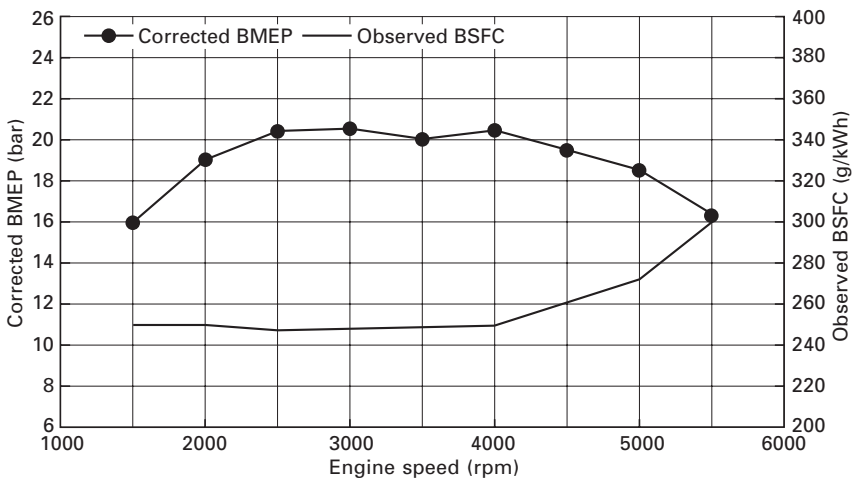


3.17 3-cylinder ‘Sabre’ research engine employing an exhaust manifold integrated into the cylinder head (‘IEM’) and close-spaced DI (courtesy Lotus Engineering).

manifold’ or IEM has many synergies with turbocharged engines. Beyond the obvious advantages in terms of cost, mass and assembly, these include the following:

- Less heat is lost from the exhaust system during a cold start, meaning that the catalyst lights off earlier.
- The heat energy that is rejected through the head heats the coolant and not the air surrounding the engine, shortening warm-up.
- At full load, because of the much increased convective heat transfer due to the use of a liquid coolant, the exhaust gases have more of their thermal energy removed. As a consequence, less component protection cooling in the form of over-fuelling is required, improving full-load fuel consumption.
- Pre-turbine volume is reduced, reducing turbo lag.
- There is an improvement in durability because of reduced distortion both from assembly and from the effect of thermal growth differential.

Because the amount of enrichment required for component protection is reduced, the full-load brake specific fuel consumption (BSFC) is as good as that presented for engines with much higher levels of technology such as cooled EGR [65] or excess air operation [68]. Fig. 3.18, reproduced from data in Reference [16], presents full-load BSFC data which is better than that typically obtained by naturally aspirated engines. That this is generally possible in turbocharged direct injection SI engines is a consequence of the turbocharger turbine removing heat energy from the exhaust gases in



3.18 Full-load BMEP and BSFC for ‘Sabre’ turbocharged DISI engine fitted with an exhaust manifold integrated into the cylinder head (IEM). Data reproduced from Coltman *et al.* [16].

order to drive the compressor and hence performing the function of catalyst protection fuelling in naturally aspirated engines. Any technology that removes the requirement for over-fuelling for turbine protection will therefore have a beneficial knock-on effect. Consequently, there are further beneficial synergies between an IEM and cooled EGR because the amount of cooled EGR required to eliminate over-fuelling operation is concomitantly reduced, and so combustion phasing can be better optimized together with a reduced impact on compressor matching and EGR routing [84]. As a result of the reduction in the mass of EGR required, it may even be possible to use the engine coolant for EGR cooling, simplifying this system and reducing any additional demands on the vehicle cooling system in general.

The synergy between turbocharging in general and mild hybridization has been noted by several researchers [85, 86]. It may become still more important when an IEM is used, since the removal of some exhaust heat by the manifold might be detrimental to low-speed driveability, reducing as it does the enthalpy available to drive the turbine at low speed (although this effect is relatively small due to the predominant transmission of energy to the turbine in pulse form at low speed). Any such deficit may be regained through the use of torque assistance from the electric motor. The use of an IEM, of course, saves some base engine costs which can be used to offset those of a mild hybrid system [16].

Other technologies studied and shown to have synergies with downsizing include variable valve train (VVT) and stratified operation. The combination of downsizing with VVT has been studied in the context of different technologies to reduce fuel consumption and CO₂ emissions, and versus downsizing alone is believed to offer the potential to approach diesel engine efficiency [87]. This supports the work conducted in References [16] and [84]. Although downsizing is commonly associated with homogeneous operation, the use of pressure charging in a stratified DI combustion system has been shown to be beneficial, providing the potential to increase the area of possible stratification and so to improve indicated fuel consumption [88, 89]. As mentioned above, however, there are cost implications for NO_x control in any stratified approach.

Other charging system developments for downsized DISI engines include the application of variable nozzle geometry to the turbine (or VTG), which has traditionally been restricted to diesel engines due to the high cost associated with the metallurgy and engineering necessary to resist gasoline engine exhaust temperatures whilst maintaining nozzle mechanism integrity. Porsche has introduced an engine with VTG [90] which simultaneously improves both driveability and performance. It should be noted, however, that the rotational inertia of the turbocharger shaft assembly may not be reduced with VTG; the improvement is due to the ability to increase the expansion ratio across the turbine and improve the flow angles to the turbine blades at low exhaust

gas mass flow rates. To improve driveability further, it may be necessary to adopt two-stage turbocharging, since this can reduce the inertia of the first, high-pressure, stage significantly [91].⁸ DISI is a particular advantage in the application of VTG to gasoline engines, producing as it does reduced peak exhaust gas temperatures which obviously ameliorate the metallurgical considerations.

On the compressor side, it is difficult to apply large-frame turbocharger technologies such as map width enhancers, recirculation passages or vaned diffusers to light-duty turbochargers on either a manufacturing or a cost basis [91, 92]. However, variable inlet guide vanes (a technology which has been commonly used in racing) have the potential to be beneficial in enhancing the compressor operating characteristics, particularly in single-compression-stage engines [93]. The connection to direct-fuel-injection SI engines, however, is chiefly with the improved low-speed knock resistance that DI affords, in return demanding more air flow at these operating points.

Water-cooled intercoolers permit an increase in charge air density at reduced boost with obvious benefits in terms of engine pumping work. Although originally introduced in series production in 1989 [94], such intercoolers have recently been applied in a production turbocharged DISI engine conceived primarily for good fuel economy [76], the advantage of the DI combustion system again being that it can make best use of the air mass being supplied to the engine.

Finally, in considering the engine–fuel system as a whole, there is little doubt that current fuel specifications are limiting the efficiency potential for pressure-charged engines. The octane appetite of pressure-charged engines is understandably high, and this has been well understood for some time [71]. In this context, direct injection can be viewed as a means of reducing the octane appetite of an engine in the same manner as intercooling or high adiabatic efficiency compressors or turbines: the heat of vaporization of the fuel lowers cycle temperatures to the benefit of knock. That better charge cooling works in this context has been demonstrated [95] and this is the underlying concept behind turboexpansion [39–42, 96] as discussed above. The octane appetite of an engine can also be significantly cut by switching from a 4-stroke cycle to a 2-stroke cycle at high loads, since the BMEP necessary to generate a given load halves in so doing, and this is the approach currently being investigated by Osborne and co-workers [97]. Such technology necessarily increases engine system cost but suggests that significant fuel consumption improvement is possible.

⁸ The inertia of the turbine wheel (or exducer) is the dominant component of the shaft assembly inertia. Turbine inertia is approximately proportional to the fourth power of the wheel diameter.

The above arguments are predicated on the specification of gasoline remaining constant in the foreseeable future, but there is a view that current mainstream SI engine technology (particularly fuel injection and pressure charging) are pushing fuels and engines into operating regions where they would benefit from significantly increased octane indices – this has been referred to by some workers as the operating points moving ‘beyond RON’ [98–102]. Considering fuels other than gasoline raises the potential to improve the thermal efficiency of SI engines by choosing fuels with significantly higher octane ratings than can easily be obtained from gasoline and, since the basic technology of the engine does not have to be changed, this approach is very pragmatic, especially if the chosen fuels possess physico-chemical characteristics which allow them to be introduced via the existing distribution and storage infrastructure. In this respect, high-blend alcohol fuels offer much: ethanol and methanol are both miscible in gasoline, and since they can be made with varying degrees of renewability they also address well-to-tank CO₂ and energy security issues [103, 104] as well as improving tank-to-wheels energetic efficiency through their ability to support higher degrees of downsizing [56, 105] (which directly supports the ‘beyond RON’ contention). Alcohols also bring significantly higher heat of vaporization, compounding the effect with an improvement in octane appetite from the engine before the octane index of the fuel itself is considered, especially in direct-fuel-injection engines where a higher proportion of this heat energy is taken from the charge air. Even in PFI engines, they can give higher thermal efficiency than diesel combustion systems [106]. Considered as a whole, therefore, perhaps history will tell whether the direct-injection turbocharged engine operating on methanol or ethanol will be the fuel–engine combination that will ultimately provide the best use of energy available for transportation, whether from the perspective of minimizing anthropogenic CO₂ emissions or of ensuring security of energy supply.

3.7 Summary

This chapter has shown that the turbocharging of the direct-fuel-injection SI engine allows many of the fundamental problems of PFI turbocharged engines (knocking tendency, turbo lag, cold start emissions behaviour, etc.) to be significantly reduced or obviated. The concept that emerges then offers the opportunity to reduce fuel consumption significantly due to its ability to dethrottle the 4-stroke SI engine in ‘downsized’ form. For this reason, the future of this class of engine is extremely strong since it provides a cost-effective platform to reduce CO₂ output from road transport.

The basic platform of the turbocharged direct-injection SI engine has also been shown to be a basis for further improvement of the concept, be it by architectural improvement, combustion system development or in

combination with other SI technologies either in series production or under development. Furthermore, the possibilities offered by the introduction of increased amounts of renewable alcohol fuel into the market will benefit this engine configuration to an extent greater than other types. Subsequent chapters will discuss some of these possibilities, most of which are aimed at improvement in fuel economy and a concomitant reduction in vehicle CO₂ output, but in conclusion here it must be stated that the turbocharged direct injection SI engine, in downsized form, is already delivering on the initial promise of direct fuel injection in a manner that under-ports stratified combustion systems never truly managed.

3.8 References

1. Turner, J., Pearson, R. and Kenchington, S., 'Concepts for improved fuel economy from spark ignition engines', *JER03504, Int. J. Engine Res.*, Vol. 6, 2005.
2. Hiereth, H. and Prenninger, P., *Charging the Internal Combustion Engine*, Springer, Vienna, 2007.
3. Bamsey, I., *A History of the Turbocharged Racing Car*, Haynes Publishing Group, Yeovil, 1989.
4. German patent number 204630, 16 November 1905.
5. Hooker, S., Reed, H. and Yarker, A., *The Performance of a Supercharged Aero Engine*, Rolls-Royce Heritage Trust Technical Series No. 3, Rolls-Royce Heritage Trust, Derby, 1997.
6. Bingham, V., *Major Piston Aero Engines of World War II*, Airlife Publishing, Shrewsbury, 1998.
7. Taylor, D.R., *Boxkite to Jet – the Remarkable Career of Frank B Halford*, Rolls-Royce Heritage Trust Historical Series No. 28, Derby, 1999.
8. http://www.holset.co.uk/files/2_4-history%20of%20turbocharging.php
9. Allard, A., *Turbocharging and Supercharging*, Patrick Stephens, Cambridge, 1982.
10. <http://en.wikipedia.org/wiki/Turbocharger>
11. Bamsey, I., *The 1000 bhp Grand Prix Cars*, Haynes Publishing Group, Yeovil, 1988.
12. Doble, I.M., 'Supercharging with an axial compressor', SAE paper 870722, Detroit, MI, February 1987.
13. Krebs, R., Szengel, R., Middendorf, H., Fleiß, M., Laumann, A. and Voeltz, S., 'The new dual-charged FSI petrol engine by Volkswagen. Part 1: Design', *MTZ 11/2005*, Volume 66, pp. 2–7, November 2005.
14. Winterbone, D.E. and Pearson, R.J., *Design Techniques for Engine Manifolds: Wave Action Methods for IC Engines*, John Wiley & Sons, London, 1999.
15. Krebs, R., Szengel, R., Middendorf, H., Sperling, H., Siebert, W., Theobald, J. and Michels, K., 'The new dual-charged FSI petrol engine by Volkswagen Part 2: Thermodynamics', *MTZ 12/2005*, Volume 66, pp. 23–26, December 2005.
16. Coltman, D., Turner, J.W.G., Curtis, R., Blake, D., Holland, B., Pearson, R.J., Arden, A. and Nuglisch, H., 'Project Sabre: a close-spaced direct injection 3-cylinder engine with synergistic technologies to achieve low CO₂ output', SAE paper 2008-01-0138, SAE 2008 World Congress, Detroit, MI, 14–17 April 2008.

17. Kapus, P.E., Fraidl, G.K., Prevedel, K. and Fuerhapter, A., 'GDI turbo – the next steps', JSAE paper 20075355 and *JSAE Proceedings*, No. 84-07, pp. 13–16, Yokohama, Japan, May 2007.
18. Hancock, D., Fraser, N., Jeremy, M., Sykes, R. and Blaxill, H., 'A new 3 cylinder 1.2l advanced downsizing technology demonstrator engine', SAE paper 2008-01-0611, SAE 2008 World Congress, Detroit, MI, 14–17 April 2008.
19. Otobe, Y., Goto, O., Miyano, H., Kawamoto, M., Aoki, A. and Ogawa, T., 'Honda Formula One turbo-charged V-6 1.5L engine', SAE paper 890877, 1989.
20. Tashima, S., Okimoto, H., Fujimoto, Y. and Nakao, M., 'Sequential twin turbocharged rotary engine of the latest RX-7', SAE paper 941030, 1994.
21. Crosse, J., 'The methanol alternative', *Autocar & Motor*, 30 May 1990, pp. 14–17.
22. Steinparzer, F., Kratochwill, H., Mattes, W. and Stuetz, W., 'Two stage turbocharging for the BMW 3.0 litre 6-cylinder diesel engine', *13. Aachener Kolloquium Fahrzeug- und Motorentechnik 2004*, Aachen, Germany, October 2004.
23. Steinparzer, F., Mattes, W., Nefischer, P. and Steinmayr, T., 'The new BMW four-cylinder diesel engine', *MTZ 11/2007*, Volume 68, pp. 932–942 (pp. 6–10 of the English translation), November 2007.
24. Heywood, J.B., *Internal Combustion Engine Fundamentals*, McGraw-Hill, New York, 1988.
25. Draper, C.S., 'Pressure waves accompanying detonation in the internal combustion engine', *J. Aero. Sci.*, Vol. 5, No. 6, pp. 219–226, April 1938.
26. Swarts, A., 'Insights relating to octane rating and the underlying role of autoignition', Ph.D. thesis, University of Cape Town, 2006.
27. Klein, R., Breitbach, H., Geratz, K.J. and Senger, W., 'Surface erosion by high-speed combustion waves', Twenty-Fifth Symposium (International) on Combustion, The Combustion Institute, pp. 95–102, 1994.
28. Lee, W. and Schaefer, H.J., 'Analysis of local pressures, surface temperatures and engine damages under knock conditions', SAE paper 830508 and *SAE Transactions*, Vol. 92, Section 2, pp. 511–523, 1983.
29. Clerk, D., 'Explosive reactions considered in reference to internal combustion engines', *Trans. Faraday Soc.*, pp. 338–340, 1926.
30. Ricardo, H.R., 'Paraffin as fuel', *Auto. Eng.*, Vol. 9, p. 2, 1919.
31. Moses, E., Yarin, A.L. and Bar-Yoseph, P., 'On knocking prediction in spark ignition engines', *Combustion and Flame*, Vol. 101, pp. 239–261, 1995.
32. Livengood, J.C. and Wu, P.C., 'Correlation of autoignition phenomena in internal combustion engines and rapid compression machines', Fifth Symposium (International) on Combustion, The Combustion Institute, pp. 347–356, 1955.
33. Curry, S., 'A three-dimensional study of flame propagation in a spark ignition engine', SAE paper 630487 and *SAE Transactions*, pp. 628–650, 1963.
34. Spicher, U., Kröger, H. and Ganser, J., 'Detection of knocking combustion using simultaneously high-speed Schlieren Cinematography and multi optical fiber technique', SAE paper 912312 and *SAE Transactions*, Vol. 100, Section 4, pp. 569–588, 1991.
35. König, G., Maly, R.R., Bradley, D., Lau, A.K.C. and Sheppard, C.G.W., 'Role of exothermic centres on knock initiation and knock damage', SAE paper 902136, SAE International Fuels and Lubricants Meeting, Tulsa, OK, October 1990.
36. Schreiber, M., Sadat Sakak, A., Poppe, C., Griffiths, J.F., Halford-Maw, P. and Rose, D.J., 'Spatial structure in end-gas autoignition', SAE paper 932758 and *SAE Transactions*, Vol. 102, Section 4, pp. 1502–1514, 1993.

37. Gu, X.J., Emerson, D.R. and Bradley, D., 'Modes of reaction front propagation from hot spots', *Combustion and Flame*, Vol. 133, pp. 63–74, 2003.
38. Rothe, M., Heidenreich, T., Spicher, U. and Schubert, A., 'Knock behaviour of SI-engines: thermodynamic analysis of knock onset locations and knock intensities', SAE paper 2006-01-0225, SAE 2006 World Congress, Detroit, MI, April 2006.
39. Turner, J.W.G., Pearson, R.J., Bassett, M.D. and Oscarsson, J., 'Performance and fuel economy enhancement of pressure charged SI engines through turboexpansion – an initial study', SAE paper 2003-01-0401 and *SAE Transactions*, June 2004.
40. Turner, J.W.G., Pearson, R.J., Bassett, M.D., Blundell, D.W. and Taitt, D.W., 'The turboexpansion concept – initial dynamometer results', SAE paper 2005-01-1853, SAE 2005 World Congress, Detroit, MI, April 2005.
41. Taitt, D.W., Garner, C.P., Swain, E., Pearson, R.J., Bassett, M.D. and Turner, J.W.G., 'An automotive engine charge-air intake conditioner system: 1st Law thermodynamic analysis of performance characteristics', *Proc. Instn Mech. Engrs, J. Automotive Engineering*, Vol. 219, Part D, no. 6, pp. 389–404, 2005.
42. Taitt, D.W., Garner, C.P., Swain, E., Blundell, D., Pearson, R.J. and Turner, J.W.G., 'An automotive engine charge-air intake conditioner system: Analysis of fuel economy benefits in a gasoline engine application', *Proc. Instn Mech. Engrs, J. Automotive Engineering*, Vol. 220, Part D, no. 9, pp. 1293–1307, 2006.
43. Moller, C.E., Johansson, P., Grandin, B. and Lindström, F., 'Divided exhaust period – a gas exchange system for turbocharged SI engines', SAE paper 2005-01-1150, SAE 2005 World Congress, Detroit, MI, April 2005.
44. Turner, J.W.G., Kalafatis, A. and Atkins, C., 'The design of the NOMAD advanced concepts research engine', SAE paper 2006-01-0193, SAE 2006 World Congress, Detroit, MI, April 2006.
45. Groff, E., Königstein, A. and Drangel, H., 'The new 2.0L high performance turbo engine with gasoline direct injection from GM Powertrain', *27th International Vienna Motor Symposium, Proceedings*, Book 1, pp. 86–114, Vienna, 27–28 April 2006.
46. Andriesse, D., Cazzolato, F., Marangoni, A., Oreggioni, A. and Quinto, S., 'A new generation of high efficiency DI gasoline engines – Serious competition for the DI diesel engine?', 18th International AVL Congress 'Engine and Environment', Graz, Austria, 7–8 September 2006.
47. Eng, J.A., Leppard, W.R., Najt, P.M. and Dryer, F.L., 'The interaction between nitric oxide and hydrocarbon oxidation chemistry in a spark ignition engine', SAE paper 972889, International Falls Fuels and Lubricants Meeting and Exposition, Tulsa, OK, October 1997.
48. Kawabata, Y., Sakonji, T. and Amano, T., 'The effect of NO_x on knock in spark-ignition engines', SAE paper 1999-01-0572, 1999.
49. Stenlås, O., Gogan, A., Egnell, R., Sunden, B. and Mauss, F., 'The influence of nitric oxide on the occurrence of autoignition in the end gas of spark ignition engines', SAE paper 2002-01-2699, SAE Powertrain and Fluid Systems Conference and Exhibition, San Diego, CA, October 2002.
50. Gunston, B., *World Encyclopaedia of Aero Engines*, Patrick Stephens, Yeovil, 1995, 3rd edition, pp. 49–50.
51. Ando, H., 'Combustion control technologies for gasoline engines', I. Mech. E. Seminar on Lean Burn Combustion Engines, paper S433/001/96, London, 3–4 December 1996.

52. Wurms, R., Grigo, M. and Hatz, W., 'Audi FSI technology – improved performance and reduced fuel consumption', *ATA*, Vol. 56, no. 3/4, March–April 2003.
53. Wirth, M., Mayerhofer, U., Piock, W. and Fraidl, G., 'Turbocharging the DI gasoline engine', SAE paper 2000-01-0251, SAE 2000 World Congress, Detroit, MI, March 2000.
54. Ranini, A. and Monnier, G., 'Turbocharging a gasoline direct injection engine', SAE paper 2001-01-0736, SAE 2001 World Congress, Detroit, MI, March 2001.
55. Fraser, N. and Blaxill, H., 'Engine downsizing and the application of gasoline direct injection to a high specific output turbocharged engine', I. Mech. E. Fuel Economy and Engine Downsizing Seminar, London, 13 May 2004.
56. Bergström, K., Nordin, H., Königstein, A., Marriott, C.D. and Wiles, M.A., 'ABC – alcohol based combustion engines – challenges and opportunities', 16th Aachen Colloquium, pp. 1031–1071, Aachen, Germany, October 2007.
57. Zhao, F., Harrington, D. and Lai, M.-C., *Automotive Gasoline Direct-Injection Engines*, Society of Automotive Engineers, Warrendale, PA, 2002.
58. Krebs, R., Boehme, J., Dornhoefer, R., Wurms, R., Friedmann, K., Helbig, J. and Hatz, W., 'The new Audi 2.0T FSI engine – the first direct injection turbo-gasoline-engine from Audi', 25th Vienna Motor Symposium, Vienna, April 2004.
59. Tanaka, S., Ayala, F. and Keck, J.C., 'A reduced chemical kinetic model for HCCI combustion of primary reference fuels in a rapid compression machine', *Combustion and Flame*, Vol. 133, pp. 467–481, 2003.
60. Anderson, W., Yang, J., Brehob, D.D., Vallance, J.K. and Whiteaker, R.M., 'Understanding the thermodynamics of direct injection spark ignition (DISI) combustion systems: an analytical and experimental investigation', SAE paper 962018, 1996.
61. Lang, O., Geiger, J., Haberman, K. and Wittler, M., 'Boosting and direct injection – synergies for future gasoline engines', SAE paper 2005-01-1144, SAE 2006 World Congress, Detroit, MI, April 2006.
62. Grandin, B., Angström, H.-E., Stalhammar, P. and Olofsson, E., 'Knock suppression in a turbocharged SI engine by using cooled EGR', SAE paper 982476, SAE 1998 World Congress, Detroit, MI, March 1998.
63. Grandin, B. and Angström, H.-E., 'Replacing fuel enrichment in a turbo charged SI engine: lean burn and cooled EGR', SAE paper 1999-01-3505, SAE 1999 World Congress, Detroit, MI, March 1999.
64. Duchaussoy, Y., Lefebvre, A. and Bonetto, R., 'Dilution interest on turbocharged SI engine combustion', SAE paper 2003-01-0629, SAE 2003 World Congress, Detroit, MI, April 2003.
65. Cairns, A., Blaxill, H. and Irlam, G., 'Exhaust gas recirculation for improved part and full load fuel economy in a turbocharged gasoline engine', SAE paper 2006-01-0047, SAE 2006 World Congress, Detroit, MI, April 2006.
66. Cairns, A., Fraser, N. and Blaxill, H., 'Pre versus post compressor supply of cooled EGR for full load fuel economy in turbocharged gasoline engines', SAE paper 2008-01-0425, SAE 2008 World Congress, Detroit, MI, 14–17 April 2008.
67. Stokes, J., Lake, T.H. and Osborne, R.J., 'A gasoline engine concept for improved fuel economy – the lean boost system', SAE paper 2000-01-2902, SAE International Fuels and Lubricants Meeting and Exposition, Baltimore, MD, October 2000.
68. Lake, T., Stokes, J., Murphy, R., Osborne, R. and Schamel, A., 'Turbocharging concepts for downsized DI gasoline engines', SAE paper 2004-01-0036, SAE 2004 World Congress, Detroit, MI, April 2004.

69. Hattrell, T., Sheppard, C.G.W., Burluka, A.A., Neumeister, J. and Cairns, A., 'Burn rate implications of alternative knock reduction strategies for turbocharged SI engines', SAE paper 2006-01-1110, SAE 2006 World Congress, Detroit, MI, April 2006.
70. Hiroshi, M., Makoto, K., Tetsunori, S. and Shinji, K., 'The potential of lean boost combustion', FISITA paper F2004V219, FISITA Conference 2004, Barcelona, Spain, 2004.
71. Institution of Automobile Engineers, 'Report of the Empire Motor Fuels Committee', Volume XVIII, Part I, Session 1923–1924.
72. Peletier, L.A., 'Effect of air–fuel ratio on detonation in gasoline engines', National Advisory Committee for Aeronautics Technical Memorandum No. 853, Washington, DC, March 1938 (originally published in French at the Second World Petroleum Congress, Paris, June 1937).
73. 'Surface vehicle information report, alternative automotive fuels', SAE Standard J1297, Society of Automotive Engineers, Warrendale, PA, 2002.
74. Wyszynski, L., Stone, C.R. and Kalghatgi, G.T., 'The volumetric efficiency of direct and port injection gasoline engines with different fuels', SAE paper 2002-01-0839, SAE 2002 World Congress, Detroit, MI, March 2002.
75. Bromberg, L. and Cohn, D.R., 'Effective octane and efficiency advantages of direct injection alcohol engines', MIT Laboratory for Energy and the Environment Report LFEE 2008-01 RP, 6 January 2008.
76. Szengel, R., Middendorf, H., Pott, E., Theobald, J., Etzrodt, T. and Krebs, R., 'The TSI with 88 kW – the expansion of the Volkswagen family of fuel-efficient gasoline engines', 28th International Vienna Motor Symposium, Vienna, 26–27 April 2007.
77. Lückert, P., Waltner, A., Rau, E., Vent, G. and Schaupp, U., 'The new V6 gasoline engine with direct injection by Mercedes-Benz', *MTZ 11/2006*, Volume 67, pp. 830–840, November 2006.
78. Schünemann, E., Langen, P., Missy, S. and Schwarz, C., 'New BMW 6- and 4-cylinder petrol engines with high precision injection and stratified combustion', *JSAE* paper 20075363 and *JSAE Proceedings*, No. 84-07, pp. 1–6, Yokohama, Japan, 23–25 May 2007.
79. Welter, A., Bruener, T., Unger, H., Hoyer, U. and Brendel, U., 'The new turbocharged BMW six cylinder inline petrol engine', *MTZ 02/2007*, Volume 68, pp. 80–88, February 2007.
80. Königstein, A., Larsson, P.-I., Grebe, U.D. and Wu, K.J., 'Differentiated analysis of downsizing concepts', 29th International Vienna Motor Symposium, Series 12, No./Vol. 672-1 No. 22, Vienna, 24–25 April 2008.
81. http://en.wikipedia.org/wiki/Trionic_T5.5
82. Inoue, T., Matsushita, S., Nakanishi, K. and Okano, H., 'Toyota lean combustion system – the third generation system', SAE paper 930873, 1993.
83. Winterbone, D.E. and Pearson, R.J., *Theory of Engine Manifold Design: Wave Action Methods for IC Engines*, John Wiley & Sons, London, 2000.
84. Turner, J.W.G., Pearson, R.J., Curtis, R. and Holland B., 'Improving fuel economy in a turbocharged DISI engine already employing integrated exhaust manifold technology and variable valve timing', SAE paper 2008-01-2449, SAE International Powertrain Fuels and Lubricants Meeting, Rosemont, IL, 6–9 October 2008.
85. Grebe, U.D., Larsson, P.-I. and Wu, K.-J., 'Comparison of charging systems for spark ignition engines', 28th International Vienna Motor Symposium, Vienna, 26–27 April 2007.

86. Fischer, R. and Kirsten, K., 'The turbo hybrid – holistic approach for a modern gasoline hybrid drive', 27th Vienna Motor Symposium, Vienna, 27–28 April 2006.
87. Atkins, M.J. and Koch, C.R., 'A well-to-wheel comparison of several powertrain technologies', SAE paper 2003-01-0081, SAE 2003 World Congress, Detroit, MI, 3–6 March 2003.
88. Kneifel, A., Buri, S., Velji, A., Spicher, U., Pape, J. and Sens, M., 'Investigations on supercharging stratified part load of a spray-guided DI SI engine', SAE paper 2008-01-0143, SAE 2008 World Congress, Detroit, MI, April 2008.
89. Lang, O., Habermann, K., Krebber-Hortmann, K., Sehr, A., Thewes, M., Kleeberg, H. and Tomasic, D., 'Potential of the spray-guided combustion system in combination with turbocharging', SAE 2008 World Congress, Detroit, MI, April 2008.
90. Kerkau, M., Knirsch, S. and Neußer, H.-J., 'The new six-cylinder bi-turbo engine with variable turbine geometry for the Porsche 911 Turbo', 27th Vienna Motor Symposium, Vienna, 27–28 April 2006.
91. Baines, N.C., 'The turbocharging challenge', Keynote Speech, I. Mech. E. Turbochargers and Turbocharging Conference, London, 17–18 May 2006.
92. Fisher, F.B., 'Application of map width enhancement devices to turbocharger compressor stages', SAE paper 880794 and *SAE Transactions*, Volume 97, Section 6, pp. 1303–1310, 1988.
93. Fraser, N., Fleischer, T., Thornton, J. and Rueckauf, J., 'Development of a fully variable compressor map enhancer for automotive application', SAE paper 2007-01-1558, SAE 2007 World Congress, Detroit, MI, April 2007.
94. Wood, S.P. and Bloomfield, J.H., 'Clean power – Lotus 2.2 Lt chargecooled engine', SAE paper 900269, SAE 1990 World Congress, Detroit, MI, February 1990.
95. Turner, J.W.G., Pearson, R.J., Milovanovic, N. and Taitt, D., 'Extending the knock limit of a turbocharged gasoline engine via turboexpansion', 8th I. Mech. E. Conference on Turbochargers and Turbocharging, London, May 2006.
96. Crooks, W.R., 'Combustion air conditioning boosts output 50 per cent', *CIMAC*, Vol. 15, pp. 475–494, 1959.
97. Osborne, R., Stokes, J., Ceccarini, D., Jackson, N., Lake, T., Joyce, M., Visser, S., Miche, N., Begg, S., Heikal, M., Kalian, N., Zhao, H. and Ma, T., 'The 2/4SIGHT project – development of a multi-cylinder two-stroke/four-stroke switching gasoline engine', *JSAE* paper 20085400 and *JSAE Proceedings*. No. 79-08, pp. 11–16, Yokohama, Japan, May 2008.
98. Kalghatgi, G.T., 'Fuel anti-knock quality – Part I, Engine studies', SAE paper 2001-01-3584, 2001.
99. Kalghatgi, G.T., 'Fuel anti-knock quality – Part II, Vehicle studies – How relevant is motor octane number (MON) in modern engines?', SAE paper 2001-01-3585, 2001.
100. Yates, A.D.B., Swarts, A. and Viljoen, C.L., 'Correlating auto-ignition delays and knock-limited spark-advance data for different types of fuel', SAE paper 2005-01-2083 and *SAE Transactions*, Volume 114, Section 4, pp. 735–747, 2005.
101. Viljoen, C.L., Yates, A.D.B., Swarts, A., Balfour, G. and Möller, K., 'An investigation of the ignition delay character of different fuel components and an assessment of various autoignition modelling approaches', SAE paper 2005-01-2084 and *SAE Transactions*, Volume. 114, Section 4, pp. 748–763, 2005.
102. Duchaussoy, Y., Barbier, P. and Schmerzle, P., 'Impact of gasoline RON and MON on a turbocharged MPI SI engine performances', SAE paper 2004-01-2001, SAE Fuels and Lubricants Meeting and Exhibition, Toulouse, France, June 2004.

103. Pearson, R.J. and Turner, J.W.G., 'Exploitation of energy resources and future automotive fuels', SAE paper 2007-01-0034, SAE Fuels and Emissions Conference, Cape Town, January 2007.
104. Hammerschlag, R., 'Ethanol's energy return on investment: a survey of the literature 1990–present', *Environmental Science and Technology*, Vol. 40, No. 6, pp. 1744–1750, 2006.
105. Turner, J.W.G., Pearson, R.J., Holland, B. and Peck, B., 'Alcohol-based fuels in high performance engines', SAE paper 2007-01-0056, SAE Fuels and Emissions Conference, Cape Town, January 2007.
106. Brusstar, M., Stuhldreher, M., Swain, D. and Pidgeon, W., 'High efficiency and low emissions from a port-injected engine with neat alcohol fuels', SAE paper 2002-01-2743.

The lean boost combustion system for improved fuel economy

T. LAKE, J. STOKES, R. OSBORNE, R. MURPHY and
M. KEENAN, Ricardo UK Ltd, UK

Abstract: Downsized engine concepts can help achieve reduced CO₂ emissions from vehicles. A key challenge is controlling octane requirement without sacrificing fuel economy. The authors have investigated Lean Boost Direct Injection (LBDI) with lean operation at full load to control octane requirement while maintaining a high compression ratio. Experimental investigations have been carried out using a 1.125 l multi-cylinder engine and C-class vehicle. Aftertreatment via a lean NO_x trap was assessed and selective catalytic reduction (SCR) compared. The authors conclude that the pressure to lower CO₂ will require lean engines in the future, of which the LBDI concept is the most attractive variant.

Key words: downsized engine, low CO₂ powertrain, lean burn, gasoline direct injection, lean NO_x aftertreatment.

4.1 Pressures on the gasoline engine

Although the gasoline vehicle of today is much cleaner and more fuel-efficient than its predecessor at the turn of the century, it is about to face its most severe test yet. Ironically, as the gasoline engine can now face up to the challenge of meeting even the toughest tailpipe emissions, it faces a new challenge as attention has now turned to improving its efficiency, and more specifically to reducing its emissions of carbon dioxide (CO₂). In recent years the emission of carbon dioxide as a result of burning fuel has become of increasing concern because of the ‘greenhouse’ effect. Environmental pressure in Europe has been steadily rising since the early 1980s and has recently culminated in a proposed new complex vehicle inertia weight-related requirement for CO₂ emissions from the vehicle fleet. This requires the achievement of an average of 130 g/km CO₂ per vehicle on the NEDC drive cycle. For a gasoline vehicle, that equates to 5.4 l per 100 km (or 52 miles per imperial gallon).

The pressure is not just in Europe; the US ‘twenty in ten’ initiative aims to reduce gasoline consumption by 20% over the next 10 years and China has introduced CO₂ legislation related to vehicle inertia weight. Other examples are being developed around the globe and initiatives to further improve powertrain efficiency and CO₂ levels are arising regularly. Whether it is for the reasons of protecting the environment or for energy security, the

pressure is on to reduce consumption of fossil fuels as we progress through the twenty-first century. The improvement of gasoline engine efficiency will have to be a large part of that achievement. In Europe, the earlier voluntary ACEA target to lead to a fleet average of 140 g/km of CO₂ by 2008 drove the manufacturers to the immediate short-term solution of applying the diesel engine to the vehicle fleet as far as economically possible. This has had significant impact on fleet average CO₂ values due to its increased market share. Market acceptance of the diesel was accelerated by favourable fuel tax incentives in some European countries, and recently improved refinement and performance despite its significantly higher (1.6–2 times) powertrain costs. However, achieving much tougher future emissions levels with the diesel engine, without its overall powertrain and aftertreatment system cost spiralling beyond that which is economic or is compromising its thermodynamic efficiency, is proving a very difficult challenge. Ultimately, the fleet failed to meet the 140 g/km target by the deadline of 2008 as there was very low execution of fuel economy technology on gasoline engines. It was and will not be enough to just ‘dieselize’.

The latest proposal is for a Europe-wide fleet average CO₂ level of 130 g/km to be achieved by 2012. At the time of writing, this will require a typical European manufacturer to improve its fleet fuel consumption by around 20% in four years – a huge challenge. The technology for improving fuel economy must be applied across the full vehicle fleet. The most important area will be to produce a high-economy family car in the C or D class. A good short-term target for this type of vehicle is to achieve a fuel consumption of 5 l per 100 km and in the longer term to approach 4 l per 100 km. A recent study at Ricardo has shown that this is indeed possible through a combination of powertrain and vehicle gains, but as about half the gain has to come from the powertrain, significant pressure remains on improving the fuel consumption of the engine.

So, after many years of researching but doing very little to actually implement the technology to improve the efficiency of gasoline engines, manufacturers are realising that to achieve the fleet average CO₂ targets requires a holistic approach involving developed gasoline engines as well as diesel engines along with their transmissions. Thus activity has increased in this area in recent years. Most notably the market has seen the application of exhaust gas recirculation (EGR), variable valvetrains, direct injection and, more recently, well-executed downsizing (i.e. maintaining engine performance via boosting whilst reducing swept volume, which has the effect of lowering friction torque, and raising BMEP to reduce pumping work and improve indicated efficiency). Introduction of these technologies, along with incremental improvements in base engine and vehicle designs, will enable some large reductions in drive-cycle CO₂ emissions to be made. Downsizing can be very effective, and it is the issue of downsizing the gasoline engine

while utilising an even more efficient lean air/fuel ratio that is the subject of this chapter.

4.2 Downsizing strategies

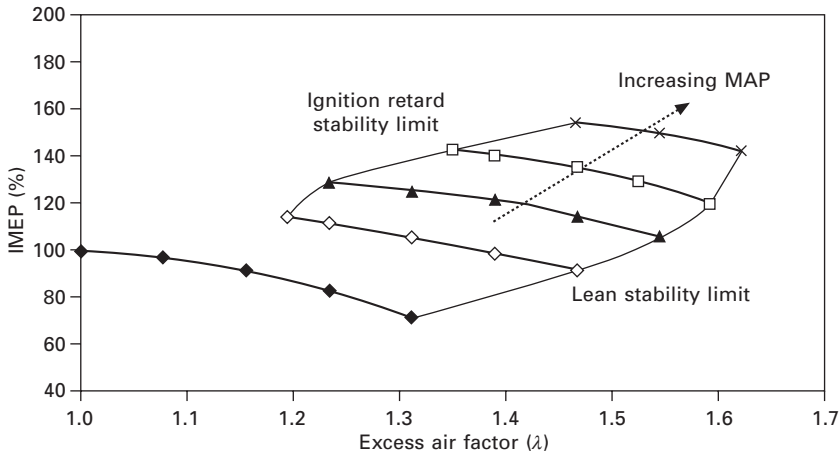
The potential benefits of engine downsizing on fuel consumption for a wide range of driving conditions are well known. However, there are obstacles to the widespread adoption of downsized engines in future vehicles. The first of these is concerned with the driving characteristics of vehicles with turbocharged engines, which may have reduced torque at low engine speeds and poor transient response. Owing to airflow and octane requirement constraints, steady-state low-speed torque is reduced compared to a naturally aspirated engine of equivalent peak torque and power. This adversely affects pull away from rest and performance feel for tip-in manoeuvres at low engine speeds. Although greatly improved with modern boosting systems, turbocharger lag is still an issue for downsized engines. A second obstacle is customer and manufacturer acceptance of downsized engines, as traditionally there has been a close association between swept volume and desirability for the consumer, and with profitability for the carmaker.

A number of technical measures can be employed to overcome the first of these obstacles, but a process of re-education and appropriate product branding and marketing must address the second. Furthermore, the issue of having to reduce compression ratio faced by conventional port-injected downsized engines must be resolved. Compression ratio must be reduced on conventional boosted engines to control knock. As well as a direct reduction in thermodynamic efficiency, this leads to higher exhaust temperatures and both earlier and increased levels of over-fuelling for component protection. Inevitably any downsizing technology package must also be economically justified in terms of a cost-benefit analysis compared to other technology packages.

4.3 The lean boost direct injection (LBDI) concept

The lean boost system is an example of such a downsized engine and combines direct injection, lean operation and pressure charging. A critical factor in the function of pressure-charged gasoline engines is octane requirement. It is normally necessary to significantly reduce the geometric compression ratio of a boosted engine in order to avoid combustion knock, and this has a negative effect on thermal efficiency. However, direct injection and homogeneous lean operation both reduce octane requirement, allowing a higher compression ratio to be used.

Figure 4.1 illustrates the theoretical basis of the lean boost combustion system. As the intake charge is boosted, the operating band of air/fuel ratio



4.1 Characteristics of the lean boost DI concept.

changes. At the rich limit, combustion stability is hindered by ignition retard due to knock, so the rich limit moves to a higher excess air-factor (λ). At the lean limit, combustion stability is limited by spark initiation and flame propagation. The lean limit improves with increasing boost pressure, so the overall operating band shifts to a higher λ value. As the air/fuel ratio is increased from the rich limit to the lean limit, the engine output decreases. The objective is to boost to a level at which the indicated mean effective pressure (IMEP) is significantly higher than the naturally aspirated stoichiometric value, to allow downsizing, but with a homogeneous lean mixture ($\lambda = 1.4$ – 1.6). To minimise the airflow demand of the engine, the richest mixture that allows stable operation at the desired IMEP would be selected. So, the fundamental precept of the lean boost system is the reduction in octane requirement due to the direct injection system and the role of excess air as a knock suppressant.

This allows operation at around 1.5 compression ratios higher than for a conventional direct injection turbocharged engine. Typically a compression ratio of 11.5–12 to 1 with 95 RON fuel is viable. LBDI requires no over-fuelling for component protection and the low peak exhaust temperature allows the use of a comparatively cheap variable nozzle turbine (VNT), currently not suitable for conventional gasoline engines due to its limited temperature capability. This gives advantages in low-speed torque and reduction of turbocharger lag.

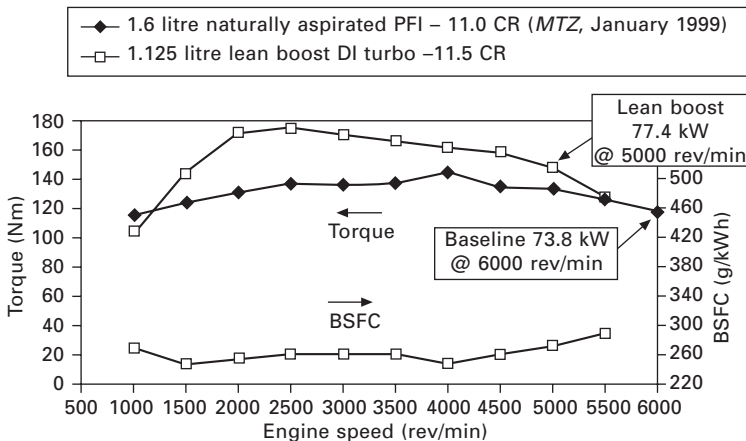
Ricardo conducted an extensive testbed programme, followed by the development and calibration of a C-class vehicle showing comparative driveability with a production 1.6 litre stoichiometric equivalent. A VNT turbocharger was used for the reasons outlined above. Owing to the lower

exhaust temperatures of the LBDI concept it was possible to use a standard production diesel VNT unit over a higher-specification, higher-cost gasoline equivalent. This results in superior transient performance compared with a conventional fixed geometry unit but at a reduced on-cost. The 1.1 litre LBDI unit developed for a European application produced 5% more power and 20% more torque than the conventional 1.6 litre PFI engine (Fig. 4.2).

Installed in the C-class vehicle, LBDI delivers 21% lower CO₂ emissions as illustrated in Table 4.1. Validated system simulation (V-Sim) showed that downsizing plus direct injection delivered 9% economy benefit (154.1 vs 169 g/km). Test results show that the addition of lean operation and higher CR gives a further 14% improvement. Lean NO_x trap regeneration added only 1% to overall cycle fuel consumption.

Transient response has been enhanced through the use of a VNT enabled by low exhaust temperatures and appropriate control strategies and allows LBDI to achieve driveability targets. The LBDI vehicle had a similar driving feel to a diesel engine vehicle, but with an extended engine speed range. The tractive effort curves in fourth and fifth gears illustrate that LBDI has the ‘fun to drive’ performance feel of a diesel vehicle (Fig. 4.3).

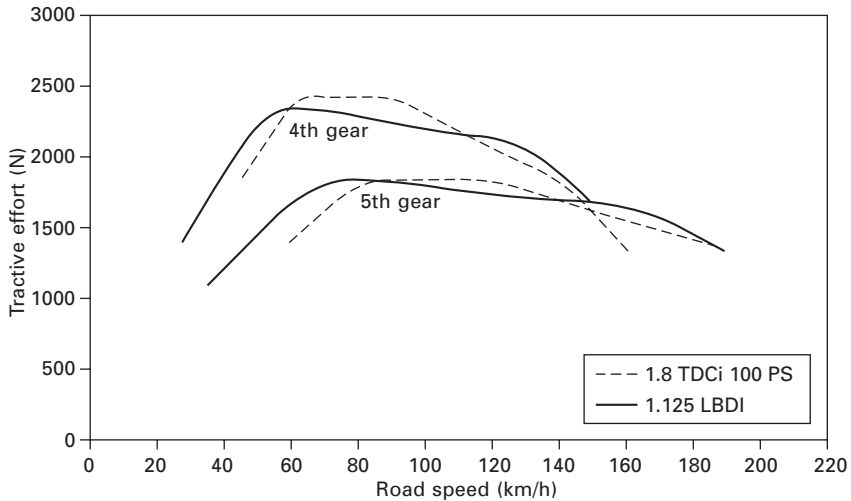
At the time, the LBDI vehicle was developed to meet emissions requirements through conventional lean NO_x trap technologies. Off-cycle NO_x had been



4.2 Power curves for the baseline engine and LBDI concept.

Table 4.1 NEDC drive-cycle CO₂ and fuel consumption results

	LBDI 1.125 litre	Baseline 1.6 litre NA
CO ₂ emissions (g/km)	130.7	166.0
Fuel consumption (litre/100 km)	5.52	7.00



4.3 Vehicle tractive effort.

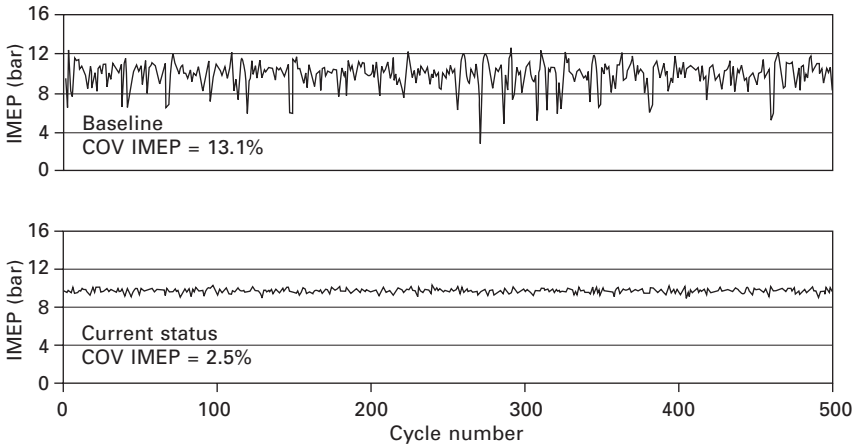
limited to 0.1 g/km at 130 kph whilst low exhaust temperatures improve NO_x trap durability. Very high load NO_x trap regeneration and desulphation were enabled through new control strategies using post-injection, variable valve timing and EGR.

The estimated on-cost for a 75 kW application in 2004 was €500–650, resulting in a cost/benefit ratio more attractive than that of a conventional diesel powertrain.

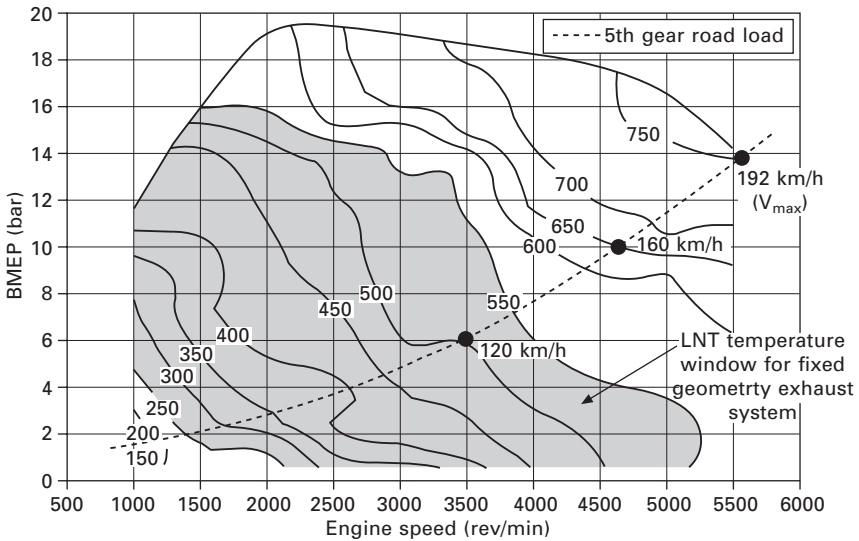
Lean operation – especially at high boost pressures – represents a more demanding environment for stable combustion, and the dual injection strategies developed in the single-cylinder work were further evolved in this programme to improve the combustion stability on the multi-cylinder engine. Additional investigations were conducted into both air motion and ignition energy effects (using a production ignition system) and significant improvements were achieved, as shown in Fig. 4.4.

One way of addressing concerns over low-speed torque and transient response is to take advantage of one of the key characteristics of the LBDI system: the cooler exhaust temperatures shown in Fig. 4.5. This made possible the use of a low-cost production VNT unit that was specified using the engine simulation code Ricardo WAVE. Transient performance of the LBDI engine with its VNT is, as shown in Fig. 4.6, directly comparable with that of the stoichiometric engine with its fixed geometry turbocharger.

The I3 engine in LBDI build specification was installed in a C-class passenger car as shown in Fig. 4.7. A full calibration was developed to deliver a LBDI vehicle demonstrator, with lean operation throughout the engine speed and load range. Acceleration tests were undertaken for the LBDI vehicle: the

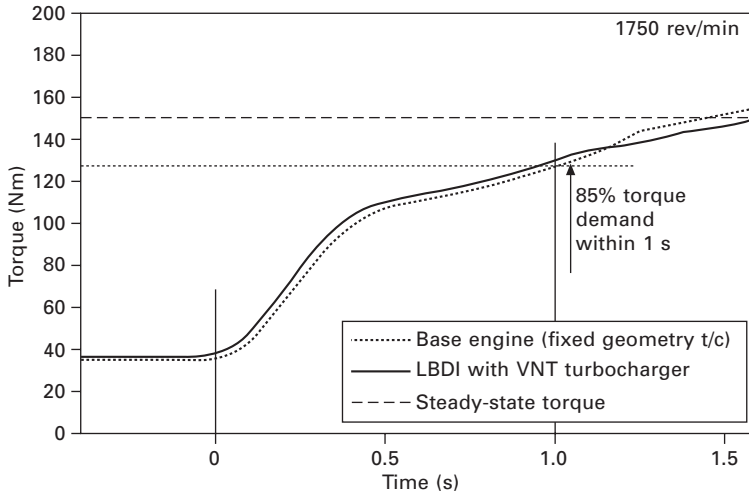


4.4 Combustion stability characteristics before and after combustion system development – 2000 rev/min, $\lambda = 1.4$, 50% MFB 26° CA ATDC.



4.5 Turbine-out temperature [°C].

time taken to accelerate from 1500 to 3000 rev/min was measured in each gear, starting under steady-state conditions at 1500 rev/min. These results are shown in Table 4.2, and are compared to the same model vehicle with a 1.6 litre naturally aspirated engine. Comparable acceleration times were achieved from the two vehicles. Table 4.1 shows the CO₂ emissions and fuel consumption results for the LBDI vehicle, compared with those for the baseline 1.6 litre naturally aspirated car. Both vehicles were tested at 1250



4.6 Transient performance comparison.



4.7 Vehicle installation of LBDI engine.

Table 4.2 Vehicle acceleration times for 1500–3000 rev/min (seconds)

Gear	LBDI vehicle	1.6L NA equivalent
2nd	3.7	3.1
3rd	7.3	6.6
4th	12.4	12.8
5th	20.2	23.4

kg inertia. The cumulative CO₂ emissions over the drive cycle are illustrated in Fig. 4.8. No LNT regeneration events occurred during the drive-cycle tests.

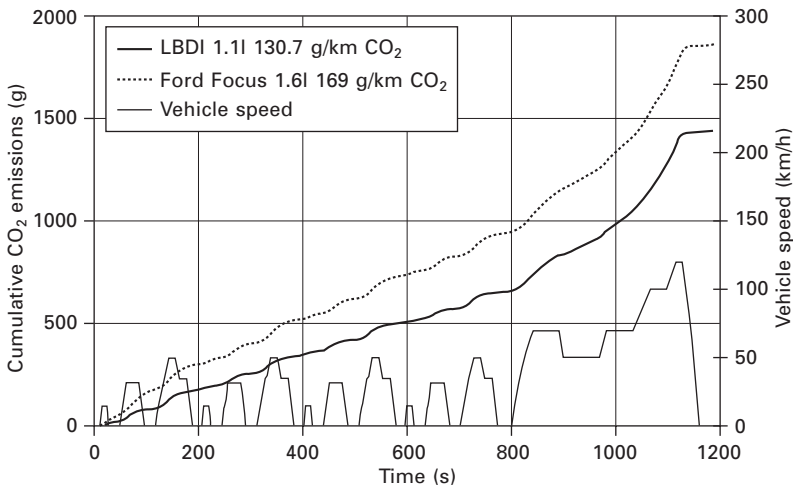
4.4 Exhaust emissions control: drive-cycle emissions

Any engine operating under lean conditions currently requires some form of lean NO_x aftertreatment and this has taken the form of a lean NO_x trap (LNT) for most successful production applications, typically in an underfloor location. As will be discussed later, an alternative is to use a urea-based selective catalytic reduction. As developed for LBDI, the system used was a LNT.

To achieve good trapping efficiency for NO_x within the LNT, its temperature must be maintained within the relatively narrow range of 250–550°C. The post-turbine exhaust temperature (Fig. 4.5) is about 60–100°C higher than the LNT inlet temperature and gives a good guide as to where there is potential for effective NO_x trapping and conversion with a fixed geometry exhaust system. The shaded region in the figure is from 250 to 550°C. Thus under drive-cycle conditions, the emissions control approach for LBDI can be broadly similar to that for a conventional lean stratified DISI engine.

4.5 Exhaust emissions control: off-cycle emissions

The emissions control system must be capable of surviving use to the maximum performance of the vehicle, as well as being durable enough to

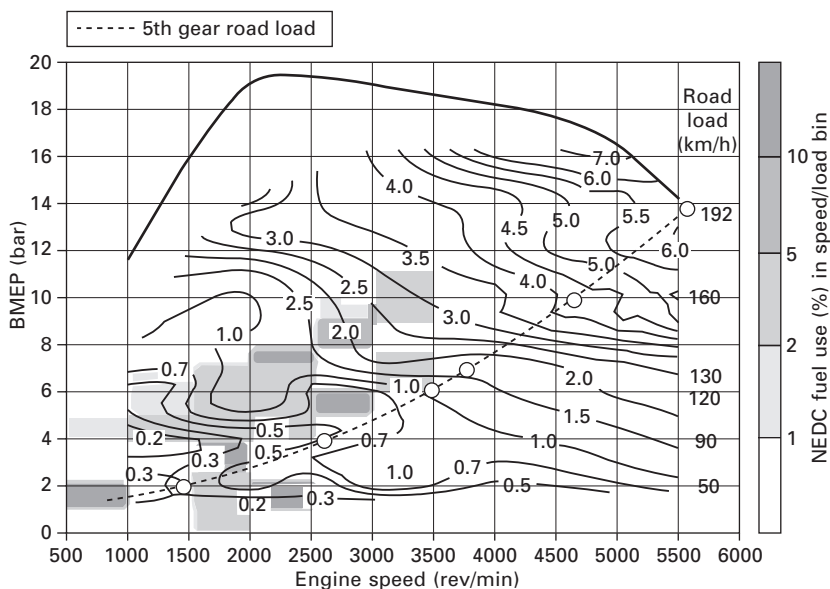


4.8 Cumulative CO₂ emissions over the NEDC drive cycle.

tolerate this routinely (referring, of course, to European high-speed driving). The temperature drop across the turbine, in addition to cooling along the exhaust system, is enough to lower the temperature to a safe level for LNT protection (750°C), even up to the maximum speed of the vehicle (Fig. 4.5). Importantly, high torque, low-to-medium speed driving (used predominantly in the real world by ordinary drivers) comfortably sits in the $200\text{--}550^{\circ}\text{C}$ exhaust temperature window where the LNT stores effectively.

Ricardo has investigated how to provide suitable conditions at the LNT for trapping and regeneration to allow clean operation over the complete operating envelope. To achieve trapping over the full range and achieve off-cycle emissions control requires shifting of the temperature seen at the LNT. Recent production approaches such as those introduced by VW on their FSI engine vehicles, and more recently by Daimler with their CGI engine in the C-class and CLK, have enabled the LNT inlet temperature to be managed, particularly to allow protection under high-speed driving conditions. Daimler showed that a temperature shift of more than 140°C was possible with their system. Clearly these approaches are valid for any LBDI installation.

LNTs require regeneration, the frequency of which will be directly related to engine-out NO_x levels and inversely related to trap storage capacity and trapping efficiency. The more frequent the regeneration, the worse the fuel economy penalty. Figure 4.9 shows the penalty of fuel economy to keep the LNT of an LBDI vehicle regenerated over the full envelope of

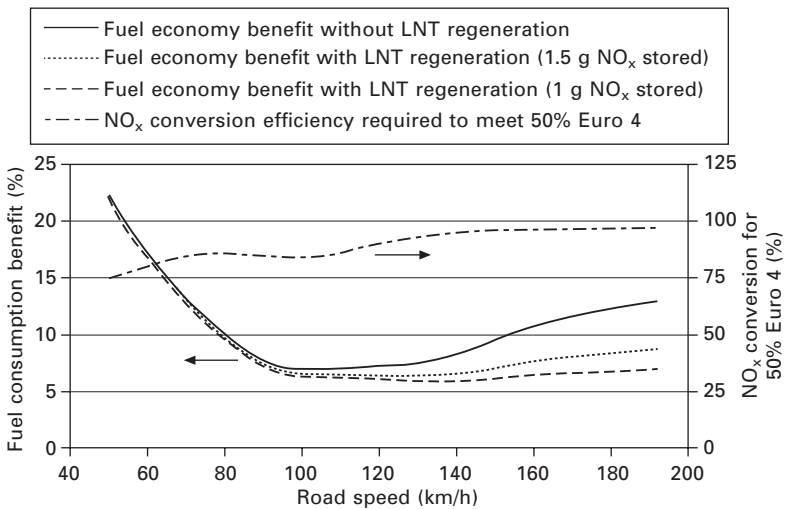


4.9 Regeneration fuel consumption penalty (%) for 1 g NO_x stored (2 g trap capacity), assuming $\lambda = 0.85$ for 4 s during regeneration.

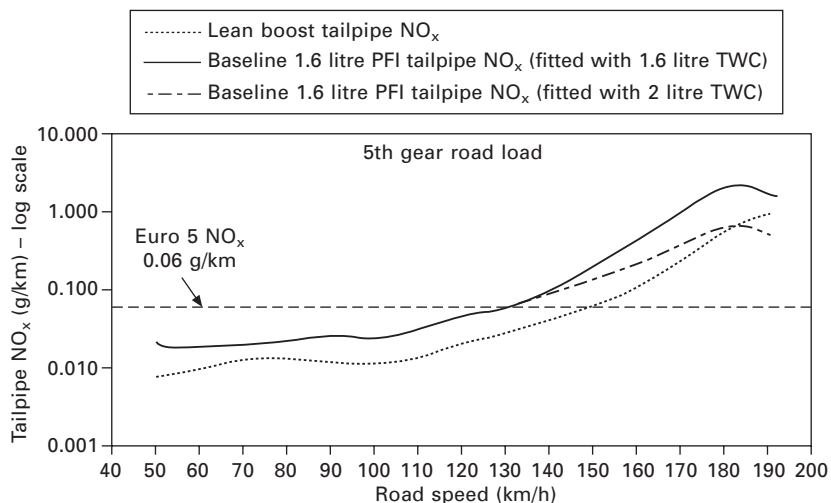
operation. Thus, an LBDI engine substituting an NA stratified DISI engine could achieve an additional 10% economy benefit over the NEDC cycle and a further 10% in the ‘real world’. Figure 4.10 shows that under some extreme driving conditions, LBDI still produces an economy benefit whilst delivering TWC-level NO_x conversion efficiencies. (As in any aftertreatment application, the conversion efficiencies are eventually limited by space velocity considerations.) The HC and CO emissions are much lower with the LBDI concept than for an enriched conventional engine. Assuming that a suitable LNT inlet temperature can be maintained, the tailpipe NO_x results shown in Fig. 4.11 would be feasible: <0.06 g/km (Euro 5) up to 130 kph and <0.1 g/km up to 160 km/h.

4.6 Selective catalytic reduction (SCR) NO_x control as an alternative to lean NO_x trap (LNT)

Selective catalytic reduction (SCR) based around urea is currently in use on European heavy-duty diesel applications and is being developed for use on light-duty diesel applications targeting US Tier 2 Bin 5 and below and Euro 6 emissions legislation. An on-board supply of aqueous urea (32.5 wt% urea in water) is required for exhaust NO_x control. Aqueous urea is injected into the exhaust upstream of an SCR catalyst. The urea undergoes the hydrolysis reaction (urea plus water produces ammonia and carbon dioxide) to deliver ammonia into the exhaust flow. Ammonia is a good reductant for NO_x under the excess oxygen conditions found in lean operating gasoline engines and



4.10 Lean Boost DI concept fuel consumption benefit – 5th gear road load.



4.11 Tailpipe NO_x emissions – 5th gear road load.

therefore can potentially be used for LBDI-type applications. The produced ammonia is stored on the SCR catalyst and reacts with the exhaust flow of NO_x to produce nitrogen and water.

There are three main issues with utilising urea-based SCR for gasoline applications. The first is to engineer the SCR catalyst temperature operating window to be favourable. SCR catalysts tend to have a broader operating window compared to LNT catalysts and therefore can potentially improve the total NO_x control of the application, independently of the drive-cycle, and hence can be more effective for NO_x control during off-cycle operation.

The secondly consideration is to allow sufficient on-board urea storage. The impact on urea consumption will be directly related to the engine-out NO_x emissions. This is analogous to the increased fuel penalty associated with more frequent LNT regeneration events under regions of high NO_x mass flow. For engines using urea-based SCR it is necessary to understand the amount of urea that needs to be stored on board the vehicle. It is understood that there will not be a European or US urea infrastructure at every fuel filling station. Therefore, the urea refill requirements will need to coincide with the annual vehicle service interval in Europe or the oil service interval in the US. Studies show that the calculated urea storage requirement for a typical US application, a 2000 kg SUV, would be in the range 14–21 litres. The lower end of the range assumes that the urea is refilled every 8000 km, at the same time as the oil change, and that the vehicle drives repeated FTP cycles. However, more aggressive US06 cycle driving may be more typical in the US and in this case the higher end of the range, 21 litres, would be required for 8000 km. In Europe, the calculated urea storage requirement

was made for a typical European application, an 1130 kg C-class passenger car. For this European application, the amount of NO_x that requires reducing is much less than for US applications over a given distance, but for a typical European 20 000 km service interval, the required urea storage is approximately 21 litres. This assumes continuous NEDC driving. Due to the large urea storage requirements, packaging of the urea tank might be a difficult issue for urea-based SCR in LBDI-type gasoline applications, but it remains an interesting alternative to LNT depending on precious metal costs, leading to the final point.

The third and final point is that the system must make economic sense against alternatives (LNT). It will be necessary to understand the cost impacts of using LNT or SCR based solutions. The LNT solution uses a precious metal based catalyst system, whereas the SCR solution requires a urea injection and storage system but uses a non-precious metal based catalyst system. In recent years the price of rhodium has increased significantly, rising by a factor of 10 in the period from mid-2003 to mid-2006. This has a big impact on the price of LNT systems. The cost differentials between SCR and LNT are related to the precious metal cost for LNT and the urea dosing and storage equipment for SCR. The price for urea dosing equipment will be fixed and independent of engine displacement, but the catalyst volume is dependent on engine displacement. Recently the price of rhodium has dropped back dramatically, changing again the balance between the cost of LNT and SCR systems.

4.7 Conclusions

Low CO_2 gasoline engines are needed as an essential part of any profitable powertrain portfolio. Further significant improvements in gasoline powertrain efficiency will be required to meet future fleet average CO_2 emission targets. A good method of achieving low CO_2 is by raising the specific torque levels of the gasoline engine; this allows a volumetrically smaller engine to replace a larger one – so-called ‘downsizing’. Downsizing approaches that are applied well not only reduce pumping losses and friction but deliver improved indicated efficiency benefits, which in turn deliver improvements over a wide range of operating conditions with a direct impact to the vehicle owner.

This chapter considers that the best fuel economy (lowest CO_2) is obtained with the lean boost direct injection (LBDI) approach. LBDI is a completely new engine operating approach and has been developed from research testbed to driveable vehicle. Operating under lean conditions throughout, the engine has been developed to deliver competitive power and torque, with superior transient low-speed torque compared to other turbocharged downsized approaches. A substantial fuel economy benefit of more than 20% has been measured compared to the base NA vehicle whilst being capable of

meeting half Euro IV emissions over the NEDC cycle. Critically, very low CO₂ performance is maintained under a wide variety of driving conditions, including high-speed autobahn use. The lean boost DI concept in particular offers CO₂ emissions comparable to that for an HSDI diesel engine with a significantly reduced cost penalty.

Production of the lean boost concept is dependent on control of NO_x emissions in an engine which operates lean at all engine operating conditions, including high load. This applies to all 'real world' driving conditions, not just over legislated drive cycles. Either LNT or urea-based SCR solutions would provide sufficient NO_x conversion in a lean boost application and the likely choice of application will be dependent on the price of precious metal loading required. At the height of the platinum and rhodium prices, the aftertreatment system costs for LNT were significantly higher than for SCR. The cost of the urea dosing and storage equipment for SCR redresses some of the higher LNT catalyst costs, but at those peak precious metal prices there was a net \$200–600 price difference for European and US applications respectively. Packaging the urea tank for SCR will be a difficult issue to resolve, but in applications where the urea tank can be packaged successfully, SCR would be the preferred solution in times of high precious metal prices.

4.8 Future trends

Extensive study has shown that lean boost provides a gasoline engine with the CO₂ emissions of a diesel at significantly reduced engine manufacturing cost. Developing economic lean NO_x aftertreatment systems to enable the widespread application of this technology across the new vehicle population is a critical issue; to date only premium vehicle applications have been made available.

The LBDI approach can be adapted to any of the other downsizing systems currently being developed for the future, including boosted ethanol-based approaches, downspeeding, boosted variable compression ratio; and deep Miller strategies. Without lean operation of the gasoline engine, there is too much fuel economy left untapped, which in the low-CO₂ world of the future will not be a tenable position. Thus, any future CO₂-optimised manufacturer's fleet must contain some or all of the elements of the lean boost strategy presented in this chapter. In the pursuit of ever better fuel economy and emissions, the future of the gasoline engine looks simultaneously promising, exciting and fascinating.

Exhaust gas recirculation boosted direct injection gasoline engines

A. CAIRNS, H. BLAXILL and N. FRASER,
MAHLE Powertrain Ltd, UK

Abstract: Downsizing is widely considered to be one promising method for improving the fuel consumption of the spark ignition engine. However, the associated rise in peak in-cylinder pressures and gas temperatures in a unit of high power density can result in an increased tendency to knock. The traditional method to avoid gasoline engine knock involves retarding the spark and/or cooling the mixture with excess fuel. While the regime of fuel enrichment is normally at loads higher than those encountered during existing drive cycle assessments, it is probable that full-load fuel economy targets and emissions legislation will emerge in future years. Various investigations have therefore been made into alternatives to fuel enrichment at high output, and the current chapter is concerned with the benefits and challenges of applying cooled exhaust gas recirculation under such higher loads.

Key words: spark ignition, direct injection, turbocharging, exhaust gas recirculation.

5.1 Introduction

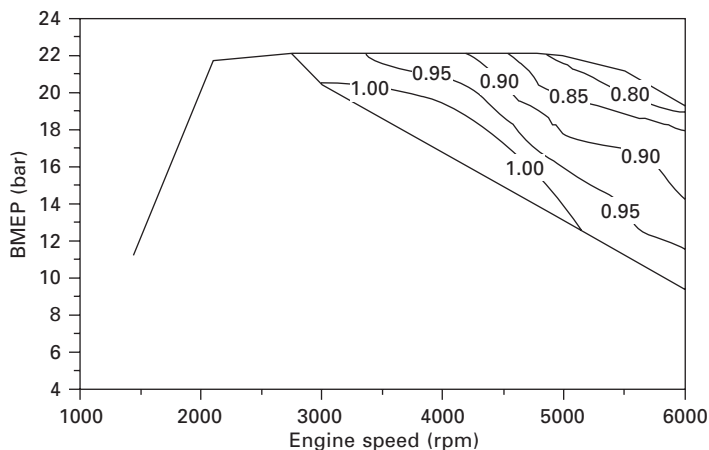
Evolving emissions legislation and concerns for diminishing fuel reserves continue to prompt automotive manufacturers to seek alternative forms of engine operation. In recent years, European CO₂ emissions targets have largely been met through increased diesel sales, rising above ~50% in some countries. However, the distillation of crude oil results in high proportions of both gasoline and diesel fuel. In terms of well-to-wheel energy expenditure and emissions, such diesel market penetration cannot continue indefinitely (1) and is not yet foreseen outside Europe (2). In order to meet future global emissions targets in the short to medium term, it will be necessary to improve the fuel consumption of the gasoline engine.

A large proportion of automotive engine operation is spent at part-load and this is where fuel economy targets are currently most concerned. However, under light loads the breathing losses of the spark ignition (SI) engine are usually at their highest levels. Downsizing has therefore become widely considered to be one promising method for improving the fuel consumption of the gasoline engine (3–5). The basic principle is to reduce the capacity of the engine and hence enforce a larger proportion of operation to higher loads.

As a result, the pumping losses of the engine can be significantly reduced for a given road load requirement. In order to compensate for the inherent power loss, some form of intake air pressure charging is usually required. However, the associated rise in peak in-cylinder gas temperatures and pressures in a unit of high power density can result in an increased tendency to knock. The onset of such knocking combustion is generally accepted to be the result of excessive energy release rate via exothermic centres in the end-gas beyond the entraining edge of the flame (6). Such auto-ignition is often multiple-centred and may occur as one or more of three identified modes (namely deflagration, detonation and developing detonation). The developing detonation mode, which can be induced via preceding deflagration events, is believed to be the most damaging in the SI engine (7).

Current methods to avoid knock involve retarding the spark and/or cooling the mixture with excess fuel, albeit with the penalty of increased fuel consumption and operation away from the fixed stoichiometric mixture strength required for efficient catalytic conversion. However, even under such conditions, in an engine of high energy inhalation rate it is usually still necessary to reduce the geometric compression ratio to avoid knock. As a result, in recent years various workers have investigated the synergy between downsizing and direct fuel injection, the charge cooling effects of which facilitate increased compression ratio and improved thermal efficiency (8–12). However, such injection systems are not without their own challenges, including maintaining robust pollutant emissions control.

Shown in Fig. 5.1 is a map of relative air-to-fuel ratio (λ) for a typical turbocharged gasoline direct fuel injection engine. While the regime of fuel enrichment is normally at loads higher than those encountered during most



5.1 Relative air-to-fuel ratio (λ) speed-load map for a typical turbocharged gasoline engine.

existing drive cycle assessments, it is possible that full load fuel economy targets and emissions legislation will emerge in future years. Furthermore, the more aggressive the downsizing approach, the more often the over-fuelling region will be encroached upon during 'real world' driving conditions. Various investigations have therefore been made into alternatives to fuel enrichment at high output. Of these, the most promising methods studied in recent years have included cooled exhaust gas recirculation (EGR), lean boost (13, 14), indirect water injection (15) and so-called turbo-expansion (16), and it is the EGR approach that is the topic of this chapter.

The concept of using cooled EGR to improve gasoline high-load fuel consumption is not a new one. Brustle and Hemmerlein (17) studied the effects of cooled external EGR on the performance of a four-cylinder turbocharged engine operating under stoichiometric gasoline fuelled conditions. At high engine speed and load and a pre-turbine temperature limit of 1000°C, an increase in brake mean effective pressure (BMEP) of ~1 bar was obtained when recycling up to ~12% EGR. These workers postulated that use of EGR could allow small increases in compression ratio to be tolerated, with improved fuel economy across the entire operating map. Specific details of the EGR circuit performance and layout were not reported.

In later work, Grandin *et al.* (18) investigated the influence of cooled external EGR at high loads in a turbocharged four-cylinder 2.3-litre gasoline port fuel injection (PFI) unit. The EGR gases were taken from before the turbine, passed through a cooler and introduced to the inlet downstream of the compressor (post-intercooler). It was concluded that EGR dilution served to decrease the rate of mass burning at high speed and load, with reduced temperature rise during combustion and significant inhibition of knock. Although the results presented were limited to 4000 rpm, these workers demonstrated the potential of EGR to replace fuel enrichment and vastly improve emissions of carbon monoxide (CO) and hydrocarbons (HC). Later on (19), the technique was compared with excess air dilution at speeds and loads of up to 5000 rpm and 16.5 bar BMEP respectively. Although combustion stability was observed to deteriorate in each case, it was apparent that EGR facilitated the more stable burn and presented significant advantages in terms of reducing emissions of nitrous oxides (NO_x). In an alternative but similar study in a turbocharged four-cylinder 2.0-litre unit, Duchaussoy *et al.* (20) concluded that introducing EGR provided significant benefits over excess air dilution in terms of transient turbocharged engine operation, with a smaller increase in compressor size required. Specific details of the pre-to-post compressor EGR feed ratio (with the flow divided via a three-way valve) were not provided. Elsewhere, Diana *et al.* (21) also demonstrated the knock inhibition effects of EGR at moderate to high output in a PFI research engine, albeit without pressure charging and hence incurring significant power loss. Regardless, these workers confirmed the effects earlier postulated by

Brustle and Hemmerlein, with up to ~10% improvement in fuel economy achieved at moderate load with the geometric compression ratio increased from 10 to 13.

In more recent work, Alger and co-workers (22) studied the benefits of EGR when applied to a modern production turbocharged gasoline DI engine. This study clearly demonstrated the potential of EGR across the entire excess fuel operating map, achieving reductions in CO₂ of up to ~20% that were associated with reduced knocking tendency and hence lower exhaust gas temperatures. Reductions in CO of up to ~95% were also recorded at high speed and load. Elsewhere, Kapus *et al.* (23) have insinuated that the EGR technique should perhaps be combined with a water-cooled exhaust manifold to reduce exhaust gas temperatures to a level where diesel-like variable geometry turbochargers could be used for spark ignition applications. In summary, partially due to strong synergy with the engine downsizing approach, the so-called ‘wide open throttle EGR’ (WOT-EGR) technique is now subject to significant research efforts, including those at MAHLE Powertrain (24, 25).

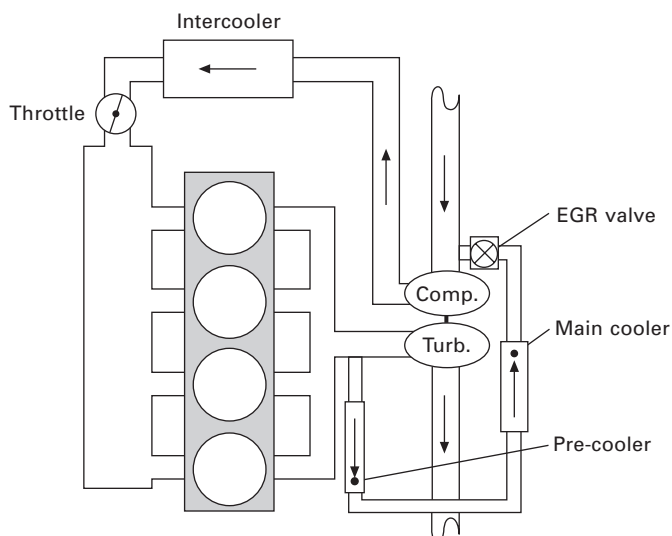
5.2 Fundamentals of wide-open-throttle exhaust gas recirculation (WOT-EGR) operation

5.2.1 Knock suppression effects

The general principle of spark-ignited WOT-EGR operation is to return cooled exhaust gases to the cylinder at moderate to high loads, reducing unburned gas temperatures to such a level where knock can be adequately suppressed and/or the temperature of the outgoing exhaust gases is sufficiently low so as to preserve the exhaust components. In order to understand the thermodynamic principles involved, a number of experiments have been made by the authors. These experiments were performed in a modern turbocharged four-cylinder direct fuel injection engine, some details of which are provided in Table 5.1. The combustion chamber of this engine was of four-valve pent-roofed design, with the fuel injector located between the two inlet valves and fuel directed towards the flat piston crown. Such a chamber layout was considered to be acceptable for the homogeneous operation intended. The EGR circuit fitted to the engine for these tests is illustrated in Fig. 5.2 and can be considered to be a ‘hybrid’ version of the conventional low-pressure and high-pressure EGR gas circuits, with EGR withdrawn pre-turbine and then passed through the two cooler assemblies and the EGR control valve. The gas was then fed back to the intake system well upstream (~0.5 m) of the turbocharger compressor in an attempt to attain accurate mixed gas temperature readings at the compressor entry. This layout was chosen to ensure that high EGR flow rates could be obtained, but is arguably not the most practical solution

Table 5.1 Details of the research engine used for the fundamental studies

Number of cylinders	4
Bore (mm)	87.5
Stroke (mm)	83.1
Geometric compression ratio	9:1
Variable valve timing	Dual independent (35°c.a. inlet, 55°c.a. exhaust)
Cam duration (end of ramp)	Inlet: 234°c.a., exhaust: 220°c.a.
Fuel injectors	Bosch (6-hole, 25 cc/s)
Peak fuel rail pressure	115 bar
Fuel	98 RON unleaded gasoline
Turbocharger	Mitsubishi model 16T-6 cm ²
Spark plugs	NGK HR7 high ignitability
Ignition coils	Bosch coil-on-plug (100 mJ)



5.2 Schematic showing the 'hybrid' EGR circuit used to uncover the fundamental effects of EGR boosted operation.

as discussed further later on. Additional details of the engine assembly have been presented elsewhere (24, 25).

The experiments were specifically concerned with directly comparing the effects of cooled EGR with those of conventional excess fuel or excess air charge dilution at fixed engine speed and load (4000 rpm, 19 bar BMEP) under knock-limited conditions. By increasing the mass of fuel, air or cooled EGR charge dilution at this site, it was possible to demonstrate the thermodynamic effects of each method of dilution on engine combustion, performance and emissions. At this speed and load it was just still possible to

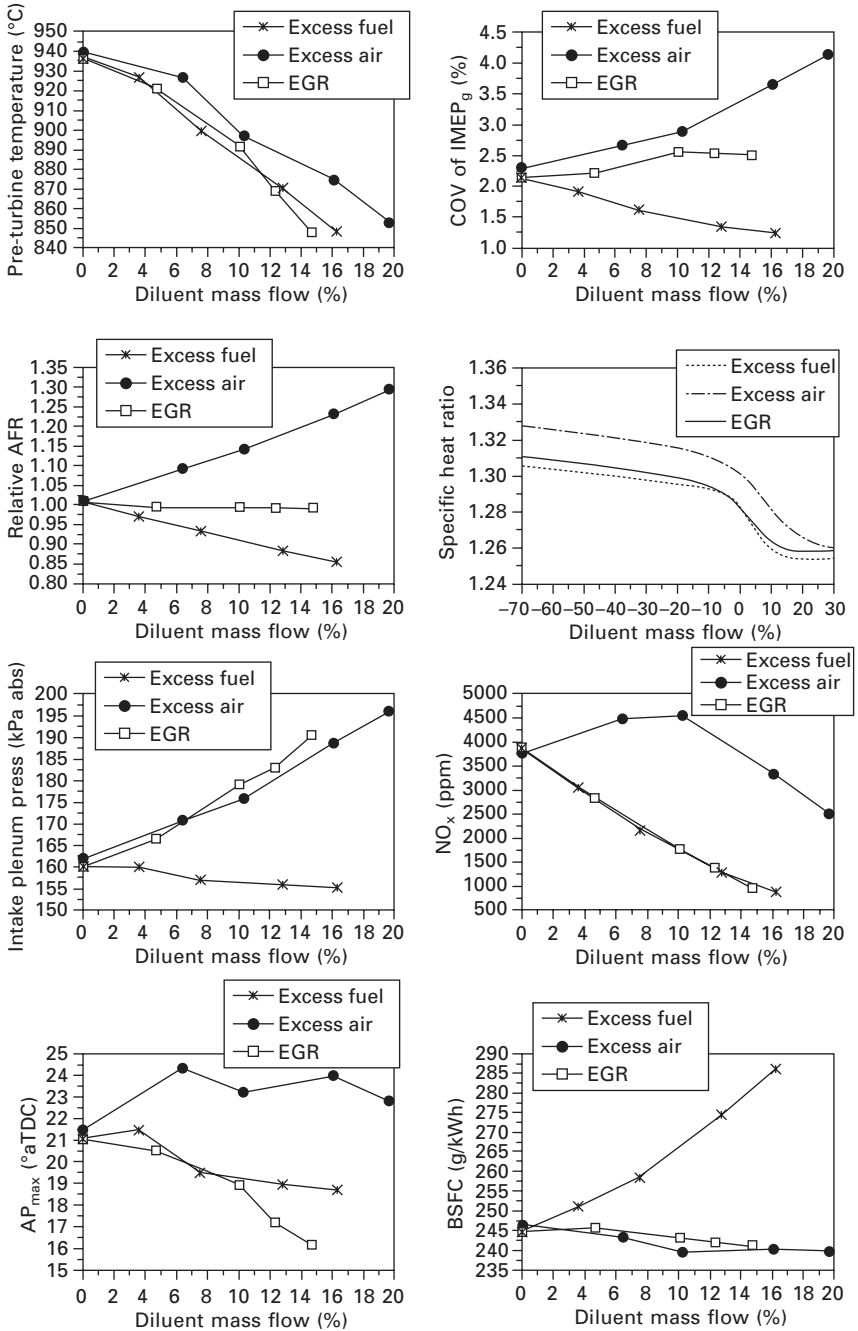
operate the engine under stoichiometric fuelled conditions. Therefore, these experiments do not allow the benefits of EGR on over-fuelling reduction to be directly quantified. Rather, the tests were performed to isolate the effects of increased EGR, excess fuel or excess air on knock-limited combustion when starting under stoichiometric conditions (as often incurred at low to moderate engine speeds).

During these tests, the spark timing was set to borderline detonation minus 1.5° (BLD – 1.5°) at all sites. The pre-turbine gas temperature under such conditions was approaching $\sim 950^\circ\text{C}$, which is the limit imposed on many current production turbocharged engines. The inlet charge temperature was fixed (40°C) as were the start of fuel injection timing (300° bTDC) and fuel rail pressure (115 bar), previously optimised for homogeneous operation. The inlet and exhaust valve timings were also held constant at 88° crank after top dead centre (88° aTDC) maximum opening position (MOP) and 100° bTDC MOP respectively.

The corresponding key measurements are shown in Fig. 5.3. Firstly, the meaning of the x -axis on the graphs is dependent on the case being considered. The hollow squares represent the data set produced using cooled external EGR dilution under stoichiometric fuelled conditions. Here, the x -axis is simply the ratio of CO_2 recorded in the inlet to that simultaneously monitored in the exhaust. The second data set (solid circles) was produced using excess air charge dilution, where the x -axis is the increase in mass of air relative to the total exhaust mass flow. Finally, the stars denote data produced using excess fuel, where the x -axis is the additional percentage of fuel relative to the original stoichiometric mass of fuel at the start of the sweep under stoichiometric conditions. Owing to these differences, the x -axes allow only qualitative comparison of each method of dilution.

Observing Fig. 5.3, it can clearly be seen that all three methods of charge dilution reduced the exhaust gas temperature as required. However, to maintain load when using either gaseous form of charge dilution, it was necessary to significantly increase the intake charge boost pressure, with the wastegate duty cycle increased to a maximum of 73% (excess air) or 100% (EGR) respectively at the end of each sweep. In contrast, the boost pressure marginally decreased when employing fuel dilution, which was the result of species dissociation and hence potentially increased indicated mean effective pressure (IMEP) under such conditions.

While all three methods seemed effective at lowering exhaust gas temperatures, in terms of knock suppression, only increasing amounts of fuel or EGR allowed the angle of peak in-cylinder pressure (AP_{max}) to be further advanced. In turn, this resulted in poor combustion stability in the leanest case, with the maximum coefficient of variation in gross IMEP (COV of IMEP_g) greater than 4% compared with a constant value of $\sim 2.5\%$ when using the highest mass flow of EGR. The lowest variation in IMEP was



5.3 Key parameters during excess fuel, excess air and cooled EGR sweeps at 4000 rpm and 300 Nm/19 bar BMEP.

observed under rich fuel conditions, associated with the faster rate of mass burning.

To fully understand these observations, a 'reverse-mode' thermodynamic analysis of the data was performed using the commercial modelling package GT-Power. The three cases simulated were those at the end of each sweep at a pre-turbine temperature of $\sim 850^\circ\text{C}$. The GT-Power engine model was constructed to ensure accurate simulation of the air path. Cylinder head port flow coefficients were determined in advance using an in-house port flow rig. Computed and measured values of volumetric efficiency were maintained within a maximum error of 3%. Combustion was simulated using the well-known Wiebe function and in-cylinder heat transfer was computed using the Woschni correlation.

Observing the corresponding predictions in Fig. 5.3, the lean charge incurred a higher ratio of specific heats (γ) throughout the cycle. This is a well-known phenomenon for lean operation and one reason why lean burn engines exhibit higher thermal efficiencies at part-load (26). At the high loads tested here, the higher value of γ was associated with higher unburned gas temperatures during compression and flame propagation, which presumably explained the lack of improvement in knock suppression observed when lean. Efforts to expand the lean operating regime by increased in-cylinder charge motion or some other technique would help but may add complexity and cost. A significant factor that must be considered is emissions after-treatment, with a vast increase in engine-out emissions of NO_x observed when lean. It could be argued that lean NO_x after-treatment could be used to alleviate these effects. However, the associated on-cost and also the high frequency at which such a NO_x trap may have to be purged if used often at high load must be considered. EGR seems to present the best compromise in terms of allowing efficient three-way catalytic conversion of all key engine-out emissions, especially if stoichiometric operation can be maintained across the entire operating map.

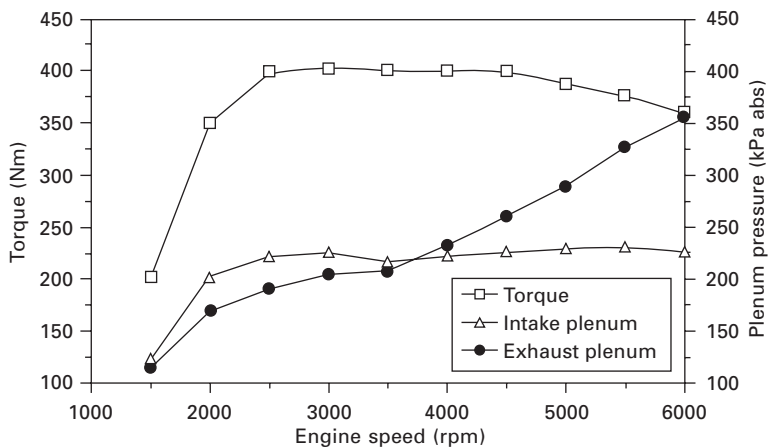
Given that the engine could still be operated under stoichiometric conditions with a pre-turbine gas temperature of 950°C , the test results in Fig. 5.3 cannot be used to quantify the real-world improvement in fuel economy when replacing excess fuel with cooled EGR, although this is shown later on. However, the results do still indicate the potential sources of fuel consumption improvement under conditions where stoichiometric operation cannot be maintained. Clearly, a large fuel economy penalty was observed when using excess fuel, with the brake specific fuel consumption (BSFC) deteriorating by 17% during the relative air-to-fuel ratio (λ) sweep from $\lambda = 1.0$ to $\lambda = 0.85$. At this particular site, a second small additional benefit in fuel economy could be incurred using EGR to advance AP_{max} further towards the optimum, arguably demonstrated during the EGR tests with BSFC improved by $\sim 1.5\%$ during the EGR sweep at $\lambda = 1$. However, it was

not always possible to achieve such combustion phasing benefit when using cooled EGR, particularly at higher engine speeds as discussed below.

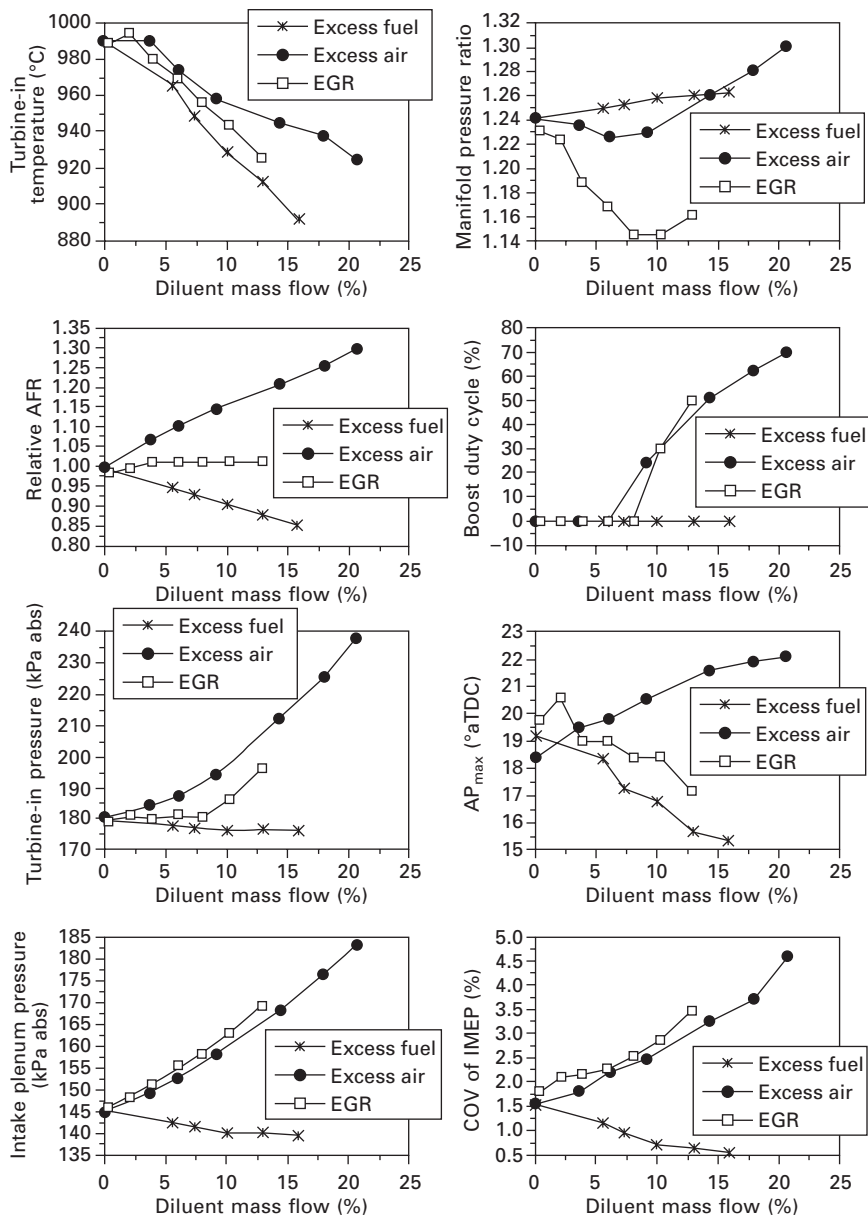
5.2.2 Engine speed effects

When specifying a single-stage turbocharger for a gasoline engine, it is usually necessary to compromise between acceptable low speed torque (compressor run-up) and peak power. As a result, the smallest possible compressor wheel must be selected, while still allowing sufficient headroom for operation at altitude. Owing to the required match of turbine and compressor and also the restrictions in the exhaust system, most turbocharged gasoline engines exhibit a significant increase in exhaust back-pressure at higher engine speeds, as illustrated in Fig. 5.4. This may become problematic to combustion if cooled EGR charge dilution is employed but sufficient hot residual gas scavenging is not achieved.

The influence of increasing exhaust back-pressure at higher engine speed is shown for the three diluent cases in Fig. 5.5. This data was produced at 5500 rpm, 250 Nm and 15.8 bar BMEP (BLD – 1.5°) using the engine described above. During these tests, the engine was initially operated near the maximum (hardware-limited) exhaust gas temperature of ~990°C under slightly rich conditions ($\lambda = 0.98$). The air charge temperature was again controlled to $40 \pm 1^\circ\text{C}$. The cam timing (inlet = 90° aTDC MOP, exhaust = 100° bTDC MOP), fuel injection timing (340° bTDC) and fuel pressure (115 bar) also remained fixed. When in use, the EGR was fed pre-compressor as described previously (hybrid EGR circuit).



5.4 Torque and plenum pressures for a four-cylinder turbocharged gasoline engine, showing typical exhaust pressure increase at high engine speeds.



5.5 Key parameters during excess fuel, excess air and cooled EGR sweeps at elevated engine speed (5500 rpm, 250 Nm).

In brief, at higher engine speeds it can be seen that the use of either cooled EGR or excess air again required the engine to be operated at significantly higher boost pressures, with the intake throttle fully opened and subsequently

the wastegate progressively closed. In turn, particularly when lean, a significant increase in exhaust back-pressure and exhaust-to-inlet manifold pressure ratio ('EGR pressure ratio') was incurred, rising from 1.24 to 1.3 during the excess air sweep. Such increase in back-pressure with the fixed cam timings may have resulted in increased trapped residuals, which would be detrimental to knock. Furthermore, the use of excess air or EGR resulted in prolonged combustion duration (25), which equally may have contributed to the retarded combustion phasing at higher speeds. Whether residual or prolonged combustion duration induced, this retarded phasing ultimately resulted in unacceptable combustion stability, especially when lean with the COV of $IMEP_g = 5.2\%$ compared with 0.63% for fuel or 3.5% with EGR.

In summary, it would appear that in the high speed and load region, some cooled EGR will be desired to reduce excess fuelling but, in turn, any increase in manifold pressure ratio and/or combustion duration may result in a retarded combustion event. Such a situation may escalate to the point where stable combustion cannot be achieved at the highest speeds and loads. The additional boost required when using EGR must also be considered. At the least, many applications will require a revised match of turbine and compressor to achieve the best fuel economy improvements. Whether such improvements can be realised in production is dependent on both the specific engine performance targets and also the EGR circuit design and it is the latter which is the next topic of this chapter.

5.3 Exhaust gas recirculation (EGR) circuit design

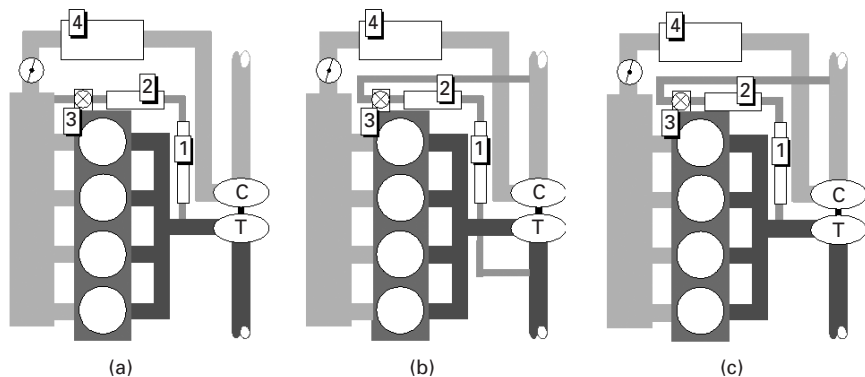
5.3.1 EGR circuit layout

The ideal EGR gas routing is highly dependent on application. Previously, external EGR has been used on gasoline engines for part-load emissions control, especially within the US market for NO_x reduction and also more recently in many DI engines employing a stratified charge (27, 28). In both applications, the exhaust gases are typically taken from either the exhaust plenum or one exhaust runner and passed back to the intake manifold. The ideal requirements of such a circuit include minimised gas dead volume, a fast-reacting EGR valve located close to the inlet ports, closed loop control of the EGR gas flow rate and valve de-icing capability (29). Such arrangements typically allow large amounts of EGR to be used at lower engine loads but may not always be suitable for the use of cooled EGR at high load.

Shown in Fig. 5.6 are three possible layouts previously considered for gasoline EGR boosted operation (22, 24, 25). A comparison of the advantages of each circuit is set out in Table 5.2. The so-called high-pressure EGR circuit involves routing the exhaust gases from pre-turbine to post-compressor. This layout is arguably easier to implement where significant transient engine

Table 5.2 Advantages and disadvantages of different EGR circuit layouts

Post-compressor (high-pressure)	Pre-compressor (low-pressure)	Pre-compressor (hybrid)
<i>Advantages</i>		
<ul style="list-style-type: none"> Compressor durability Compressor efficiency Minimised EGR dead volumes 	<ul style="list-style-type: none"> Reduced EGR cooling demand Equal EGR distribution Improved turbine wheel response 	<ul style="list-style-type: none"> High EGR rate Equal EGR distribution
<i>Disadvantages</i>		
<ul style="list-style-type: none"> Limited EGR driving forces, especially at low speeds Difficulties in achieving equal EGR distribution Moderate to high EGR cooling 	<ul style="list-style-type: none"> Compressor durability (e.g. water droplet impact) Compressor efficiency Increased compressor size Increased EGR dead volumes 	<ul style="list-style-type: none"> Compressor durability (e.g. water droplet impact) Compressor efficiency Increased compressor size Transient response High EGR cooling demand



5.6 (a) High-pressure, (b) low-pressure and (c) hybrid EGR circuits. Key to components: 1 = pre-cooler, 2 = secondary cooler, 3 = EGR valve, 4 = intercooler, C = compressor, T = turbine.

operation is expected, with the gases ideally fed directly to the inlet ports for best response. Such circuit designs are currently employed in many diesel engine applications, albeit often in conjunction with variable geometry turbochargers that provide an additional degree of control over the EGR rate (30).

The so-called low-pressure EGR circuit involves post-turbine to pre-compressor EGR gas routing. This layout reduces EGR cooling demand and

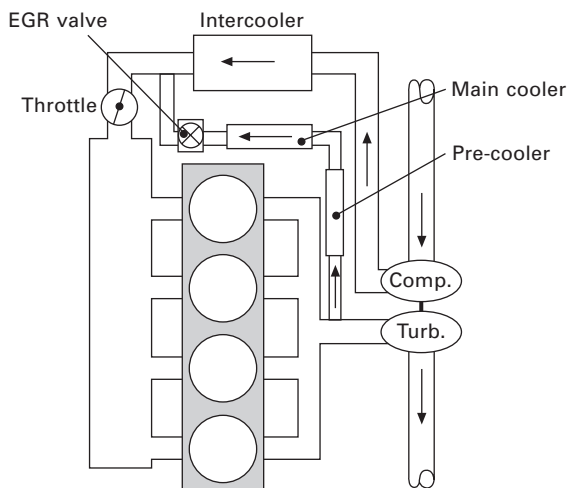
more easily ensures thorough mixing of the gases. However, large EGR gas dead volumes are inherently incurred and complex gas/coolant temperature control and/or filters may be required to minimise water pooling and/or droplet impact on the compressor wheel. Compressor wheel coatings and/or enhanced materials may help alleviate such effects but these are not currently readily available. The final layout, previously used by the authors, is the so-called hybrid EGR circuit, which is arguably the least practical solution. This layout incurs similar disadvantages to the low-pressure circuit design but is also a poorer arrangement for the turbocharger, with the possibility of both reduced turbine efficiency and high compressor work. However, the hybrid circuit potentially allows the highest EGR rates to be obtained and has been used by the authors to compare the effects of pre-versus post-compressor supply of cooled EGR at high speed and load, as summarised below.

5.3.2 Pre-versus post-compressor EGR feed

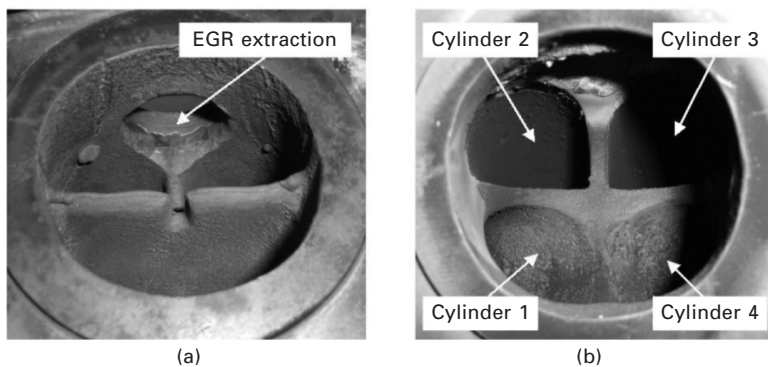
For a typical production single-stage turbocharged DI engine, post-compressor EGR routing may be preferred in many cases to reduce excess fuelling at high speed and load. This approach reduces issues with EGR dead volumes and compressor wheel durability. However, successful application is dependent on achieving good cylinder-to-cylinder EGR distribution, maintaining stable combustion and achieving sufficient EGR rate, which is not always readily feasible. Simply increasing the back-pressure via some external means is usually unfavourable to fuel economy. A pre/post compressor switching feed may help alleviate such effects but could be very difficult to control on a transient basis and possibly requires a complex setup of EGR valve(s).

Regardless of such problems, there has been little detailed published information on the possible thermodynamic differences of pre- and post-compressor EGR for gasoline applications. As such, a comparison has been undertaken at constant high engine speed and load (5500 rpm, 250 Nm and 15.8 bar BMEP, BLD – 1.5°). The pre-compressor circuit used was based on the hybrid system first shown in Fig. 5.2. A schematic of the post-compressor gas routing used is set out in Fig. 5.7, with the EGR returned post-intercooler rather than post-intake throttle. This was not ideal but avoided EGR distribution issues. The location of the pre-turbine EGR gas pick-up was similar in each case and is illustrated in Fig. 5.8. Observing Fig. 5.8(b), it was necessary to machine down the original exhaust runner splitter plates to maximise the EGR rate. The fact that the EGR gases were taken before the turbine in either case means that the current comparison cannot identify any benefits of a low-pressure post-turbine EGR pick-up. However, differences in compressor performance would still be identifiable and this comparison was therefore considered to be an appropriate first step.

A dual gas-to-water EGR cooler assembly was employed in both circuits,



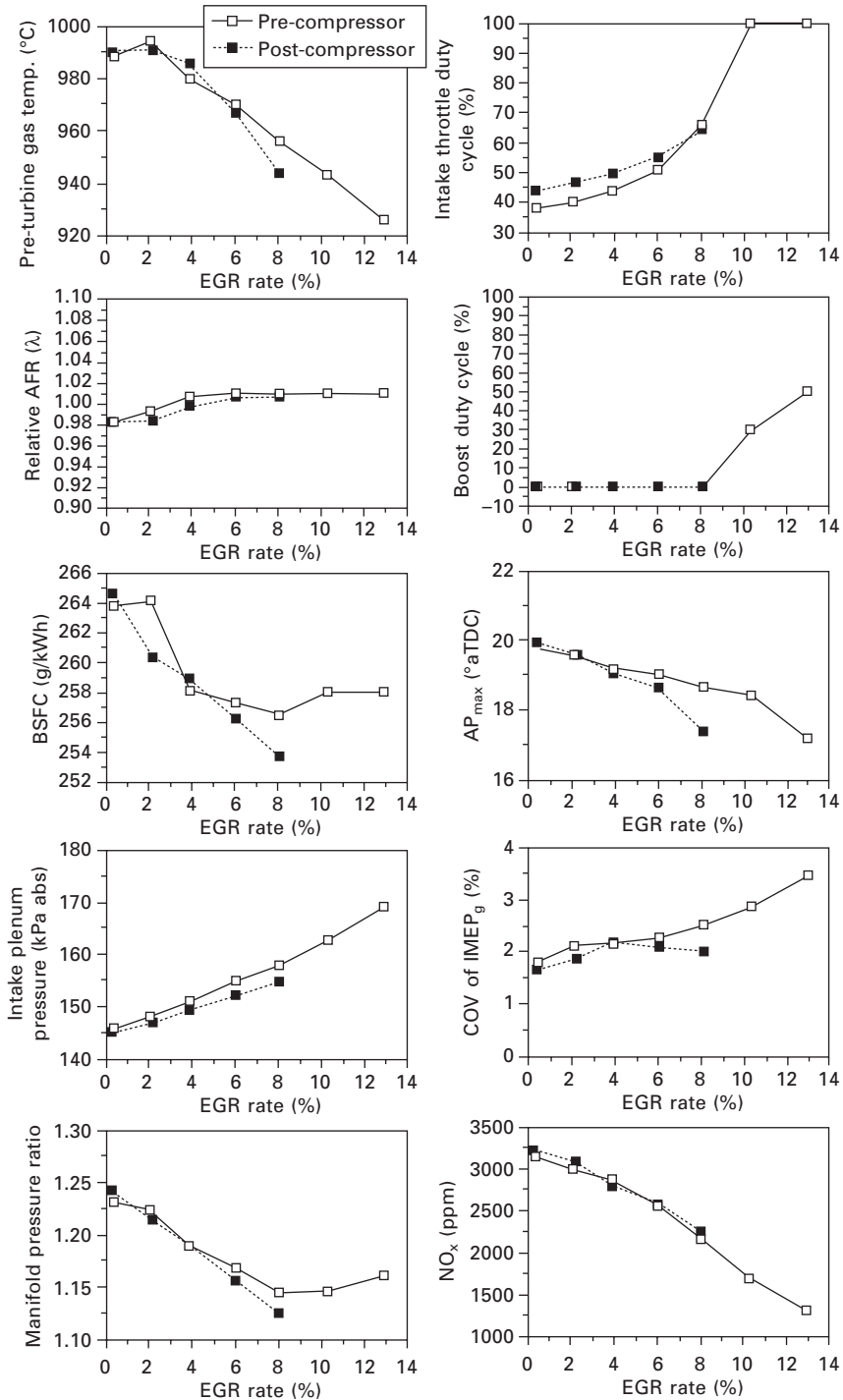
5.7 Schematic showing the high-pressure EGR circuit used for the experiments.



5.8 (a) Original and (b) modified exhaust plenum showing the machining of the exhaust runner splitter plates.

where the first cooler was of stainless steel construction and was used to remove the bulk of the heat, and the second was of more conventional multi-tube design and was used to achieve the required EGR temperature set point. The intake plenum gas temperature had again been closely controlled to 40°C via the intercooler and EGR coolers. All other test conditions remained as described previously at this site (see Section 5.2.2).

Shown in Fig. 5.9 are the key test results. Initially, the engine was operated with the exhaust gas temperature at ~990°C, under slightly rich fuel conditions. The maximum post-compressor EGR rate was ~8%. At this EGR level, both systems could be operated with a stoichiometric fuel-air

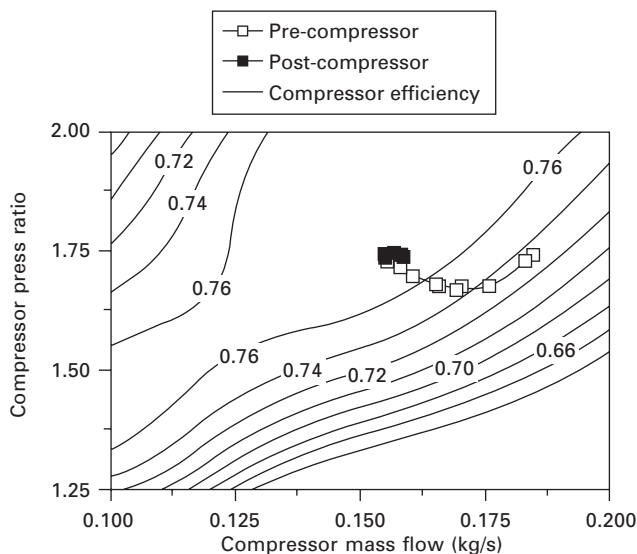


5.9 Key parameters during pre- and post-compressor EGR sweeps at elevated engine speed (5500 rpm and 250 Nm/15.8 bar BMEP).

mixture. However, the post-compressor route appeared to incur a slightly lower exhaust temperature ($\sim 10^\circ\text{C}$), marginally better fuel consumption (254 vs 257 g/kWh), reduced intake plenum pressure (154 vs 158 kPa), lower compressor work (~ 9.4 vs ~ 10.5 kW), decreased demand on the turbine and hence lower exhaust-to-inlet manifold pressure ratio. The total increase in intake plenum pressure with 8% EGR was 13 kPa (pre) or 9 kPa (post) respectively. Without EGR at this relatively moderate load site, the engine was still operating with a partially closed intake throttle. As EGR was added, this throttle was fully opened, then, for pre-compressor feed, the wastegate was partially closed.

Given the observed differences in manifold pressure ratio at 8% EGR, it is possible that an increased mass of internal EGR was trapped in the pre-compressor case. Such marginal increase in internal EGR cannot be easily computed but is possibly evident in the results, with combustion phasing further advanced and better combustion stability in the post-compressor case. The fact that engine-out emissions of NO_x were similar, despite an earlier angle of peak in-cylinder pressure in the post-compressor case, may also be indicative of the small differences in EGR rate incurred. The timing of the spark was 38° bTDC or 39° bTDC for pre- or post-compressor feed respectively. The engine-averaged peak in-cylinder pressure was 74.5 bar (pre) or 76.8 bar (post). The air charge temperature had again been closely controlled to 40°C .

Finally, shown in Fig. 5.10 are the loci of the EGR sweeps superimposed on



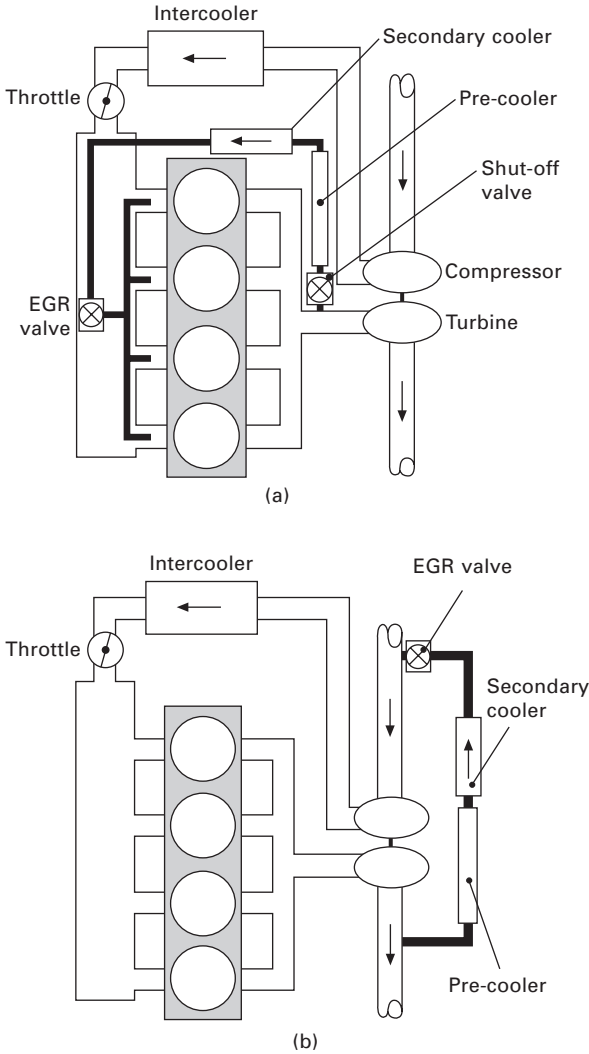
5.10 Loci of operation superimposed on the turbocharger compressor map.

the turbocharger compressor map. In the post-compressor case, the compressor pressure ratio remained around a constant value of ~ 1.74 due to the intake throttling at the start of each sweep (as the throttle was further opened the compressor pressure ratio would have dropped without EGR being added). In summary, when sufficient EGR rate could be achieved, post-compressor supply appeared favourable at high speed and moderate load, allowing reduced compressor work and with higher compressor efficiency maintained under the conditions tested. Despite these observations, it is still likely that a revised match of compressor and turbine would be required to achieve the highest engine loads due to the additional boost requirement when using EGR with any EGR circuit design (as quantified over a mapped area later on). Further work is required at different sites to verify the observations of increased internal EGR using pre-compressor supply, but this observation arguably also seems logical given that passing the EGR through the compressor clearly required higher compressor (and hence turbine) work.

5.3.3 EGR valve location effects

The location of the EGR valve is critical to the dead volume of EGR and hence the transient response of the engine. Shown in Fig. 5.11 are example solutions for a high-pressure and a low-pressure EGR circuit. For the high-pressure circuit, ideally the EGR control valve should be located as close as possible to the intake ports to allow fast EGR gas shut-off and also to minimise any EGR fouling within the intake air path. However, if a pre-turbine gas pick-up is to be used in a high-pressure or hybrid circuit, the detrimental effects of the open volume of the circuit upstream of the EGR valve must also be considered. In this case an additional or replacement hot-side valve may be required for reasons discussed in more detail below. For the low-pressure circuit, such effects on the turbine are eliminated and a cold-side valve located close to the compressor entry may suffice provided hot spots on the compressor wheel can be avoided and the EGR pipework is installed so as to avoid water trapping.

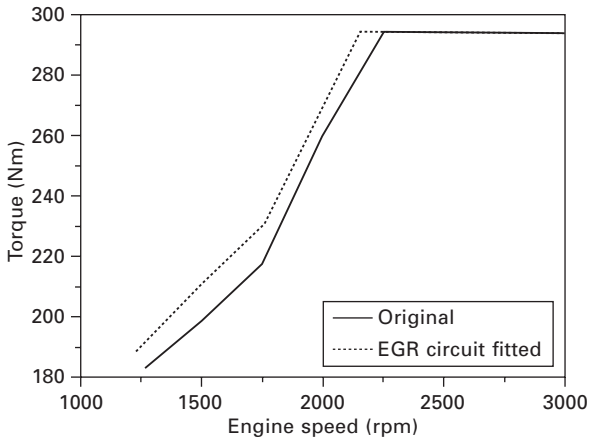
The influence of large EGR dead volume with a pre-turbine gas pick-up is evident in the two full-load torque curves set out in Fig. 5.12. This data was produced using a modified four-cylinder turbocharged production engine. The details of this engine and the high-pressure EGR circuit employed are provided later in Section 5.4. Shown in Fig. 5.13 are corresponding crank angle resolved measurements of the pressure in the exhaust plenum. In brief, the torque curves illustrate a reduction in low-speed torque when the EGR circuit was fitted, even with the EGR flow fully closed off. Potential EGR valve leakage was eliminated from this experiment by removing the valve and simply blocking the end of the pipe. Therefore, this drop in torque has been associated with the EGR dead volume acting as a dampener, reducing



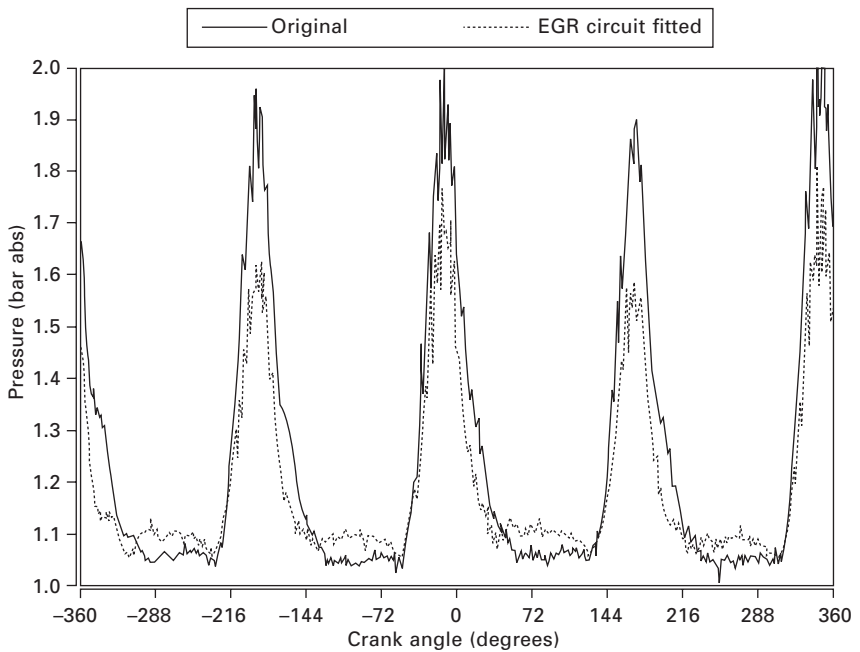
5.11 Example valve locations for the a) high-pressure and b) low-pressure EGR circuit layouts.

the exhaust blowdown pressure peaks (as seen in Fig. 5.13) and hence decreasing the available turbine work.

In conclusion, the use of a pre-turbine EGR pick-up necessitates minimised EGR circuit dead volume and in some cases may require an EGR circuit shut-off valve to avoid such dampening effects. A single hot-side EGR control valve may be considered too expensive in some cases and also insufficient in terms of quickly shutting off the EGR supply at the intake side of the



5.12 Low-speed torque curves with and without an EGR circuit fitted.



5.13 Crank angle resolved measurements of exhaust plenum pressure with and without an EGR circuit fitted (1500 rpm, wastegate fully closed).

engine. However, an additional, simple wastegate-type valve fitted prior to the entry to the cooler may perhaps suffice and could also perhaps be used to simultaneously control an EGR cooler bypass, enabling an additional degree of control over the EGR gas temperature.

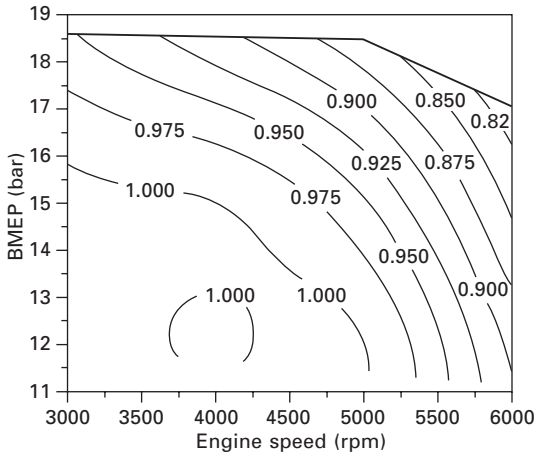
5.4 Exhaust gas recirculation (EGR) operating maps

In order to demonstrate the real-world fuel economy benefits of EGR-boosted operation at high speeds and loads, a second engine (a modern production turbocharged DI) was modified and tested. Some general details of the unit are provided in Table 5.3. The combustion chamber included side direct fuel injection, designed for homogeneous operation with a shallow central bowl in the piston crown. Shown in Fig. 5.14 are the corresponding maps of relative air-to-fuel ratio and exhaust-to-inlet manifold pressure ratio when operating the engine using excess fuel alone with an imposed pre-turbine gas temperature limit of 950°C. It can be seen that a positive EGR pressure ratio was available across the excess fuel regime, thus allowing high-pressure EGR to be adopted. The EGR circuit layout used during the test was identical to that shown previously in Fig. 5.7.

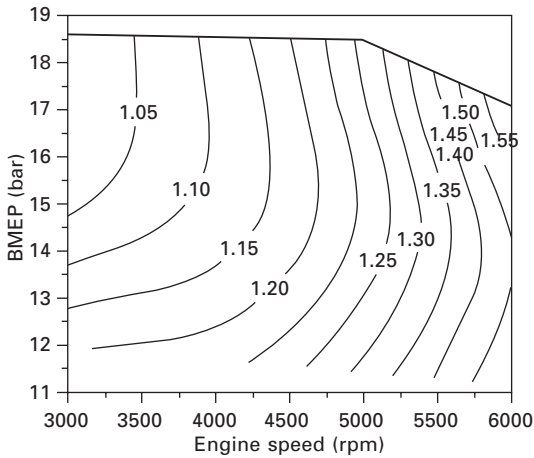
Shown in Fig. 5.15 are selected maps with the engine operated under steady-state EGR-boosted conditions, with the intake plenum gas temperature controlled to 35°C. The fuel injection and cam timings were fixed for each speed-load site. It was possible to operate the engine using cooled EGR over the entire required map. With the EGR control valve fully open, up to 14% EGR could be driven at moderate loads, falling to 12% at full load with the turbocharger wastegate fully closed. In turn, this allowed the engine

Table 5.3 Details of the modified production engine used for the high-pressure EGR operating maps

Number of cylinders	4
Bore (mm)	82.5
Stroke (mm)	92.8
Geometric compression ratio	9.8:1
Variable valve timing	Inlet only (42°C.a.)
Target peak power	170 kW at 6000 rpm
Cam duration (1 mm lift)	Inlet: 190°C.a., exhaust: 210°C.a.
Fuel injectors	Swirl type, 20 cc/s
Peak fuel rail pressure	120 bar
Fuel	98 RON unleaded gasoline
Turbocharger	BorgWarner K04
Spark plugs	Bosch single electrode
Ignition coils	Bosch coil-on-plug



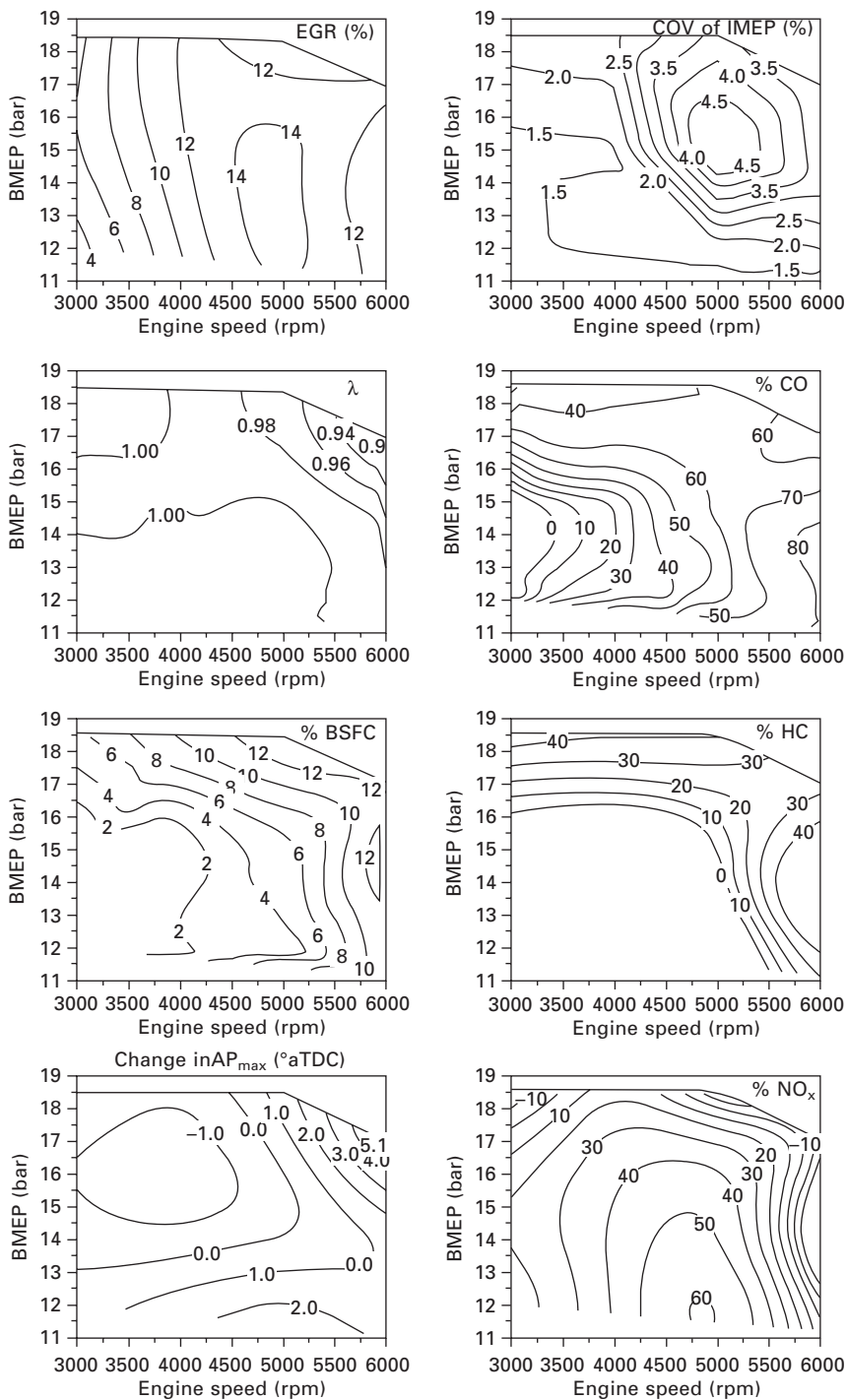
(a)



(b)

5.14 (a) Relative air-to-fuel ratio, λ , and (b) exhaust-to-inlet manifold pressure ratio for the engine when operating in conventional excess fuel mode (pre-turbine gas temperature limit = 950°C).

to be operated under stoichiometric fuelled conditions over the majority of the speed-load map. At peak rated power (6000 rpm, 17 bar BMEP), less excess fuel was required (i.e. $\lambda = 0.91$ vs $\lambda = 0.81$ using excess fuel alone). Consequently, up to 12% improvement in brake specific fuel economy was observed. Up to moderate engine speeds (<4500 rpm), the phasing of the peak in-cylinder pressure was marginally advanced ($\sim 1^\circ$ crank) when using EGR (vs. excess fuel). However, at higher engine speeds, increased exhaust back-pressures were incurred and significantly increased combustion



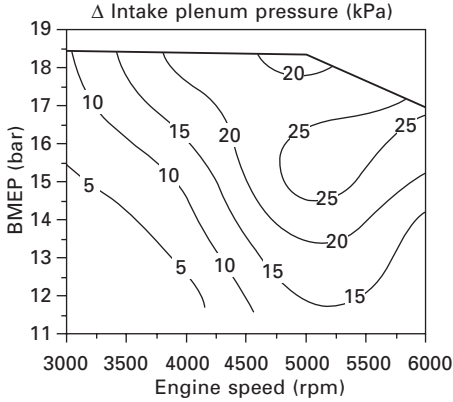
5.15 EGR operating maps produced using a modified four-cylinder production engine (pre-turbine gas temperature limit = 950°C).

duration was also noted. For example, at peak rated power, the 0–10% and 10–90% mass fraction burned periods increased by 7° and 6° crank respectively. Associated with this was retarded combustion phasing (up to ~5°) and deteriorated combustion stability, with the COV of gross IMEP approaching the acceptable high load limit of 5%. Efforts to improve the EGR tolerance and combustion stability may therefore probably be required for a robust production solution (e.g., in-cylinder flow and/or ignition system development). Nonetheless, the maps show that EGR-boosted operation using a high-pressure EGR circuit should be feasible in the short to medium term, for mildly downsized engine applications at least. Finally, also shown in Fig. 5.15 are maps of percentage reduction in engine-out emissions. As well as the aforementioned improvements in real-world fuel economy, up to ~70% reduction in CO and ~40% decrease in hydrocarbons were recorded. Such large reductions, together with engine operation nearer to constant stoichiometric fuelling conditions, demonstrate that even greater improvements in tailpipe emissions are possible using just a standard three-way catalyst, especially if EGR tolerance can be improved for continuous $\lambda = 1$ operation. The higher emissions of engine-out NO_x at high load were associated with operation nearer to stoichiometric conditions.

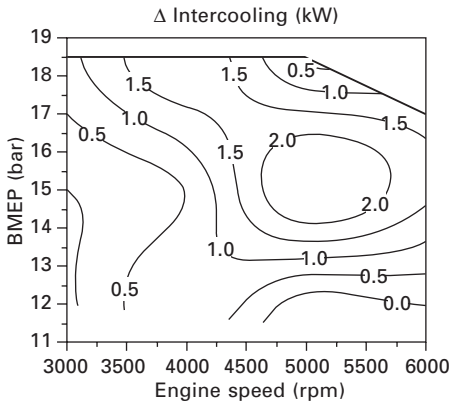
5.5 In-vehicle requirements

One major challenge of WOT-EGR operation is achieving the combined additional heat rejection from the recycled exhaust gases and increased air charge cooling. Ideally the EGR gases should be cooled to ~100°C; higher temperatures may reduce the knock suppression effect while lower temperatures can lead to excessive water trapping around the EGR circuit. While low-pressure EGR gas routing may reduce the EGR heat rejection requirements, challenges still remain with compressor performance, durability and transient engine operation.

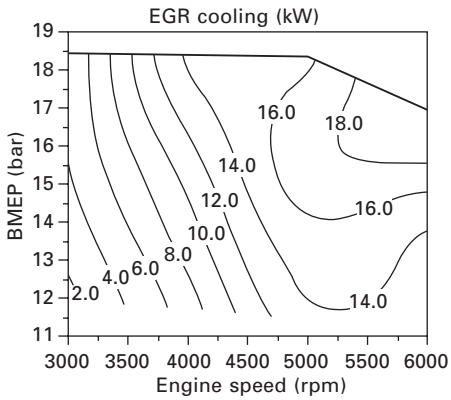
Shown in Fig. 5.16(a) is a map of the increase in intake manifold pressure required when using post-compressor EGR in place of fuel alone. This data was produced using the same engine and identical operating conditions as described above in Section 5.4. In order to drive ~12% EGR at 6000 rpm and 17 bar BMEP, an additional 25 kPa boost was required. Set out in Fig. 5.16(b) is the associated increase in intercooler heat rejection required to maintain the intake plenum charge temperature at 35°C. Such increase in air charge heat rejection should arguably be manageable with minor modifications in many typical vehicle installations. Shown in Fig. 5.16(c) is the corresponding heat rejected in the EGR cooler assembly (pre- and main cooler). The EGR gas temperature at the exit to the EGR control valve could be controlled to a maximum of 100°C at the highest speed and load. Strong synergy with exhaust gas heat recovery is clear.



(a)



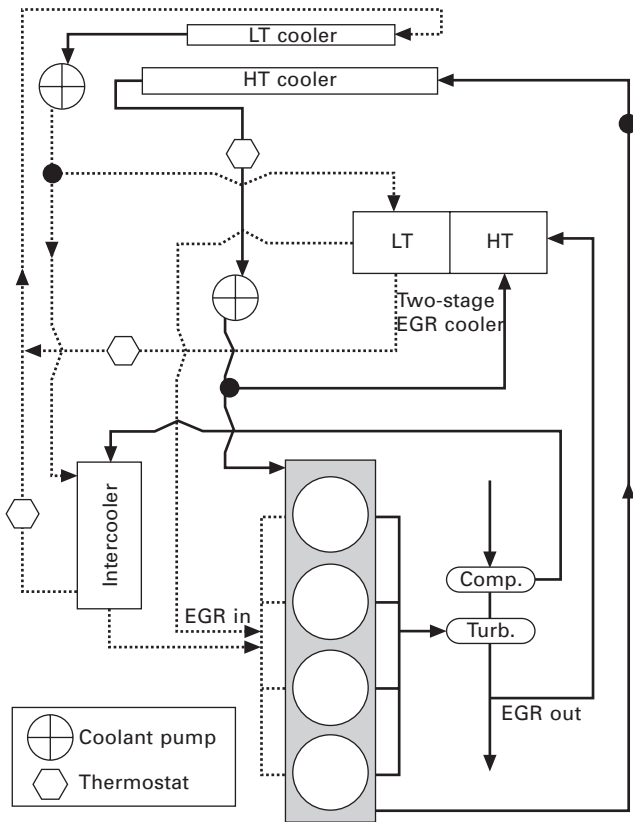
(b)



(c)

5.16 Example values of additional (a) boost pressure (b) intercooler heat rejection and (c) EGR cooler heat rejection for EGR-boosted operation.

Such EGR heat rejection imposes a significant demand on any existing vehicle installation. How this issue might be overcome is highly dependent on the application. However, one possible solution for the vehicle coolant circuit is illustrated in Fig. 5.17. A similar layout was proposed elsewhere (31) but for future diesel applications. In summary, the coolant circuit would incorporate a dual EGR cooler assembly. The first cooler could be constructed to withstand the highest exhaust gas temperatures and be fed with engine coolant through the so-called high temperature (HT) circuit. The second section of the cooler could then be supplied from the intercooler low temperature (LT) coolant circuit. The main advantage of such a dual EGR cooler application is that cooler inefficiencies that develop over time can be more easily compensated for; it would be difficult to maintain the cooler efficiencies required to reduce the EGR gas to $\sim 100^{\circ}\text{C}$ using engine coolant alone (itself at $\sim 90^{\circ}\text{C}$). Some form of integrated cooler bypass could also be made available for EGR temperature control.



5.17 One potential solution for a WOT-EGR vehicle coolant circuit.

5.6 Future trends

At present, most turbocharged spark ignition production engines use excess fuel at high speed and load to cool the exhaust gases and protect the exhaust components from excessive thermal loading. Such excess fuelling results in poor high-load fuel consumption, a significant decrease in three-way catalyst efficiency and hence a vast increase in tailpipe pollutant emissions. At present, the regime of such fuel enrichment is often at loads higher than those encountered during existing drive cycle assessments. However, 'real-world' fuel economy is becoming increasingly important and it seems feasible that high-load fuel economy and emissions legislation will emerge in future years. Downsized spark-ignition engines are beginning to emerge and such units will inherently spend more time operating at higher loads. Furthermore, these engines still need a high geometric compression ratio for good part-load fuel efficiency, but a high compression ratio can also lead to yet increased over-fuelling at full load.

From the research performed to date, it is clear that EGR boosted operation provides a viable alternative to excess fuel, allowing vast reductions in tailpipe pollutant emissions ($\sim 70\%$ CO and $\sim 40\%$ hydrocarbons) using just a standard three-way catalyst. Reasonable fuel economy improvements have also been measured at high engine speeds and loads (e.g. $\sim 12\%$). In addition, EGR has often been observed to be a more effective alternative suppressant of knock than excess air, involving a gas mixture of a lower ratio of specific heats and with improved combustion stability maintained over a wider speed-load range.

However, challenges remain to bring the EGR boosted technique to market and further research is required. In the currently reported work, high-pressure EGR gas routing was applied to a modified production engine retaining the original turbocharger assembly. Such routing arguably has potential for improved compressor wheel durability, minimised EGR circuit dead volume and fast transient engine response. Furthermore, a comparison of pre- and post-compressor EGR supply in this work indicated that post-compressor routing may allow higher compressor efficiencies to be maintained (and hence reduced compressor work) under some conditions. However, with this high-pressure routing, attaining sufficient EGR rate was not always possible over the required operating map, which limited the thermodynamic benefits achieved. In addition, when using the pre-turbine EGR pick-up, the EGR circuit dead volume had to be closed off in order to maintain low-speed torque, insinuating that a hot-side EGR circuit shut-off valve may be required at additional cost. Low-pressure EGR gas routing may therefore be unavoidable where EGR is most required at low speeds and higher loads (e.g., knock suppression in the most aggressively downsized engine applications) and corresponding research is still required.

At the highest engine speeds and loads, EGR tolerance has been shown to deteriorate and measures to improve such tolerance may be required in some cases. Whether the highest loads proposed for advanced downsizing concepts can ever be efficiently reached via EGR boosted operation remains to be seen. At the very least, those engines employing very high levels of EGR on top of already high levels of boost will require sophisticated pressure charging systems. Suitable in-vehicle EGR heat rejection technologies must also be developed, ideally in tandem with EGR heat recovery systems. The associated on-costs of the EGR components and vehicle cooling circuit may be partially offset by the possibility of running lower peak gas temperatures and using cheaper cylinder head and/or exhaust component materials.

5.7 References

1. Louis, J.J.J.: 'Well-to-wheel energy use and greenhouse gas emissions for various vehicle technologies', SAE paper 2001-01-1343, 2001.
2. Hurden, J., DeBoer, C. and Cairns, A.: 'Towards the optimum use of crude oil in passenger cars', *Proceedings of the Global Powertrain Congress*, 2004.
3. Overington, M.T. and DeBoer, C.: 'Vehicle fuel economy – high compression ratio and supercharged compared', SAE paper 840242, 1984.
4. Guzzella, L., Wenger, U. and Martin, R.: 'IC-engine downsizing and pressure-wave supercharging for fuel economy', SAE paper 2000-01-1019, 2000.
5. Petitjean, D., Bernardini, L., Middlemass, C. and Shahed, S.M.: 'Advanced gasoline engine turbocharging technology for fuel economy improvements', SAE paper 2004-01-0988, 2004.
6. Konig, G. and Sheppard, C.G.W.S.: 'End-gas autoignition and knock in SI engines', SAE paper 902135, 1990.
7. Pan, J. and Sheppard, C.G.W.S.: 'A theoretical and experimental study of the modes of end gas autoignition leading to knock in SI engines', SAE paper 942060, 1994.
8. Pearson, R., Turner, J. and Kenchington, S.: 'Concepts for improved fuel economy from gasoline engines', IMechE Fuel Economy and Engine Downsizing Conference, 2004.
9. Fraser, N. and Blaxill, H.: 'Engine downsizing and the application of gasoline direct injection to a high specific output turbocharged engine', IMechE Fuel Economy and Engine Downsizing Conference, 2004.
10. Lang, O., Geiger, J., Habermann, K. and Wittler, M.: 'Boosting and direct injection – synergies for future gasoline engines', SAE paper 2005-01-1144, 2005.
11. Wirth, M., Mayerhofer, U., Piock, W.F. and Fraidl, G.K.: 'Turbocharging the DI gasoline engine', SAE paper 2000-01-0251, 2000.
12. Lecointe, B. and Monnier, G.: 'Downsizing a gasoline engine using turbocharging with direct injection', SAE paper 2003-01-0542, 2003.
13. Lake, T., Stokes, J., Murphy, R., Osborne, R. and Schamel, A.: 'Turbocharging concepts for downsized DI gasoline engines', SAE paper 2004-01-0036, 2004.
14. Hiroshi, M., Makoto, M., Yuichi, O., Tetsunori, S. and Shinji, K.: 'The potential of lean boost combustion', SAE paper 2004-05-0417, 2004.
15. Harrington, J.A.: 'Water addition to gasoline – effect on combustion, emissions, performance and knock', SAE paper 820314, 1982.

16. Turner, J.W.G., Pearson, R.J., Bassett, M.D., Blundell, D.W. and Taitt, D.W.: 'The turboexpansion concept – initial dynamometer results', SAE paper 2005-01-1853, 2005.
17. Brustle, C. and Hemmerlein, N.: 'Exhaust gas turbocharged SI engines and their ability of meeting future demands', IMechE paper C484/039/94, 1994.
18. Grandin, B., Angstrom, H.-E., Stalhammar, P. and Olofsson, E.: 'Knock suppression in a turbocharged SI engine by using cooled EGR', SAE paper 982476, 1998.
19. Grandin, B. and Angstrom, H.-E.: 'Replacing fuel enrichment in a turbo charged SI engine: lean burn or cooled EGR', SAE paper 1999-01-3505, 1999.
20. Duchaussoy, Y., Lefebvre, A. and Bonetto, R.: 'Dilution interest on turbocharged SI engine combustion', SAE paper 2003-01-0629, 2003.
21. Diana, S., Giglio, V., Iorio, B. and Police, G.: 'A strategy to improve the efficiency of stoichiometric spark ignition engines', SAE paper 961953, 1996.
22. Alger, T., Chauvet, T. and Dimitrova, Z.: 'Synergies between high EGR operation and GDI systems', SAE paper 2008-01-0134, 2008.
23. Kapus, P.E., Fraidl, G.K., Prevedel, K. and Fuerhapter, A.: 'GDI turbo – the next steps', JSAE paper 20075355, 2007.
24. Cairns, A., Irlam, G. and Blaxill, H.: 'Exhaust gas recirculation for improved part and full load fuel economy in a turbocharged gasoline engine', SAE paper 2006-01-0047, 2006.
25. Cairns, A., Fraser, N. and Blaxill, H.: 'Pre versus post compressor supply of cooled EGR for full load fuel economy in turbocharged gasoline engines', SAE paper 2008-01-0425, 2008.
26. Heywood, J.B.: *Internal Combustion Engine Fundamentals*, McGraw-Hill, New York, 1988.
27. Wirth, M., Zimmermann, D., Friedfeldt, R., Caine, J., Schamel, A., Davies, M., Peirce, G., Storch, A., Riese-Muller, K., Gansert, K.P., Pilgram, G., Ortman, R., Wurfel, G. and Gerhardt, J.: 'A cost optimised spray guided direct injection system for improved fuel economy', IMechE Fuel Economy and Engine Downsizing Conference, 2004.
28. Kawamoto, M., Honda, T., Katashiba, H., Sumida, M., Fukutomi, N. and Kawajiri, K.: 'A study of center and side injection in spray guided DISI concept', SAE paper 2005-01-0106, 2005.
29. Blank, H., Dismon, H., Kochs, M.W., Sanders, M. and Golden, J.E.: 'EGR and air management for direct injection gasoline engines', SAE paper 2002-01-0707, 2002.
30. Weber, O., Jorgl, V., Shutty, J. and Keller, P.: 'Future breathing system requirements for clean diesel engines', 14th Aachen Colloquium, 2005.
31. Muller, R. and Pantow, E.: 'Engine cooling and the Euro 5 standard for diesel cars', ATZ Article 09/2005, 2005.

Direct injection gasoline engines with autoignition combustion

H. ZHAO, Brunel University, UK

Abstract: This chapter begins by presenting the principle of autoignition combustion operation in the automotive gasoline engine. Following an overview of the main technical approaches to achieve autoignition combustion in gasoline engines, the chapter discusses in detail the operational characteristics of controlled autoignition (CAI) combustion with residual gas trapping. It then describes ways of switching between spark ignition (SI) and CAI operations in order to develop a practical automotive engine with autoignition combustion. The chapter concludes with a summary of state-of-the-art autoignition direct injection (DI) gasoline research and development and its future trends.

Key words: homogeneous charge compression ignition (HCCI), controlled autoignition (CAI), low temperature combustion, gasoline direct injection.

6.1 Introduction

One of the main motivations in the development of direct injection (DI) gasoline engines is the potential of DI for improving the vehicle's fuel economy. The potential fuel economy benefit of a DI gasoline engine is mainly achieved by employing stratified lean-burn operation at part-load as discussed in the previous chapters. Stratified charge operation is necessary in order to burn an overall very lean mixture at wide open throttle so that the pumping losses associated with the partly closed intake throttle are minimised. It is achieved by placing a rich mixture near the spark plug by means of fuel spray, in-cylinder flow (tumble or swirl), piston geometry and accurate fuel injection controls as discussed elsewhere.

However, combustion of the stratified charge lean-burn mixture in a DI gasoline engine presents a number of difficulties. Firstly, optimisation of fuel injection, in-cylinder flow and piston geometry is crucial to the stratified charge operation by placing the combustible charge at the right place (around the spark plug) and at the right time (spark ignition timing). Mismatching between the fuel distribution and ignition timing will lead to excessive unburned hydrocarbons (uHC) and smoke emissions, partial burn or even misfire, which restricts the unthrottled lean-burn stratified charge operation to a limited engine operating range.

Secondly, as combustion takes place in the stratified stoichiometric mixture, a larger amount of NO_x is produced in the stratified charge operation than

in homogeneous lean-burn combustion at the same operating condition. In addition, because the spark timing is inextricably linked to the timing of the fuel injection, the spark timing is often too advanced for minimising in-cylinder NO_x formation.

Most importantly, the lean-burn operation necessitates the use of less efficient, more expensive and more fuel-sensitive NO_x aftertreatment. These factors have contributed to the slower market penetration of gasoline DI engines than initially predicted, and the absence of stratified charge operation in the current gasoline DI engines in the market.

However, direct injection has a greater potential for the downsized gasoline engine and better full-load performance than the port fuel injection as discussed in the previous chapters. Therefore, there is a strong industrial need to develop a gasoline DI engine that is able to operate with low fuel consumption and low emissions at part-load as well as to produce superior full-load performance.

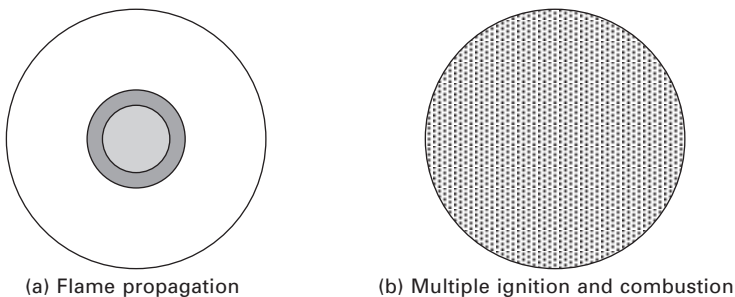
In the last decade, significant advances have been made in an alternative combustion mode, commonly known as homogeneous charge compression ignition (HCCI) or controlled autoignition (CAI). In contrast to the conventional spark-ignited flame propagation, the autoignition combustion process involves the simultaneous reactive envelopment of the entire premixed fuel/air mixture, allowing a more uniform and repeatable burning of the very lean and/or highly diluted mixture in a gasoline engine. Results from both single (Lavy *et al.*, 2000; Law *et al.*, 2001; Koopmans and Denbratt, 2001) and multi-cylinder engines (Li *et al.*, 2001; Zhao *et al.*, 2002) have shown that autoignited combustion of a premixed fuel and air mixture is characterised by significant improvement in part-load fuel economy and ultra-low NO_x emissions. In addition, it is shown that the DI gasoline engine with autoignition combustion can also lead to substantial reduction in CO emissions whilst producing similar uHC emissions to that of stratified charge SI combustion. Therefore, the autoignition combustion of a premixed mixture represents a very attractive solution for vehicle use that enables simultaneous reductions in CO_2 and NO_x emissions from a lean burn engine without the necessity for expensive and less efficient aftertreatment.

In this chapter, after a brief description of its operating principle, a review of the major engine technologies will be given on the autoignition combustion operation in gasoline DI engines. The engine performance and emission characteristics of gasoline engines with autoignition combustion will be presented and discussed. The chapter then describes the ways to switch between SI and autoignition combustion operations in a four-stroke automotive gasoline engine. The chapter will conclude with a summary of the state of the art in autoignition DI gasoline research and development and its future trends.

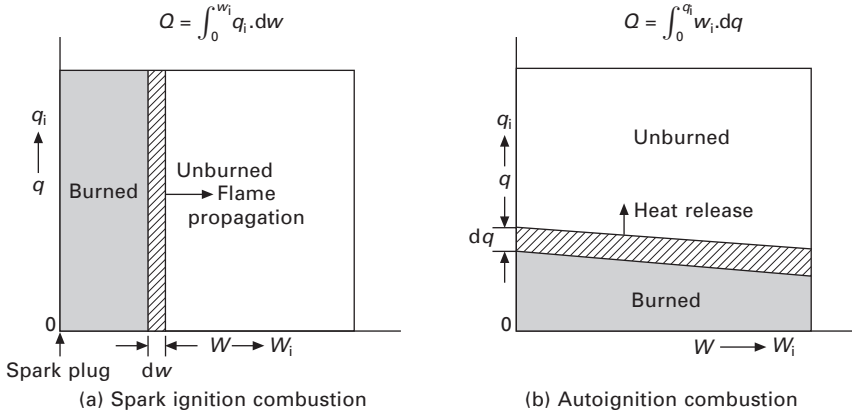
6.2 Principle of autoignition combustion in the gasoline engine

The concept of autoignition combustion in four-stroke gasoline engines had been identified as the cause of ‘after-run’, ‘run-on’ or ‘dieseling’ in carburetted engines (Benson, 1972; Ingamells, 1979), an abnormal combustion phenomenon that occurs when a spark-ignition gasoline engine continues to run after the ignition is turned off. Similarly, two-stroke part-load operation was found to be plagued with irregularities of spark ignited flame propagation and autoignition combustion (Souk *et al.*, 1973). However, this ‘abnormal’ combustion process had been harnessed by researchers at Nippon Clean Engine (NiCE) to achieve remarkable improvements in stability, fuel efficiency and exhaust emissions in the two-stroke gasoline engine, which was subsequently commercialised in the form of a portable two-stroke electric generator (Onishi *et al.*, 1979).

In principle, autoignition combustion of a premixed air/fuel mixture is realised in two steps, as shown in Fig. 6.1. The first step involves the initiation of high temperature combustion through the autoignition process of a premixed air/fuel mixture. This is followed by the simultaneous burning of the entire combustible charge. Figure 6.2(a) and (b) show ideal models of spark ignition (SI) flame propagation combustion and autoignition combustion respectively. In each case, the x -axis represents the fraction of total mixture mass, while the y -axis represents the specific heating value of the fuel. During SI combustion, each element of the fuel (dw) in the flame region is burned completely. In comparison, heat release occurs in almost all parts of the charge simultaneously during the autoignition combustion of the premixed fuel and air mixture. The incremental heat released at each time interval, dq , represents the total heating value of the intermediate reactants that continue the chain branching reactions. In this way, with autoignition combustion, combustion duration is limited chemically by kinetic reaction rates, while the speed of SI combustion is limited by the physics of flame propagation.



6.1 Schematic of (a) spark ignition and (b) autoignition combustion.



6.2 Ideal heat release models of (a) spark ignition and (b) autoignition combustion.

Since the combustion process is dominated by the autoignition and simultaneous burning of a combustible mixture at multiple sites, an extremely lean (with excess air) or diluted (with excess recycled exhaust gases) fuel and air mixture can be burned beyond the flammability limits. It is no longer necessary to restrict the air flow through an intake throttle to keep the fuel and air mixture closer to its stoichiometric value so that a spark-ignited flame can propagate in the premixed combustible mixture. Instead, wide-open throttle operation can be achieved at part-load conditions with excess air and/or diluents. As a result, better fuel economy can be achieved by removing the pumping losses associated with a partly closed intake throttle. Ultra-low NO_x emissions are realised through the low combustion temperature of a highly diluted mixture of internal or externally recycled burned gases, and through the absence of a high-temperature flame front and a localised high-temperature burnt gas region.

In order to achieve autoignition in a gasoline engine, the kinetics of autoignition would suggest that the charge temperature at the end of the compression stroke must be elevated to above the autoignition temperature of gasoline fuel, which is typically around 1000 K. However, gasoline fuel is characterised by high resistance to autoignition as measured by its high octane number. In addition, the gasoline engine is designed with a relatively low compression ratio in order to avoid knocking combustion at full load operations. Therefore, autoignition combustion does not occur in the conventional four-stroke gasoline engine unless additional measures are introduced to the engine design.

In addition, autoignition combustion is governed mostly by chemical kinetics and depends on the history of temperature, pressure and composition of the

combustible mixture. Unlike the spark-ignited flame that can be accurately controlled by the spark timing, autoignition combustion cannot be directly controlled. Either too early or retarded combustion phasing will lead to reduced fuel economy and poor emission characteristics. Furthermore, some means of slowing down the rapid heat release rate is necessary to prevent an excessive rate of pressure rise and knocking combustion at high load operations.

6.3 Approaches to autoignition combustion operation in gasoline engines

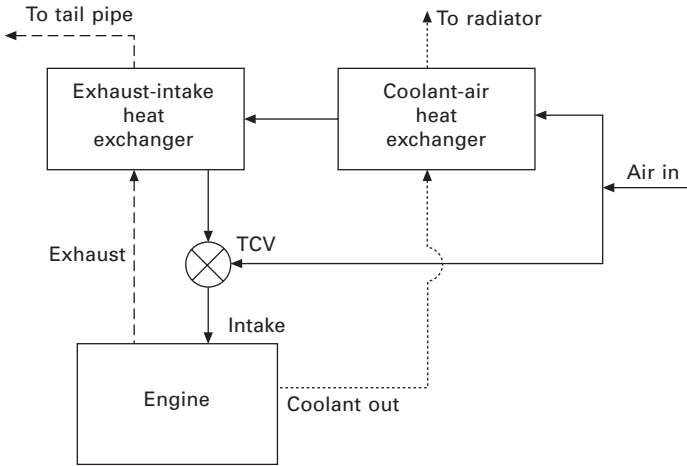
Based on the discussion in the previous section, it is apparent that there are three basic requirements for a gasoline engine to operate with controlled autoignition combustion: (1) a sufficient charge temperature for autoignition to occur; (2) the presence of diluents (air or recycled exhaust gas) to restrict the heat release rate; and (3) a method to alter the combustion phasing. In this section, major approaches to achieving controlled autoignition combustion in a gasoline engine will be presented and discussed.

6.3.1 Gasoline autoignition combustion with thermal management

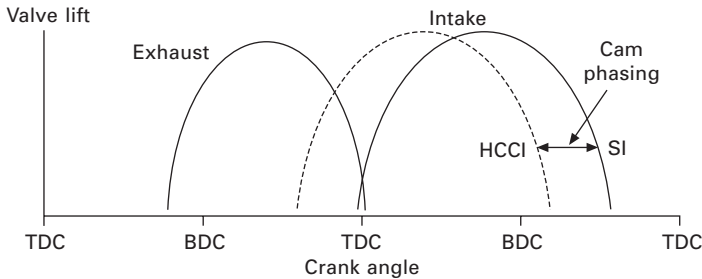
The most straightforward approach to achieving autoignition combustion involves the use of an external heating source to heat the intake air and provide the thermal energy needed to the combustible charge to reach its autoignition temperature. This can be in the form of a simple electric heater, or heat recovered from exhaust gases or/and coolant. The use of an electric heater or any other form of external heating may be suitable for research purposes but will have little practical use for automotive applications. A more realistic approach is to utilise thermal energy in exhaust gases and coolant (Yang and Kenney, 2002; Hyvoenene *et al.*, 2003).

The first effort towards a practical thermal management system for autoignition combustion in a gasoline engine was reported by Stockinger *et al.* (1992). In their system, the intake charge temperature was increased by forcing part of the hot exhaust gases back into the pressurised intake system. The amount of recycled exhaust gases was controlled by flow control valves located in the exhaust and intake systems. The fast thermal management requirement was met by the mixture temperature control through the amount of recycled exhaust gas, while the slow thermal management was obtained by a coolant temperature control device.

Figure 6.3 shows such an intake system with two heat exchangers to heat the intake air implemented in the OKP engine concept by Yang and Kenney (2006). One stream of intake air is heated up by passing it through



6.3 Fast thermal management system adopted in the OKP engine.



6.4 Valve timing diagram for the OKP engine concept.

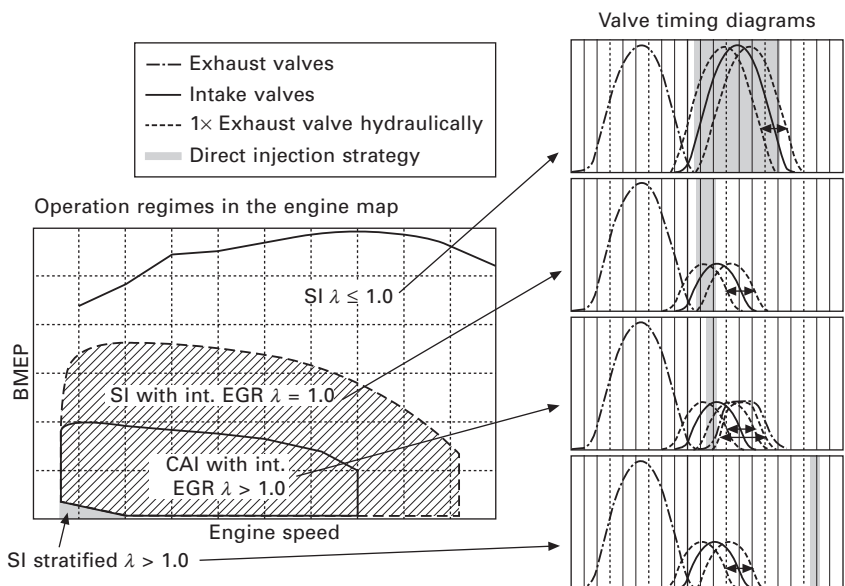
a coolant-air heat exchanger and then an exhaust heat exchanger, and the rest of the air is unheated. A temperature control valve (TCV) regulates the ratio of heated and unheated air in order to achieve flexible adjustment of the intake air temperature for autoignition and combustion timing control. The engine’s geometric compression ratio is increased to about 15:1 in order to achieve autoignition combustion at part-load condition. To avoid knocking combustion at high load, an extended intake cam profile in conjunction with a variable cam timing (VCT) device is used to operate the engine with a reduced effective compression ratio and conventional valve overlap through retarded intake valve closing, as shown in Fig. 6.4. In addition, to compensate for the loss in volumetric efficiency due to retarded intake valve closing, supercharging with intercooling is needed to regain the full-load performance in the SI mode. The OKP engine concept was demonstrated in a single-cylinder direct injection gasoline engine at steady state from 750

rpm to 4750 rpm. The autoignition combustion was achieved from 1 bar to 5.5 bar of net indicated mean effective pressure (NMEP) at 1500 rpm. It was shown that, at part-load operation, the autoignited combustion operation of the OKP engine could achieve a 50% improvement over that of conventional PFI engines and 30% over the original stratified charge direct injection gasoline engine.

The use of fast thermal management for closed-loop control of autoignition combustion was investigated by Hyvoenene *et al.* (2003) on a prototype five-cylinder Saab variable compression ratio (VCR) engine. Similar to the thermal management system shown in Fig. 6.3, one stream of intake air was heated by the exhaust gas through a heat exchanger after an electric heater, which was primarily designed for start-up. The other stream of cold air was mixed with a hot air flow after the heat exchanger at a location that was more than 500 mm away from the intake ports. The closed-loop combustion control using fast thermal management was implemented by setting the mean CA50 (50% burn crank angle) from all cylinders to a desired value through a PID controller. The intake air temperature was altered by adjusting the ratio of hot and cold airstreams through two throttles working in opposite duty cycles. Since the same intake air was supplied to all the cylinders, the thermal management is effectively an engine-global control. It was found that a delay of several engine cycles was present due to a combination of slow response thermocouple measurement and a large air volume between the mixing point and the inlet ports. In addition, a very large temperature increase in the inlet air temperature was required to accomplish speed changes in a transient operation.

6.3.2 Gasoline autoignition combustion with internal exhaust gas recirculation (iEGR)

In the previous section, the fast thermal management approach utilises the exhaust thermal energy indirectly through heat exchangers and introduces the dilution effect of burnt gases by externally recirculating exhaust gas from the exhaust manifold through an EGR runner back into the intake manifold. However, the dead volume of exhaust gases in the EGR system and the maldistribution of EGR between cylinders can cause cycle-to-cycle and cylinder-to-cylinder variations, as well as slow transient response. In addition, the heat loss through the EGR system is significant. A method of overcoming deficiencies of the external EGR approach is the use of 'intern EGR'. The most significant research on the use of such internal exhaust gas recirculation to achieve autoignition combustion in a four-stroke direct injection gasoline engine was carried out by Fuerhapter *et al.* (2003, 2004). Figure 6.5 shows the schematic valve timing diagrams for different operation modes. In order to achieve autoignition combustion, one of the two exhaust valves was set to



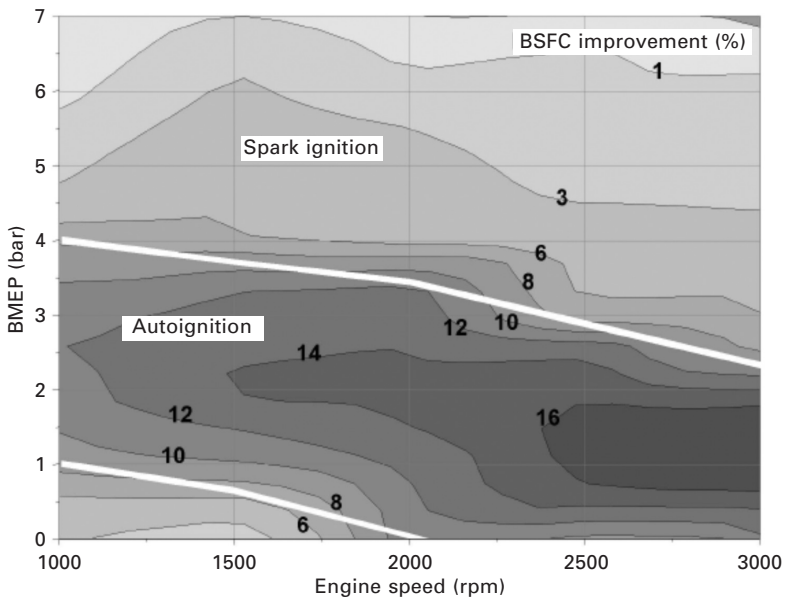
6.5 Valve timing diagram for autoignition combustion in the AVL-CSI engine (adapted from Fuerhapter *et al.*, 2007).

reopen during the intake stroke. If the second opening of the exhaust valve occurs during the first half of the intake stroke, the hot burnt gases will be sucked back from the exhaust port into the cylinder and mixed with cold air from the intake port. The hot rebreathed exhaust gas will then experience a cooling-down period in the cylinder as the cylinder volume expands and heat is lost to the cylinder wall. In comparison, if the second opening of the exhaust valve takes place towards the end of the intake stroke after the fresh air has been admitted into the cylinder, the hot burnt gases will be sucked back into the cylinder shortly before the start of the compression process. As a result, the rebreathed burnt gases will remain hot as they stay in the hot exhaust port rather than in the expanding cylinder volume. In addition, the late rebreathing approach allows the effective compression ratio to be altered by the same actuator for the reopening of the exhaust valve. In both cases, the rate of iEGR is primarily controlled by the reopening exhaust valve duration and timing. It should also be noted that a shorter intake valve opening period is needed to restrict the air flow into the cylinder so that a large amount of EGR can be trapped in the cylinder. It is also noted that the same low-lift intake valve profile is used for part-load SI operations outside the autoignition combustion range, with early intake valve closing time so that the engine is operating effectively unthrottled in a Miller cycle.

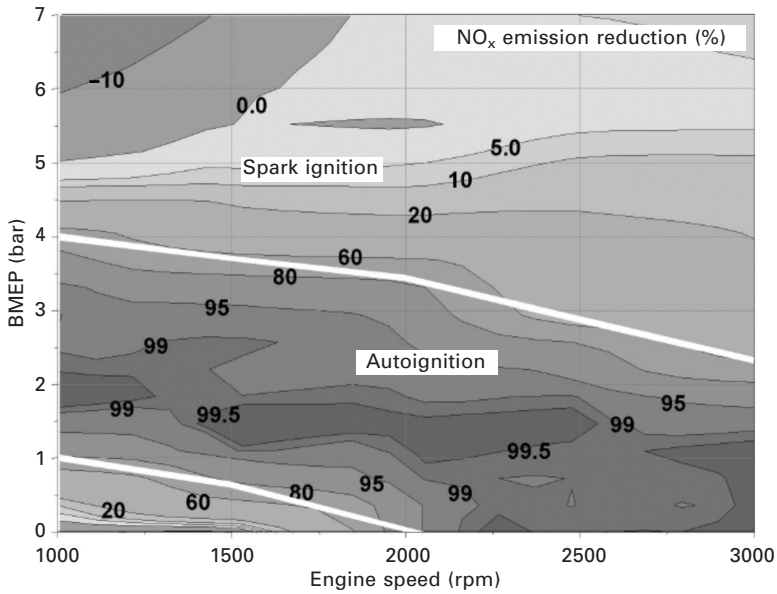
A 2.0 litre direct injection gasoline engine was modified to accomplish

autoignition combustion as well as spark ignition combustion. The intake camshaft was equipped with a VCT device and a two-stage valve lift shifting mechanism. A standard exhaust camshaft was used to actuate the two exhaust valves in the exhaust stroke. An electro-hydraulic valve actuation (EHVA) system was implemented to reopen one exhaust valve towards the end of the intake stroke. The EHVA system was able to adjust the opening timing and duration of the exhaust valve individually for each cylinder so that the combustion in each cylinder could be controlled independently and on a cycle-to-cycle basis. This was realised by implementing a closed-loop combustion control through an in-cylinder pressure sensor and a physically based model that was capable of predicting the autoignition combustion behaviour.

Figures 6.6 and 6.7 show the relative improvement in brake specific fuel consumption (BSFC) and NO_x emissions with autoignition combustion compared to a purely SI operation without the flexible valve train system. The range of autoignition operation is indicated by the two white lines and extends from 1000 rpm to 3000 rpm, which is likely to be the limit imposed by the EHVA system. The upper load limit is given by the limitation of the maximum cylinder pressure rise, which was defined as $3 \text{ bar}/^\circ\text{CA}$, whereas misfiring due to reduced exhaust gas temperature prevents autoignition occurs at the lowest load and speed operations. Within the range of autoignition



6.6 BSFC improvement achieved with the AVL-CSI engine (adapted from Fuerhapter *et al.*, 2007).



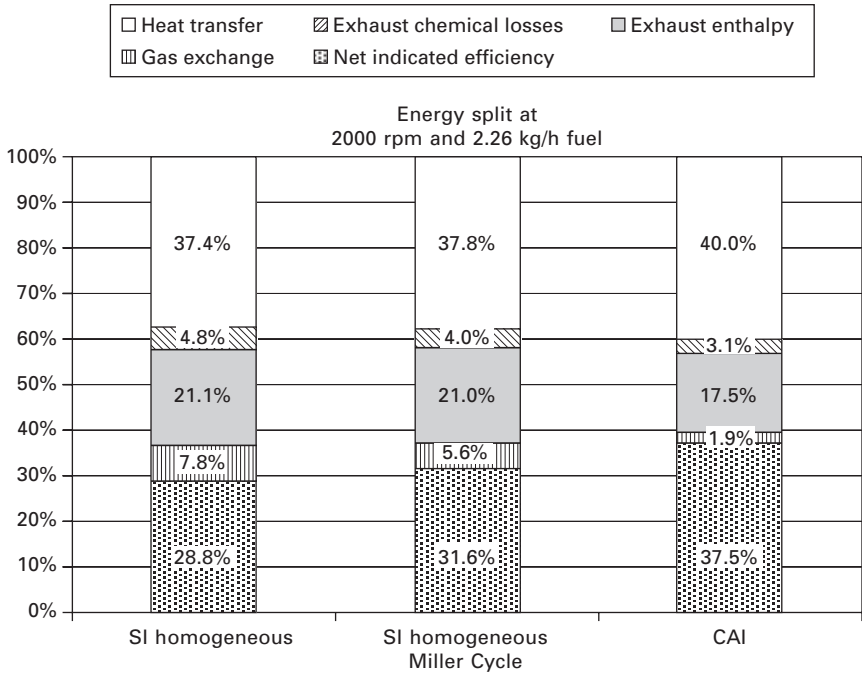
6.7 NO_x emission reduction achieved with the AVL-CSI engine (adapted from Fuerhapter *et al.*, 2007).

combustion operation, NO_x emissions are reduced by a factor of 10 to 100 compared with the values with spark-ignition combustion.

In order to understand the source of improvement, Fuerhapter *et al.* (2007) carried out an energy balance analysis of the different combustion modes. As shown in Fig. 6.8, at the selected operating point, the net indicated efficiency is increased from 29% in SI homogeneous operation to 37.5% in CAI mode, representing an improvement of about 30%. The energy split analysis shows that the pumping losses account for about two-thirds of the overall improvement of the net indicated efficiency of autoignition combustion and the remaining one-third is due to the reduced exhaust enthalpy and chemical energy losses caused by the high internal exhaust gas recirculation rates.

6.3.3 Gasoline autoignition combustion through residual gas trapping

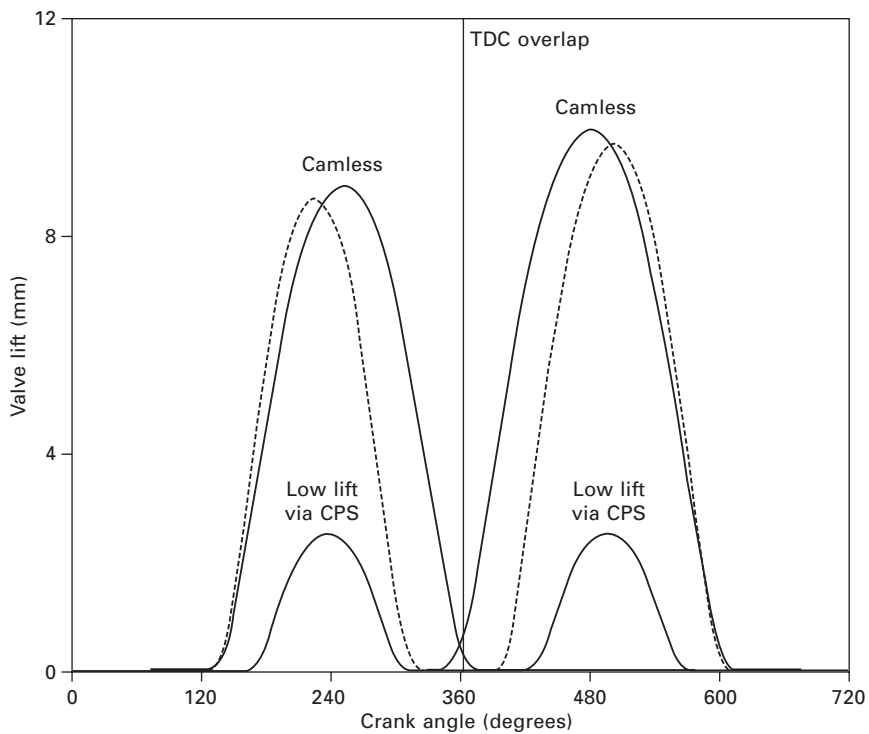
In addition to the internal EGR approach described in the previous section, hot burnt gases from the previous cycle can be trapped within the cylinder through negative overlap. As shown in Fig. 6.9, by closing the exhaust valve earlier in the exhaust stroke, a large quantity of burnt gases can be kept in the cylinder. The burnt gas trapped will then be compressed towards Top Dead Centre (TDC), resulting in a recompression peak in the pressure



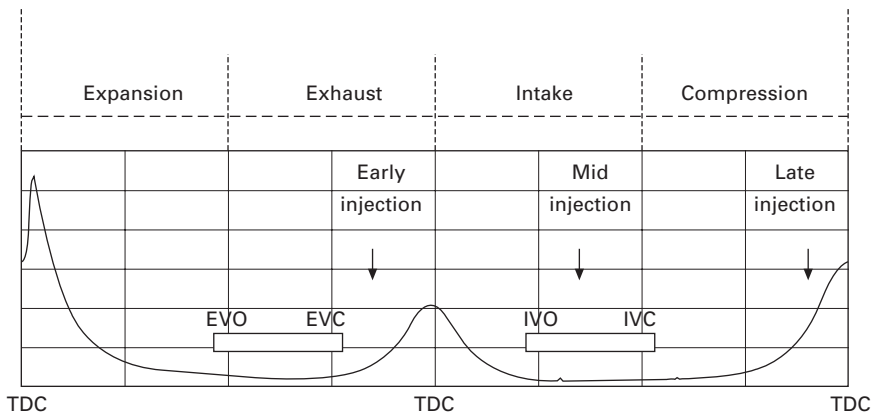
6.8 Energy balance analysis of three different engine operations (adapted from Fuerhapter *et al.*, 2007).

diagram shown in Fig. 6.10. The earlier the exhaust valve closes, the more burnt gases will be trapped, and vice versa. At the same time, the intake valve opening time has to be retarded to a position where the in-cylinder pressure is equalised to that in the intake port to minimise the backflow into the intake manifold. This can be realised ideally by a fully variable valve actuation (VVA) camless system, through either electrohydraulic (Law *et al.*, 2001) or electromechanical actuation (Koopmans *et al.*, 2002, 2003). A VVA camless system in theory is capable of independent control of the valve lift and duration so that full intake and exhaust valve lifts can still be used during the negative valve overlap operation. As the opening and closing speed of valves in a camless system is limited by the speed of actuators, such a system is often characterised by reduced valve lifts as the valve opening period is reduced at higher engine speeds. The reduced valve lift and duration restrict the intake air flow into the cylinder at high engine speeds.

However, a more practical approach to the negative valve overlap is through the use of a camshaft with a low lift cam profile (Lavy *et al.*, 2000; Li *et al.*, 2001) or a mechanical continuous variable valve lift mechanism (Xie *et al.*, 2008). By replacing the standard intake and exhaust camshafts with a set of low-lift camshafts, autoignition combustion was achieved for

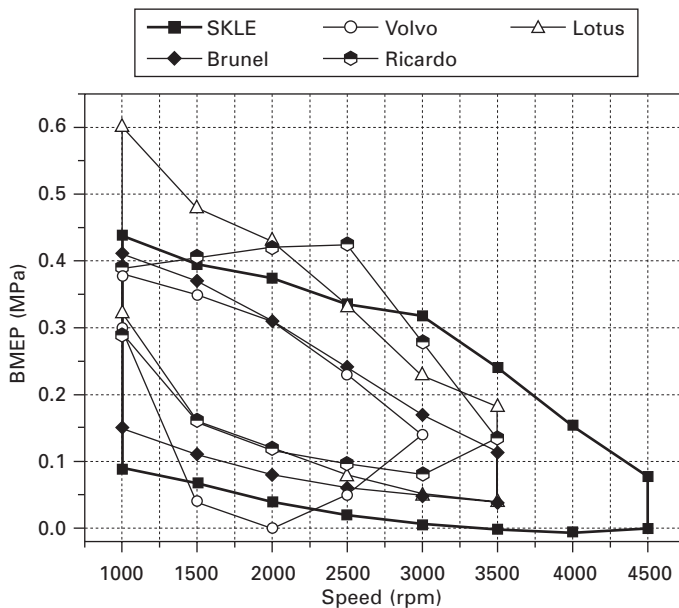


6.9 Negative valve overlap achieved by camless and mechanical actuation.

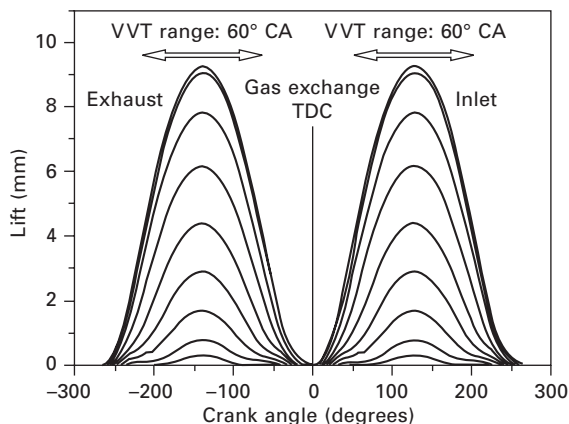


6.10 In-cylinder pressure diagram with negative valve overlap.

the first time in a production type on a four cylinder production type gasoline engine (Zhao *et al.*, 2002) over a range of speed and load conditions, details of which will be further discussed in the next section as shown in Fig. 6.11. A mechanical, fully variable valve lift system in production has been employed to achieve controlled autoignition combustion in a four-stroke gasoline engine by the author and his colleagues (Xie *et al.*, 2008). A pair of BMW Valvetronic devices are installed in a specially designed cylinder head to actuate the intake and exhaust valves respectively. Figure 6.12 shows the valve lift curves that can be achieved with such a system. The valve lift of both intake and exhaust valves can be adjusted continuously from less than 1 mm to 9 mm. In combination with two independent cam phasers, the timing and duration of intake and exhaust valves can be altered and optimised for different engine operating conditions. Figure 6.11 compares the operational ranges of controlled autoignition combustion in the four-stroke gasoline engine through different valve actuation setups (Koopmans and Denbratt, 2001; Li *et al.*, 2001; Law *et al.*, 2001; Stokes *et al.*, 2005). It can be seen that the mechanically fully variable valve lift system leads to significant enlargement of the operating range of controlled autoignition combustion compared to the fixed low-lift cam profile operations. The improvement in the upper limit at high-speed operations is due to the higher volumetric efficiency achieved by operating the engine with a higher intake valve lift and wider duration.



6.11 Operational region of autoignition combustion reported in the literature.



6.12 Variable intake and exhaust valve lifts of a mechanical VVA system.

It is interesting to note that the mechanically fully variable valve lift system even outperformed the camless system of electromechanical actuations by a significant margin at the upper load limit. This may be attributed to the limited opening and closing speed of the camless system used, which limited the opening duration for a set valve lift and hence the flow area and rate. In addition, the results in Fig. 6.11 show that controlled autoignition combustion could be extended to lower loads through the optimisation of valve lifts using the variable valve lift device.

6.4 Operation and control of direct injection gasoline engines with autoignition combustion

In order to implement autoignition combustion in a gasoline engine for automotive applications, the engine must be able to perform well throughout its speed and load range. Such an engine is subjected to varied and rapid changes in load and speed as the vehicle is driven. One or more throttles are typically used to control the power output of current automotive gasoline engines. In the case of unthrottled operation, such as in controlled autoignition combustion, any alternative load control device must be able to match the throttle operation in order to meet the customer's requirements.

In addition, the lack of direct control over the combustion phasing during the autoignition combustion operation needs to be considered and compensated for by other engine controlling parameters in conjunction with closed-loop control of individual cylinders as well as each combustion cycle. The wider the autoignition combustion operational range becomes, the better will be the fuel economy and the less the exhaust emissions. However, even with

all the measures in place to achieve optimised autoignition combustion, it will not be feasible to operate autoignition combustion across the whole operating range of the gasoline engine. The engine must be able to operate in both spark-ignition and autoignition modes and achieve rapid and seamless switch between the two modes of operation.

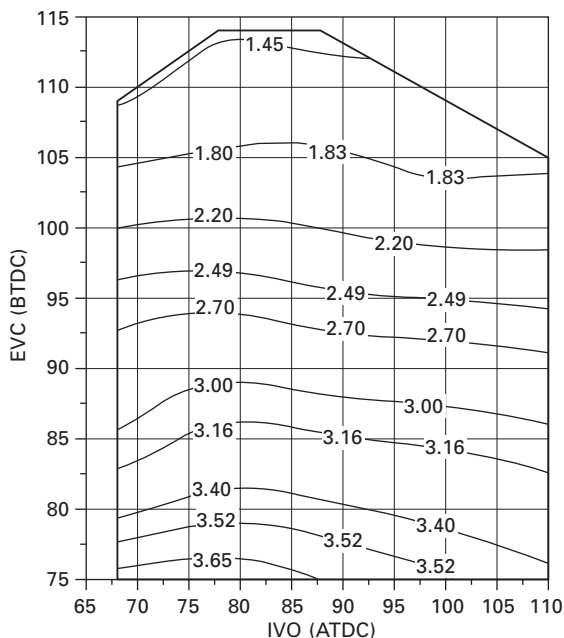
The operation of autoignition combustion and its control in a gasoline engine vary depending on how the autoignition combustion is achieved. Given the author's experience and its adoption in prototype engines by major automotive OEMs (GM in 2007, Mercedes in 2007), the discussion will focus mainly on the operation and control of autoignition combustion through the residual gas trapping method. The performance and operation of autoignition combustion engines with alternative approaches can be found in the recently published book on HCCI/CAI combustion engines (Zhao, 2007).

In this section, the load control of the autoignition combustion operation will be discussed first. This is followed by an examination of other engine control parameters that can be altered to achieve optimised autoignition combustion. Experimental results on the enlargement of the autoignition combustion operation will then be presented.

6.4.1 Operation of gasoline engines with autoignition combustion

The power output of a gasoline engine operating with autoignition combustion is fundamentally determined by the amount of combustible mixture presented in the cylinder. In spark-ignition combustion, a premixed flame front travels through the near-stoichiometric unburnt fuel and air mixture. Departure from the stoichiometric mixture will hinder the flame propagation and quickly extinguish the flame front. As the load on the engine is reduced, less fuel is needed to meet the power requirement. In order to keep the fuel and air mixture near the stoichiometric air/fuel ratio, air flow is throttled in current gasoline engine operations. Therefore, the opening of the intake throttle is directly linked to the power output of the gasoline engine.

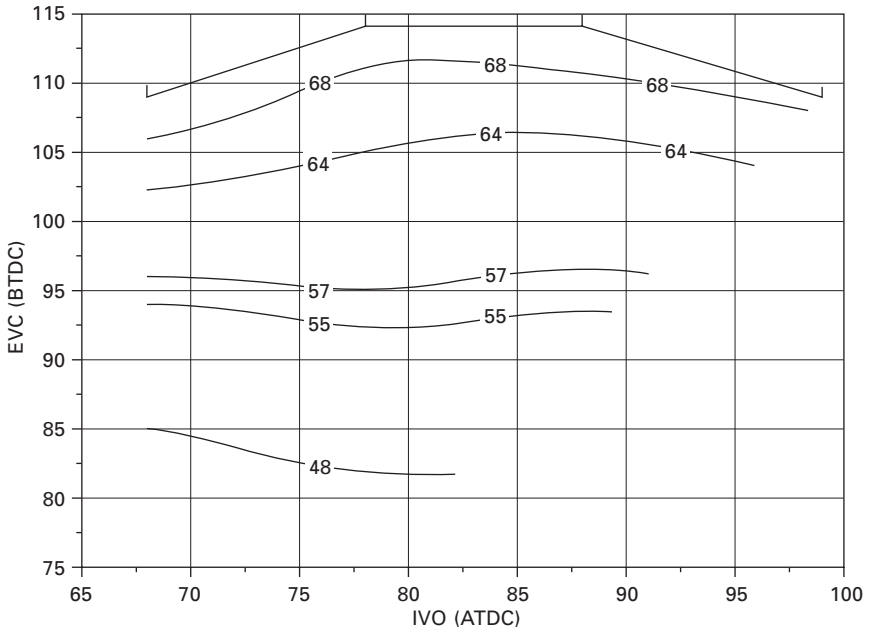
In the case of autoignition combustion with residual gas trapping, the power output of the engine is directly controlled by the valve timings. Figure 6.13(a) shows brake mean effective pressure (BMEP) contours as a function of EVC (exhaust valve closing) and IVO (intake valve opening) at 1500 rpm and $\lambda = 1.0$ in a four-cylinder four-stroke gasoline engine (Li *et al.*, 2001; Zhao *et al.*, 2002). The engine was equipped with a pair of low-lift camshafts and two independent VCT devices that allowed the intake and exhaust valve timings to be altered by 40° crank angles. As shown in Fig. 6.13, when the EVC is retarded from 115 CA BTDC to 75 CA BTDC the engine output increases from 1.45 bar BMEP to 3.65 bar BMEP. This can be understood



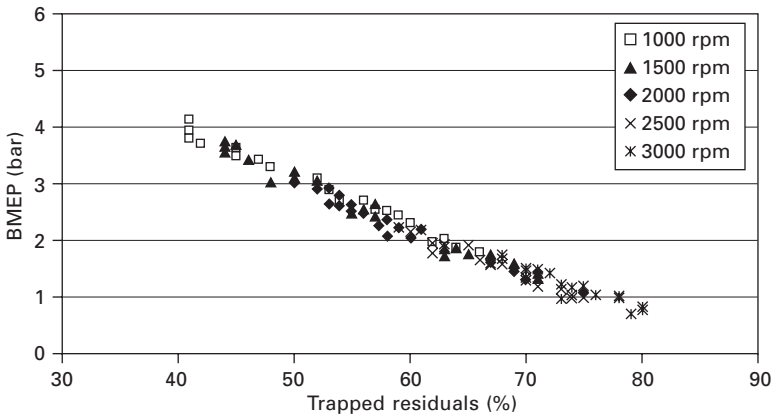
6.13 Contours of brake mean effective pressure (bar).

by referring to the plots in Figs 6.14 and 6.15. It can be seen in Fig. 6.14 that as the exhaust valve closes earlier the residual gas fraction increases. Figure 6.15 shows that there was a linear correlation between the residual fraction and the engine’s performance, independent of the engine speed. The higher the residual fraction, the lower the torque became. As the engine was operated at WOT during autoignition combustion, the mass in the cylinder was more or less the same and only the mixture concentration changed. The more residuals were trapped, the less air/fuel mixture the engine could breathe in, and hence the lower torque could be generated. Therefore, changing the residual fraction by adjusting the valve phasing is an effective means of controlling the engine load during the CAI combustion operation, resulting in throttleless engine operation and hence reduced pumping losses.

Figure 6.11 also shows that for each engine speed there were upper and lower limits of BMEP and IMEP outputs. The upper limit was a consequence of the restrictions of the gas exchange process imposed by the special camshafts. The lower end of the torque output was limited by misfires. The range of torque output was dependent upon the engine speed. At lower engine speed, the breathing capability of the engine was improved and hence a higher maximum torque output could be obtained. As the engine speed went up, the maximum fresh charge that the engine could take in was reduced, as



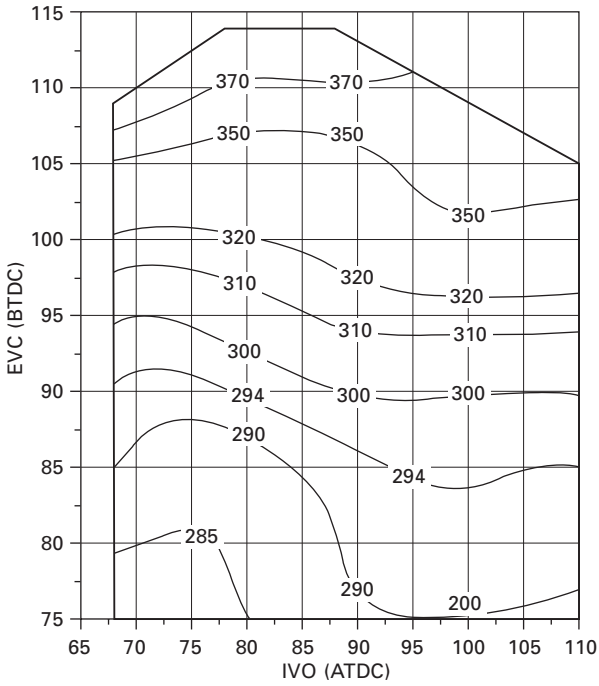
6.14 Contours of concentration of residual gas concentration.



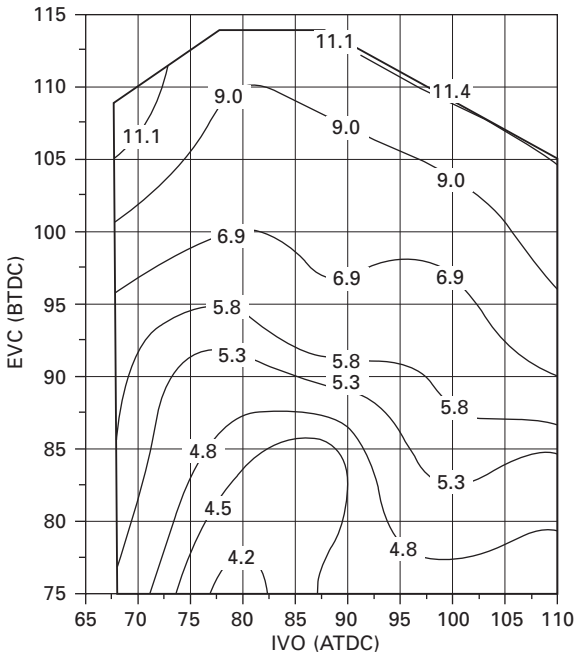
6.15 Relationship between BMEP values and the percentage of trapped residual gas.

less time was available for the gas exchange process to take place through the low lift valves, leading to a lower maximum torque output.

In addition to controlling the engine's output, the valve timings are found to affect the engine's fuel consumption and exhaust emissions. As shown in Figs 6.16 and 6.17, at the same BMEP value of 3.4 bar, both the fuel

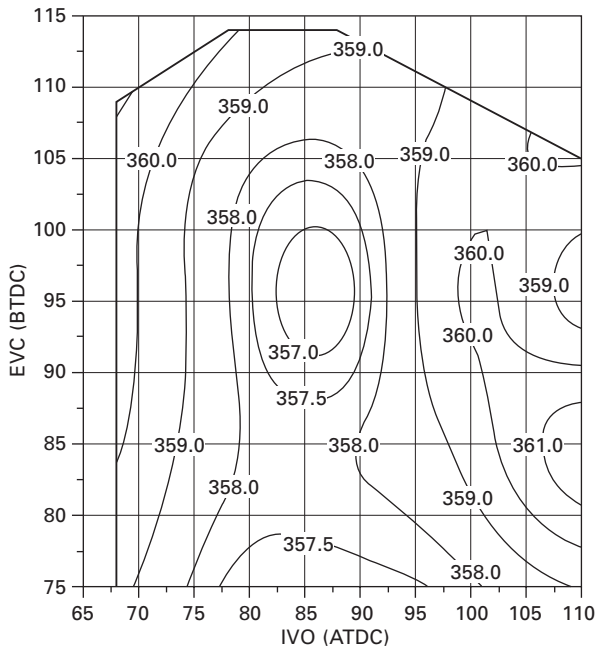


6.16 Contours of brake specific fuel consumption (g/kWh).



6.17 Contours of brake specific hydrocarbon emissions (g/kWh).

consumption and HC emissions increase with the retarded intake opening as the effective compression ratio is decreased and combustion becomes less complete. Furthermore, in-cylinder pressure measurements and the subsequent heat release analyses indicate that the autoignition and heat release processes are also affected by the valve timings. As shown in Fig. 6.18, autoignition occurs earliest at the intermediate EVC and IVO timings, corresponding to the middle range of the autoignition combustion region. This is because at the same EVC timing or load point, retarded IVO reduces the effective compression ratio, giving a lower compression temperature and retarded autoignition. Earlier opening of the inlet valve induces more backflow of the hot residual gases into the intake port immediately after the opening of the inlet valve due to higher in-cylinder pressure than that in the intake port. This portion of residual gas will lose heat to the intake port and the in-cylinder gas mixture will start the compression process at a lower charge temperature, resulting in delayed autoignition combustion. For the same IVO setting in Fig. 6.18, the change of combustion timing with EVC timing is associated with the variation in engine output. As EVC is advanced, the concentration of residual gas increases at reduced load. Combustion takes place with a more diluted mixture and hence lower combustion and burnt gas temperature. The trapped residual gas from the previous cycle will therefore



6.18 Contour of the position of 10% mass fraction burned.

be at a lower temperature, retarding the autoignition process. On the other hand, the increase in load with retarded EVC leads to a higher residual gas temperature but the quantity of residual gas will be reduced. Beyond a certain load and EVC setting, the total thermal energy of residual gas, which is proportional to its temperature and mass, will start to drop when the effect of mass becomes dominant. This will cause the autoignition to be delayed at the upper load region of CAI operations. Therefore, the start of combustion is delayed or even misfire can occur as EVC timing is changed to produce either higher output or lower torque.

The above discussion demonstrates that EVC timing can be used to achieve rapid load control. The IVO timing should be adjusted accordingly to achieve the optimised combustion, lower fuel consumption and lower exhaust emissions, when the residual gas trapping method is employed.

6.4.2 Effects of injection strategy on autoignition combustion

The direct injection of fuel can take place at different parts of an engine cycle, as shown in Fig. 6.10. The cylinder pressure diagram is obtained with a negative valve overlap and shows the recompression peak as well as the normal combustion peak. The injection timing is grouped into categories: early injection during the negative valve overlap period, mid injection during the intake process, and late injection in the compression stroke. The effects of injection timing on autoignition combustion are summarised in Table 6.1.

When injection takes place during the negative valve overlap period, the liquid fuel is injected into hot residual gas left from the previous cycle. As the liquid fuel evaporates, it introduces a charge cooling effect to the cylinder charge, which is shown by a negative heat release in the heat release diagram during the negative valve overlap period. During the subsequent mixing of fuel vapour with hot residual gas, intermediate species are produced due to fuel-reforming reactions and some heat release can take place when there is oxygen in the residual gas from the lean-burn combustion or if a mixture of air and fuel is injected (Li *et al.*, 2007; Cao *et al.*, 2008). The overall effect

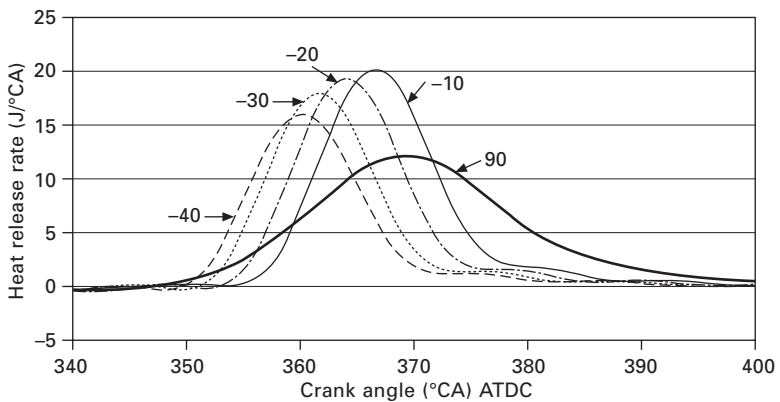
Table 6.1 A Summary of fuel injection timing effects

Injection timing	Charge cooling	Volumetric efficiency	Fuel reforming	Charge heating	Charge/thermal stratification
Early injection	✓		✓	✓	
Mid injection		✓			
Later injection	✓				✓

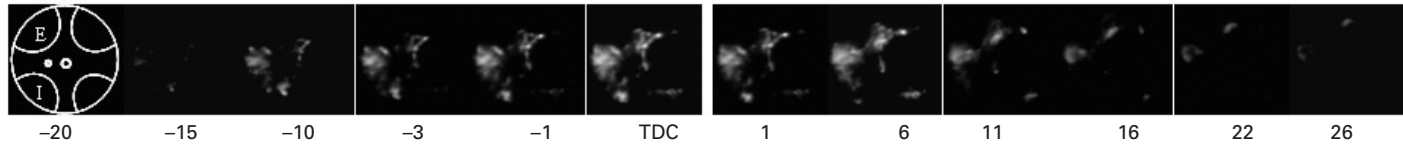
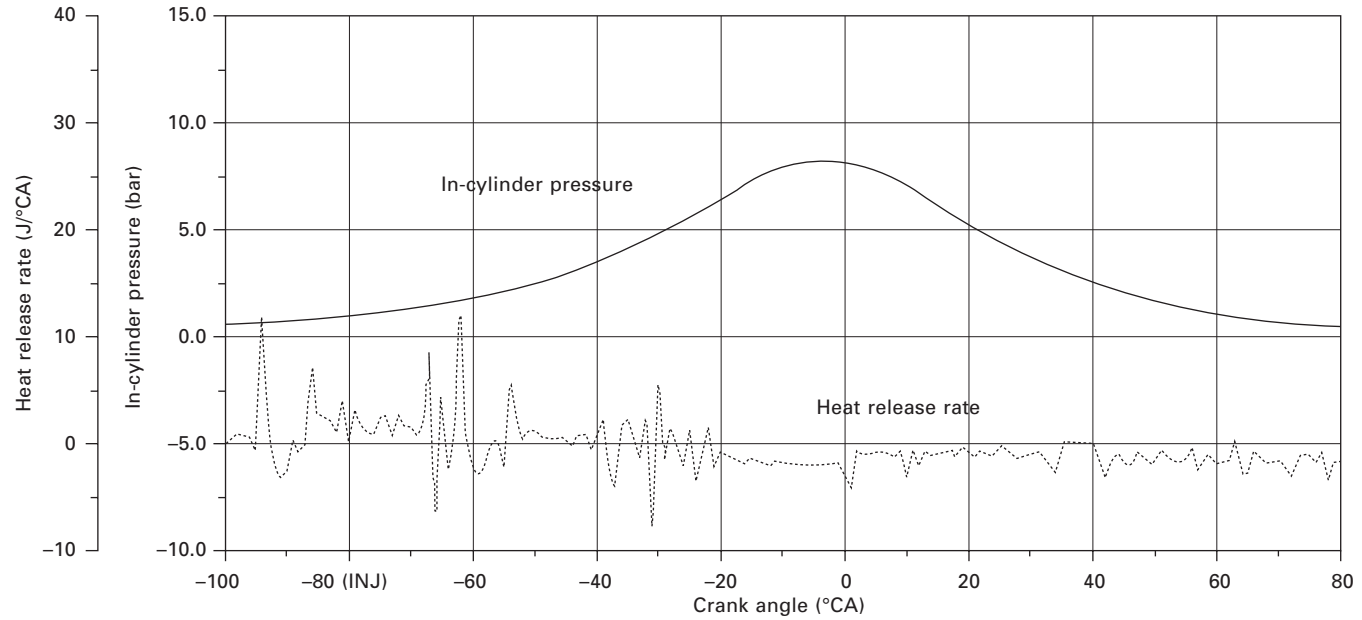
of early injection is the advancement of autoignition as shown in Fig. 6.19, which was obtained from a four-cylinder DI gasoline engine (Standing *et al.*, 2005). Analytical studies (Cao *et al.*, 2008) have shown that when fuel is injected into hot residual gases with oxygen, heat release from the high temperature reactions has a predominant effect on advancing the start of main combustion. Intermediate species formed during the negative valve overlap period, on the other hand, are responsible for the advanced combustion phasing for stoichiometric operations. Further evidence of fuel reforming was recently obtained through in-cylinder high speed chemiluminescence measurements (Yang, 2008), shown in Fig. 6.20. The images were taken at 10000 fps through an intensified high-speed video camera during the negative valve overlap period together with the in-cylinder measurements. A small mixture of air and fuel is injected through an air-assisted injector at 80°CA BTDC just after the exhaust valves are closed. Although no heat release can be detected in the heat release diagram, the occurrence of chemical reactions is confirmed by the chemiluminescence images detected from 15°CA BTDC to 26°CA ATDC, lasting over 40 CA.

When fuel injection takes place in the intake period, more air is inducted into the cylinder due to the charge cooling effect and a slight increase in the engine output is observed for the same valve timings. As the fuel injection is retarded into the compression stroke, the creation of a fuel-rich zone due to charge stratification can lead to an early combustion phasing as autoignition is promoted by the presence of a fuel and air mixture region at higher temperature between the fresh fuel and hot cylinder gas. Late injection is accompanied, however, by a penalty of higher NO_x and soot emissions (Cao *et al.*, 2006).

In order to take advantage of the individual effect of injection timings,



6.19 Effect of injection timing on the heat release process in a four-cylinder DI gasoline engine.



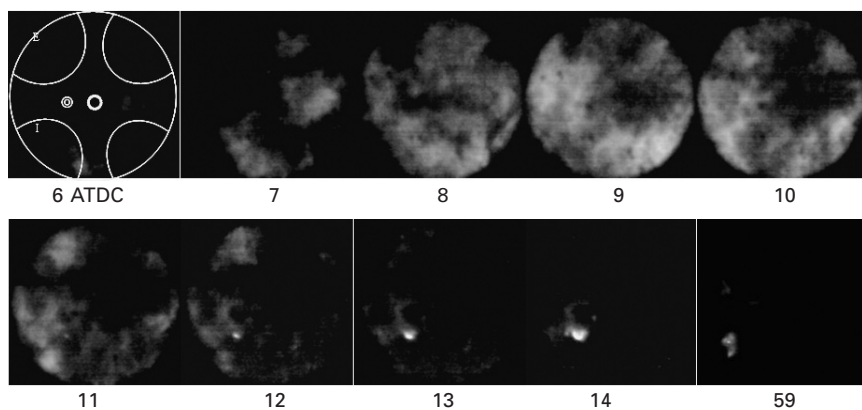
6.20 Mini combustion with simultaneous in-cylinder pressure, heat release rate and full chemiluminescence images at λ_1 , 1600 rpm, gain 50%, SOI = 80° CA BTDC.

split injections have been employed to alter the combustion phasing and engine performances (Li *et al.*, 2007; Cao *et al.*, 2005, 2006; Urushihara *et al.*, 2003). As discussed previously, the principal effect of early injection into lean-burnt residual gas is the heat release reactions during the negative overlap period and the resulting increase in the compression temperature. Experimental results indicate that the charge temperature at IVO can be increased by up to 150 K as the quantity of pre-injection during the negative valve overlap is varied from zero to 10% of the total fuel delivered in a split injection operation. This is translated to about an 80 K increase in the peak compression temperature near compression TDC. Since the autoignition temperature of gasoline fuel is typically around 1000 K, a temperature difference of around 50 K will be sufficient to trigger autoignition to occur at more desirable timings for optimised combustion, with improved efficiency and lower emissions. Such control over the combustion phasing can be realised through a closed-loop control of 50% burn angle through in-cylinder pressure measurements that can now be accomplished using the low cost piezo-resistive pressure transducer being developed for mass production. A control algorithm can be applied to adjust the timing and quantity of pre-injection for the desired CA50 values. In addition, the main injection can be adjusted to compensate for cylinder-to-cylinder variations in IMEP due to imbalance in air flows and different thermal boundaries in each cylinder.

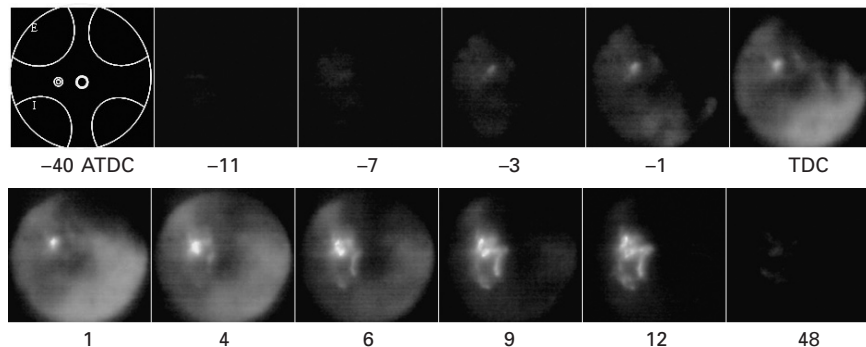
6.4.3 Effects of spark discharge on autoignition combustion

Following some initially conflicting reports on the effect of spark discharge from a standard spark plug on autoignition combustion, it has been established that spark can be harnessed for stabilising and altering the autoignition combustion process under conditions when part of the mixture is ignitable. In the middle region of the CAI operation, there is a large percentage of diluents, whether air or recycled exhaust gas. In the case of CAI operation with residual gas trapping, the residual gas concentration is typically more than 50% when there is sufficient thermal energy to cause the combustible charge to reach the autoignition temperature without spark assistance. As the mixture becomes less diluted, it becomes more flammable by spark discharge, while the autoignition tendency is diminishing with less thermal energy. As a result, a flame kernel can be initiated and expands as a flame front, which in turn can compress the unburned fuel and air mixture to reach the autoignition temperature. Because of the slow flame propagation speed in the diluted combustible mixture, there can be sufficient time for autoignition reactions to take place, as the initial reactions leading to autoignition combustion are fairly slow compared to the high-temperature heat-release reactions. As a result, hybrid combustion of flame and autoignition can occur

under such conditions. This is best demonstrated by the high-speed video chemiluminescence images of such a combustion process shown in Figs 6.21 and 6.22 (Yang, 2008). They were taken at 10000 fps from the single-cylinder direct injection gasoline engine with optical access through the extended piston. The images in Fig. 6.21 were taken without spark ignition and are characterised by multiple combustion sites distributed around the peripheral region of the combustion chamber. The first visible combustion occurs at 6°CA ATDC. With the spark ignition switched on, Fig. 6.22 shows that first combustion images appears at 11°CA BTDC near the spark plug as the flame kernel expands. In addition, an autoignition combustion site appears at 1°CA BTDC at the bottom right corner of the image. The chemiluminescence



6.21 Simultaneous in-cylinder pressure, temperature, heat release rate, MFB rate and full chemiluminescence images at λ_1 , 1600 rpm, gain 60%, SOI = 80° CA ATDC and without spark.



6.22 Simultaneous in-cylinder pressure, temperature, heat release rate, MFB rate and full chemiluminescence images at λ_1 , 1600 rpm, gain 60%, SOI = 80° CA ATDC and with spark.

intensity is higher and combustion images appear more dense than in pure autoignition combustion. This is in agreement with the in-cylinder pressure measurement and heat release analysis which showed earlier combustion and a higher heat release rate when spark ignition was present.

Spark-assisted autoignition combustion has been used to optimise the combustion phasing for minimum fuel consumption and lower emissions (Standing *et al.*, 2005; Urushihara *et al.*, 2005). The presence of spark has also been used to reduce the cycle-to-cycle variations (Koopmans *et al.*, 2003). It has also been found that spark-assisted autoignition combustion can be employed to achieve a smooth transition between SI and CAI operations in both a two-stroke (Onishi *et al.*, 1979) and a four-stroke gasoline engine (Zhang *et al.*, 2007), which will be discussed further in Section 6.5.

6.4.4 Extending the autoignition combustion operational range

As shown in Fig. 6.11, autoignition combustion can be achieved over a limited range of speed and load conditions. It would be desirable to operate the engine with autoignition combustion over a wider range of engine operating conditions.

One obvious solution to extend the high load limit of autoignition combustion is to increase the density of air in the cylinder by pressure charging. It has been demonstrated by Christensen *et al.* (1998) that boost pressures of up to ~2 bar could be tolerated during supercharged autoignition combustion provided the inlet air temperature was varied accordingly. In a later work, Olsson and co-workers (2004) showed the importance of turbocharger efficiency on fuel economy and emissions. In the case of CAI combustion operation by residual gas trapping, both an externally driven supercharger rig and a turbocharger (Cairns and Blaxill, 2005b; Martins and Zhao, 2008) have been used to raise the upper limit of CAI combustion by about 2 bar in IMEP values. The improvement is more noticeable in the high speed region where the limited flow area imposed by the low valve lift and duration is the limiting factor. However, in order to avoid a too rapid heat release rate, increase in the air supply pressure needs to be accompanied by an increase in the air to fuel ratio of the in-cylinder mixture (Cairns and Blaxill, 2005b).

In addition to intake boosting, exhaust boosting has also been proposed. The supercharging by exhaust blowdown method proposed by Hatamura (2007) generates high-pressure burnt gas by opening one of the exhaust valves early in the power stroke before it is closed before BDC and stores it in a separate exhaust manifold that is shut off from the exhaust system during the autoignition combustion, while the other exhaust valve is allowed to operate normally to expel the exhaust gas during the exhaust stroke. After the intake valve is closed, the first exhaust valve reopens around BTDC

before compression so that the stored high-pressure exhaust gas is forced into the cylinder, hence supercharging by exhaust. As the burnt gas is recycled after the air has been inducted and trapped in the cylinder, the proportion of recycled burnt gas, which acts as the heating source to promote autoignition and as the diluent to slow down the heat release rate, to the fresh fuel and air mixture can be maintained at the elevated pressure or charge density required for higher engine output. A similar idea but using inter-cylinder exhaust charging was demonstrated on a four-cylinder DI gasoline engine equipped with electromagnetic valves (Takanashi *et al.*, 2006), in which the additional effect of the exhaust wave from the other cylinder is also utilised by forming two separate high-pressure exhaust gas manifolds.

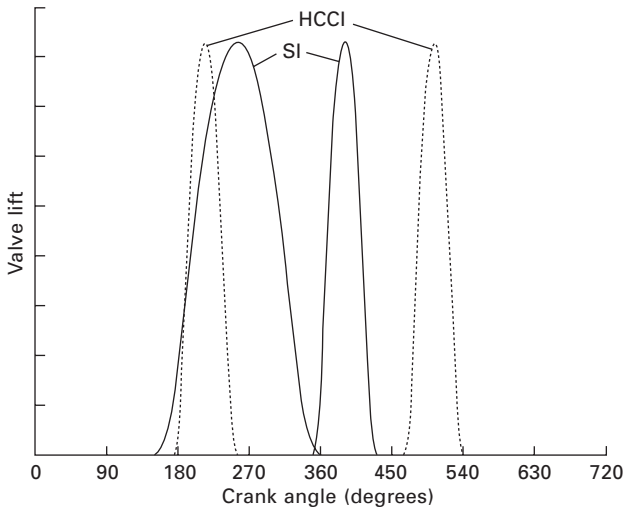
The advantage of extended CAI operation by boosting should be considered together with potential difficulties associated with managing the transition from naturally aspirated SI combustion to boosted CAI at high loads with the turbo lag. The use of a mechanical supercharger may provide a better response, but the implication of its parasitic losses on the overall fuel economy benefit needs to be considered.

Even without pressurising the intake air supply, it has been found that the introduction of externally cooled EGR (Cairns and Blaxill, 2005a) can extend the upper limit of naturally aspirated CAI operation by 20–65% between 1000 rpm and 3000 rpm, with the greatest benefit achieved at speeds of 1500 rpm to 2000 rpm. Under these conditions, the presence of additional external exhaust gas helped to retard ignition, reduce the rate of heat release and limit the peak knocking pressure.

6.5 Development of practical gasoline engines with autoignition and spark-ignition (SI) combustion

As discussed in the previous sections, it will not be possible to operate a gasoline engine in the autoignition combustion mode over the entire engine speed and load range. A practical engine has to be developed that can operate in and switch between flame propagation and autoignition combustion operations.

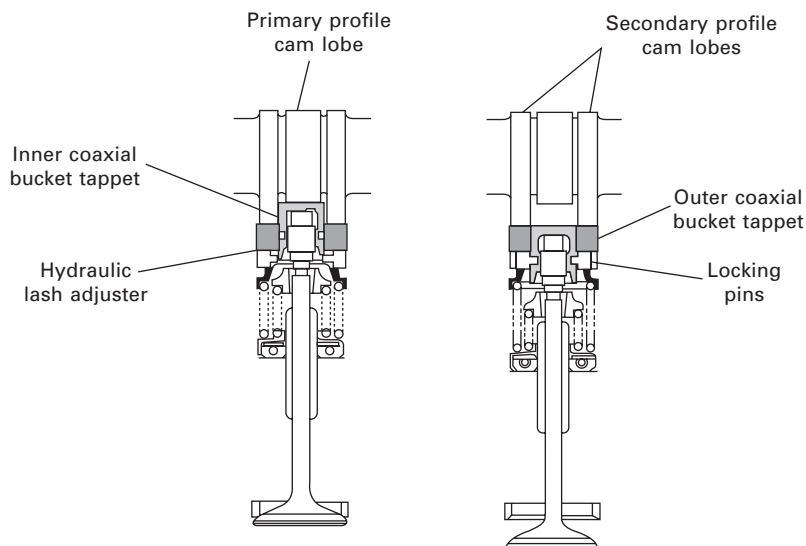
The first demonstration of switched operation between SI and autoignition combustion was carried out in a four-stroke single-cylinder research engine and a five-cylinder engine both equipped with the electromechanical camless valve actuation system (Koopmans *et al.*, 2003). When it is necessary to change from SI to CAI engine operation, the residual mass has to be increased and the air excess ratio and fuel amount often also have to change. As shown in Fig. 6.23, the spark ignition operation was operated with a typical exhaust valve lift profile but the intake valve lift profile was set to a much narrower duration in order to achieve unthrottled SI operation. When change to CAI was required, the exhaust valves were closed much earlier to trap sufficient



6.23 Valve lift profiles adopted for SI and HCCI operations by the electromechanical camless system.

burnt gas and the intake valve opening was shifted to the mid-intake stroke. Although the change in the valve lift profiles could be achieved within one cycle, the first few cycles of CAI operation were characterised by earlier, quicker and faster combustion than the later cycles, due to the hotter exhaust gas from the previous SI cycle and hotter boundary conditions created by the hotter SI combustion operations. This was accompanied by a jump in torque as the thermal efficiency of CAI combustion was higher. Koopmans *et al.* (2003) suggested that optimisation of valve timings and fuel adjustment were needed to achieve improved SI to CAI switching operations. Switching from CAI to SI operation did not have many complications as SI combustion was such less sensitive to the ambient conditions.

A much more practical approach is to achieve both SI and CAI operations in a gasoline engine with a cam profile switching (CPS) mechanism in conjunction with twin independent variable cam timing (VCT) devices. The CPS device allows operation with two different valve lift modes, whilst the valve timing is altered by the VCT devices. The components of the CPS mechanism are typically inner and outer co-axial bucket tappets and three cam lobes per engine valve (Fig. 6.24). The inner tappet operates directly on the engine valve via a hydraulic lash adjuster and is controlled by the central cam lobe. The outer tappet is driven by a pair of outer cam lobes of identical profiles and has its own set of lost motion springs within the tappet to absorb lost motion and to ensure that it remains in correct contact with its cams at all times. To achieve profile switching (from the outer to the inner cam profile) the valves within a chosen cylinder are switched by releasing



6.24 Cam profile switching device with coaxial bucket tappet.

the locking pins and allowing the inner and outer tappets to slide relative to each other. The engine valve is now controlled purely by the inner tappet. If the inner lobe has been manufactured with a small lift relative to the outer lobes, the engine valve will be lifted with a small lift. During normal engine operation the locking pins are held in the locked position by engine oil pressure. When a profile switch is required to the lower lift value, the oil pressure supplied to the tappets is reduced to a lower level by the use of a simple pressure-modulating solenoid valve, thus allowing a light spring to move the locking pins to the unlocked position.

One example of such work was reported by Cairns and Blaxill (2007). They applied two-stage cam profile switching to the transition between SI and CAI combustion in a four-cylinder direct injection research engine. They found that in order to avoid individual cylinder misfires, it was necessary to employ sequential CPS strategies. Furthermore, they stated that to improve the response of the switching tappets, the oil circuit dead volumes needed to be minimised and the inlet and exhaust tappet oil supply pressures were decreased to the minimum value possible for robust SI operation (~1 bar gauge). Following these modifications, it was possible to achieve transition without misfire on the four-cylinder direct injection gasoline engine.

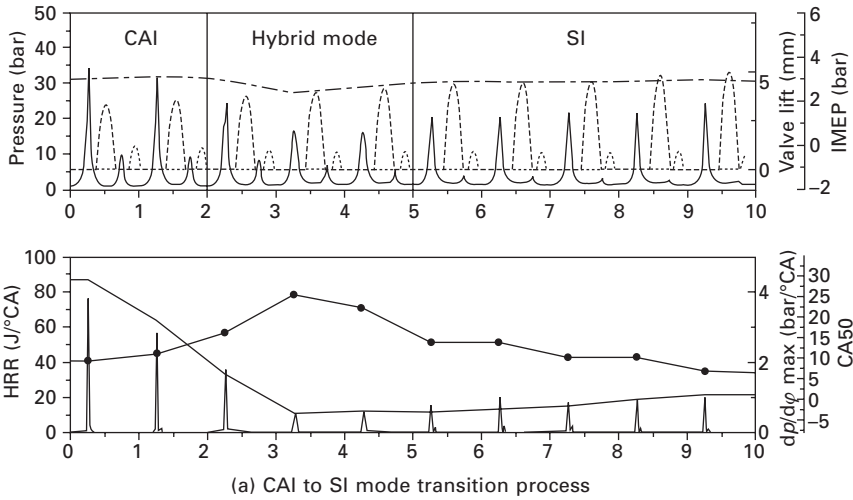
In a similar study carried out on a 3.0 litre V6 DI gasoline engine with twin CPS and twin VCT devices in the author's laboratory (Kalian and Zhao, 2008), it was found that the control strategy had to be tuned in order to realise a successful transition from the SI mode to the CAI mode. First,

the control program was modified so that two different sets of parameters, namely ignition timing, injection timing and valve timing, could be pre-set, one for the high-lift SI mode and one for the low-lift CAI mode. Hence, when a transition was undertaken, the parameters would change instantly. However, the values of these parameters did not correspond to their steady-state operation and would need careful calibration through the closed-loop control. In addition, the throttle setting and speed of its opening and closing may need to be adjusted to avoid misfire due to excessive fluctuation in the air inducted into each cylinder.

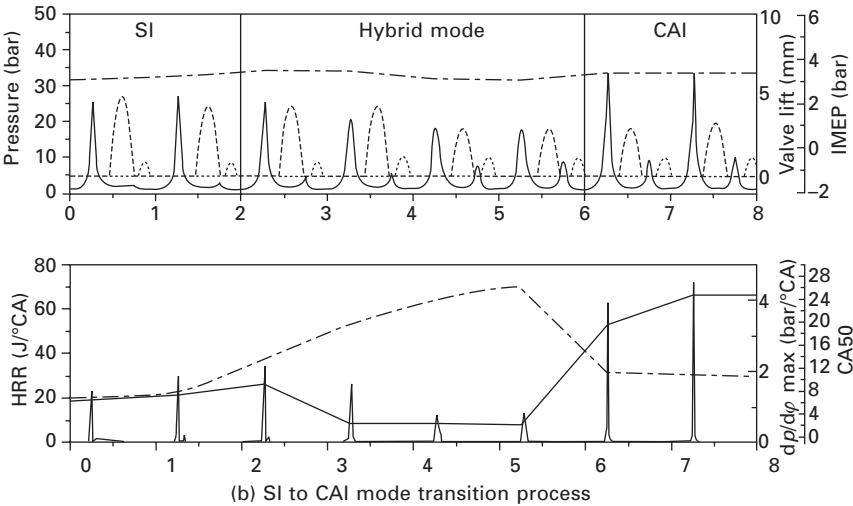
Recently, a more flexible and practical approach to achieving SI and CAI combustion in a production-type four-stroke gasoline engine has been researched and developed by the author and his colleagues in SKLE (Zhang *et al.*, 2007) by making use of mechanically variable valve lift systems in production engines which are capable of continuously varying the valve lift from less than 1 mm to the full lift of 9 mm (Fig. 6.10). Examples of successful CAI–SI and SI–CAI transitions are shown in Fig. 6.25. Figure 6.25(a) shows the sequence of cycles during the SI to CAI operation. In the first two cycles, the engine was operated in the CAI combustion mode with a low exhaust valve lift and early EVC. The switching process started as the exhaust valve lift was increased and the EVC was retarded in order to reduce the level of residual gases. During the switching cycles (from cycle 3 to cycle 5), spark-assisted autoignition took place, the spark-ignition combustion process became more dominant and the heat release rate decreased. In order to maintain the engine output and efficiency, the effective compression ratio was adjusted by altering the IVC timing. As a result, the CAI–SI switching process lasted about three cycles. Similarly, by simultaneously controlling the residual gas concentration through adjusting the exhaust valve lift profile and heat release process through spark timing and IVC, swift and smooth switching was achieved from SI to CAI mode operation, as shown in Fig. 6.25(b). If IMEP fluctuations (δ IMEP) are employed to indicate the stability of the transition process, experimental results show that δ IMEP in the 4VVAS engine can be reduced to 0.2 bar in the CAI–SI transition and to less than 0.3 bar during the SI–CAI transition process through the optimised control strategies, which represents perhaps one of the best results reported in the literature.

6.6 Future trends

The state of the art in direct injection gasoline engines with autoignition combustion is demonstrated by GM and Mercedes in their concept cars. GM has implemented its HCCI engines in an Opel Vectra and a Saturn Aura vehicle. The Aura car is powered by a 2.2-litre Ecotec engine that makes 134 kW and has a torque of 230 Nm. It features a central direct-injection system,



(a) CAI to SI mode transition process



(b) SI to CAI mode transition process

6.25 Valve lifts, IMEP, in-cylinder pressure, heat release rate (HRR) and CA50 during the switching process between the two combustion modes.

with CPS on both the intake and exhaust sides, dual electric camshaft phasers, and individual cylinder pressure transducers to control the combustion as well as deliver a smooth transition between combustion modes. Its latest achievements include the engine's ability to operate in autoignition combustion mode from idle to a vehicle speed of 50 mph.

Another recent development is the Dies-Otto engine developed by Mercedes which was on show at the 2007 Frankfurt Motor Show. The 1.8-

litre direct injection gasoline engine employs piezo injectors, sequential two-stage turbo-charging and advanced electronic controls. CPS and VCT are used to switch between SI and autoignition combustion. In addition, a variable crank mechanism is employed to alter the geometric compression ratio.

On the research front, the scope of autoignition combustion is being expanded and redefined. The widely accepted acronym of HCCI has become merely symbolic, as ‘homogeneous charge’ and ‘compression ignition’ do not reflect the truth of the combustion process involved. The use of stratified charge (whether fuel, air or recycled exhaust gas) can be advantageous to expand the operational region of autoignition combustion to both low and higher load regions. Compression ignition does not reflect the thermal process leading to autoignition combustion and the fact that the spark-assisted autoignition combustion process has been shown to extend the low-temperature dilution combustion operation. In fact, stratified charge and hybrid combustion of spark ignition and autoignition could be used to bridge the gap between the conventional SI combustion with moderate exhaust dilution and autoignition combustion at high exhaust gas dilution, opening up the possibility of low-temperature combustion of a diluted premixed fuel and air mixture over a much wider range of the entire engine operation for the benefit of lower fuel consumption and low exhaust NO_x emissions. It is therefore the author’s view that the current focus on achieving HCCI or CAI combustion should be broadened so that the automotive direct injection gasoline engine can be operated in the low-temperature combustion mode of stoichiometric air/fuel mixture with variable exhaust dilutions throughout its load range.

6.7 References

- Benson J (1972), ‘The influence of engine and fuel factors on after-run’, SAE paper 720085.
- Cairns A and Blaxill H (2005a), ‘The effects of combined internal and external exhaust gas recirculation on gasoline controlled autoignition’, SAE paper 2005-01-0133.
- Cairns A and Blaxill H (2005b), ‘Lean boost and exhaust recirculation for high load controlled autoignition’, SAE paper 2005-01-3744.
- Cairns A and Blaxill H (2007), ‘The effects of two stage cam profile switching and external EGR on SI-CAI combustion transitions’, SAE paper 2007-01-0187.
- Cao L, Zhao H, Jiang X and Kallian N (2005), ‘Mixture formation and CAI combustion in four-stroke gasoline engines with single and split fuel injections’, *International Journal of Engine Research*, Volume 6, Number 4, pp. 311–329.
- Cao L, Zhao H, Jiang X and Kallian N (2006), ‘Investigation into the effect of injection timing on stoichiometric and lean CAI operations in a 4-stroke GDI engine’, SAE paper 2006-01-0417.
- Cao L, Zhao H and Jiang X (2008), ‘Analysis of controlled auto-ignition/CCI combustion in a direct injection gasoline engine with single and split fuel injections’, *Combustion Science and Technology*, Volume 180, pp 176–205.

- Christensen M, Johansson B, Amneus P and Mauss F (1998), 'Supercharged homogeneous charge compression ignition', SAE paper 980787.
- Fuerhapter A, Piock W F and Fraidl G K (2003), 'CSI – controlled auto ignition – the best solution for the fuel consumption – versus emission trade-off?', SAE paper 2003-01-0754.
- Fuerhapter A, Piock W F and Fraidl G K (2004), 'The new AVL CSI engine – HCCI operation on a multi cylinder gasoline engine', SAE paper 2004-01-0551.
- Fuerhapter A *et al.* (2007), 'Four stroke CAI engines with internal exhaust gas recirculation (EGR)', Chapter 6, in *HCCI and CAI Engine for the Automotive Industry*, by H. Zhao, Woodhead Publishing, Cambridge.
- Hatamura K (2007), 'A study on HCCI (homogeneous charge compression ignition) gasoline engine supercharged by exhaust blow down pressure', SAE paper 2007-01-1873.
- Hyoenene J, Haraldsson G and Johansson B (2003), 'Operating range in a multi-cylinder HCCI engine using variable compression ratio', SAE paper 2003-01-1829.
- Ingamells J (1979), 'Effect of gasoline octane quality and hydrocarbon composition on after-run', SAE paper 790939.
- Kalian N and Zhao H (2008), 'Investigation of transition between spark ignition and controlled auto-ignition combustion in a V6 DI engine with cam-profile switching', *Part D: Proc. IMechE, Journal of Automobile Engineering*, Volume 222, Number 10, pp. 1911–1916.
- Koopmans L and Denbratt I (2001), 'A four stroke camless engine, operated in homogeneous charge compression ignition mode with a commercial gasoline', SAE paper 2001-01-3610.
- Koopmans L, Backlund O and Denbratt I (2002), 'Cycle to cycle variations: their influence on cycle resolved gas temperature and unburned hydrocarbons from a camless gasoline compression ignition engine', SAE paper 2002-01-0110.
- Koopmans L, Strom H, Lundgren S, Backlund O and Denbratt I (2003), 'Demonstrating a SI–HCCI–SI mode change on a Volvo 5-cylinder electronic valve control engine', SAE paper 2003-01-0753.
- Lavy J, Dabadie J, Angelberger C, Duret P, Juretzka A, Schaflein J, Ma T, Lendresse Y, Satre A, Schulz C, Kramer C, Zhao H and Damiano L (2000), 'Innovative ultra-low NO_x controlled auto-ignition combustion process for gasoline engines: the 4-SPACE project', SAE paper 2000-01-1837.
- Law D, Allen J, Kemp D, Kirkpatrick G and Copland T (2001), 'Controlled combustion in an IC-engine with a fully variable valve train', SAE paper 2001-01-0251.
- Li J, Zhao H, Ma T and Ladommatos N (2001), 'Research and development of controlled autoignition (CAI) combustion on a multi-cylinder 4-stroke gasoline engine', SAE paper 2001-01-3608.
- Li Y, Zhao H, Brouzou N and Ma T (2007), 'Parametric study on CAI combustion in a GDI engine with an air-assisted injector', SAE paper 2007-01-0196.
- Martins M and Zhao H (2008), '4-stroke multi-cylinder gasoline engine with controlled auto-ignition (CAI) combustion: a comparison between naturally spirited and turbocharged operation', SAE paper 2008-36-0305, 2008.
- Olsson J-O, Tunestal P and Johansson B (2004), 'Boosting for high load HCCI', SAE paper 2004-01-0940.
- Onishi S, Souk H, Shoda K, Pan D and Kato S (1979), 'Active thermo-atmosphere combustion (ATAC) – a new combustion process for internal combustion engines', SAE paper 790507.

- Souk H J, Pan D J, Gomi T and Onishi S (1973), 'Development of a low emissions and high performance 2-stroke gasoline engine (NICE)', SAE paper 730463.
- Standing R, Kalian N, Ma T, Zhao H, Shamel A and Wirth M (2005), 'Effects of injection timing and valve timings on CAI operation in a multi-cylinder DI gasoline engine', SAE paper 2005-01-0132.
- Stockinger V, Schapertons H and Kuhlmann U (1992), 'Investigations on a gasoline engine working with self-ignition by compression', *MTZ*, Volume 53, pp. 80–85.
- Stokes J, Lake T, Murphy R, Osborne R, Patterson J and Seabrook J (2005), 'Gasoline engine operation with twin mechanical variable lift (TMVL) valvetrain. Stage 1: SI and CAI combustion with port fuel injection', SAE paper 2005-01-0752.
- Takanashi J, Awasaka M, Kakinuma T, Takazawa M and Urata Y (2006), 'A study of a gasoline HCCI engine equipped with an electromagnetic VVT mechanism – increasing the higher load operational range with the inter-cylinder EGR boost system', F2006P360, FISITA.
- Urushihara T, Hiraya K, Kakuhou A and Itoh T (2003), 'Expansion of HCCI operating region by the combination of direct fuel injection, negative valve overlap and internal fuel reformation', SAE paper 2003-01-0749.
- Urushihara T, Yamaguchi K, Yoshizawa K and Itoh T (2005), 'A study of gasoline-fueled compression ignition engine – expansion of HCCI operation range using SI combustion as a trigger of compression ignition', SAE paper 2005-01-0180.
- Xie H, Zhang Y and Zhao H (2008), 'Effects of valve management on in-cylinder residuals inhomogeneity in a gasoline HCCI engine with 4VVAS', SAE paper 2008-01-0052.
- Yang C-Y (2008), 'Investigation of combustion and performance characteristics of CAI combustion engine with positive and negative valve overlap', a PhD thesis, Brunel University.
- Yang J and Kenney T (2002), 'Development of a gasoline engine system using HCCI technology – the concept and the test results', SAE paper 2002-01-2832.
- Yang J and Kenney T (2006), 'Robustness and performance near the boundary of HCCI operating regime of a single-cylinder OKP engine', SAE paper 2006-01-1082.
- Zhang Y, Xie H, Zhou N, Chen T and Zhao H (2007), 'Study of SI–HCCI–SI transition on a port fuel injection engine equipped with 4VVAS', SAE paper 2007-01-0199.
- Zhao H (2007), *HCCI and CAI Engine for the Automotive Industry*, Woodhead Publishing, Cambridge.
- Zhao H, Li J, Ma T and Ladommatos N (2002), 'Performance and analysis of a 4-stroke multi-cylinder gasoline engine with CAI combustion', SAE paper 2002-01-0420.

Design and optimization of gasoline direct injection engines using computational fluid dynamics

J. YI, Ford Research and Advanced Engineering Research and Innovation Center, USA

Abstract: This chapter discusses the role of computational fluid dynamics (CFD) modeling in gasoline direct injection (DI) engine combustion system design and development. It starts with a brief review of injector technologies and the impact of the spray characteristics on the combustion system optimization. The main challenges to the optimization of a homogeneous-charge DI combustion system are to improve volumetric efficiency and fuel–air mixing homogeneity with reduced surface fuel wetting. Examples are included to demonstrate how CFD modeling is utilized to optimize the intake port design for improved flow capacity while providing adequate in-cylinder flow motion, to optimize combustion chamber design to improve fuel–air mixing at high speed and high load condition by alleviating the impact of intake flow on fuel spray, and to optimize fuel injection and cam strategy for improved fuel–air mixing homogeneity. For stratified-charge operation, CFD modeling has been applied to optimize the matching between intake flow motion and the spray configuration to generate stable charge stratification with the least amount of smoke emissions over a wide operation window. The boosted DI combustion system promotes its unique challenges in fuel–air mixing, knock mitigation, and higher heat flux requirement for catalyst warm-up in turbo-charged DI engines. However, it also provides further opportunity for combustion system optimization with fewer requirements on intake flow capacity. CFD modeling has been applied to optimize the intake port design to improve in-cylinder flow motion and mixing homogeneity. This chapter also provides a perspective view of CFD modeling in future combustion system development. CFD computational speed and simulation accuracy are two equally important aspects of CFD simulation in combustion system development and optimization. Better physical models are essential to the development of future advanced combustion systems with better fuel economy, higher power density, and cleaner emissions.

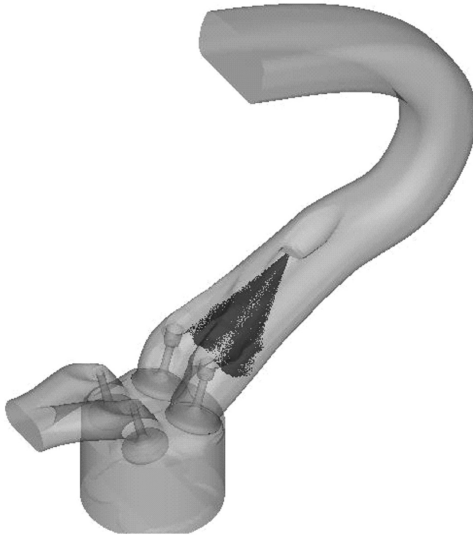
Key words: combustion system, direction injection, DI, DISI, gasoline, optimization, fuel–air mixing, homogeneity, stratified-charge, stratification, turbo-charged, super-charged, boosted, intake port, chamber, piston, spray, fuel injector, injection, split-injection, modeling, CFD, computational fluid dynamics, emission, computer speed and accuracy, physics, physical models.

7.1 Introduction

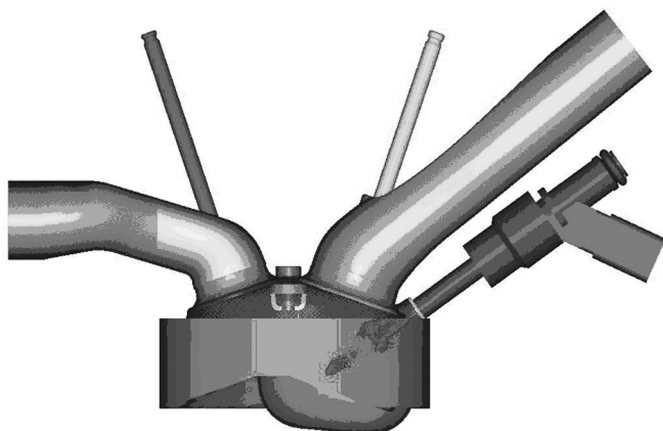
In the engineering of internal combustion (IC) engines, computational fluid dynamics (CFD) modeling is realizing an increasingly important role in

combustion system development thanks to an improved understanding of the physical processes and improved computer power. CFD modeling has become an integrated tool for engine combustion system development. Major automakers are using CFD extensively to develop and optimize their combustion systems. Development of high quality and optimized combustion systems follows from the insight of detailed physical processes that CFD modeling provides. CFD modeling also helps to reduce engine development costs and time due to reduced hardware design iterations.

CFD simulation has long been applied in diesel combustion system development. The application of CFD modeling in gasoline engine combustion system development has grown significantly in the last decade as the research and development of DISI (direct injection spark ignition) engines increases at universities and OEMs. In conventional PFI (port fuel injection) gasoline engines (Fig. 7.1), fuel is injected onto intake port surfaces and closed intake valves. Most of the injected fuel evaporates and mixes with the fresh intake air before it flows into the cylinder. This mixture is typically very well mixed before ignition occurs. In terms of modeling the combustion system operating processes, zero-dimensional or quasi-dimensional engine cycle simulation serves as an adequate tool to understand the engine operating process (Tabaczynski *et al.*, 1977; Davis and Kent, 1979; Matthews *et al.*, 1991; Dai *et al.*, 1995). However, in a DISI engine (Fig. 7.2), the fuel is injected directly into the cylinder. The in-cylinder dynamics involve a number of complex, closely coupled physical and chemical processes. These include



7.1 Schematic of Ford Duratec 3.5L V6 PFI engine combustion system with injector mounted in the intake port.



7.2 Typical combustion system for a DISI engine with side-mounted swirl injector (Yi *et al.*, 2002).

the transient three-dimensional dynamics of fuel injection and evaporation, spray-wall impingement, fuel-air mixing, ignition, combustion, and heat transfer between gas and surfaces such as the liner, cylinder head, and piston. A three-dimensional CFD simulation is necessary to capture these spatially and temporally dependent processes. Many commercial CFD software packages have been applied for such applications. The series of KIVA codes for IC engine cycle simulation (Amsden *et al.*, 1985, 1989, 1997; Torres and Trujillo, 2006) offers a unique platform for physical model development.

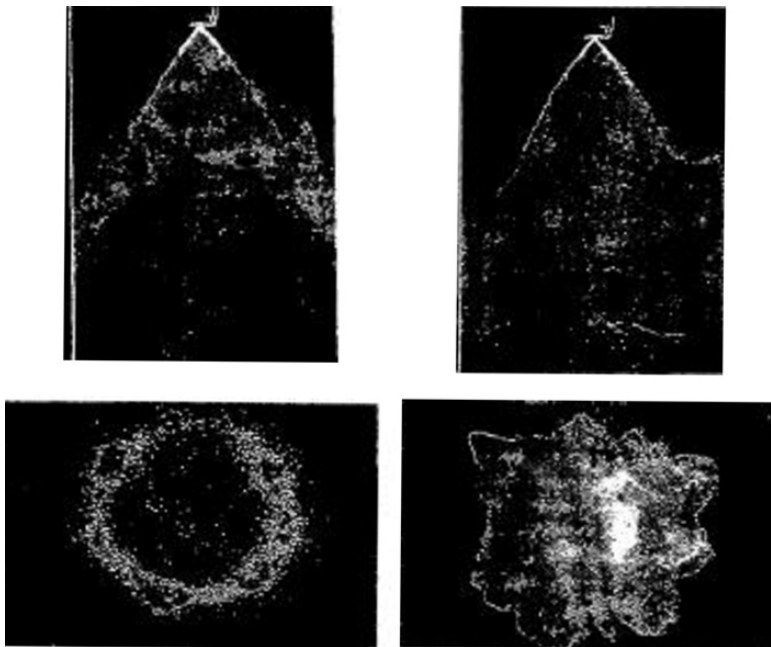
The design targets and the associated optimization procedure of a DISI combustion system depend on many different factors. Among the major influential factors are the operating mode, intake air system, injector type, and stratification generating mechanism. The major advantages of gasoline DI engines over existing PFI engines are improved fuel economy, quicker and cleaner engine start, and faster transient response. The advantages in start and transient response in DISI engines are directly related to the fact that the fuel is directly injected into the cylinder, instead of in the intake port as in PFI engines. There are four major factors that give improved fuel economy in gasoline DI engines. These include increased compression ratio, reduced pumping losses, higher specific heat ratio, and reduced heat losses to the cylinder walls. The compression ratio increase in DI engine is enabled by the charge cooling effect (Anderson *et al.*, 1996) due to the fuel evaporation in the cylinder charge as compared with on intake port surfaces in a PFI engine. The latter three benefits are mainly associated with stratified-charge DI engines, in which fuel-air mixing is stratified with a rich mixture around the spark plug and a lean mixture in the region away from the chamber center and close to the chamber surface. In the stratified-charge operating

mode, the fuel is injected during the compression stroke. In contrast, in a homogeneous charge operating mode, the fuel is injected during the intake stroke to achieve a homogeneous mixture.

7.2 Direct injection spark-ignition (DISI) injector technologies

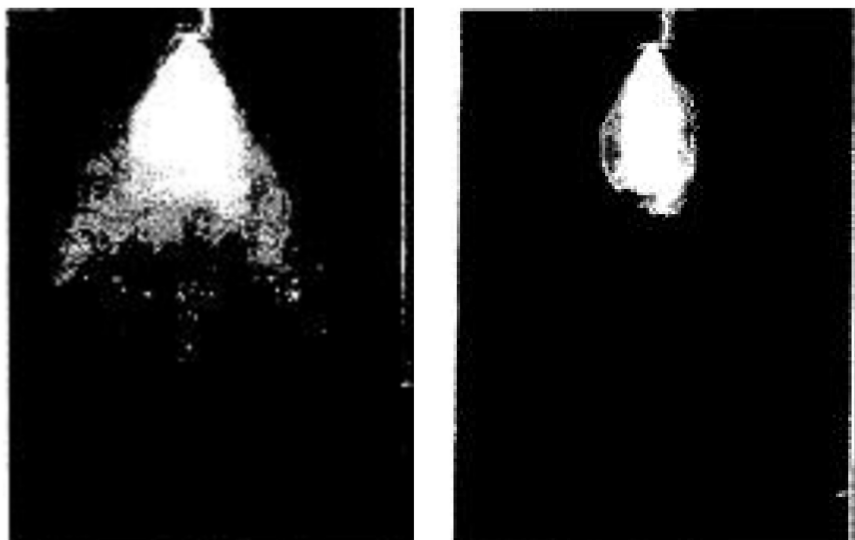
Fuel spray characteristics such as the spray shape, spray droplet size, penetration, and fuel flow rate are critical to the fuel spray evaporation, fuel–air mixing, and fuel–wall impingement. The selection of these injector characteristics to match the in-cylinder flow field and spark-plug location is an important aspect of the combustion system optimization process. It is worthwhile to briefly review DISI injector technology before discussing combustion system optimization.

DISI injector technologies have been evolving tremendously in the last two decades in order to improve the spray characteristics. There are five major types of DISI injectors: swirl injector, air-assisted injector, multi-hole injector, outwardly opening injector, and slit injector. Shown in Fig. 7.3 are



7.3 Spray images of Siemens swirl injector at 4 ms after start of injection with injection pressure of 2.9 MPa (left) and 8.4 MPa (right) (Zhao *et al.*, 1996); top row shows side view and bottom row shows cross-sectional view at 50 mm from the injector tip; Injection duration = 5 ms, Ambient pressure = 0.1 MPa.

the spray images of a Siemens swirl injector at 4 ms after start of injection with injection pressure of 2.9 MPa and 8.4 MPa by Zhao *et al.* (1996). It can be identified that a hollow-cone structure exists at the lower fuel injection pressure case. Due to its hollow-cone structure, the swirl injector is often referred to as a hollow-cone injector. It can also be seen that there is an air-entrainment zone at the edge of the spray cone. The other feature of the hollow-cone spray is that the spray cone decreases as the ambient pressure increases, as shown in Fig. 7.4. In DISI engine operations, the ambient pressure could go as low as 0.03 MPa at an idle condition with a homogeneous-charge mode. It could also reach as high as 1 MPa for injection late in the compression stroke during stratified-charge operation. The back pressure sensitivity of the spray shape coincides with the trend of the spray shape requirements for both homogeneous-charge and stratified-charge operations. For homogeneous-charge operation, the fuel is injected during the induction event. A widely dispersed fuel spray (a wide cone angle) is helpful in achieving good fuel–air mixing. For stratified-charge operation, the fuel is injected during the compression stroke. A compact spray (small cone angle) is preferred to achieve a stratified-charge mixture distribution. However, the spray-cone angle sensitivity to ambient pressure also adds further complexity to the combustion system design and optimization.

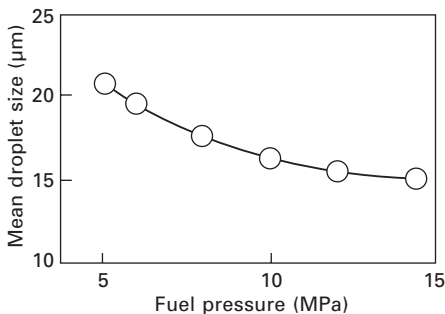


7.4 Spray photographs of a Siemens swirl injector with gasoline at 2 ms after start of injection at ambient pressure of 0.1 MPa (left) and 1.48 MPa (right) (Zhao *et al.*, 1996); fuel injection duration = 5.0 ms, fuel injection pressure = 5.5 MPa.

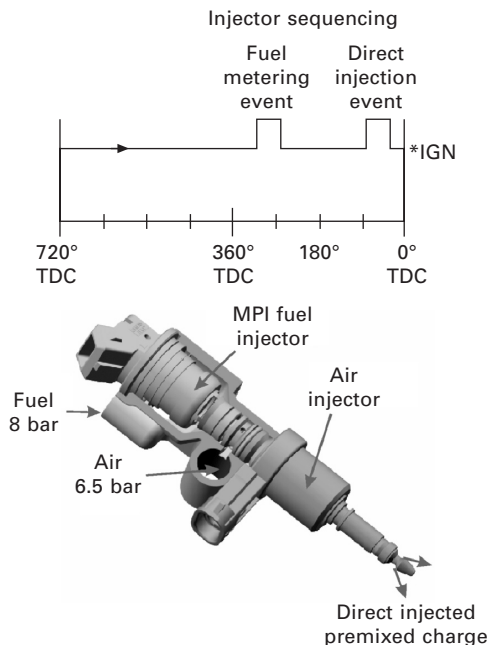
Figure 7.5 shows a typical fuel droplet size dependency on the fuel injection pressure reported by Harada *et al.* (1997). It is evident that as fuel pressure increases, the droplet size decreases. Based on his modeling work, Dodge (1996) recommended that a mean droplet size of 15 μm or smaller is required in DISI engines. The recent development in injector technology to generate such small droplets makes DISI engines feasible engine design solutions (Anderson *et al.*, 1996).

Air-assisted injection is a technology that produces sprays with well-atomized distributions even operating at relatively low fuel supply pressures. Shown in Fig. 7.6 is a typical air-assisted injector and its injection sequence developed by Orbital (Cathcart and Zavier, 2000). This fuel system comprises a direct injector, a conventional PFI-type fuel injector, and an interface region that provides the path between the air and the fuel. The conventional PFI injector provides the fuel metering function, operating with a constant differential pressure of normally 0.5 to 1.0 MPa. The metered fuel is combined with air in the interface region, and this charge, comprising fuel and air, is injected by the direct injector at a gauge pressure of normally 0.65 MPa. Fuel droplet shearing forces enable the air-assisted injector to produce smaller droplet sizes as compared with swirl injectors. Figure 7.7 shows the droplet distribution for a typical low load fueling event, with a SMD of approximately 10 μm . It is evident that the injection window of the air-assisted injector is limited by the available air pressure. During late compression stroke injection, the in-cylinder pressure may be too high to have positive differential pressure across the direct injector of this injection system.

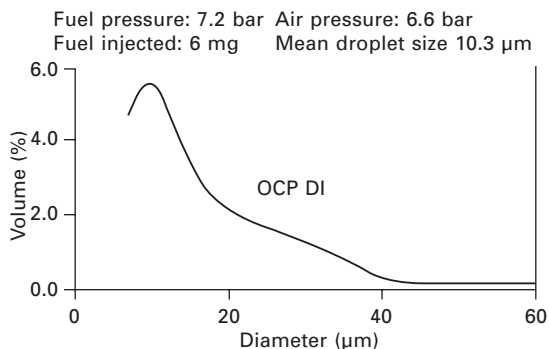
The multi-hole injector for a DISI engine is an extension of gasoline PFI and diesel injectors. The main difference between these injectors concerns the operating fuel pressure. PFI injectors typically operate at around 0.4 MPa, and diesel injectors with rail pressures as high as 200 MPa. Multi-hole DISI injectors operate in the range of 3 to 20 MPa. Shown in Fig. 7.8 is a Bosch six-hole injector and a representative spray image (Stach *et al.*,



7.5 Spray characteristics of a swirl injector (Harada *et al.*, 1997).

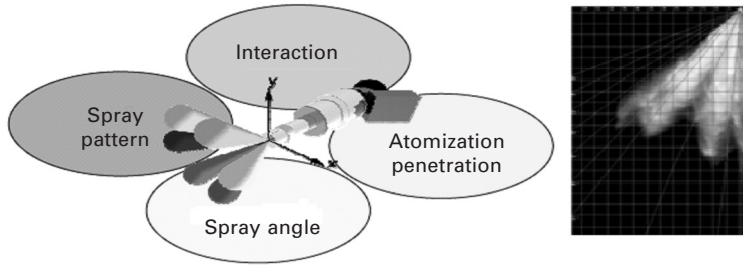


7.6 Schematic of Orbital air-assisted direct fuel injection system (Cathcart and Zavier, 2000).



7.7 Air-assisted fuel injection system PDPA particle size data (Cathcart and Zavier, 2000).

2007). One of the unique features of multi-hole injectors is the wide range of available flow rates. The other important feature is that the spray shape is not significantly dependent on the ambient gas pressure, even though the penetration of each jet decreases as the ambient pressure increases. Another important feature of the multi-hole injector in combustion system development is that the orientation of each individual spray plume (or jet) can be varied



7.8 Schematic of a Bosch 6-hole injector (left) and corresponding spray image (Stach *et al.*, 2007).

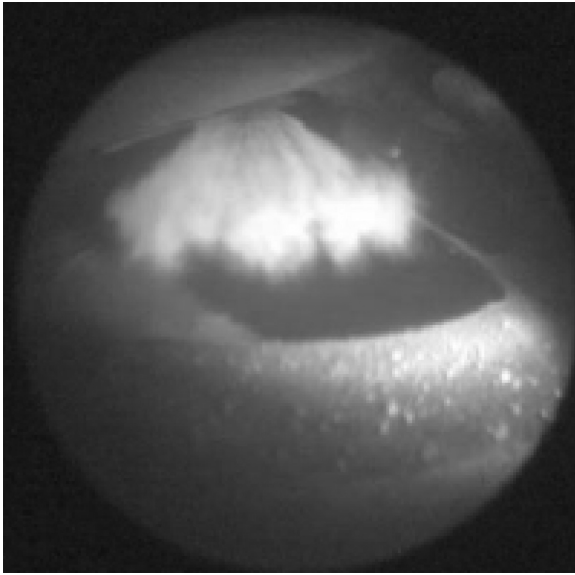
almost independently relative to the other spray plumes. This provides design engineers with great freedom for optimizing the injector spray patterns.

An outwardly opening piezo injector has a similar spray shape to the swirl injector but is formed through a conical annulus between the body of the injector and an outwardly opening pintle. The outward motion and quick, repeatable spray formation of this spray type lends itself well to being actuated by a piezoelectric stack. Such a piezo injector has a much wider dynamic fuel flow rate range and a quick transient response time. Shown in Fig. 7.9 is an image from a Siemens piezo injector. A characteristic feature described in the caption is the very small injection durations for both first and second injections, of the order of 200 μs . The capability to deliver fuel at short pulse widths with robust spray characteristics is a unique feature of the piezo injector. This feature also enables highly flexible multiple injection pulses per engine cycle.

Slit injectors emit fuel sprays from a rectangularly shaped slit. The resulting spray shape is similar to that of a fan. This injector design has been applied in Toyota DISI engines (Ikoma *et al.*, 2006). More details of this combustion system design will be discussed in Sections 7.3 and 7.4.

7.3 Homogeneous-charge direct injection (DI) system design and optimization

As mentioned in the preceding sections, the optimization of a homogeneous-charge combustion system has unique design targets compared with that of a stratified-charge combustion system. Likewise, the optimization of a turbo-charged or super-charged DI combustion system is different from that of a naturally aspirated combustion system. The differences are rooted mainly in the functional requirements and the optimization goals of each system. Section 7.3 will focus on the optimization of a homogeneous-charge combustion system, Section 7.4 describes stratified-charge combustion

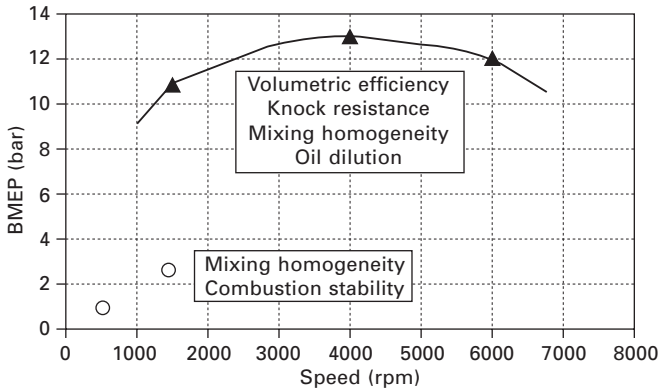


7.9 Endoscopy image taken at 26.4 CAD BTDC in an optically accessible engine, operating condition 2000 rpm, $IMEP_n = 2.7$ bar, $EOI_{1/2} = 29.5/23.5$ CAD BTDC, $TI_{1/2} = 197/141$ μ s (Baecker *et al.*, 2007).

system optimization, and Section 7.5 briefly discusses the unique aspects of optimization of turbo-charged combustion systems.

The combustion system of a homogeneous-charge DISI engine is very similar to that of a PFI engine. Both engines require the port design to achieve maximum volumetric efficiency while generating enough turbulent energy to promote combustion stability and a fast burn rate. However, the DISI engine has additional unique challenges. These include improving fuel–air mixing homogeneity, reducing engine smoke emissions, and ensuring low oil dilution. An optimized DISI combustion system needs to deliver a well-balanced performance over the entire engine operating map. Generally, a few representative points, i.e. mini-map points, are used to evaluate and guide the combustion system optimization. Figure 7.10 shows the mini-map points and associated design objectives for a DISI engine combustion system optimization utilized by Yi *et al.* (2004a).

As indicated in Fig. 7.10, the challenges at the full-load conditions, marked with triangles, are the volumetric efficiency, knock resistance, mixture homogeneity, and oil dilution. At the part-load conditions, marked with circles, the main challenges are to ensure sufficient mixture homogeneity and combustion stability. The following sections detail methods to optimize the intake port, injector spray pattern, and injection strategy to address these challenges.



7.10 Mini-map points and associated optimization targets for a naturally aspirated DISI engine combustion system development (Yi *et al.*, 2004a).

7.3.1 Intake port optimization

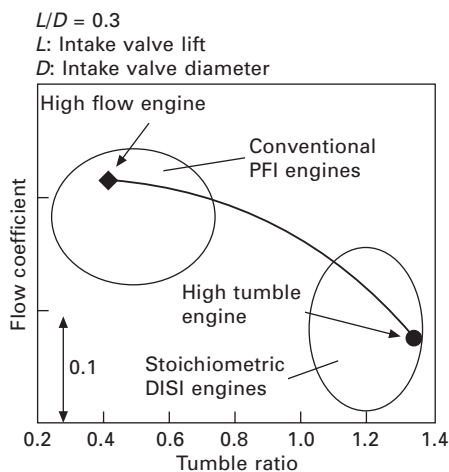
There are two factors that drive the intake port optimization. The first is the requirement for port flow capacity that is a key to high volumetric efficiency for improved engine torque and power. The second is the in-cylinder flow motion. With induction of intake air, a rotating flow structure forms within the cylinder that persists up to combustion. The principal axis of this coherent rotational flow structure forms an inclined angle relative to the cylinder axis. The rotational component with its axis parallel to the cylinder axis is called swirl, and the component having an axis perpendicular to the cylinder axis is referred to as tumble. The angular velocity of the rotational flow is roughly proportional to the engine speed. Therefore, swirl ratio and tumble ratio, which are defined as the angular velocity normalized by the engine speed, are often used to represent the strength of the in-cylinder flow motion. As explained by Zhao *et al.* (1997), there are four key controlling features of the in-cylinder flow field: the mean flow components, the stability of the mean flow, the temporal turbulence evolution during the compression stroke, and the mean velocity near the spark plug gap at the time of ignition.

The flow requirements differ between homogeneous-charge and stratified-charge operation. The flow structure in the induction stroke is more critical to mixture preparation for homogeneous-charge operation, while the flow in the compression stroke is the driving force for mixture stratification for stratified-charge operation. Generally, a tumble flow structure during the intake stroke works better than a quiescent flow or a swirl flow structure to distribute the fuel spray evenly for homogeneous-charge operation. The tumble flow can effectively decay into smaller-scale flow structures, eventually

converted to turbulent kinetic energy during the compression stroke. High kinetic energy available late in the compression stroke is essential for rapid combustion. For stratified-charge operation, swirl motion works better because it generally experiences less viscous dissipation than tumble motion, and it is preserved longer into the compression stroke to generate and maintain charge stratification.

This section will focus mainly on the intake port optimization for high flow capacity and high tumble motion. The port design with swirl motion will be discussed in the section on stratified-charge design. Figure 7.11 shows the typical trade-off between port flow capacity and tumble ratio (Ikoma *et al.*, 2006). As shown in the figure, as the tumble ratio increases, the flow capacity decreases. Plate I (between pages 172 and 173) illustrates the fundamental physics behind the trade-off between flow capacity and tumble flow strength. Here, the design with high flow capacity (Plate Ia) produces an evenly distributed flow field around the periphery of the intake port, while the port design with high tumble motion (Plate Ib) generates a biased flow structure with higher flow momentum towards the longer side of the port and very low flow momentum along the short side of the port. This flow also separates from the wall on the short side. Obviously, the biased flow with flow separation is the reason for high tumble motion and also the reason for reduced flow capacity.

The art of intake port optimization is centered on improvement of both flow capacity and tumble motion and determination of the best balance between these two objectives. Traditionally, flow rig experiments have been the main tool for port optimization. One of the obvious disadvantages of this experimental method is the requirement of building hardware. CFD



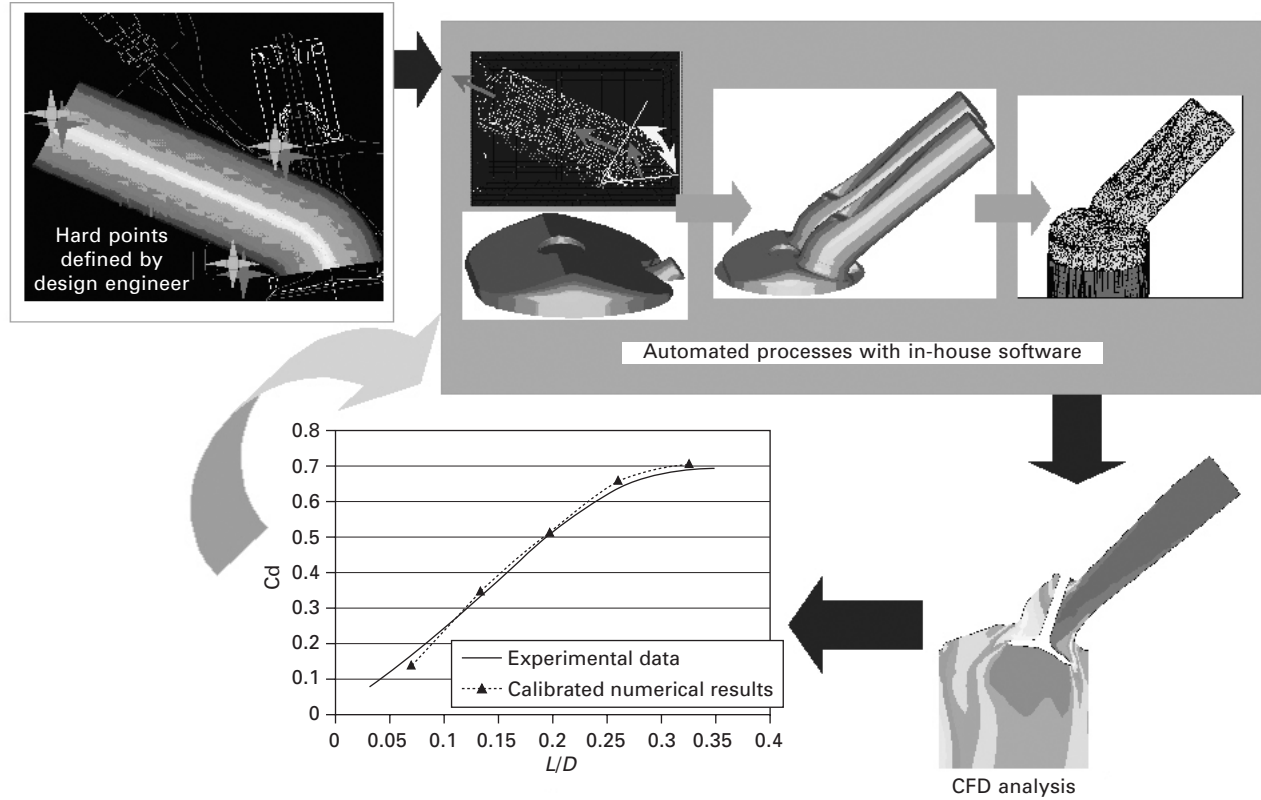
7.11 Typical trade-off between port flow capacity and tumble ratio (Ikoma *et al.*, 2006).

modeling has been applied to accommodate or even replace hardware testing for port optimization. Figure 7.12 shows the CFD-based port optimization methodology developed at the Ford Motor Company (Yi *et al.*, 2002). The optimization process starts with a set of hard points that define the envelope of the port geometry. The chamber and port geometry are then generated and assembled together automatically. Computational meshes for the port–chamber assembly are then generated automatically for a series of valve lifts. The flow capacity and tumble ratio are evaluated with CFD numerical simulations. The predicted flow structure details are used to understand the detailed physics and guide the iterative port design.

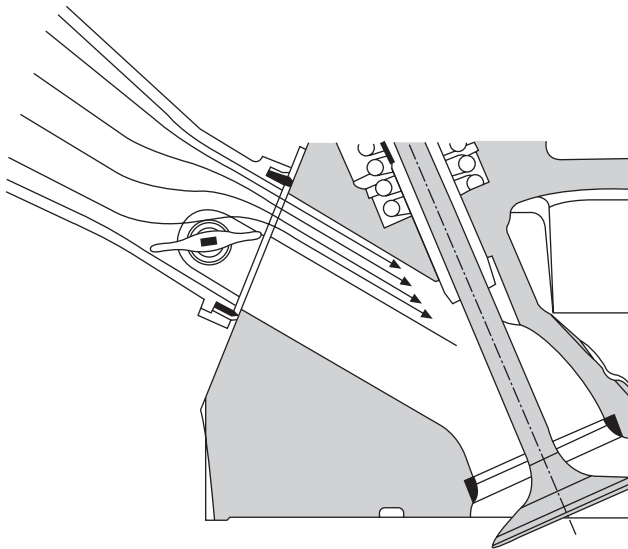
With the understanding that it is difficult to design an intake port that can concurrently produce high in-cylinder flow motion and high flow capacity, efforts have focused on decoupling these two requirements with the help of supplementary device. An example is the variable tumble design in the 2.0 Audi FSI combustion system (Fig. 7.13, Wurms *et al.*, 2002). In this system, the intake port itself was optimized for maximum flow capacity. When the engine operates at high-load or full-load conditions, the valve is at its low position parallel to the flow streamline direction (bottom configuration in Fig. 7.13). In this configuration, there is very little flow resistance across the valve plate. At part load, where high tumble motion is needed, the valve is set to its high position (top configuration in Fig. 7.13). The lower part of the intake port is blocked by the valve. The flow is forced to separate at the tip of the flapper to generate high tumble motion.

7.3.2 Mixing homogeneity improvement

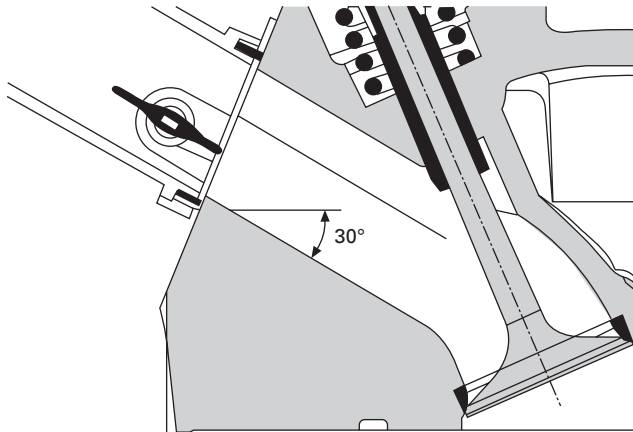
The fuel–air mixing process for homogeneous-charge operation starts with fuel injection into the cylinder at a prescribed fuel pressure. The fuel spray is atomized into fuel droplets, and the fuel droplets are transported throughout the combustion chamber. The droplets subsequently vaporize and mix with fresh air through turbulence mixing and molecular level mixing, then form a well-mixed fuel–air mixture for combustion. Even though all these processes are important to the mixture homogeneity, even distribution of fuel droplets and sufficiently rapid droplet evaporation are the overriding characteristics essential for good mixture quality. The evaporation process is determined by the droplet size, the droplet temperature, and the surrounding gas thermodynamic environment. The droplet size depends on the injector type, the nozzle opening size, and the operating fuel pressure. The fuel dispersion is dominated by the interaction between the fuel spray and the in-cylinder flow motion. This interaction depends on the spray droplet characteristics such as droplet size and penetration, injector plume orientation, and also the in-cylinder flow structure. This interaction can be optimized through adjustment of the injector spray pattern, through controlling the injector



7.12 Schematic of a CFD-based port optimization process (Yi *et al.*, 2002).



(a)



(b)

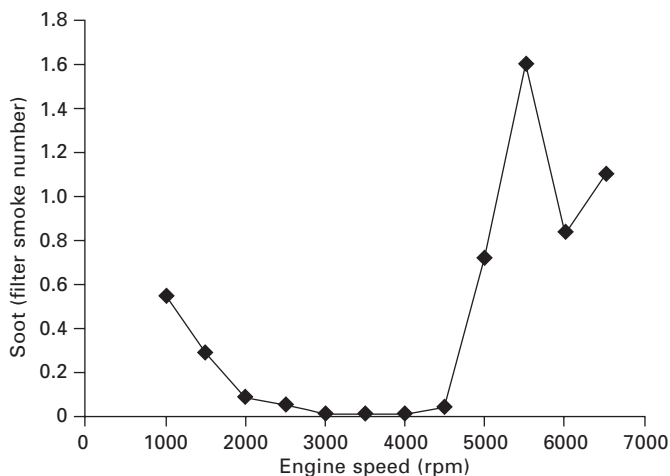
7.13 Audi FSI combustion system with a valve in the intake port to improve tumble motion, (Wurms *et al.*, 2002).

operating conditions, such as fuel pressure or injection timing, and through intake port or chamber design. This interaction is highly three-dimensional and time dependent, and is also a strong function of engine operating conditions such as speed and load.

There are two major factors that make fuel–air mixing homogeneity very challenging at high engine speeds and high-load operation. One factor is that it is very hard to distribute the fuel spray evenly in the cylinder, because

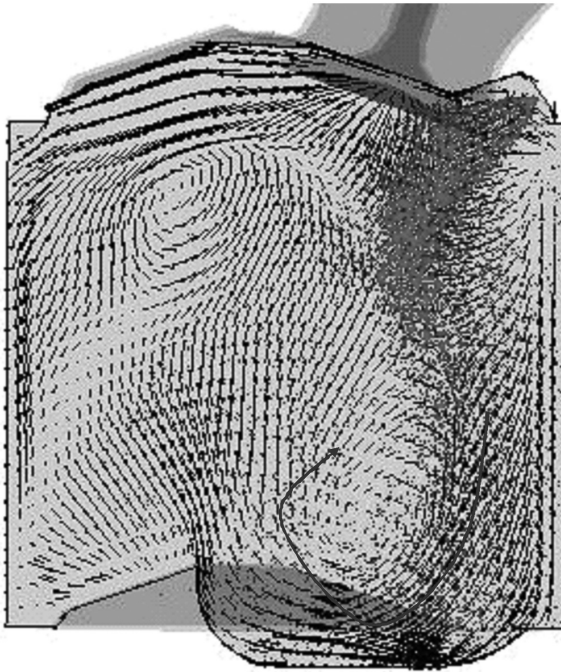
the fuel spray trajectory is highly influenced by the intake flow with high momentum. The other factor is that there is very limited flexibility in the fuel injection timing due to the fact that the injector flow rate is generally designed such that the injection window is about the same as the duration of the intake process at high-speed, high-load conditions. Increasing the injector flow rate helps mixing homogeneity at high-speed, high-load conditions. However, it may cause fuel metering difficulty at low loads such as idle conditions. At a moderate engine speed and high-load conditions, such as 3000 rpm WOT (wide open throttle), the unique challenge to mixing homogeneity is that the injection duration is not short enough to allow much flexibility for the injection strategy, such as split injection, while at the same time the engine speed is not high enough to promote strong turbulence mixing. At low-speed, full-load operation, some flexibility exists for advanced fuel injection strategies. However, low turbulence mixing, due to the low engine speed, creates a challenge for good mixing. Shown in Fig. 7.14 are engine smoke emission measurements from a research DISI engine at full-load operation over a wide engine speed range. It can be seen that the smoke emissions are higher at both low and high speed operations. The smoke emissions can be used as an indicator of the mixture homogeneity, because the smoke emission is believed to be closely associated with fuel-rich mixtures at these operating conditions.

The work of Yi *et al.* (2000a, 2002b, 2002) illustrated how three-dimensional modeling can help to optimize combustion chamber design with improved



7.14 Engine soot emission measurements vs. engine speed for a typical DISI engine with a high tumble intake port. The engine is equipped with a SCV (swirl control valve) in one of its two intake ports. The corresponding operation mode is full-load operation with the SCV open (Yi *et al.*, 2002).

fuel–air mixing homogeneity at high-speed and high-load conditions by alleviating the intake flow impact on the fuel spray trajectory. Shown in Plate II is the simulated air–fuel ratio distribution at 6000 rpm and full-load condition with the initial design of this combustion system (Yi *et al.*, 2002). The combustion system is based on a typical tumble port concept. As shown in Plate II (between pages 172 and 173), even at 20° bTDC (before TDC) during the compression stroke, about the time of ignition, there is still very strong stratification in the mixture. A rich mixture pocket is located on the intake side, while a lean mixture exists on the exhaust side. Yi *et al.* identified the root cause of the mixing inhomogeneity as uneven spray droplet distribution inside the cylinder. The fuel spray trajectory was strongly affected by the intake flow motion, which pushed the fuel spray away from its axial penetration direction towards the intake port. The bowl-in-piston geometry in this DISI engine further complicated the interaction between the intake flow and the fuel spray by drawing the airflow into the bowl and forming a vortex structure. The direction of the left branch of the vortex structure was opposite to that of the fuel droplet penetration, which further prevented the fuel droplets from penetrating across the cylinder, as shown in Fig. 7.15.

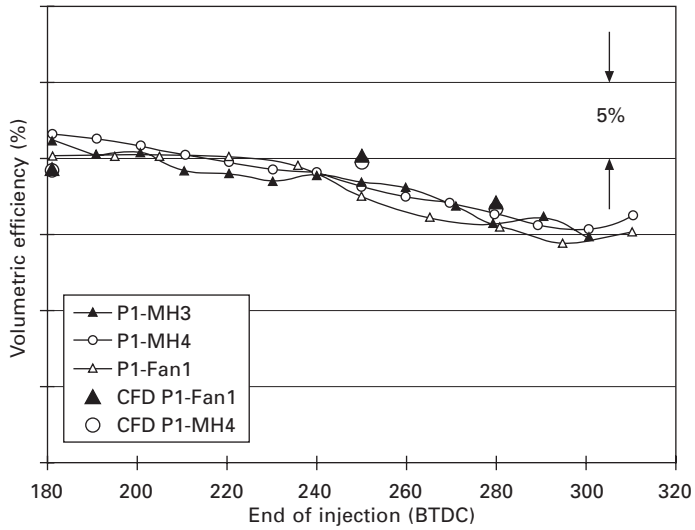


7.15 Corresponding velocity and fuel spray distribution at BDC. The intake flow pushes the fuel spray to the intake side, which causes fuel–air mixing inhomogeneity as shown in Plate II (Yi *et al.*, 2002).

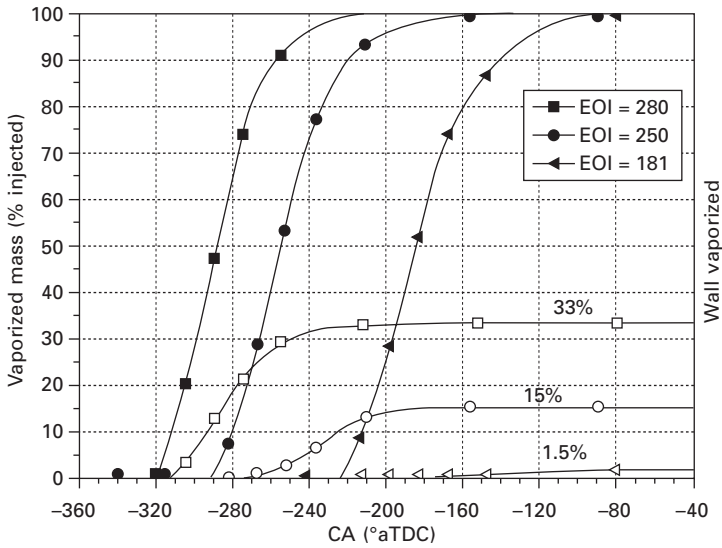
It was found that such an interaction between the intake flow and the fuel spray could be alleviated by designing a mask around the injector pocket to deflect the intake flow from impinging on the injected fuel spray. As a result of this local redirection of the intake flow motion, the fuel spray was more evenly distributed and the fuel–air mixing homogeneity was improved, as shown in Plate III (between pages 172 and 173).

Lippert *et al.* (2004a) demonstrated that three-dimensional modeling can be used to reveal the physical insight of the injection timing effect on the engine torque and volumetric efficiency as observed in dynamometer testing at 3000 rpm full-load condition in a four-valve pent-roof DISI engine. The dynamometer results indicated that as the injection timing advanced, the volumetric efficiency decreased between EOI (end of injection) of 180° to 320° bTDC. Their modeling showed that at early injection timings with an EOI of 280° bTDC, as much as 33% of the injected fuel impinges on the cylinder liner. However, the liner wetting with EOI of 180° bTDC is only about 1.5%, as shown in Fig. 7.16. The high liner wetting with early injection timings results in the fuel spray absorbing significant heat from the cylinder wall, which reduces the charge cooling effect that is characteristic of DISI engines. Lippert *et al.* also noted that the predicted fuel evaporation due to impingement may be greater than in the actual engine due to the Leidenfrost effect, whereby a vapor cushion insulates the liquid droplet from the hot wall. The wide spectrum of the fuel composition may also contribute to a discrepancy in the predicted evaporation compared with that observed. Another factor that can contribute to the discrepancy is the existence of an oil film on the cylinder liner. However, the proper trend of the fuel impingement over the injection timing range is valid. Excessive liner impingement could also impact engine durability, due to oil dilution, and fuel impingement on the piston surface could be a source of soot emissions. In engine combustion system optimization, it is important to minimize both liner wetting and piston wetting.

Ikoma *et al.* (2006) applied CFD modeling to optimize their slit injector spray pattern in the new Toyota 3.5-liter DISI gasoline engine (2GR-FSE) development. This engine is equipped with a dual fuel system with both PFI and DI fuel injection systems as shown in Fig. 7.17. The combustion system is an evolution of Toyota's 3GR-FSE engine with a pent-roof-type chamber, tapered squish, and an SCV (swirl control valve) in one of its intake ports. The DI fuel system in the dual fuel system employs a slit injector that generates a dual-fan-shaped spray with wide dispersion. CFD modeling was utilized to assist the selection of the DI fuel spray pattern. The CFD modeling results shown in Plate IV (between pages 172 and 173) suggest that the slit injector emits fuel perpendicularly to the piston with wide dispersion in the cylinder, while the conventional spray causes the fuel to be trapped by the piston cavity and prevents penetration toward the exhaust side of the combustion

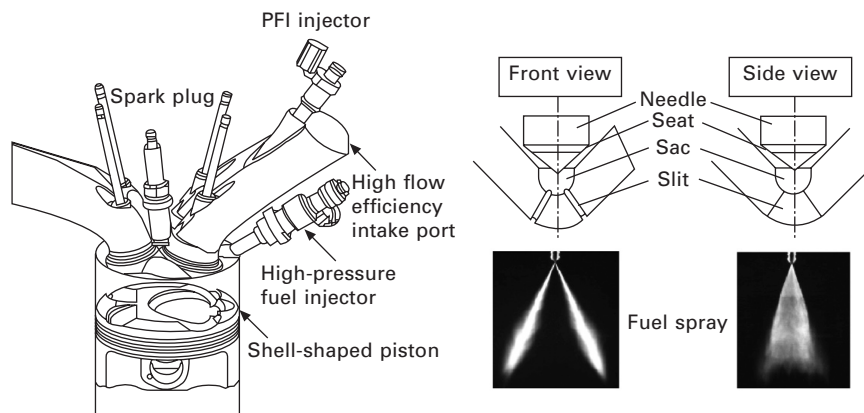


(a)



(b)

7.16 (a) Injection timing effect on volumetric efficiency, and (b) vaporized fuel from cylinder wall, at 3000 rpm full-load conditions with multi-hole (MH) and slit (fan) injector sprays (Lippert *et al.*, 2004a).

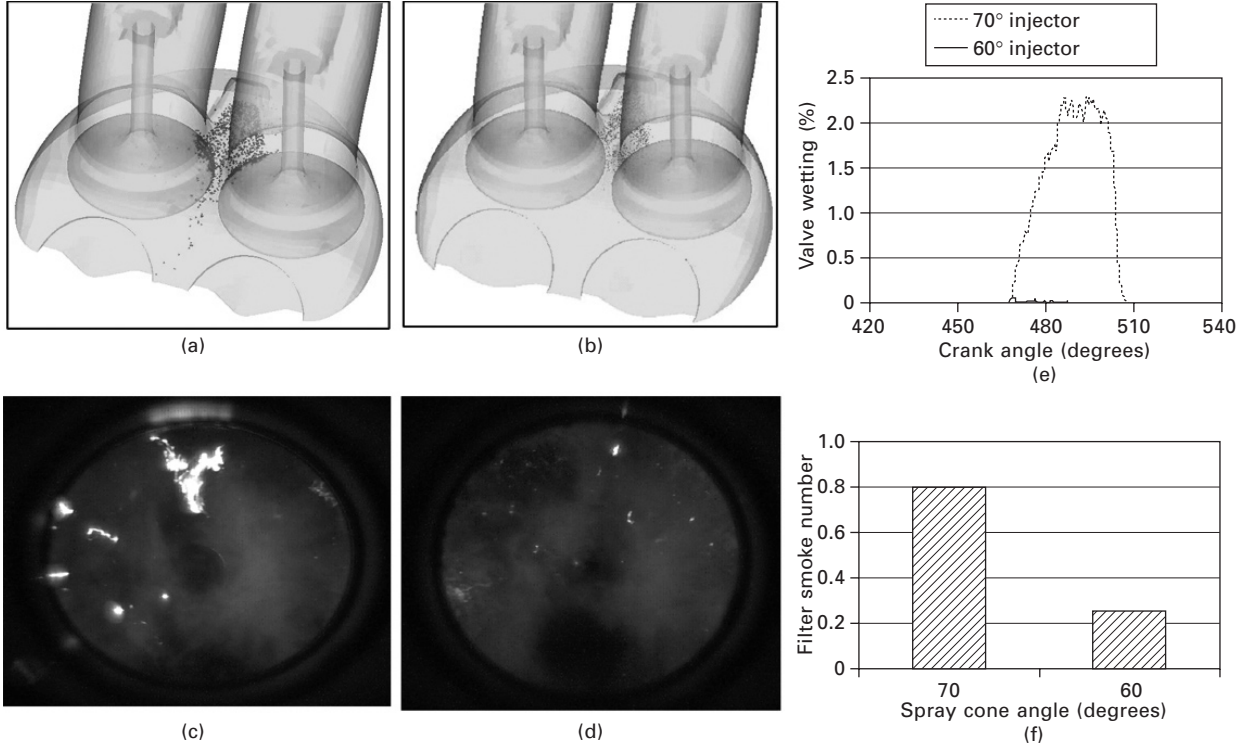


7.17 Toyota D-4S combustion system equipped with both PFI and DI fuel injection systems (left); and DI fuel system with dual-fan-shaped spray (right) (Ikoma *et al.*, 2006).

chamber. The combination of the new fuel system and elimination of SCV valve improves the low speed torque by about 7%.

As mentioned earlier, excessive fuel impingement on the cylinder and chamber surfaces could cause damage to a DISI engine. As in PFI engines, liner wetting may cause oil dilution that affects engine durability. Surface impingement can also cause soot emissions in a DISI engine, whereas that is seldom the case in PFI engines. Soot formation is a very complex process that includes many stages of soot particle generation and growth (Heywood, 1988). The capability to accurately predict soot formation in CFD modeling is limited by the understanding of the fundamental physical and chemical processes during soot formation. Even if the steps to soot formation were well understood, the computational resources required for three-dimensional simulation of practical engine geometry could still be beyond current computer power. Certain correlations between predicted wall wetting and oil dilution or soot emissions have been developed to provide an engineering guideline for combustion system optimization. Significant progress has been made in the last two decades in the understanding of the physics of the fuel impingement and fuel film dynamics on a solid surface for engine operating conditions (Naber and Reitz, 1988; Bai and Gosman, 1996; Han *et al.*, 2000).

Yi *et al.* (2004a) identified that excessive amounts of fuel impingement on the intake valve surfaces could cause high soot emissions in their DISI engine equipped with a swirl injector mounted underneath the intake ports. They further established a correlation between the amount of fuel impinging on the intake valves and the engine-out soot emissions. Shown in Fig. 7.18 is the correlation between CFD predicted intake valve fuel wetting and the engine-out soot emissions for two swirl injectors with 70° and 60° spray

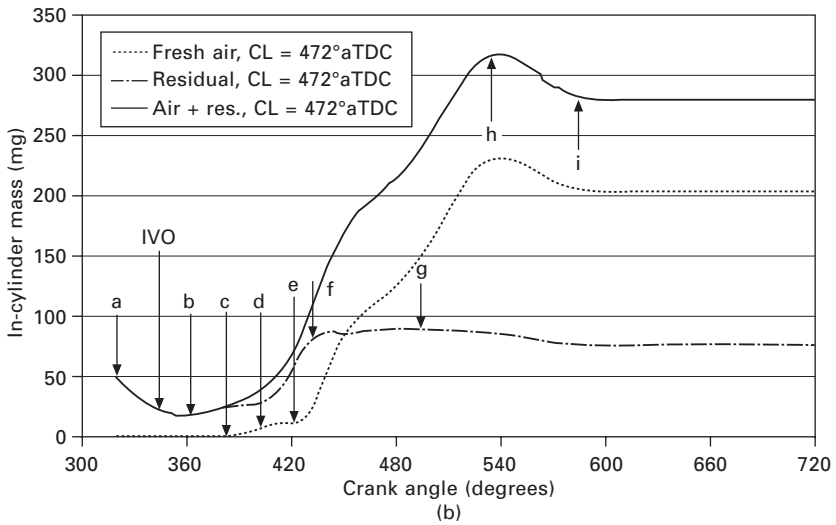
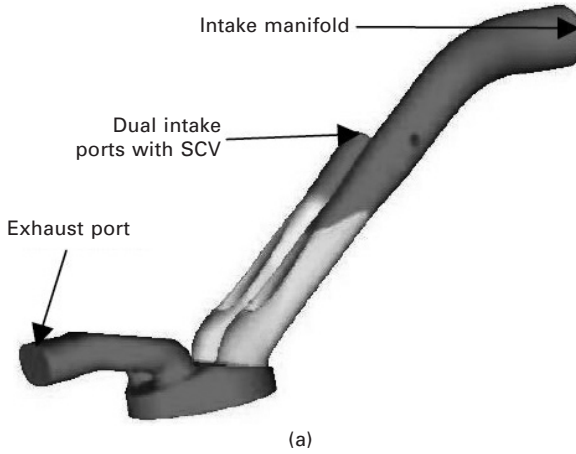


7.18 Fuel impingement on the intake valve surface was found to be the root cause of soot emissions in a DISI engine equipped with a swirl injector at 1500 rpm WOT conditions with $EOI = 260^\circ$ bTDC. (a) and (b) CFD predicted fuel impingement near the injector pocket with a fuel spray cone angle of 70° and 60° , respectively; (c) and (d) corresponding combustion flame images observed in an optically accessible engine for sprays of cone angle of 70° and 60° ; (e) and (f) CFD-predicted valve wetting and dynamometer-measured engine-out soot emissions (Yi *et al.*, 2004a).

cone angles. The operating conditions are 1500 rpm WOT with $\text{EOI} = 260^\circ$ bTDC. The 70° injector impinges fuel on the intake valve surface. Newly developed fuel impingement and wall dynamics models by Han *et al.* (2000) were employed to capture the fuel impingement and fuel–wall interactions. The predicted instantaneous valve wetting was the net result of the incoming fuel spray impinging onto the intake valve, and the fuel evaporating from the surface. It was found that the predicted fuel impingement location correlated well with the location of a pool fire observed in the corresponding optical engine, and the peak value of CFD-predicted valve wetting correlated with engine-out smoke emissions. The peak surface wetting value was used to guide the design process. The peak value of the valve wetting for the spray with 70° cone was about 2% and the measured engine-out soot emission was about 0.8 units of filter smoke number (FSN), using an AVL415 smoke meter. In the modified injector design with a 60° cone angle spray, the valve impingement was significantly reduced, and the resulting engine-out soot emission was reduced to 0.2 FSN.

For part-load operation, a short injection duration facilitates further injection strategy development, as compared with full-load conditions. For example, split injection strategies or the use of lower fuel pressures are feasible in part-load conditions. The added challenge to optimal mixing homogeneity is the interaction between valve event timing (alternatively, variable cam timing or VCT) and the DISI fuel injection and mixing process. As in a PFI engine, VCT has been proven to be a very effective method to improve engine fuel economy by reducing engine pumping losses with retarded intake cam closing time. In DISI engines, however, VCT can also affect the fuel–air mixing by altering the in-cylinder flow structure, turbulence intensity, and time available for mixing. Yi *et al.* (2004b) investigated the detailed air-exchange and fuel–air mixing processes with different intake cam phasing.

Yi *et al.* (2004b) revealed that the valve events, with late intake valve closing, together with the piston motion result in many different flow patterns. For a specific operating condition with intake valve maximum opening position (intake MOP) at 472° aTDC, several characteristic processes were identified. During the period between the late stage of the exhaust stroke, marked as point ‘a’ in Fig. 7.19b, and intake valve opening (IVO, 349° in this case), the piston moves up and pushes combustion products into both exhaust ports. For the period from IVO to TDC, marked as ‘b’ in Fig. 7.19b, the piston keeps moving up, and the combustion products in the chamber are pushed into both exhaust and intake ports. During the period between TDC and point ‘c’, both intake and exhaust valves are open. The burned gas is drawn back into the combustion chamber from the exhaust ports. The characteristic of the flow pattern in the period between points ‘c’ and to ‘e’ is that the air flows in the primary and the secondary intake ports are in

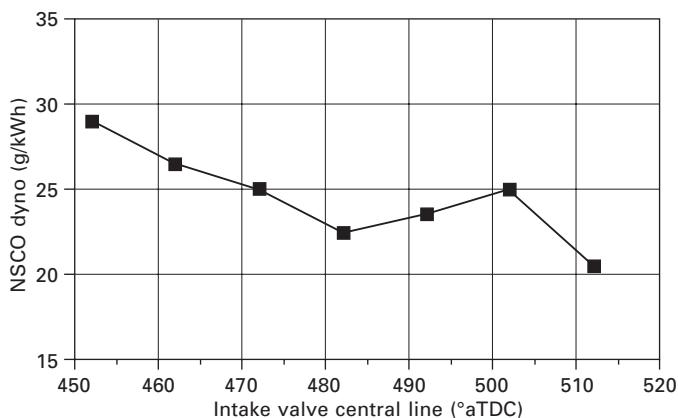


7.19 In-cylinder gas evaluation process at 1500 rpm, 2.62 bar BMEP with intake cam MOP (maximum opening position) at 472° after TDC, in a DISI engine with a swirl injector mounted underneath the intake ports. The SCV in the secondary intake port (left port) was closed at this operating condition. The intake cam duration is 246° (Yi *et al.*, 2004b).

opposite directions. The flow is drawn in from the secondary intake port to the combustion chamber, and the flow goes out to the primary intake port. In the next period, between points ‘e’ and ‘f’, the flow in the primary port reverses. The gases in the lower part of the primary intake port are drawn into the combustion chamber. The next period is characterized as the true air

induction process, where only fresh air is drawn into the combustion chamber. This period corresponds to the duration from points ‘f’ to ‘h’ in Fig. 7.19b. At point ‘h’, around BDC, the total in-cylinder mass reaches a maximum. It is very interesting to note that the residual gas has remained constant from ‘f’ to ‘g’, then starts to decrease from point ‘g’. The decrease is caused by flow of some of the residual gas into the secondary intake port. The final period of the induction process is the pushback process, as marked from ‘h’ to ‘i’ in Fig. 7.19b. During this period, the mixture of residual gas and fresh air in the chamber is pushed back into both the primary and the secondary intake ports, until the intake valve closes at point ‘i’, around 595° aTDC for this specific cam. It should be emphasized that a multi-cycle simulation may be necessary to take into account the true pushback effect on the fuel–air mixing process for late intake cam phasing.

Yi *et al.* (2004b) utilized CFD modeling, together with single-cylinder engine and optical engine, to investigate the intake cam phasing effect on fuel–air mixing homogeneity. Dynamometer testing with the single-cylinder engine showed that as the intake cam was retarded the engine-out CO emissions decreased, which indicated that mixing homogeneity was improving (Fig. 7.20). Both CFD modeling and fuel–air images from the optical engine (Plate V (between pages 172 and 173)) agreed with the mixing homogeneity trend observed in the single-cylinder testing. The authors argued that the improvement was mainly due to the local small flow structure, instead of the large structure such as tumble or swirl motion, or turbulence intensity. As shown in Plate VI (between pages 172 and 173), in the case of $MOP = 472^\circ$, there is a strong downward motion as indicated by the arrows. The shape of the flow motion coincides with the shape of the air–fuel ratio distribution.



7.20 Experimentally measured engine-out emission (NISCO dyno) at 1500 rpm, 2.62 bar BMEP, with an EOI of 280° b TDC. The injector has a 60° spray cone (Yi *et al.*, 2004b).

In the case with retarded cam with MOP of 512° , there is a tumble flow structure, which moves the fuel cloud upward and toward the exhaust port side. Comparing these two flow patterns suggests that the downward motion in the case of MOP = 472° is likely responsible for keeping the richer mixture from moving to the upper left side, i.e., toward the exhaust side.

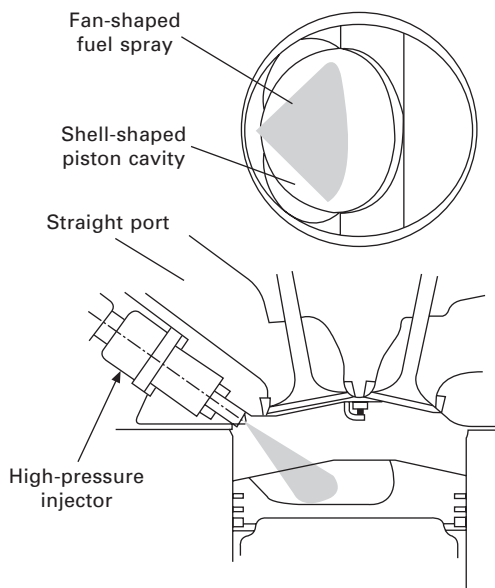
7.4 Stratified-charge direct injection (DI) combustion system design and optimization

A stratified-charge DI engine is operated in mixed modes. It is operated with a stratified air–fuel mixture at lower loads and speeds, while at higher loads and speeds it is operated with a ‘homogeneous’ mixture. The fuel economy benefit in stratified-charge mode originates from four aspects: reduced pumping loss due to an overall lean mixture, reduced heat losses to the cylinder walls due to lower gas temperatures, higher thermal efficiency due to increased specific heat ratio, and improved thermal efficiency due to higher compression ratio. The requirement of the fuel–air mixture for a stratified-charge condition is fundamentally different from that required for homogeneous-charge conditions. A locally rich fuel–air cloud around the spark-plug gap is required at the time of ignition, with a lean mixture outside this rich region. The capability to operate the engine at an overall lean condition is the key enabler for fuel economy improvement. The quality of mixture stratification directly affects the combustion stability and emissions such as UHC, NO_x , and soot. A good stratified-charge combustion system should be able to operate stably in a wide speed and load window with low emissions.

There are many different ways to achieve such charge stratification with the help of the injector spray pattern, piston geometry, and in-cylinder flow motion. Stratified-charge combustion systems can be categorized as wall-guided, air-guided, and spray-guided according to the main mechanism to form the charge stratification. In wall-guided systems, different in-cylinder flow patterns along with the typical interaction between the fuel spray and a piston bowl can be used to achieve mixture stratification. Engineers at Mitsubishi (Kume *et al.*, 1996) and Ricardo (Jackson *et al.*, 1997) first proposed a reverse tumble concept in conjunction with a specially designed piston cavity that created a stratified charge near the spark plug gap. The cavity was designed to control the spray impingement and flame propagation. Volkswagen (Krebs *et al.*, 1999) utilized a forward tumble motion in their DI engine. Recently, swirl motion together with a piston bowl design has been widely adopted by Toyota (Harada *et al.*, 1997), Ford (Han *et al.*, 2002), and GM (Lippert *et al.*, 2004b) in their stratified-charge engine combustion systems. One of the advantages with swirl motion is that the swirl flow structure can be preserved longer in the compression stroke to help stabilize the stratified

charge around the spark-plug location. FEV's stratified-charge system is an example of an air-guided system (Geiger *et al.*, 1999). It utilizes intake air forward tumble motion together with a large but shallow piston cavity to control the mixture formation. VanDerWege *et al.*'s (2003) VISC (vortex induced stratified combustion) concept is a typical spray-guided system with a piezo injector mounted in the center of the combustion chamber. It utilizes the vortex naturally formed on the outside of a wide spray cone that is enhanced by bulk gas flow control and piston crown design. This vortex transports fuel vapor from the spray cone to the spark gap. The main advantages of a spray-guided system are reduced piston fuel wetting and more optimum combustion phasing, as compared with wall-guided systems.

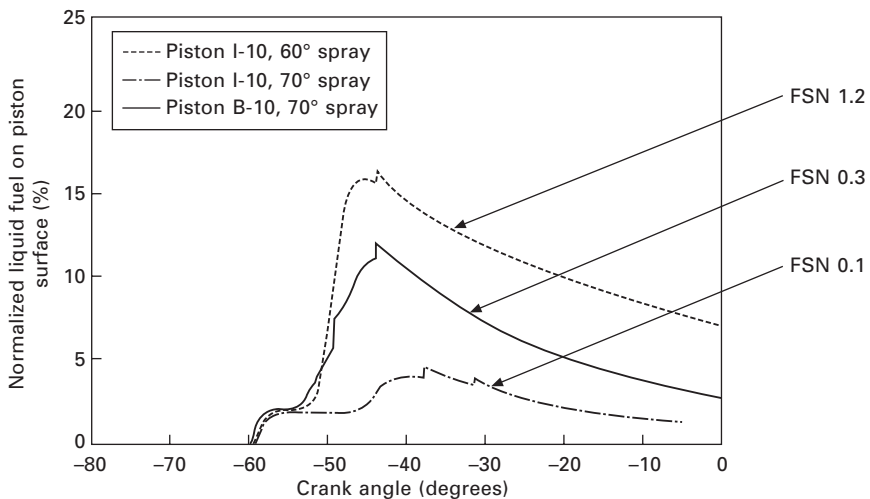
CFD modeling has played a very important role in the design optimization of chamber, piston cavity, and spray configurations in stratified-charge combustion systems. Abe *et al.* (2001) applied CFD modeling to investigate the fuel–air mixture formation process for combustion with a side-mounted fan (slit) injector spray and straight intake ports (Fig. 7.21). The modeling aided understanding of the piston shape effects on the stratification and emissions. Their modeling results indicated that with an oval wall cavity, the mixture was more concentrated around the spark plug compared with the case of a shell-shaped piston (Plate VII (between pages 172 and 173)).



7.21 Toyota stratified-charge combustion system with side-mounted fan (slit) spray, piston cavity, and straight intake port in a 4-cylinder DOHC, 4-valve engine with bore and stroke of 86 mm and 86 mm, (Abe *et al.*, 2001).

Han *et al.* (2002) optimized the swirl injector spray pattern design for reduced piston wetting at stratified-charge operation, based on the physical insight of the fuel–wall interaction gained through the CFD modeling. They investigated the fuel spray, fuel–air mixing, and the flow field evolution process, shown in Plate VIII (between pages 172 and 173), in a stratified-charge engine with bore of 89 mm and stroke of 79.5 mm, equipped with a swirl injector beneath the intake ports. Based on the results of the CFD study, most of the impinged fuel adhered to the wall surface. The adhering liquid fuel either vaporized and contributed to very rich mixtures near the wall or remained as liquid phase at the time of spark (e.g., 20–25° BTDC). Based on their modeling and the ‘foot printing’ of fuel impingement observed in the dynamometer engine, they believed that the piston wetting caused ‘pool fires’ burning in the fuel-rich region in the piston bowl, and hence was a major soot formation source. With the help of the correlation and CFD modeling, a new piston design and new spray pattern with larger spray cone were proposed for the optimized combustion system. The engine test confirmed that the new spray pattern and piston design produced much less soot emissions, as shown in Fig. 7.22.

Lippert *et al.* (2004b) investigated the effect of the spray pattern on fuel economy and emissions in stratified-charged modes with engine experiments and CFD modeling. Their dynamometer tests indicated that the fan spray injector resulted in equal or better (lower) values for specific fuel consumption



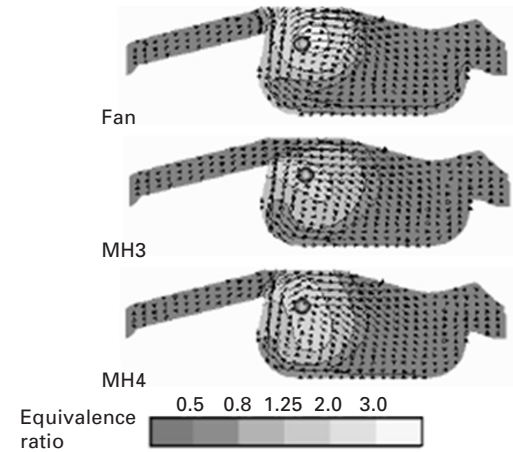
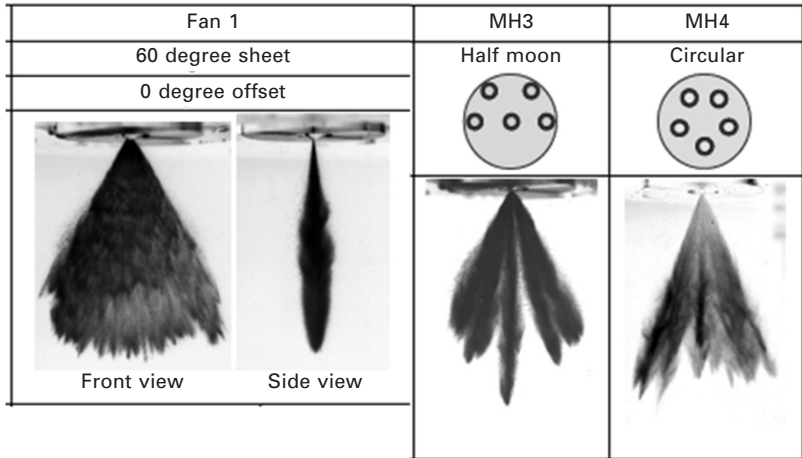
7.22 Effect of spray cone angle for a swirl injector on CFD-predicted piston wetting and dynamometer-measured soot emissions. The simulated engine conditions are the same as in Plate VIII, except that the spray cones are varied (Han *et al.*, 2002).

and emissions than the MH (multi-hole) injectors, except at idle. At idle, MH4 had considerably better HC emissions, as well as a COV of IMEP that was 50% lower than the other injectors. CFD modeling was employed to understand this phenomenon. The CFD modeling results, some of which are shown in Fig. 7.23, indicated that the better idle performance of MH4 could be due to a better-contained spray within the bowl, and this also contributed to a wider ignition window at idle. Owing to the particular distribution of mass and momentum from the MH4 injector, a much tighter recirculation of the fuel cloud around the spark gap was formed and maintained. This caused more of the mixture to be contained within the bowl, resulting in better HC emissions and greater combustion stability. However, the fan spray injector had a stronger global vapor penetration and, as a result, the fuel vapor quickly traveled up towards the head. This resulted in a higher peak in equivalence ratio at the spark gap, but a more rapid decay. Higher HC emission and less stable combustion was the result.

Iyer *et al.* (2004) investigated the stratified-charge formation mechanism in their spray-guided, stratified-charge combustion system with CFD modeling. The simulations showed that a vortex structure is formed on the periphery of the spray, due to the viscous shear between the high velocity spray droplets and the low velocity surrounding gas. This vortex structure provides an ignitable mixture to the spark plug. The CFD modeling also explained the physics underlying the effect of the relative position between injector and spark plug on misfires and combustion stability. The CFD modeling results in Plate IX (between pages 172 and 173) show that the misfire elimination with the raised injector position was due to two main mechanisms. First, the vortex at the periphery of the spray has more room to form before it impinges on the piston with the raised injector position than with the initial injector position. In this way, air entrainment can develop with less interference from the piston motion. Second, the spark plug has a better placement relative to the fuel vortex because the mixture cloud is higher around the spark plug for the raised injector position.

7.5 Turbo-charged or super-charged direct injection (DI) combustion system design and optimization

Pressure-charging gasoline engines have been employed either to improve engine performance (torque and power) for fixed engine displacement or to improve fuel economy by downsizing the engine displacement (Wirth *et al.*, 2000; Stan *et al.*, 2003; Lake *et al.* 2004). Within the category of pressure-charged DISI engines, turbo-charged, super-charged, or a combination of these two are the common alternatives. Even though there are numerous similarities, turbo- and super-charged engines have their unique requirements



7.23 Cross-section (right) through the spark gap at 25° bTDC for idle operation (650 rpm, MAP = 80 kPa, SI = 1.4, EOI = 50, EGR = 51%, AF = 32) for Fan1 (left), MH3 and MH4 (middle) injectors (Lippert *et al.*, 2004b).

for combustion system optimization and CFD modeling. For pressure-charged engine systems, the wave dynamics in both the air intake and the exhaust system have a significant impact on the engine performance through affecting the volumetric efficiency and mass of trapped residual gas. The trapped residual amount significantly affects the engine knock tendency. In order to capture these system interactions and accurately model a turbo- or super-charged engine, it is ideal to conduct three-dimensional (3-D) modeling of the entire engine system including in-cylinder phenomena with multi-cylinders, intake and exhaust system, and turbo- or super-charger system. However, such detailed CFD modeling can be extremely time-consuming, on the order of months, given current computational capabilities. Alternatively, a 1-D and 3-D coupled modeling approach provides a good method that captures the overall system dynamics with 1-D modeling and resolves detailed in-cylinder physics with 3-D modeling (Bohbot *et al.*, 2006).

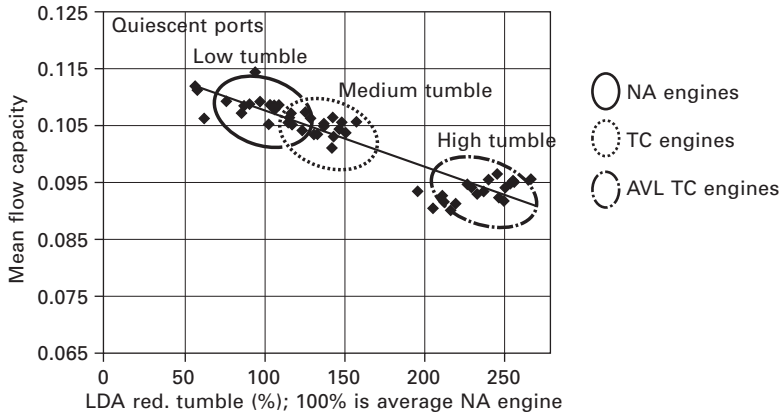
The requirements for pressure-charged DISI combustion systems are quite different from those of naturally aspirated DISI combustion systems. The difference imposed further challenges, and at the same time some opportunities. The challenges include three major aspects. First, it is increasingly difficult to ensure well-mixed fuel and air, since the fuel droplet trajectory is highly influenced by the intake air due to its higher momentum when compressed. Secondly, the engine is more prone to knock at boosted conditions. Finally, turbo-charged engines require more exhaust gas heat flux to light off the catalyst at cold start due to increased heat losses across the turbo charger. The opportunity that comes with the boosted combustion system is that the intake port flow capacity is not as critical as in the naturally aspirated engine.

Fraidl *et al.* (2006) indicated that turbo-charged (TC) engines could be designed with much less flow capacity for a much high tumble ratio (Fig. 7.24). The higher tumble motion improves mixing, burn rate (thus engine knock resistance), and combustion stability.

Higher tumble motion introduces a much stronger impact on the fuel spray trajectory and the fuel–air mixing. Iyer and Yi (2008) showed that a good match between the intake flow and the fuel spray pattern can improve fuel–air mixing and reduce wall wetting. As shown in Plate X (between pages 172 and 173), the intake flow from the high tumble port design effectively deflects the fuel spray downward and keeps it from impinging on the cylinder liner on the exhaust side (left wall).

7.6 Future trends

CFD computational speed and simulation accuracy are two equally important aspects of CFD simulation in combustion system development and optimization. CFD simulations need to be accurate enough to provide



7.24 Turbo-charged engines require much lower flow capacity but much higher tumble motion (Fraidl *et al.*, 2006).

design optimization direction. On the other hand, the CFD simulation must be fast enough to be used as a valuable tool for evaluating multiple design iterations. The rapidly growing computational power during the last decade has changed the role of CFD simulation in combustion system development from a research tool to an upfront optimization tool. Currently, a complete assessment of a combustion system design can be performed in less than one week. CFD simulations allow engineers to develop high quality combustion systems with reduced development time and cost due to a decreased need for hardware iterations.

The development of advanced combustion systems for better fuel economy, higher power density, and cleaner emissions promotes the need for more accurate CFD simulations. In addition to improved computer resources, better physical models are required to resolve the detailed physics. For example, in order to capture engine cold-start performance, multi-component fuel and associated physical fuel models to deal with fuel atomization, evaporation, and combustion are necessary to simulate the fuel behavior under a wide range of operating conditions. In order to understand the formation and evolution of engine-out emissions, more detailed chemistry with more species and reactions and better techniques for reduced chemistry are needed, in addition to more accurate fuel representations. Knock mitigation is key to the success of a turbo-charged or super-charged engine combustion system development. The capability to predict knock onset and evolution is essential to the understanding of the knock phenomenon, and to improve engine designs to suppress knock. Liang *et al.*'s (2007) recent work is a good start to address this challenge by coupling CFD modeling and detailed chemistry.

7.7 References and further reading

- Abe, S., Sasaki, K., Baika, T., Nakashima, T. and Fujishiro, O., Combustion analysis on piston cavity shape of a gasoline direct injection engine, SAE 2001-01-2029 (2001).
- Amsden, A.A. KIVA-3V: a block-structured KIVA program for engines with vertical or canted valves, Los Alamos National Laboratory report LA-13313-MS (July 1997).
- Amsden, A.A., Ramshaw, J.D., O'Rourke, P.J. and Dukowicz, J.K., KIVA: a computer program for two- and three-dimensional fluid flows with chemical reactions and fuel sprays, Los Alamos National Laboratory report LA-10245-MS (February 1985).
- Amsden, A.A., O'Rourke, P.J., and Butler, J.T., KIVA-II: a computer program for chemical reactive flows with sprays, Los Alamos National Laboratory report LA-11560-MS (May 1989).
- Anderson, R.W., Brehob, D.D., Yang, J., Vallance, J.K., and Whiteaker, R.M., A new direct injection spark ignition (DISI) combustion system for low emissions, FISITA-96 technical paper, No. P0201 (1996).
- Arai, J., Oshima, M., Oshima, N., Ito, H., and Kubota, M., Large eddy simulation of spray injection to turbulent duct flow from a slit injector, SAE 2007-01-1403 (2007).
- Baecker, H., Kaufmann, A., and Tichy, M., Experimental and simulative investigation on stratification potential of spray-guided GDI combustion systems, SAE 2007-01-1407 (2007).
- Bai, X. and Gosman, A.D., Mathematical modelling of wall films formed by impinging sprays, SAE 960626 (1996).
- Bohbot, J., Chryssakis, C., and Miche, M., Simulation of a 4-cylinder turbocharged, gasoline direct injection engine using a direct temporal coupling between a 1D simulation software and a 3D combustion code, SAE 2006-01-3263 (2006).
- Cathcart, G. and Zavier, C., Fundamental characteristics of an air-assisted direct injection combustion system as applied to 4-stroke automotive gasoline engines, SAE 2000-01-0256 (2000).
- Dai, W., Davis, G.C., Hall, M.J., and Matthews, R.D., Diluents and lean mixture combustion modeling for SI engines with a quasi-dimensional model, SAE 952382 (1995).
- Davis, G.C., and Kent, J.C., Comparison of model calculations and experimental measurements of the bulk cylinder flow processes in a motored PROCOCO engine, SAE 790290 (1979).
- Dodge, L.G., Fuel preparation requirements for direct-injected spark ignition engine, SAE 962015 (1996).
- Fraidl, G.K., Kapus, P., and Philipp, H., Development of knock-optimized combustion systems for highly boosted gasoline engines, presented in IAV Congress, 2006.
- Geiger, J., Grigo, M., Lang, O., Wolters, P., and Hupperich, P., Direct injection gasoline engines – combustion design, SAE 1999-01-0170 (1999).
- Han, Z., Reitz, R., Claybaker, D., Rutland, C., Yang, J., and Anderson, R.W., Modeling the effect of intake flow structures on fuel–air mixing in a direct-injected spark ignition engine, SAE 961192 (1996).
- Han, Z., Xu, Z., and Trigui, N., Spray/wall interaction models for multidimensional engine simulation, *International Journal of Engine Research*, **1**, 127–146 (2000).
- Han, Z., Yi, J., and Trigui, N., Stratified mixture formation and piston surface wetting in a DISI engine, SAE 2002-01-2655 (2002).
- Harada, J., Tomita, T., Mizuno, H., Mashiki, Z., and Ito, Y., Development of a direct injection gasoline engine, SAE 970540 (1997).

- Heywood, J.B., *Internal Combustion Engine Fundamentals*, McGraw-Hill, New York, pp. 635–648 (1988).
- Ikoma, T., Abe, S., Sonoda, Y., Suzuki, H., Suzuki, Y. and Basaki, M., Development of V-6 3.5-liter engine adopting new direct injection system, SAE 2006-01-1259 (2006).
- Iyer, C. and Yi, J., High tumble intake port development and assessment with 3D CFD modeling, Ford Research Report, January 2008, submitted to SAE for publication.
- Iyer, C.O., Han, Z., and Yi, J., CFD modeling of a vortex induced stratification combustion (VISC) system, SAE 2004-01-0550 (2004).
- Jackson, N.S., Stokes, J., Whitaker, P.A., and Lake, T.H., Stratified and homogeneous charge operation for the direct injection gasoline engine – high power with low fuel consumption and emissions, SAE 970543 (1997).
- Jhavar, R. and Rutland, C.J., Using large eddy simulations to study mixing effects in early injection diesel engine combustion, SAE 2006-01-0871 (2006).
- Krebs, R., Spiegel, L., and Stiebels, B., Direct injection SI engines by Volkswagen, Aachen Colloquium on Automotive and Engine Engineering (1999).
- Kume, T., Iwamoto, Y., Iida, K., Murakami, M., Akishino, K., and Ando, H., Combustion control technologies for direct injection SI engines, SAE 960600 (1996).
- Lake, T., Stokes, J., Murphy, R., Osborne, R., and Schamel, A., Turbocharging concepts for downsized DI gasoline engines, SAE 2004-01-0036 (2004).
- Liang, L., Reitz, R.D., Iyer, C., and Yi, J., Modeling knock in spark-ignition engines using G-equation combustion model incorporating detailed chemical kinetics, SAE 2007-01-0165 (2007).
- Lippert, A.M., Tahry, S.H., El Huebler, M.S., Parrish S.E., Inoue, H. and Noyori, T., Development and optimization of a small-displacement spark-ignition direct-injection engine – full-load operation, SAE 2004-01-0034 (2004a).
- Lippert, A.M., El Tahry, S.H., Huebler, M.S., Parrish, S.E., Inoue, H., Noyori, T., Nakama, K., and Abe, T., Development and optimization of a small-displacement spark-ignition direct-injection engine – stratified operation, 2004-01-0033 (2004b).
- Lippert, A.M., Chang, S., Are, S., and Schmidt, D.P., Mesh independence and adaptive mesh refinement for advanced engine spray simulations, SAE 2005-01-0207 (2005).
- Matthews, R.D., Sarwar, M.G., Hall, M.J., *et al.*, Predictions of cyclic variability in an SI engine and comparisons with experimental data, SAE International Fuels and Lubricants Conference, Toronto, 1991.
- Naber, J. and Reitz, R., Modeling engine spray/wall impingement, SAE 880107 (1988).
- Stach, T., Schlerfer, J., and Vorbach, M., New generation multi-hole fuel injector for direct-injection SI engines – optimization of spray characteristics by means of adapted injector layout and multiple injection, SAE 2007-01-1404 (2007).
- Stan, C., Stanciu, A., Troeger, R., Martorano, L., Tarantino, C., Antonelli, M., and Lensi, R., Direct injection concept as a support of engine down-sizing, SAE 2003-01-0541 (2003).
- Tabaczynski, R.J., Ferguson, C.R., and Radhakrishnan K., A turbulent entrainment model for SI engine combustion, SAE 770647 (1977).
- Torres, D.J. and Trujillo, M.F., KIVA-4: an unstructured ALE code for compressible gas flow with sprays, *Journal of Computational Physics*, **219**, 943–975 (2006).
- VanDerWege, B.A., Han, Z., Iyer, C.O., Muñoz, R.H., and Yi, J., Development and analysis of a spray-guided DISI combustion system concept, SAE 2003-01-3105 (2003).

- Wirth, M., Mayerhofer, U., Piock, W.F., and Fraidl, G.K., Turbocharging the DI gasoline engine, SAE 2000-01-0251 (2000).
- Wurms, R., Grigo, M., and Hatz, W., Audi FSI technology – improved performance and reduced fuel consumption, SAE 2002-33-0002 (2002).
- Yi, J., Han, Z., Yang, J., Anderson, R., Trigui, N., and Boussarsar, R., Modeling of the interaction of intake flow and fuel spray in DISI engines, SAE 2000-01-0656 (2000a).
- Yi, J., Trigui, N., and Han, Z., Direct injection spark ignition engines, US patent 6378488 (2000b).
- Yi, J., Han, Z., and Trigui, N., Fuel–air mixing homogeneity and performance improvements of a stratified-charge DISI combustion system, SAE 2002-01-2656 (2002).
- Yi, J., Han, Z., Xu, Z., and Stanley, L.E., Combustion improvement of a light stratified-charge direct injection engine, SAE 2004-01-0546 (2004a).
- Yi, J., Wooldridge, S., McGee, J., and Han, Z., Understanding of intake cam phasing effects on the induction and fuel-air mixing in a DISI engine, SAE 2004-01-1947 (2004b).
- Zhao, F.-Q., Yoo, J.-H., Liu, Y., and Lai, M.-C., Spray dynamics of high pressure fuel injectors for DI gasoline engines, SAE 961925 (1996).
- Zhao, F.-Q., Lai, M.-C., and Harrington, D., A review of mixture preparation and combustion control strategies for spark-ignited direct-injection gasoline engines, SAE 970627 (1997).

Abstract: This chapter covers the features of internal combustion engines burning natural gas directly injected into the cylinder near TDC. Different approaches to building an engine of this kind are briefed, followed by determination of the engine compression ratio, requirements of the engine fuelling systems, for either compressed natural gas or liquefied natural gas, and selection of ignition methods. Potential of the engines to curb air pollution and carbon emission, to improve power density and thermal efficiency on gaseous fuels, to reduce operation cost of a fleet, and to improve energy security of a region, are also discussed.

Key words: direct injection gas engines, natural gas, compression ratio, fuelling systems, carbon emission.

8.1 Introduction

Natural gas has been used as an energy resource for over a century. The proven world reserves of natural gas are comparable to those of oil on energy contents. With increased awareness of air pollution in urban areas caused by automobiles burning oil fuels, such as petrol and diesel, natural gas becomes an attractive candidate to replace or partially replace oil as a transportation fuel in big cities due to its potential of generating less regulated pollutant emissions than petrol and diesel. Replacing oil fuels with natural gas in vehicles can also reduce their greenhouse gas (GHG) emission, which has caused increasing concerns over its possible role of causing global warming. Using natural gas can substantially reduce the fuel cost of a vehicle in most countries, where natural gas is less expensive than petrol or diesel. Applying natural gas in transportation sectors, where oil fuels are dominant, can also increase energy security by offering another energy source of a size comparable to that of oil.

With reductions in new discoveries of oil deposits and increased oil consumption, world oil production has reached, or is approaching, the peak [1]. World energy consumption increases every year, and does not show any declining trend in the future. Other alternative fuels, such as ethanol, biodiesel and hydrogen, have demonstrated their potential to be used as automobile fuels, but are unlikely to play an important role in replacing oil, because they can be produced neither in such massive quantities nor at a cost comparable to those of fossil oil fuels. It is reasonable to expect that natural gas will play an increasingly important role in controlling regulated emissions

and in limiting GHG emissions, and in filling the gap between increasing energy demand and dwindling oil production, especially in transportation sectors.

Natural gas has been used as a fuel for internal combustion (IC) engines of premixed combustion. Usually conventional petrol engines or conventional diesel engines are converted to burn premixed natural gas and air with the assistance of an ignition device, such as an electric spark. Such natural gas engines can be made with thermal efficiency better than that of conventional petrol engines, because they can take advantage of the high octane number of natural gas to elevate their compression ratios higher than those of petrol engines. The thermal efficiency of these natural gas engines is, however, still not as high as that of their diesel rivals, because their compression ratios are limited by knocking due to premixed combustion, and because they need throttling to control the air-fuel ratio.

Direct injection (DI) natural gas engines have the potential to achieve thermal efficiency as good as that of diesel engines, while keeping the regulated emissions, such as NO_x and particulate matter (PM) emissions, lower than those from diesel engines, due to the differences in chemical properties between natural gas and diesel fuel. To realize their potential, much work has been done during the last two decades to develop natural gas IC engines with direct in-cylinder injection for vehicle applications. Commercial applications of DI natural gas engines on heavy duty trucks have been reported recently.

In IC engines, direct injection of natural gas could support premixed combustion, or diffusion combustion, or a combination of both, i.e. partially premixed combustion and partial diffusion combustion. The diffusion combustion can be further categorized as open chamber diffusion combustion and pre-chamber diffusion combustion. In this chapter the discussions are more relevant to open chamber diffusion combustion than to pre-chamber diffusion combustion and premixed combustion. In Section 8.2 technologies to realize the potential of burning natural gas with high efficiency and low emissions are discussed. Section 8.3 discusses potential applications of DI natural gas engines. In Section 8.4 the pros and cons of the engines in comparison with conventional diesel engines are discussed. The rest of the chapter projects the future trends of the technologies, and lists the sources related to the contents of the chapter, which could be useful to readers who may have further interest in the technologies.

8.2 Technologies

DI natural gas engines share technologies common to both petrol engines and diesel engines, and also have their own unique features that are necessary to make them deliver performance comparable to their petrol or diesel

counterparts. Before building a DI natural gas engine, a number of questions have to be answered:

- How to build an IC engine that is suitable for burning natural gas directly injected into the cylinder?
- How to store natural gas on board a vehicle?
- How to supply the engine with the gaseous fuel?
- How to deliver the gaseous fuel into the engine cylinder against elevated cylinder pressure?
- How to start the combustion?
- How to burn the gaseous fuel efficiently?
- How to control the regulated emissions?

Technically there could be multiple answers to each of these questions. No attempt has been made to explore all the possibilities. Discussions will cover knowledge fundamental to conventional IC engines, and emphasize the technologies that have been specifically developed for DI natural gas engines, especially for those that have found commercial applications or appear to have potential for commercial applications.

8.2.1 Building an engine

In this section we will discuss different options to build an IC engine for DI natural gas combustion, and what needs to be considered when determined the engine compression ratio.

Options

There are at least three options to build a direct injection natural gas IC engine. The first option is to design a new engine for the specific purpose of burning natural gas. The second option is to convert from an existing conventional petrol engine, i.e. a commercially mass-produced IC engine that generates mechanical work by burning premixed petrol and air using one or more ignition devices, such as electrical spark plugs, to initiate combustion. The third option is to convert from an existing conventional diesel engine, i.e. a commercially mass-produced IC engine that generates mechanical work by diffusion combustion of diesel fuel, which is directly injected into the cylinder near TDC. The diesel fuel jets, once partially mixed with the in-cylinder charge, are ignited under elevated temperature due to compression of the charge.

Designing a new engine

Designing a new engine provides the maximum flexibility and probably the most efficient design for operation with gaseous fuel, but tends to bear

mounting costs, which prevent it from being a commercially viable option, because direct injection natural gas engines are unlikely to find large-scale commercial application in the near future, due to the well-established product lines of conventional petrol and diesel engines. Known world oil reserves are declining but can still keep supplying conventional IC engine fuels, i.e. petrol and diesel, for decades at costs acceptable to most consumers. The mighty network of fuelling stations for petrol and diesel also binds drivers to conventional automobile fuels. Any motivation for switching from conventional fuels to natural gas, whether for cost savings or for environmental protection, will face the challenge of accessing natural gas fuelling facilities, which are on a much smaller scale than those for petrol and diesel. The market for natural gas engines, therefore, tends to be small. The cost of designing a new engine is unlikely to be recovered in a market of such a scale. Designing a new engine specifically for burning natural gas does not appear to be an attractive option in the near future.

Converting from a petrol engine

The second option does not have to bear the high cost of the first option, and fits the niche market of commercial applications of natural gas engines. By converting the fuel system, petrol engines can operate on natural gas at a cost much less than by designing a new engine. Conventional petrol engines convert chemical energy to mechanical energy by so-called premixed combustion. The petrol fuel is mixed with air, or air plus recirculated exhaust gas, before being inducted into the cylinder(s). The compression ratio of a petrol engine has to be low enough to avoid autoignition of premixed air and petrol fuel, because autoignition can cause a very rapid increase of cylinder pressure and could cause severe damage to the engine. The structure of a conventional petrol engine is designed for a low compression ratio (around 10:1). Making a DI natural gas engine by converting a conventional petrol engine would limit the potential for improving fuel efficiency by increasing the compression ratio, because the structure of the petrol engine does not allow a substantial increase of compression ratio. There is still the benefit of fuel efficiency, especially at partial load, from direct injection combustion, because the engine does not have to use the intake throttle to reduce intake air. Recently car manufacturers have started to introduce DI petrol engines on their high performance vehicles. A turbocharger is usually used with the direct injection engine to improve fuel efficiency and to increase power density. Converting a DI petrol engine to a DI natural gas engine involves fewer modifications than converting a conventional petrol engine. The fuel system needs to be redesigned for the gaseous fuel. The engine electronic control module (ECM) may be retained, but modification to the software in the ECM is necessary.

Converting from a diesel engine

The third option is to build a DI natural gas engine from a diesel engine. Replacing the fuel system of a diesel engine by a gas fuel system is less expensive than designing a new gas engine. Converting from a diesel engine has the structural advantage of adopting a higher compression ratio for better fuel economy than the second option. The cost of a diesel engine is usually higher than that of a petrol engine of the same rated power. Diesel engines, however, tend to last longer than petrol engines. For heavy duty applications, durability is important, because a heavy duty truck is normally driven for over 100 000 miles a year. Converting from a diesel engine is a logically sound choice for heavy duty applications.

Major tasks in building a DI natural gas engine from a diesel engine include (i) replacing the fuel system, (ii) adding an ignition system, and (iii) modifying the ECM. The diesel fuel system is designed for liquid fuel and is incapable of handling gaseous fuel, such as natural gas. The components of the fuel system, especially the fuel tank, the injector and the fuel pump/compressor, have to be redesigned or enhanced in order to store and deliver the fuel. An important difference between a DI natural gas engine and a diesel engine is that a DI natural gas engine needs an ignition source. In a diesel engine, diesel jets are ignited near TDC under high temperature due to compression of the in-cylinder charge. In a natural gas engine, however, the temperature increase due to compression is usually not sufficient to initiate combustion, because natural gas has a much higher ignition temperature than diesel fuel. An ignition system is necessary in a DI natural gas engine to create a zone or zones of sufficiently high energy to ignite the gaseous fuel jets. The major functions of the ECM in a modern diesel engine include (i) controlling the timing and amount of fuelling, (ii) controlling emission reduction devices, and (iii) de-rating the engine to protect the engine components. To operate on natural gas, function (i) has to be modified to account for the physical and chemical differences between two fuels. An emission control device can be either a physical unit or a virtual one. The purpose of an emission control device is to control the emissions to meet the levels regulated by legislation, such as EPA 2004 or Euro IV. In an EGR engine, for instance, an EGR valve is an emission control device. A logic scheme to change the fuelling rate and timing, depending on the engine operation mode and the environmental condition to meet the emission regulations, is also an emission control device. Modification to function (ii) can be optional, and is usually required for optimizing trade-off between fuel efficiency and emission reduction. Function (iii) can usually be retained unless the rating and the operating conditions of the gas engine are dramatically different from those of the diesel engine.

Compression ratio

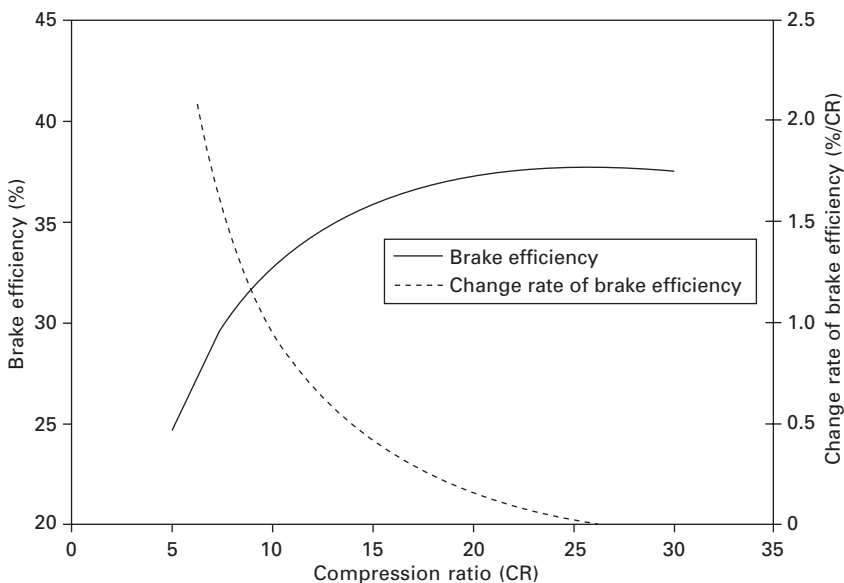
With direct injection, we are free to choose a compression ratio exceeding what otherwise would be limited by knock with premixed combustion. Now the question is what is the preferred compression ratio of a DI natural gas engine? There could be many answers to this question, depending on a number of factors, for example cold start, engine brake efficiency, and the limit of the maximum cylinder pressure. No attempt will be made to offer a number that can be applied to determine the compression ratio of all applications. Instead, boundaries or ranges of the compression ratio that a DI natural gas engine should not exceed are discussed in this section.

Cold start usually determines the lower limit of the compression ratio of diesel engines. The compression ratio of a diesel engine has to be high enough so that the temperature of the in-cylinder charge can be raised sufficiently high before TDC to evaporate the fuel and to ignite the fuel–air mixture. In a DI natural gas engine, fuel injected into the cylinder is in the gaseous phase and fuel vaporization is no longer an issue. To raise the temperature by compression to initiate combustion of natural gas, an excessively high compression ratio would be needed, which would raise the cylinder pressure beyond the limit that a conventional engine could endure. An ignition device is, therefore, needed in a DI natural gas engine. The lower limit of the compression ratio is more likely determined by engine brake efficiency rather than cold start if spark ignition or glow plug ignition is used. If the pilot diesel is used for ignition, the lower limit of the compression ratio tends to be bounded by the cold start, similar to the scenario in diesel engines. The cold start limit of diesel engines with direct injection open chamber combustion can be used as a start point for DI natural gas engines with pilot diesel ignition. Attempts to use numerical models to predict autoignition of the gaseous fuel jets have been reported recently. Unfortunately the numerical models currently available are not accurate enough to determine the cold start limit that would be useful to engine designers, due to the complexity of the ignition process. The engine test is the best way so far to make a final decision on the cold start limit of a DI gas engine.

The engine brake efficiency and the engine structure are two major factors in deciding the compression ratio of a DI natural gas engine with an ignition device. For an ideal diesel cycle without heat transfer and friction, a high compression ratio leads to higher thermal efficiency, and also higher cylinder pressure, than a low compression ratio. The brake efficiency of an engine is directly related to the thermal efficiency of the ideal diesel cycle, and is also related to engine friction and cylinder heat transfer. The general trend is that, as compression ratio increases, there are increases in thermal efficiency, friction heat transfer, the maximum cylinder pressure, and the weight and cost of the engine.

Using an engine cycle model, such a GT Power model or a Wave model, we can simulate a high speed diesel cycle engine to generate a curve of engine brake efficiency vs. compression ratio, as shown in Fig. 8.1. The engine has a bore size of 100 mm, and a stroke of 100 mm, and is naturally aspirated. The engine operates at a speed of 3000 rpm and IMEP between 8.5 and 12.5 bars, with a given heat release rate shape to represent combustion.

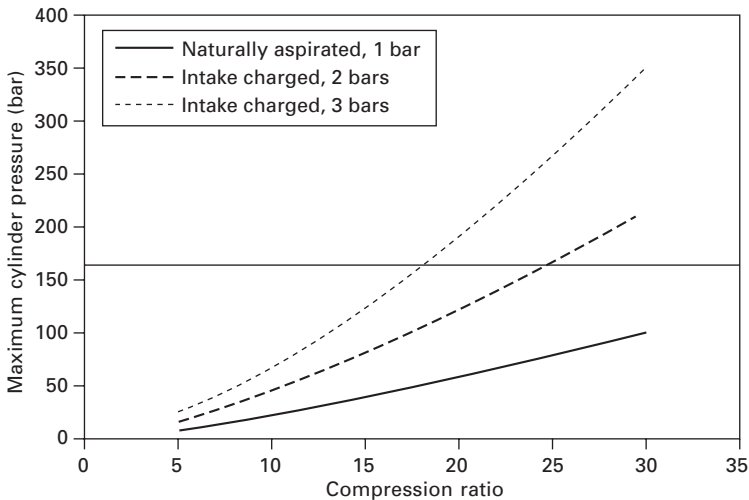
The engine brake efficiency increases from 25% to 36% as the compression ratio increases from 5:1 to 15:1, as we can see from Fig. 8.1. As the compression ratio further increases from 15:1, the gain of brake efficiency reduces, and it begins to diminish when the compression ratio passes 25:1. It is straightforward to pick up an upper limit of compression ratio due to engine brake efficiency, say 25:1, where the gain of engine brake efficiency becomes minimal or disappears if the compression ratio increases further. Picking up a lower limit of compression ratio is not as straightforward, and tends to be arbitrary. To reduce the weight and cost of an engine, one would like to keep the maximum cylinder pressure, which is positively related to compression ratio, as low as possible. As a trade-off between the brake efficiency and engine weight/cost, one may choose a compression ratio at which the rate of change of brake efficiency, which is defined as the ratio of the brake efficiency change to the compression ratio change, becomes small, say 0.5%, i.e. with an increase of compression ratio by 1, the gain of engine brake efficiency is 0.5%. For gas engines converted from diesel engines, one



8.1 Brake efficiency vs. compression ratio, I-6 engine, naturally aspirated, 4.7 litres, 3000 rpm, IMEP 8.5–12.5 bar.

may pick up a compression ratio of about 13:1 as the lower limit from the solid line in Fig. 8.1, where the rate of change of brake efficiency is about 0.5% from the dotted line in the same figure. For gas engines converted from petrol engines, one may pick up a compression ratio of about 10:1 as the lower limit, where the rate of change of brake efficiency is about 1.0%, because the structures of petrol engines are not as strong as those of diesel engines.

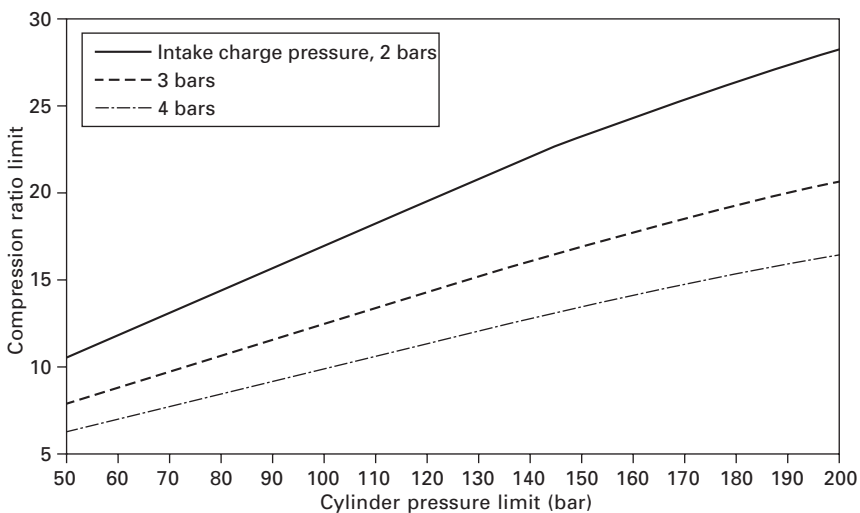
Now we have chosen a compression ratio of 25:1 as the upper limit due to brake efficiency, and a compression ratio of 13:1 for those converted from diesel engines, and of 10:1 for those converted from petrol engines, as the lower limits due to the trade-off between brake efficiency and engine structural strength, according to the modelling results of a naturally aspirated diesel cycle engine. With a turbocharged or a supercharged engine, simply termed an intake charged engine, the change of brake efficiency with compression ratio is similar to that of a naturally aspirated engine. The maximum cylinder pressure, however, from an intake charged engine could be substantially higher than that from a naturally aspirated engine. Using the same model, we can calculate the cylinder pressure of an engine with different intake manifold pressures. The maximum cylinder pressures in this case were kept at TDC due to in-cylinder charge compression by setting the combustion event sufficiently late, and can be plotted against compression ratio under different intake manifold pressures, as shown in Fig. 8.2. At a compression ratio of 25:1, the naturally aspirated engine at sea level would have a maximum cylinder pressure of about 80 bars. At the same compression ratio the maximum pressure of an intake charged engine can easily exceed



8.2 Maximum cylinder pressure vs. compression ratio.

150 bars, as shown in Fig. 8.2. In a modern diesel engine, the maximum cylinder pressure allowed for continuous operation is usually below 200 bars. If we take the 160 bars as the limit of the maximum cylinder pressure, the maximum compression ratio of an intake charged engine has to be below 24:1 with intake charge pressure of 2 bars, and below 18:1 with intake charge pressure of 3 bars, as we can find from Fig. 8.2.

By changing the limit of the maximum cylinder pressure we can find another set of data for the compression ratio versus the maximum cylinder pressure. Repeating the process, we may generate a plot of the compression ratio limit versus the cylinder pressure limit, as shown in Fig. 8.3. The plot covers the limit of the maximum cylinder pressure from 50 bars to 200 bars, and the intake charge pressure from 2 bars to 4 bars. Using Fig. 8.3, one can find the maximum allowed compression ratio once the cylinder pressure limit and the maximum manifold charge pressure of an engine are known. From the thick solid line in Fig. 8.3, for example, with the maximum charge pressure of 2 bars and the maximum cylinder pressure limit of 75 bars, one can find that the maximum allowed compression ratio is about 14:1. If we convert a petrol engine to an intake charged direct injection natural gas engine, we may have to limit the engine compression ratio below 14:1. In the analysis made in this section, we defined the upper limits of compression ratio by assuming that the combustion timing is sufficiently late so that the cylinder pressure reaches a maximum at TDC due to compression. If the combustion takes place before or close to TDC, and at a sufficiently high rate, the maximum cylinder pressure can be much higher than that due to in-cylinder charge compression.



8.3 Compression ratio limit vs. cylinder pressure limit.

In case the maximum combustion pressure is higher than the TDC compression pressure, the maximum compression ratio allowed has to be below the boundaries defined in Fig. 8.3, to ensure that the cylinder pressure limit is not exceeded. In modern diesel cycle engines with brake mean effective pressure near or above 20 bars, the TDC compression pressure is likely the maximum pressure at full load, because the timing of combustion has to be sufficiently delayed to control NO_x emission, as well as to control the cylinder pressure. Assuming an intake charge pressure of 3.5 bars, for example, we can find from Fig. 8.3 that the compression ratio has to be below 19:1 if the cylinder pressure limit is 200 bars, and below 12:1 if the cylinder pressure limit is 100 bars. This implies that the combustion timing may have to be sufficiently delayed only for the reason of not exceeding the cylinder pressure limit.

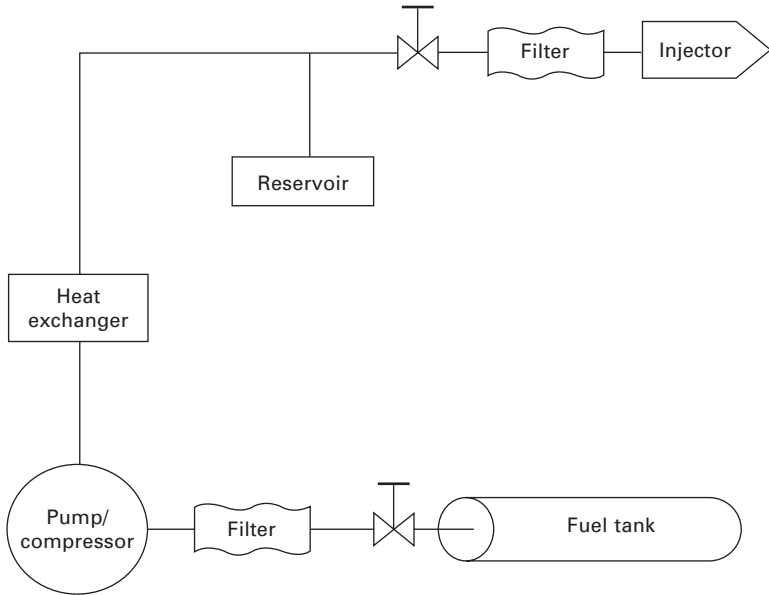
So far, we have discussed the limits of compression ratio based on the numerical results from an engine cycle model. In diesel cycle engines of different sizes and configurations, the absolute values of engine operation parameters, such as brake efficiency, heat transfer, and friction, can be different from those produced by the model, but the trends showing how engine efficiency and cylinder pressure change with compression ratio are very similar to those from the model. Engineers can either directly use the chart in Fig. 8.3, or follow the procedure to generate a chart to determine the compression ratio limit of a specific engine.

Summarizing the discussion in this section:

- The compression ratio of a direct injection gas engine should be roughly in the range of 10:1 to 24:1; the lower end of the compression ratio is the result of a trade-off between engine brake efficiency and engine weight and cost, while the upper end is imposed by the cylinder pressure limit.
- In DI natural gas engines with intake highly charged, the compression ratio may have to converge to a narrow range near the lower end, say from 12:1 to 18:1, because a reduced compression ratio provides more room for emission reduction and power density enhancement, and is also favourable for vibration and noise reduction.

8.2.2 Fuel storage and supply

A fuel supply system mainly consists of a fuel tank, fuel filters, a fuel pump/compressor, a heat exchanger, valves and connecting pipes, as shown in Fig. 8.4. The functions of the fuel supply system are to store and supply natural gas to the fuel injector(s) under a predetermined pressure and temperature at the desired rate. The natural gas is in the form of either compressed natural gas (CNG) or liquefied natural gas (LNG). The components of a fuel supply



8.4 Fuel supply system.

system could differ from one to another substantially, depending on whether the gas is stored in the form of CNG or LNG. Major components and their functions will be discussed in this section individually.

Fuel tanks

The natural gas fuel tank is a closed container impermeable to natural gas with sufficient volume to store fuel to run the engine for a desired period of time. The size, structure and material of a fuel tank are determined by its application, and whether the stored fuel is CNG or LNG.

The maximum size of a fuel tank is limited by the weight allowed and the space available on a vehicle. On a passenger car, for example, one may not want the tank bigger than the size of the trunk, so that the space of the passenger compartment will not be compromised. The minimum size of the fuel tank depends on the minimum travel distance within a refuelling cycle. On a garbage dump truck, for example, the fuel tank should be big enough to complete at least one round trip from a fuelling station to the garbage pickup, and to a dump site, and back to the fuelling station.

Cylindrical tanks made of layered composite materials with an impermeable inner shell are the preferred structure for CNG. The inner shell is usually made of aluminium due to its corrosion resistant property, light weight and

low cost. The composite outer layers, commonly made of inorganic fibres such as fibreglass, and inorganic bonding materials such as epoxy, due to their stable chemical properties, low thermal conductivity and low cost, are light in weight and highly fracture resistant. A single cylinder or a cluster of cylinders can be used on a vehicle to store CNG. The maximum mass of the gas carried is determined by the total size of the tank(s), and the maximum pressure of the gas.

To store LNG, the cylindrical tank made of two metallic layers with a vacuum insulation layer in between has been commonly used. The inner cylinder is exposed to the cryogenic temperature as low as about -162°C , at which natural gas is in liquid form. The inner layer should be made of corrosion and low temperature resistant materials, such as titanium, aluminium or stainless steel. The outer layer of the tank can be made of less expensive materials, such as carbon steel, but is preferably made of the same material as the inner layer. The outer layer does not directly contact LNG, but is still exposed to the freezing temperature locally, and tends to be exposed to LNG accidentally due to leakage and spillage. Besides, using the same material helps to ease the design to handle thermal expansion and contraction, and helps to reduce the cost of inventory and manufacturing.

A LNG tank would carry more fuel mass than a CNG tank of the same size, but tends to be more expensive and heavier than the CNG tank. For applications where travel distance is critical, such as long-haul trailers, the LNG tank is preferred. For applications where CNG fuelling stations are easily accessible and the travel distance is not critical, such as transit buses in a big city, the CNG tank is a good option.

Fuel compressors/pumps and heat exchangers

A compressor in a CNG fuel system is not necessary, but is usually desirable. In a fully charged CNG tank, the gas pressure can be over 300 bars, which is sufficiently high to supply fuel to the injectors and to inject the fuel into the engine cylinder. As CNG is consumed, the tank pressure drops, to the level at which fuel delivery to the engine cylinder cannot be sustained. We have two options to resume the fuel injection: (i) by recharging the CNG tank, or (ii) by using a compressor. Option (i) further reduces the travel distance of a vehicle, because only part of the CNG in the tank can be available. A compressor can be used to raise the CNG pressure, so that most of the fuel in a tank can be utilized.

In a LNG fuel system, a pump or a compressor is always needed, because LNG is usually kept under a pressure of less than 10 bars, which is not sufficient to deliver the fuel into the engine cylinder. There are two options to raise the gas fuel pressure. The first option is to pump the LNG to a high pressure and then to vaporize the fuel. The second is to vaporize the LNG and

then compress the gaseous fuel to a high pressure. The major advantages of pumping LNG directly are the compact size of the pump and high efficiency [2]. The main drawbacks of the first option are burdens to address the issues involving pumping cryogenic fluid, such as sealing, insulation, thermal stress and material durability. The major advantages of the second option are that mature compressor designs are available, the compressors tend to be durable and the compressors can be made of less expensive materials. The major disadvantage of the second option is that a gas compressor tends to have lower efficiency and bigger size than a liquid pump to deliver the same amount of fuel.

In both CNG and LNG systems, the temperature of the gas fuel entering the injector should be kept stable for consistent fuel injection. For this purpose, a heat exchanger is needed. With the CNG system, the heat exchanger is used for reducing the fuel gas temperature after it is compressed. With the LNG system, the heat exchanger is used for vaporizing the LNG after its pressure is raised by the pump. If the second option is used, i.e. the LNG is vaporized first and then compressed to increase its pressure, two heat exchangers may have to be used. One is for vaporizing the LNG before the compressor, and another is for regulating the gas temperature after the compressor to the level required by the fuel injection. Where LNG is directly injected into the engine cylinder, as claimed by White *et al.* [3], a heat exchanger may not be needed.

Reservoirs and accumulators

Reservoirs or accumulators are usually used in a fuel system, where the fuel injection is activated by means other than the fuel pressure itself (refer to Section 8.2.3 for detailed discussion). An accumulator can be in the form of a canister, a piece of cylindrical pipe, or a channel in an engine block or in a cylinder head. The fuel flow to injectors is intermittent and transient in IC engines. The fuel delivery rate from the pump or compressor usually does not match the fuel consumption rate of the injectors. This mismatch causes undesirable fluctuation of fuel pressure between the pump or compressor and the injectors. The volumes of the pipelines connecting the pump or compressor and the injectors are usually not sufficient to damp the fluctuation. An accumulator can be placed just before the injectors to reduce the fluctuation of fuel supply pressure to an acceptable level.

The volume of the accumulator determines the amplitude of the pressure fluctuation: the larger the volume, the smaller is the amplitude. The volume of the accumulator can be determined with a given target of pressure fluctuation by numerical modelling or by testing. For a given target bandwidth of pressure fluctuation, an accumulator is preferably made as small as possible, because a smaller accumulator takes less space and more importantly has a

quicker response time than a bigger one if the injection pressure needs to be modulated.

The accumulator could be a passive device or an electronically controlled device. To maintain a single level of pressure, a passive accumulator with a mechanical pressure release valve is sufficient. To maintain multiple levels of pressure at different operation conditions, an electronically controlled accumulator may have to be used.

Fuel filters

The natural gas from the fuel tanks and to the injectors may contain impurities, such as solid particles and liquid droplets, which can cause failure of the components. Filters have to be used in a fuelling system to remove the impurities to prevent the compressor/pump and injectors from damage or premature wear-out. There is a variety of filters for different applications, which can be classified into three categories based on the pore size of the filtration elements. They are micro filters, ultra filters, and nano filters. Micro filters have pore sizes ranging from 0.1 to 10 μm , ultra filters have pore sizes from 0.001 to 0.1 μm , and nano filters have pores in the order of molecules in size. The filtration elements can be made of organic materials, such as activated carbon, activated clay, diatomaceous earth, cotton, paper and sand, or synthetic materials, such as polyethersulfone (PES), polypropylene (PP), polytetrafluoroethylene (PTFE), glass fibre, ceramics and metals. For natural gas filtration on IC engines, micro filters and ultra filters can be used. Filtration elements made of materials with stable chemical properties and mechanical strength, such as PTFE, glass fibre and metal, are desired under severe temperature and vibration conditions for automobile applications.

8.2.3 Fuel injection

Injectors

The injector is a device to deliver fuel intermittently into the engine cylinder at times that are synchronized with the engine camshaft position. The injector needle in an injector acts as a valve to open or close the passage to the injector hole(s). In a fuel pressure-activated injector, one end of the needle is preloaded with a spring force, and the other end is exposed to the fuel pressure. The needle is closed against the seat when the spring force is greater than the force due to fuel pressure. The fuel pressure can be changed by a pump which is either separated from the injector(s) by pipelines or directly connected to an injector. When the fuel pressure increases to overcome the spring force, the needle starts moving away from the seat, and fuel injection starts. When the fuel pressure drops to a level not sufficiently

high to overcome the spring force, the needle closes to end fuel injection. In a pneumatically activated injector one end of the needle is connected to a pneumatic chamber, and the other end is exposed to the fuel pressure. By changing the hydraulic pressure in a chamber, the force on the needle changes to open or close the needle against the needle seat. Recently injectors with needles activated by piezoelectric devices have been mass-produced. An element made of piezoelectric materials is mechanically connected to one end of the needle. By changing the electrical potential across a piezoelectric element, the element expands or shrinks, due to the converse piezoelectric effect, to change the needle position to start or to stop the fuel injection. Similar to the piezoelectric injector, magnetostrictive materials can also be used to actuate the needle. In this case the dimension of a magnetostrictive element can be changed by applying a magnetic field on it. The position of the needle, which is physically connected to the element, can be controlled electronically. In a solenoid activated injector, the injector needle is connected to an armature magnetically coupled to a magnetic coil and a ferromagnetic core. By changing the electrical current through a coil surrounding the ferromagnetic core, the position of the armature changes to open or close the needle against the seat.

Fuel pressure-activated injectors are simple and compact, but sensitive to fluctuation of fuel pressure. A fuel pressure-activated gas injector has slower response than a liquid injector, because the pressure wave propagation in gas is much slower than that in liquid, and tends to compromise the accuracies of fuelling timing and fuelling rate. A pneumatically activated injector can be made to have quicker response than a fuel pressure-activated injector, because the pressure wave propagation in a hydraulic fluid is quicker than that in a gas. A piezoelectrically activated injector has quicker response than a pneumatically activated injector. The travel distance of the needle in a piezoelectrically activated injector is very limited due to the characteristics of the piezoelectric element. In large engines, such as those used in heavy duty trucks and mining trucks, the fuelling quantity tends to be large and the injection interval is long; pneumatically driven injectors can be a good candidate. Piezoelectrically or magnetostrictively activated injectors are suitable for small high-speed engines, such as those used in passenger cars and pickup trucks, where fuelling quantity is small and quick response is important. In a direct injection engine, the fuelling pressure tends to be very high, and the fuelling event tends to be very short. A pneumatic device, a piezoelectric device or a magnetostrictive device is able to provide sufficient actuating force to meet the needs. For high pressure fuel injection, the solenoid actuators have to be made very big to provide sufficient actuating force. They are therefore more suitable for low pressure fuel injection, such as intake port fuel injection, than direct in-cylinder fuel injection under high pressure.

Injectors can also be classified into two categories based on whether they can inject a single fuel or two types of fuels in a single unit, i.e. mono fuel injectors and dual fuel injectors. A mono fuel injector can inject either a single liquid fuel, such as diesel, petrol or ethanol, or a single gaseous fuel, such as natural gas or hydrogen. Mono fuel injectors have been used in diesel engines for diesel injection, and sometimes in direct injection petrol engines to inject petrol directly into the cylinders. Engines running on gaseous fuels directly injected to the cylinder by mono fuel injectors have recently been developed and tested by a number of engine developers and automobile manufacturers. A dual fuel injector is capable of injecting two types of fuels from a single injector, such as the dual fuel injector invented by Hill *et al.* [4] which can inject a small portion of diesel fuel for pilot ignition and a major portion of natural gas to provide most of the fuel to run an engine.

Injection pressure

The injection pressure here refers to the fuel pressure at the fuel entrance of an injector. In an injector with an internal intensifier the injection pressure refers to the fuel pressure at the exit of the intensifier. A positive pressure difference between the injection pressure and the cylinder pressure, to which the injector holes are exposed has to be sufficiently large to deliver the fuel to the cylinder in a short time period. Considering the pressure loss inside an injector, we may express the desired injection pressure, P_{inj} , as

$$P_{inj} > P_{max} + \delta P_1 + \delta P_2 \quad 8.1$$

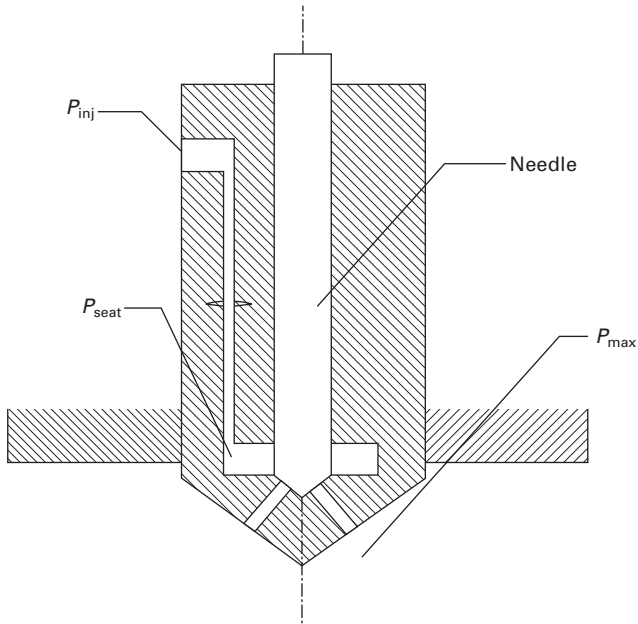
where P_{max} is the maximum cylinder pressure, $\delta P_1 = P_{seat} - P_{max}$ is the pressure difference across the injector holes, and $\delta P_2 = P_{inj} - P_{seat}$ is the pressure drop inside the injector. Here P_{seat} is the fuel pressure at the needle seat, shown in Fig. 8.5.

The pressure difference across the injector holes, i.e. δP_1 , is a driving force of fuel injection. For successful fuel injection, two conditions should be met: (i) δP_1 is positive; (ii) δP_1 is sufficiently high to inject fuel at a desired rate. Considering the pressure variations, we may express condition (i) as

$$\delta P_1 = (P_{seat} - 3\sigma_{P_{seat}}) - (P_{max} + 3\sigma_{P_{max}}) > 0 \quad 8.2$$

where $\sigma_{P_{seat}}$ is the standard deviation of P_{seat} , and $\sigma_{P_{max}}$ is the standard deviation of P_{max} . In practice, $\sigma_{P_{seat}}$ is difficult to measure, and can be replaced by $\sigma_{P_{inj}}$, i.e. the standard deviation of the injection pressure. Using the relation $P_{seat} = P_{inj} - \delta P_2$, we may rewrite equation (8.2) as

$$P_{inj} - P_{max} - \delta P_2 - 3*(\sigma_{P_{inj}} + \sigma_{P_{max}}) > 0 \quad 8.3$$



8.5 Fuel injection pressure (P_{inj}) and maximum cylinder pressure (P_{max}).

or

$$P_{inj} > P_{max} + \delta P_2 + 3*(\sigma_{P_{inj}} + \sigma_{P_{max}}) \tag{8.4}$$

In Equation (8.4), P_{max} can be measured or can be a design target; δP_2 , the pressure drop inside the injector, can be measured from a given injector; the standard deviation of injection pressure, $\sigma_{P_{inj}}$, can be measured from a given fuel supply system; and the standard deviation of P_{max} , $\sigma_{P_{max}}$, can be measured from an engine or estimated from data of similar engines. Equation (8.4) defines the lower boundary of the injection pressure.

For an injection event to complete in a given time interval, condition (ii) has to be met, i.e.

$$P_{inj} - P_{max} - \delta P_2 - 3*(\sigma_{P_{inj}} + \sigma_{P_{max}}) = \text{IPS} \tag{8.5}$$

or

$$P_{inj} = \text{IPS} + \delta P_2 + P_{max} + 3*(\sigma_{P_{inj}} + \sigma_{P_{max}}) \tag{8.6}$$

where IPS is a positive number that can be termed the ‘injection pressure surplus’. The pressure surplus in equation (8.6) is a driving force for a positive fuel flow from an injector to a cylinder. The greater the driving force,

the greater is the fuel injection rate. For effective conversion of chemical energy to mechanical energy from burning a fuel in an IC engine, the injection momentum of the fuel jets should be kept as high as possible. This means that the pressure surplus should be kept as high as possible. The increased pressure surplus, however, requires increased strength of the components of the fuel injection system and increased pumping power. As long as the engine performance and emission targets are met, the injection pressure should be kept as low as possible, because a low injection pressure helps the reliability of a fuel system, and helps to reduce its cost and power consumption. In a modern diesel engine, the IPS can be in the order of 10^3 bars. For natural gas injection, the IPS may have to be kept at least an order of magnitude lower than that of diesel engines, i.e. in the order of 10^2 – 10^1 bars, because pumping natural gas is more difficult and consumes more power than pumping diesel.

Hole size vs. hole number

For a multi-hole injector, the injector hole size usually refers to the nominal diameter of the channel connecting the in-cylinder charge and the sac volume, the volume right behind the needle seat in the injector. The fuel injection rate is proportional to the total cross-sectional area of the injector holes and the injection pressure surplus, IPS, defined by equation (8.5). The cross-sectional area of a gas injector has to be made much greater than that of a diesel injector due to the difference in the volumetric energy density between the natural gas and diesel fuel. Taking the energy densities at the injector holes of 8 MJ/litre of a natural gas fuel, and of 35.5 MJ/litre of a diesel fuel, for example, the cross-sectional area of a gas injector has to be about four times that of a diesel injector to deliver the same amount of energy under the same IPS. If the IPS of the diesel injection is 10 times higher than that of the gas injection, the cross-sectional area of the gas injector has to be about 40 times that of the diesel injector. The hole size of a gas injector has to be approximately six to seven times as large as that of a diesel injector if both injectors have the same hole number and deliver fuel at the same energy rate.

In a multi-hole injector, the total cross-sectional area of the jet flow is proportional to both the hole size and the hole number. For a given cross-sectional area, the larger the hole size the fewer the hole number is, and vice versa. For a given total fuel amount, determination of the hole number depends mainly on the thickness of the fuel jet, and on the in-cylinder swirl. The thickness of a fuel jet, which refers to the linear dimension perpendicular to the jet direction, is determined by the design parameters of the injector, such as the hole diameter, the length to diameter ratio of the hole, and the orientation of the hole. In the case of thick fuel-jets and high swirl, for

instance, the hole number may have to be kept small to avoid overlap of the adjacent fuel jets for effective fuel air mixing. The hole size affects the maximum penetration of a fuel jet. A fuel jet from a bigger hole travels further than that from a smaller hole. In a small combustion chamber, a small hole size is preferred to prevent excessive wall impingement of the fuel jets, which usually has a negative effect on fuel–air mixing and combustion. In a big combustion chamber, a big hole size can ensure sufficient fuel jet penetration to fully utilize the air in the chamber. The cylinder pressure also affects the maximum penetration of a fuel jet. A jet travels further in a low pressure cylinder than in a high pressure cylinder. Determination of the hole size and the hole number involves a number of factors, such as the injection pressure, the cylinder pressure, the combustion chamber configuration, and the in-cylinder air flow pattern and intensity.

8.2.4 Ignition

In a conventional diesel engine, the diesel sprays are ignited by compression. In a direct injection natural gas engine, it is difficult to ignite the gas sprays directly by compression. An ignition method has to be applied to initiate the combustion of the gaseous fuel. There are a number of methods for initiating combustion of natural gas in an IC engine, such as spark plug ignition, hot surface ignition or glow plug ignition, plasma ignition, laser ignition, and pilot fuel ignition. Three of them, i.e. spark plug ignition, hot surface ignition and pilot fuel ignition, have found applications in commercial products and prototype developments, and will be discussed in the following.

Spark plug ignition

Spark plug ignition uses electric arcs crossing electrodes of a spark plug to initiate combustion. The electric arcs can be generated by a high voltage from rapid collapse of the magnetic field in a coil or from a high voltage capacitor. Spark ignition has been used to ignite premixed combustible mixtures in petrol engines since they were invented over a century ago. In a direct injection natural gas engine, combustion can also be initiated by spark ignition. With spark ignition, the discharge time period of an electric arc is usually very short. The total energy release from the spark is limited. To ignite a gas jet, the location and timing of the spark release have to be carefully controlled so that an ignitable fuel–air mixture can meet the spark, and so that its temperature can be raised sufficiently high by the spark to initiate combustion. Spark ignition tends to cause misfire because it is difficult to generate a spark at the right timing and at the right location under all engine operation conditions. There are a couple of methods to improve the reliability of spark ignition. One method is to create multiple sparks: by

generating sparks one after another in a prolonged time period, the chance that the combustible fuel–air mixture meets the spark increases. Another is to use multiple spark plugs in a cylinder: by creating multiple sparks at different locations, the chance that the combustible fuel–air mixture meets the spark increases too.

As we discussed on page 204 direct injection gas engines tend to have higher cylinder pressures than petrol engines for thermal efficiency. At an elevated cylinder pressure, the voltage required to jump a spark a cross electrodes is higher than at a low cylinder pressure for a given gap width between an anode and a cathode. The increased voltage can have two negative impacts on the ignition system. One is the increased burn rate of electrodes, which shortens the life of a spark plug. Another is the difficulty of insulating the ignition system. In a direct injection gas engine, since the cylinder pressure can be too high to use spark ignition due to the issues of reliability and durability, alternative ignition methods may have to be used to overcome its shortcomings.

Glow plug ignition

Glow plugs have been used to assist cold starts of diesel engines. The surface temperature of a heating element on the tip of the glow plug increases as an electric current passes through it. The hot surface heats the charge surrounding it (usually in a pre-chamber or a swirl chamber) to speed up evaporation of the liquid diesel fuel and to assist ignition of the fuel–air mixture when an engine starts under low ambient temperature. The glow plug can generate a continuous heat flux that is not sensitive to the surrounding pressure, and is suitable as an ignition source for direct injection gas engines. Placement and surface temperature of the heating element, and control of the combustible mixture formation, are three key elements for successful ignition. The glow plug should be located where the combustible mixture is likely to form and to stay for a sufficiently long time so that chemical chain reactions in the mixture sustain to initiate combustion.

Pilot fuel ignition

The gas jets in the cylinder can also be ignited by high temperature zones from burning a small quantity of another fuel, which can be ignited by compression under normal engine operation conditions. The fuel for the purpose of ignition is usually called the pilot fuel, and this ignition method can be termed the pilot fuel ignition method. It is a method of indirect compression ignition. The pilot fuel can be introduced into the cylinder either by another injector, a pilot injector, or by mixing with the gas in a gas injector and then entering the cylinder along with the gas jets. For

convenience we may call the method of introducing the pilot fuel by another injector as separate-entrance, and call the method of introducing the pilot fuel along with the gas jets as co-entrance.

The separate-entrance method needs another injector, and increases the complexity and cost of the fuel injection system. The advantages of the separate-entrance are its flexibilities of timing and placement. The timing when the pilot fuel starts to enter the cylinder can be independent of the main gas injection event. This is important especially at partial or light load conditions, where we want the pilot fuel entering the cylinder ahead of the gas jet to establish the ignition zones to meet the gas jet before the gas jet becomes highly diluted. The location and number of ignition zones can also be tailored independently of those of the gas jets for efficient ignition of the gas jets. An injection system with co-entrance tends to be simpler and cost less than that with separate-entrance. The penalties of this simple system are lack of flexibility of the timing and placement of the ignition zones, and poor mixing of the pilot fuel with air. With co-entrance, the pilot fuel has to travel along the gas jets, where fresh air is less available than away from the gas jets, and the ignition zones created by burning the pilot fuel can only be formed after the gas jets enter the cylinder.

With separate-entrance we have two options to design the injectors. The first option is to design the pilot injector as a separate unit from the gas injector, which can be called the option of dual-fuel–two-injectors. The second option is to design the pilot injector as part of a combined unit with the gas injector, which can be called dual-fuel–single-injector. With the option of dual-fuel–two-injectors, substantial modification to the cylinder head may be needed to convert a diesel engine to a DI natural gas engine, because there is usually only a single hole on each cylinder for an injector. With the option of dual-fuel–single-injector, a dual-fuel injector can be made of the same size as the diesel injector replaced, and mounted to the existing hole in the cylinder head with minor or no modifications.

There are many fuels with cetane number sufficiently high for reliable compression ignition, such as diesel, dimethyl ether, Fischer–Tropsch fuel, rape seed oil, etc. Among them diesel appears to be the most attractive candidate, because it is readily available in many fuel stations, and its cost is lower than other candidates. Under the pioneering work of Hill *et al.* [4], dual-fuel injectors of the dual-fuel–single-injector design, which use pilot diesel fuel to ignite the gas fuel, have been successfully applied to heavy duty engines for commercial applications. The injector is of the same size as the diesel injector replaced, so that it can be fitted into the original hole without modification. With dual-fuel injectors, heavy duty engines operating on the directly injected natural gas with a small quantity of diesel fuel are able to match the brake power and the fuel economy of those operating on pure diesel fuel.

8.2.5 Combustion

Combustion of natural gas jets differs from that of diesel jets mainly in four aspects. First, the gas jets enter the cylinder in the gas phase, and do not need evaporation. Secondly, the rate at which a gaseous jet mixes with air is usually slower than for a diesel jet, due mainly to the difference in the injection pressures. The slow fuel–air mixing leads to a slow burning rate. Third, natural gas needs more air to burn than diesel fuel. The stoichiometric air–fuel ratio of natural gas is about 17:1, while that of diesel is about 14.3.1 The low heating value of natural gas is about 49 MJ/kg and that of diesel about 43 MJ/kg. To generate the same amount of energy, natural gas needs about 4% more air than diesel fuel. In other words, there is less air left after combustion in a DI natural gas engine than in a diesel engine if the amounts of intake air and fuel energy input are the same.

To achieve engine brake efficiency comparable to that of a diesel engine, the combustion system of a direct injection natural gas engine may have to be different from that of a diesel engine. To modify diesel engines, the major parameters that need to be considered include: (i) the combustion chamber configuration, (ii) the fuel jet orientation and placement, (iii) the injection timing and duration, and (iv) the large-scale flow pattern and turbulence intensity. The configurations of the combustion chambers of diesel engines are designed for burning diesel fuel jets and are not necessarily suitable for burning gaseous jets, and may need to be redesigned. Gaseous jets are much thicker than diesel jets of the same energy content. The number and orientation of the gaseous fuel jets may have to be different from those of the diesel jets for a good match with combustion chamber configuration and for good utilization of the in-cylinder air. The burning rate of natural gas jets tends to be slower than that of diesel jets, and should be improved by enhancing the large-scale charge motion, such as swirl or tumble, and by increasing the turbulence intensity. The timing and duration of the gas fuel injection have to be tailored to accommodate the differences as well.

8.2.6 Emission control

The NO_x formation from combustion increases exponentially as the adiabatic flame temperature increases. The NO_x emission from burning natural gas is inherently lower than that from burning diesel fuel, because natural gas has a lower adiabatic flame temperature than that of diesel fuel.

The low NO_x emission from burning natural gas offers a number of opportunities. First, we may advance the timing of combustion to improve fuel economy. In a diesel engine, a commonly used method to control NO_x emission is ignition delay. The fuel economy is usually negatively affected by this practice. In a natural gas engine, we may advance the combustion timing

for improved fuel economy while maintain the same NO_x emission level as that from a diesel engine with the delayed combustion timing. Secondly, we may use less EGR to meet the NO_x emission limit. Introducing cooled EGR has been an effective method to control NO_x emission from diesel engines, but has negative impacts on an engine. Using less EGR in a natural gas engine leads to a number of benefits compared to a diesel engine, such as small and less expensive EGR components, small engine cooling system, increased power density, and reduced particulate matter (PM) emission.

Even at the same EGR level a natural gas engine tends to emit less PM than a diesel engine, because the tendency to form particulates from burning natural gas is much weaker than from burning diesel fuel. This leads to the possibility of eliminating a particulate filter, or of increasing EGR for further NO_x reduction without exceeding the limit of PM emission.

A DI natural gas engine tends to have higher specific unburnt hydrocarbon emission and higher specific carbon monoxide emission than a diesel engine, especially under high engine speed and low load conditions, because natural gas burns more slowly than diesel. Measures that reduce the amount of over-lean or over-rich mixtures and enhance the burning rate help to reduce emissions, such as increasing the ignition energy, increasing the flame propagation speed, optimizing the combustion chamber configuration, etc.

8.3 Potential applications

Direct injection natural gas engines have great potential to replace conventional diesel engines and conventional petrol engines in road transportation and off-road applications. Technically, IC engines on heavy duty trucks, buses, light duty trucks and passenger cars can be replaced by direct injection natural gas engines.

8.3.1 Heavy duty trucks

Heavy duty trucks are good candidates for natural gas engines for a number of reasons. First, they usually have a large space available to accommodate the increased volume of the gas fuel system, due to the larger fuel tanks and fuel pumps. Secondly, the high cost of heavy duty trucks makes it easier to absorb the extra cost of the gas fuel system. Third, their high operation intensity makes the recovery period of the extra cost short. A heavy duty truck can travel several hundred thousand kilometres a year, and the fuel cost alone can run to over \$100,000 a year. In areas where the price difference between diesel and natural gas is substantial, the saving on the fuel cost can offset the extra cost of the gas engines in few years.

8.3.2 Buses

Buses, especially fleet-operated city buses, are also suitable for DI natural gas engines. Most bus fleets are powered by diesel engines. There are also tens of thousands of city buses powered by premixed natural gas engines. Replacing the diesel engines with DI natural gas engines can improve air quality in cities, because the latter emit fewer pollutants than diesel engines. Replacing the premixed natural gas engines with DI natural gas engines can reduce the fuel cost, because the latter have better fuel efficiency than the premixed natural gas engines. Premixed natural gas engines in buses are usually not as powerful as those diesel engines of the same displacement, because they have lower power density than the diesel engines due to knock limitation. Direct injection natural gas engines are capable of delivering the same torque and power as the diesel engines they replace, and tend to provide a smoother ride than diesel engines due to reduced noise and vibration.

8.3.3 Light duty trucks and passenger cars

Applying gas engines to light duty trucks and passenger cars presents three major challenges. The first is accessibility to natural gas fuelling facilities. Current gasoline stations rarely have fuelling facilities for natural gas. Most natural gas fuelling stations are built in big cities, and are mainly for fleet operations. People in small cities and rural areas usually do not have access to natural gas fuelling facilities. The second challenge is the reduced driving range of vehicles powered by natural gas, which limits their application to short-distance travel. The third is the extra cost of the natural gas engine, which is not as easily absorbed as in the case of heavy duty trucks, because passenger cars and light duty trucks travel less than heavy duty trucks and the fuel cost is a smaller portion of the total cost.

The first challenge can largely be overcome by having either a stationary compressor in each household or an onboard compressor to fill the CNG tanks in areas with access to natural gas supply. The second can only be partially overcome by increasing the maximum pressure of the CNG tanks or by reducing the vehicle mass and friction loss. If mass-produced, natural gas fuelled vehicles could be purchased at a price premium over the conventional diesel vehicles that is more acceptable than that shown by current projections, and in most regions this price premium could soon be recovered by the reduced fuel cost.

8.4 Strengths and weaknesses

In this section the strengths and weaknesses of DI natural gas engines are discussed mainly in comparison with those of diesel engines, because both

types of engine have a similar structure of the fuel system and operate in a diesel cycle.

8.4.1 Emissions

Natural gas has a lower adiabatic flame temperature than that of diesel fuel. The NO_x formation increases exponentially with the adiabatic flame temperature. DI natural gas engines therefore inherently emit less NO_x than diesel engines. The tailpipe NO_x emission from a DI natural gas engine is about half that from a diesel engine at the same operation condition.

DI natural gas engines tend to emit less PM mass than a diesel engine, especially at high EGR levels, because of the physical and chemical differences between the two fuels. The tendency to form particulates from burning natural gas is much weaker than from burning diesel fuel. As to whether the total number and size of the particulates from burning natural gas are different from those from burning diesel, and whether their effects on public health are different, further research work is needed.

Natural gas, which usually contains more than 90% methane, has a lower C/H ratio than diesel fuel. For the same amount of energy released, burning natural gas forms less CO_2 than burning diesel fuel. A DI natural gas engine usually emits 20–25% less CO_2 than a diesel engine.

Burning of natural gas is not as complete as the burning of diesel fuel in an IC engine, because natural gas has a slower burning rate than diesel fuel. In an IC engine, combustion usually can only be sustained for less than 60° of crank angle before the flames are quenched by expansion of the in-cylinder charge. If the flame speed is not sufficiently high, a portion of the fuel or a portion of the intermediate products from combustion of the fuel will not be fully oxidized before the exhaust valves open, and is emitted as unburnt hydrocarbon. The amount of unburnt hydrocarbons from a DI natural gas engine is higher than that from a diesel engine, but tends to be lower than that from a premixed natural gas engine.

8.4.2 Operation cost

The fuel cost of natural gas tends to be lower than that of diesel in most regions. The price of natural gas varies greatly from country to country and also fluctuates significantly from time to time. In countries where the oil price is suppressed by their huge oil reserves, natural gas can be more expensive than diesel fuel. In countries with abundant reserves of natural gas, it is much less expensive than diesel. Generally speaking, the cost of natural gas is lower than that of diesel fuel in most countries. The current natural gas price is less than 50% of the diesel price in North America and in Australia, based on the same energy content. The world-averaged price of

natural gas in the future is predicted to be about 60% of that of petroleum, as projected by EIA of the United States [5].

Much less particulate matter is formed in natural gas engines than in diesel engines. The low PM content in the cylinders has two major benefits. The first is the reduced soot accumulation in the lubricant oil, which can be directly translated into an extended oil change period. For a heavy duty truck, the cost of an oil change for a natural gas engine can be less than half of that for a diesel engine. The second is reduced wear of engine components, such as cylinder liners, valves and seats, pistons and rings. The savings due to the extended oil change period and the reduced engine component failure can be substantial on a heavy duty truck.

8.4.3 Fuel resources

The total world reserves of conventional natural gas are about 2016 billion barrels oil equivalent (BBOE), and the total world reserves of oil are about 1966 billion barrels (BB), including proved reserves and potential reserves [6, 7]. The world potential reserves from the US Geological Survey are exclusive of the United States. The *proven* reserves are estimated quantities demonstrated with reasonable certainty by analysis of geological and engineering data, and are recoverable under existing economic and operating conditions. The *potential* reserves are estimated quantities suggested with reasonable extrapolation by analysis of geological and engineering data, and tend to be difficult to recover under existing economic and operating conditions. The world oil consumption increased from 30.04 BB/year in 2004 to 31.39 BB/year in 2007 [8]. The world consumption of natural gas was 16.67 BBOE/year in 2004, and is projected to be about 25.39 BBOE/year in 2030 [9]. If the trends of increasing consumption do not change in the future, conventional oil reserves will be exhausted in about 50 years, and conventional natural gas reserves will be used up in about 70 years.

Unconventional natural gas reserves, mainly hydrate natural gas, could be a greater energy source than even the total oil and coal reserves combined [10]. Deposits of hydrate natural gas are found mainly on the bottom of offshore sea beds, where the temperature is near freezing and the pressure is sufficiently high to keep the composite stable. They are also found underground in high-latitude areas where a sub-zero temperature is maintained year round, such as in Alaska and northern Canada. Exploration for hydrate natural gas has been reported from the US, Japan and Canada. The cost of recovering energy from this source tends to be much higher than that from conventional natural gas. More investments in recovery technologies are needed. As conventional fossil fuel resources dwindle, hydrate natural gas may have to take a leading role in meeting world energy demand for the next century.

8.4.4 Cost of fuel systems

Fuel systems for DI natural gas engines tend to be more expensive than those for diesel engines. First, fuel tanks, either for CNG or for LNG, are more expensive than those for diesel. A CNG tank has to withstand over 200 bars of internal pressure. Both the costs of materials and the cost of manufacturing are higher than those of a diesel tank. A LNG tank is subjected to only a few bars of internal pressure, but has to use expensive material to withstand the cryogenic temperature, and requires sufficient insulation to preserve the low temperature of LNG for an extended period of time, making it more expensive than a diesel tank, or a CNG tank, of the same capacity. Second, the fuel pump/compressor, which either compresses gaseous fuel or pumps liquid LNG, tends to cost more to build than a diesel pump. Third, a gas injector is more difficult to seal than a diesel injector, and tends to cost more, though the cost difference could be reduced if the production volume of gas injectors becomes comparable to that of diesel injectors. Fourth, a DI gas engine also needs an additional ignition device, which is not necessary in a diesel engine. The ignition system, such as spark ignition, glow plug ignition or pilot fuel ignition, adds extra cost to a gas engine.

8.4.5 Fuel energy densities

Natural gas has a lower volumetric energy density than diesel or petrol, whether stored either as gas in CNG tanks or as liquid in LNG tanks. CNG usually has a lower energy density than LNG. At atmospheric pressure, natural gas in the gaseous phase occupies about 600 times the volume of liquefied natural gas. When compressed to 200 bars, the energy density of CNG is about 8.1 MJ/litre. The energy density of LNG is about 21.4 MJ/litre, and those of petrol and diesel are about 31.8 MJ/litre and 35.6 MJ/litre respectively. With CNG a vehicle would travel about 38% of the distance that would be travelled with LNG, about 25% of the distance that would be travelled with petrol, and about 23% of the distance that would be travelled with diesel fuel, if the fuel tank size and the fuel consumption rate are the same. In other words, to match the travelling distance with diesel fuel, a CNG tank would have to be about four times as large as the diesel tank, and a LNG tank would have to be about 70% larger than the diesel tank.

8.5 Future trends

We have seen increased numbers of IC engines using natural gas, mainly in the sector of transportation applications such as buses and heavy duty trucks. There are three major factors driving this trend: fuel price, emission control, and energy security. In most countries, natural gas is less expensive

than diesel or petrol. A gas engine tends to be more expensive than a diesel engine, though the lower cost of natural gas can usually offset the high initial cost of the gas engine. The lifetime cost of operating a natural gas engine can be less than that of a diesel engine. It is expected that more IC engines will use natural gas as fuel for economic reasons. To meet EPA 2010 or Euro VI emissions, aftertreatment devices for NO_x and PM are necessary for diesel engines. Replacing diesel fuel with natural gas tends to reduce NO_x and PM emissions from the engine exhaust, so that natural gas engines can use less expensive aftertreatment devices than diesel engines. As oil production reaches a peak while oil consumption is increasing, the gap between demand and the supply will merge and widen in the near future. Natural gas is the only chemical energy resource that is capable of filling that gap. Replacing oil with natural gas in IC engines will reduce dependency on oil, especially in regions and countries that depend heavily on imported oil.

Traditionally, heavy duty trucks are powered by diesel engines. There are few applications using premixed natural gas engines to replace the diesel engines. Those gas engines have, however, lower fuel efficiency and lower power density than diesel engines, and the drivability of the trucks has to be compromised in those cases. Premixed natural gas engines are also sensitive to the composition of natural gas and to ambient conditions. On the other hand, DI natural gas engines are able to replace diesel engines in heavy duty trucks while retaining the fuel efficiency and power density. Commercial applications and demonstrations of DI natural gas engines in heavy duty trucks have already begun in the United States and in Australia, and it is anticipated that more DI natural gas engines will be installed in heavy duty trucks for commercial operations. Emission control and fuel cost reduction are two major reasons driving the trend.

In recent years, the control of CO_2 emissions has become a hot issue. The signing of the Tokyo treaties, which proposed quotas for CO_2 emissions of industrial countries, attempting to address the global warming issue, signalled the beginning of an era of CO_2 emission control. Recently, France introduced a passenger car rebate/penalty system based on CO_2 emission. Under the system, a rebate will be offered to a purchaser of a car whose CO_2 emission is less than 130 g/km, and a penalty will be applied to a purchaser of a car whose CO_2 emission is more than 160 g/km. The European Commission has also proposed mandatory limits on CO_2 emissions from new passenger cars. Under the proposal, the average CO_2 emission from a new car of average weight 1289 kg in the EU would decrease from today's level of about 160 g/km to 130 g/km in 2012. The proposal imposes penalties on manufacturers. With conventional fuels, such as diesel or petrol, vehicle manufacturers have to either redesign their products to meet the limit, or pay the penalty. Both can be costly. The penalty for selling a vehicle of current CO_2 emission of 160 g/km will be €600 in 2012, and up to €2850 in 2015.

Replacing diesel and petrol with natural gas in IC engines will lead to an immediate reduction of CO₂ by about 20%, e.g. from 160 g/km to 128 g/km, without the need to redesign the vehicles. The control of CO₂ emissions can be a powerful driving force for manufacturers to produce vehicles with natural gas engines, but commercial applications of DI natural gas engines in passenger cars and light duty trucks still need further investment and government incentives.

8.6 Sources of further information and advice

More information about reserves and world production and consumption of oil and natural gas can be found in the following reports:

- Energy Information Administration, US DoE; website <http://www.eia.doe.gov/>
- International Energy Agency, an international forum for countries committed to advancing global energy security, policy and technology through co-operation; website <http://www.iea.org/>
- US Geological Survey, Department of the Interior; website <http://infotrek.er.usgs.gov/pubs/>

and in the *Oil & Gas Journal* (PennWell Corporation) and *World Oil* (Gulf Publishing Co.).

DI natural gas engines have found applications on commercial vehicles in the United States and in Australia. In August 2007, the South Coast Air Quality Management District of California approved US\$2.9 million to subsidize the deployment of 20 Kenworth T800 trucks powered by DI natural gas engines from Westport Innovations, Inc. at Port of Long Beach, as part of the initiatives to improve air quality in the port area [11]. In Australia, DI natural gas engines were installed in four Kenworth trucks (T4-T404 and T4085AR) for commercial operations by Mitchell Corporation, Sands Fridge Lines, and Murray Coulburn Co-operative under the Alternative Fuels Conversion Program of the Australian government [12]. More information about the developer and the supplier of the engines, can be found on the website <http://www.westport.com/about/index.php>.

Based on the CO₂ reduction system of the French government, the range of the rebate is from €1000 for cars with CO₂ emission below 100 g/km, to €200 for cars of 121–130 g/km; and the range of the penalty is from €200 for cars with CO₂ emission of 161–165 g/km, to €2600 for cars above 250 g/km. Buyers of vehicles rated at 130–160 g/km will neither receive a rebate nor pay a penalty. More information about the system can be found from the news release: ‘Le bonus écologique incitera dès aujourd’hui les acheteurs de voitures neuves à se porter vers les véhicules les plus sobres en carbone’, Ministère de l’Écologie, du Développement et de l’Aménagement durables,

Paris, 5 December 2007, <http://www.ecologie.gouv.fr/Le-bonus-ecologique-incitera-des.html>.

The European Parliament has proposed mandatory CO₂ emission limits from passenger cars and light commercial vehicles. The proposal sets a CO₂ limit equal to 130 g/km + 0.0457 × (vehicle mass – 1289 kg). Based on this proposal, a manufacturer has to pay a penalty based on the number of g/km of CO₂ emission from a vehicle sold by the manufacturer above the limit. A penalty of €20 per car per g/km of CO₂ exceeding the limit has been proposed in the first year (2012), gradually rising to €35 in the second year (2013), €60 in the third year (2014), and €95 in 2015. More information can be found from the proposal: ‘Setting emission performance standards for new passenger cars as part of the Community’s integrated approach to reduce CO₂ emissions from light-duty vehicles’, Proposal for a Regulation of the European Parliament and of the Council, Commission of the European Communities, Com(2007) 856 final, 2007/0297 (COD), Brussels, 19 December 2007.

8.7 References

1. Heinberg, R., ‘The view from oil’s peak’, *MuseLetter* No. 184, a joint publication with the journal *Public Policy Research*, August 2007; <http://www.ippr.org/publicationsandreports/?id=2385>.
2. Goto, Y., ‘Development of a liquid natural gas pump and its application to direct injection liquid natural gas engines’, *International Journal of Engine Research*, Volume 3, Number 2, pp. 61–68, 1 June 2002.
3. White, G.W. *et al.*, US Patent 5566712, 22 October 1996.
4. Hill, P.G., ‘Intensifier-injector for gaseous fuel for positive displacement engines’, US patent 5067467, 26 November, 1991.
5. *Annual Energy Outlook 2008, Energy Trends to 2030*, Energy Information Administration, Office of Integrated Analysis and Forecasting, US Department of Energy, February 2007.
6. *Oil & Gas Journal*, Volume 104.47, 18 December 2006.
7. USGS World Petroleum Assessment 2000, <http://pubs.usgs.gov/fs/fs-062-03/FS-062-03.pdf>.
8. *Oil Market Report*, International Energy Agency, 10 August 2007.
9. *International Energy Outlook 2007*, US Energy Information Administration, 2007.
10. ‘Natural gas hydrates – Vast resource, uncertain future’, USGS Fact Sheet FS-021-01, US Geological Survey, US Department of the Interior, March 2001.
11. ‘Heavy duty trucks to deploy at California ports’, *AltFuels Advisor*, August 2007.
12. ‘Direct response’, *Diesel*, pp. 66–67, November–December 2007.

J. D. PAGLIUSO, University of São Paulo, Brazil and M. E. S. MARTINS, Sygma Motors, Brazil

Abstract: Biofuels are an important alternative to reduce CO₂ emissions, improve fuel security and bring other environmental and economic benefits. For spark-ignition engines the only large-scale biofuel used today is ethanol, mostly in Brazil and the USA. It should be noted, however, that new sources of biofuels might become available in the near future. This chapter discusses the production and use of biofuels for spark-ignition engines, including sources, environmental impacts in both production and use of the fuel and engine operation and performance.

Key words: biofuels for spark-ignition engines, environmental impacts of biofuels production, environmental benefits in biofuels usage, performance and emissions of biofuels engines.

9.1 Introduction

Biogasoline can be understood as a liquid fuel for spark-ignition engines obtained from biomass, either vegetal or animal, or from wastes of both. In a strict sense it would exclude the alcohols once alcohols are typically oxygenated, in contrast with oil-derived fuels. However, alcohols, mainly ethanol, are by far the most used biofuels for engines today and so will be included in this chapter.

The main driving forces to use biofuels are that they are renewable, representing a kind of liquid solar energy. Depending on how they are produced, they contribute very little to carbon emissions and climate change. Moreover, their use is good for the local economy and they are more evenly distributed over the planet than fossil fuels. For countries with limited availability of oil they are a strategic option as well. According to IPCC [1], in 2004 road transport accounted for 74% of total CO₂ transport emissions, which in turn represented 23% of the world's energy-related CO₂ emissions. Biofuels could mitigate a significant fraction of these emissions.

Biofuels can be obtained from fermentation as, for example, in the large-scale ethanol production from sugar cane in Brazil [2,3] and corn in the USA [4]; by gasification, followed by a Fischer–Tropsch synthesis [5–7]; and by fast pyrolysis [5, 8]. Many other processes are under research and development.

The idea of using biofuels, in this case ethanol, as an automotive fuel is not new. In fact, ethanol was used in Europe as early as 1892 [9]. In America,

Henry Ford experimented with ethanol in 1914 and stated to the *New York Times* in 1925 that ethanol was ‘the fuel of the future’. On the other hand, the synthesis of fuels from gasification of solid or gaseous feedstocks, which is a route to the production of transportation biogasoline, was employed by Germany in the Second World War and is used today by Sasol in South Africa to produce gasoline and diesel from coal and natural gas. However, biomass gasification for liquid fuels is not being used as a feedstock on a significant scale so far [10], partly because of costs and partly because it is more heterogeneous and difficult to handle.

In Brazil, the country with the largest fleet fueled by ethanol, the first car reported as running on ethanol was a Ford that in 1925 ran for 230 km using hydrated ethanol with a percentage of water as high as 30% [11]. Average fuel economy was 20 liters per 100 km. Later, in the 1970s Brazil started an ambitious program for developing ethanol as an automotive fuel, which placed the country as a leader in this field. Today, about 75% of the 2.8 million light vehicles per year produced in Brazil are flex, meaning that they can use gasoline, ethanol or any mixture of them [12]. In fact, there is no pure gasoline in the country; the fuel sold at the pump contains 22–25% of ethanol.

Many other processes aimed at producing fuels for spark-ignition engines from biomass are under research and development. A few examples are enzymatic hydrolysis of cellulosic materials followed by fermentation; microorganisms able to deliver a diesel-like fuel instead of an alcohol; and conversion of butyric acid obtained from sugar fermentation to hexane [13]. Others include microorganisms that could produce ethanol from syngas (see Section 9.2.2); blends of glycerol (a by-product of biodiesel) with propanol, propanediol and gasoline [14]; and even conversion of dehydrated ethanol to biogasoline [15].

Some of these processes seem promising; some seem more difficult to be successful. Production of dehydrated ethanol is energy demanding, in fact dehydration is one of the most important factors that drops energy efficiency in US corn-based production, taking about 14% of the gross energy input in the process. Likewise, conversion of dehydrated ethanol to biogasoline surely takes some extra energy, dropping energy efficiency still further. Finally, in small fractions, ethanol can be mixed easily with gasoline without any deleterious effect for the engine and even benefiting the environment.

As the concerns with climate change and the limited supply of oil increase, so does the research on transportation fuels from biomass. At a time of fast and diversified developments, surprises may lie ahead.

9.2 Types and sources of biofuels

9.2.1 Fast pyrolysis

Fast pyrolysis is the thermal decomposition of matter in the absence of oxygen. It yields solids (char), liquids and gas. Usually liquid is the main target for this process, which can deliver 65–75% of the dry original fuel in this form. The liquid, known by a variety of names, including bio-oil, is a viscous and oxygenated substance that contains some solids (char) and water and has a low calorific value (about 50% of that of gasoline). It is also chemically unstable and has an oxygen content as high as 40 wt%.

The composition of bio-oil from pyrolysis includes a large number of alcohols and carboxylic acids. In its complex composition, bio-oils resemble more fossil fuels than the fuels obtained from biomass distillation, in the sense that these are usually pure substances with only a fraction of water.

The fuel can be upgraded and used as a transportation fuel by mixing it with ethanol or methanol or by means of other chemical or thermal processes, including gasification and Fischer–Tropsch synthesis. Hot filtration brings some benefits as it removes most of the char but it also decreases the liquid yield as the vapors are cracked when they pass over the char retained in the filter.

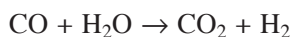
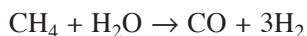
A review of fast pyrolysis fuel can be found in Bridgwater *et al.* [8]. At the moment bio-oils obtained from fast pyrolysis do not seem to be an economically feasible source of biogasoline.

9.2.2 Gasification

Gasification is a process of partial oxidation of a fuel that delivers a gas, usually rich in CO and H₂, with smaller amounts of CH₄. This gas can be used as an energy source through its direct combustion, as a chemical feedstock (syngas) to produce liquid fuels and other chemicals through the Fischer–Tropsch (FT) process or a combination of both, in order to improve energy efficiency. Gasification agents can be air, oxygen, steam or a combination of them.

To produce liquid fuels from biomass the steps are pre-processing, gasification, cleaning and conditioning of the gas, application of the FT synthesis, and finally upgrade and refining of the product. The Fischer–Tropsch process is catalytic and requires a very clean gas, free from sulfur, tars, ammonia, dust and some other contaminants to avoid catalyst poisoning [16]. Nitrogen is also not accepted by the FT process, so the bio-syngas for liquid fuels must be produced with oxygen as oxidant or with steam and an indirect heating source. Although methane is good for thermal use of the gas since it improves its calorific value, it must be kept at a minimum for fuel synthesis.

An approximate syngas composition is given in Table 9.1. The CO/H₂ ratio in the syngas is an important parameter as well, and may have to be adjusted in order to obtain the desired product. Methane and hydrogen concentrations may be adjusted using the steam reforming and water gas shift reactions:



The economic feasibility of the gasification route to produce liquid fuels is still controversial today and most of the biomass to liquid gasification plants are pilot or demonstration facilities [10], but it seems that as oil prices increase and climate change concerns grow, a point will be reached where it will be a profitable activity.

A proposal has been made [17] to enrich the syngas with external H₂ and use H₂ as a fuel for the gasification process. H₂ would come from windmill, nuclear and other possible sources. The authors estimate that under this scenario the 1.36 billion dry tons per year of biomass that could be available in the USA without displacing other crops or natural habitats would be able to replace all the oil consumption of that country.

Ethanol from cellulose, i.e. from materials like sugarcane bagasse and other leftovers, is a promising route to obtain additional biofuel and to improve overall energy efficiency. Although many processes for cellulosic ethanol are being investigated and developed, none has yet achieved commercial operation, and gasification followed by the FT process is presently a promising alternative since the technology already exists.

9.2.3 Fermentation and distillation

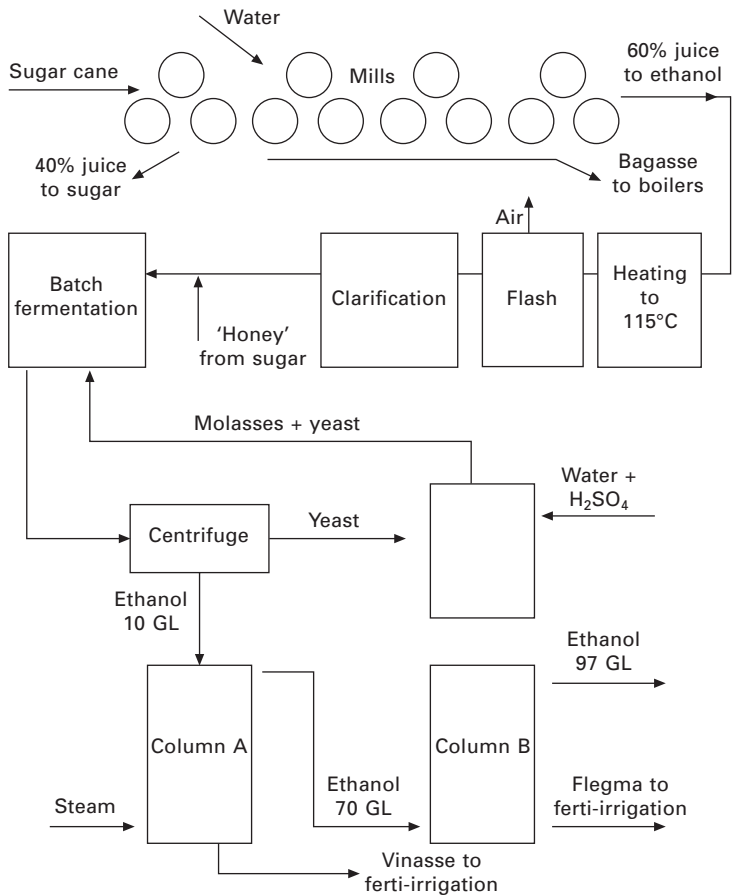
Fermentation and distillation is perhaps the most frequently used process for biofuel production, and ethanol is its most important product. Several crops can be used, such as sugar cane, corn, beetroot, wheat and sorghum, depending on where on the planet the raw material is cultivated. The largest producers are Brazil (sugar cane) and the USA (corn). In Brazil this process has been used since the 1970s to power cars with dedicated engines, either

Table 9.1 Approximate composition of typical syngas

Component	% dry volume
Methane, CH ₄	5
Hydrogen, H ₂	25
Carbon monoxide, CO	40
Carbon dioxide, CO ₂	25
Other	5

pure or blended 22–25% with gasoline. More recently, its use has increased again through the advent of flex-fuel vehicles (FFVs). Today Brazil has about 30 000 gas stations that can fuel cars with ethanol all over its territory [2] and produces about 17 million cubic meters of ethanol per year. About 75% of the new spark ignition vehicles are flex-fuel [12], meaning that they can use any mixture of ethanol and gasoline. The use of flex vehicles has the additional – and very important – benefit of stabilizing the biofuel market.

Ethanol production from sugar cane is often associated with sugar production. The first step in the process is the reception and washing of the cane that is sent to the mills, usually using six sets of three rolls (Fig. 9.1), where it is smashed to extract the juice. The first set of rolls delivers about 40% of the total juice, generally used to produce sugar; the remaining rolls



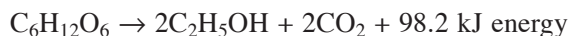
9.1 Simplified flow diagram for sugar cane based ethanol production in Brazil.

receive an addition of water to facilitate extraction, and this juice is used to produce ethanol.

Bagasse is extracted at the end of the mill and sent to the boilers that will produce electricity and steam for the process. This way, no external input of energy is required. There is a bagasse surplus of about 15% that is sold, but changes in the process could easily increase this amount and make more energy available.

The juice is first heated and flashed to eliminate bacteria and air, and then sent for clarification to complete the cleaning process. This ensures that unwanted microorganisms will not compete with the yeast for the sugars.

After treatment, the juice is blended with about 10% ‘honey’, a sugar-rich by-product of sugar production, and it then goes to the fermentation tanks where it is mixed with molasses and yeast. The fermentation process is done in batches and lasts about 12 h, so to keep ethanol production continuous, several fermentation tanks are used. During this process, sugars are broken up according to the following reactions:



These produce ethanol and CO_2 , this last being released to the atmosphere. The fermentation process is exothermic and cooling must be used.

After fermentation, the material is sent to centrifuge separators where yeast is separated from the ‘wine’ (ethanol 10 GL). Yeast is sent back to tanks where it is recovered with water and sulfuric acid, whereas the ‘wine’ follows the distillation columns, leaving column ‘A’ with 70 GL and column ‘B’ with 93 GL, ready to be used in ethanol or flex-fueled engines. Columns A and B produce a liquid waste (vinasse or stillage), rich in organics, that is used as a fertilizer to irrigate the land (ferti-irrigation).

There are some concerns about the use of ethanol as a transportation fuel that deserve some discussion. Economics, including costs and subsidies, is one of them. At least in Brazil there are no subsidies to ethanol production. Although this activity is clearly profitable in Brazil, consumers pay for ethanol about US\$0.60 per liter (average national cost, 2008), that is, half the price of gasoline. The user spends from US\$0.04 to US\$0.10 per km traveled, depending on the vehicle used. The cost of ethanol energy for the consumer is about US\$0.02 per MJ.

Greenhouse gas emissions are another important point, mainly the carbon dioxide (CO_2) balance. It is important to say that CO_2 emissions from the biomass itself, no matter whether it is caused by the fermentation process, biomass burning in the field or the use of the fuel in the engine, is carbon neutral, if the crop needs the same amount of CO_2 taken from the atmosphere to grow next year. However, some gaseous emissions in the field, such as

methane and N_2O , are not compensated, nor are the emissions that come from fossil fuels used in the process or from the use of indirect sources of energy and materials.

Macedo *et al.* [18] produced a comprehensive LCA (life cycle assessment) study for ethanol production in Brazil that included sources of greenhouse gases as diversified as external fuels, fertilizers, lime, seeds, herbicides, sulfuric acid, lubricants, and energy for the manufacture, construction and maintenance of equipments and buildings. Table 9.2 shows the results for two scenarios. Scenario 1 is for average consumption of energy and materials and Scenario 2 is for best values being practiced today.

In both scenarios, greenhouse gas emissions quantified as CO_2 equivalent are negative if the avoided emissions, brought by the substitution of gasoline by ethanol and of oil by surplus bagasse, are taken into account. On a fuel basis the avoided emissions are 2.6 and 2.7 kg/L of anhydrous ethanol (Scenarios 1 and 2 respectively), and 1.7 and 1.9 kg/L for hydrous ethanol.

It is worth noting that the largest shares of CO_2 equivalent emissions in Table 9.2 are fossil fuels, used in trucks and agricultural machinery (19 and 17 kg/ton) followed by methane due to the burning of sugar cane, that is still partially practiced before harvesting (about 9 kg CO_2 /ton of cane for both scenarios), and N_2O emissions, from the use of fertilizers. The first could be

Table 9.2 CO_2 emissions and avoided emissions in ethanol production and use

	Average (kg CO_2 e/t)*	Best values (kg CO_2 e/t)*
<i>Emissions</i>		
Fossil fuels	19.2	17.7
Methane and N_2O from field burning	9	9
Soil N_2O	6.3	6.3
Total emissions	34.5	33
<i>Avoided emissions</i>		
Surplus bagasse	12.5	23.3
Ethanol use		
average consumption of energy	242.5(A)	259.0(A)
best values	169.4(H)	180.8(H)
<i>Total avoided emissions</i>		
average consumption of energy	255.0(A)	282.3(A)
best values	181.9(H)	204.1(H)
<i>Net avoided emissions</i>		
average consumption of energy	220.5(A)	249.3(A)
best values	147.4(H)	171.1(H)

* kg of CO_2 equivalent per ton of sugar cane processed; anhydrous ethanol, (H) hydrous ethanol.

Source: adapted from [17].

avoided by using heavy duty ethanol engines that are under development by a few companies. Methane emissions are decreasing fast and should disappear within a few years because mechanical harvesting is quickly taking over from manual harvesting, so burning will become unnecessary.

The main reason for such a favorable situation regarding CO₂ emissions is that sugar cane produces a large amount of bagasse that holds about one-third of the total energy in the crop. This bagasse is burned in boilers producing all the electricity, heating and mechanical power needed by the process and a surplus of bagasse and electricity that can be sold. External direct energy comes only as diesel fuel, used for trucks and agricultural machinery. In the USA the situation is not so favorable, although it is still positive [4]. The main reason is that corn produces much less bagasse, so fossil energy inputs are higher.

Some alternatives to improve the energy balance of corn ethanol have been proposed, such as the use of HCCI engines that would be able to operate with 65% wet ethanol [19]. The present net energy is about 21% (6% ethanol, 15% co-products) but this could be raised to 55% (40% ethanol, 15% co-products), reducing energy use in distillation and eliminating energy in dehydration. On bench tests, conventional spark-ignited engines can run on 22% wet ethanol with no drop in efficiency or perceptible problems in transient regimes [20], just by increasing the compression ratio.

The ratio of bioenergy output to fossil energy input changes according to the crop used for ethanol production, but is by no means negligible. Table 9.3 shows the results for a few crops. It is worth noting that the sugar cane ratio of 8.9 can reach 11 or even more, as new plants are constructed and old ones rebuilt using higher-pressure boilers, able to deliver more efficiently so that bagasse and wastes currently not used or left in the field could be employed to produce additional fuel and power. Gasification and enzymatic hydrolysis are two routes for this. In just four Brazilian states, currently (2008) there are 210 projects with conventional technology that together have a potential to deliver 10.2 GW to the grid – equivalent to the output

Table 9.3 Ratio of bioenergy output to fossil energy

Raw material	Bioenergy output/fossil energy input
Corn (USA)	1.3
Sugar cane (Brazil)	8.9
Beetroot (Germany)	2.0
Sweet sorghum (Africa)	4.0
Wheat (Europe)	2.0
Cassava	1.0

Source: adapted from [21].

of Itaipu, the largest hydropower plant in Brazil and the second largest in the world [2].

The potential competition between biofuels and food and the devastation of forests to cultivate crops for biofuels are often mentioned as an obstacle to use liquid biofuels. However, as some authors point out [22], the price of corn affects the price of some food, but the price of fuels affects practically everything we eat, as it has impacts on cultivation, harvesting, processing, transportation and storage. Biofuels are a way to slow down the increasing cost of oil-derived fuels. An extensive analysis on liquid biofuels production and its impacts on sustainability can be found in Reference [23].

Another point is the misconception that the production of biofuels will necessarily destroy native forests. In Brazil the present (2008) production is 17 million cubic meters, delivered by 310 existing industrial plants and enough to supply half of the fuel used for the approximately 20 million light vehicles in the country [24]. Moreover, the prospects for future growth are high: production should double by 2012/13 [2] with the start-up of 77 new plants under construction in the southeast.

However, the cultivated area for current ethanol and sugar production is about 7 million hectares, which represents only 0.8% of the country's 850 million hectares or 2% of its arable land, while worldwide arable land for fuel accounts for only about 1% of all arable land [25]. Compared with the 210 million hectares destined for pastureland, the area for ethanol and sugar is only 3%. Considering that today half of the spark-ignition fuels used in the country are ethanol, if only 3% of the pastureland area were converted to produce ethanol and sugar, the total production would be enough to fuel the entire fleet of light vehicles in Brazil. If the share of sugar production in the new plants is reduced (today it is about 50%), less land would be necessary.

9.3 Performance

9.3.1 Fuel economy, torque and power

Alcohol-based fuels or fuel blends are currently being discussed as potential substitutes for fuels from crude oil. For SI engines, the main alcohols used are methanol and ethanol, with a much smaller proportion of butanol. Table 9.4 lists some properties of these alcohols as well as gasoline and iso-octane.

Alcohols and, more specifically, methanol have a long-established reputation as racing fuels [26]. On the other hand, ethanol, as a consequence of the phasing out of leaded fuel, became popular as an octane enhancer, replacing benzene and other toxic chemicals often used by refiners and proving to be a valuable additive to mid- to low-octane gasoline [27]. Both ethanol and methanol have been blended with gasoline. At the present time, the most

Table 9.4 Properties of alcohol fuels, gasoline and iso-octane

Property	Methanol	Ethanol	Butanol	Gasoline	Iso-octane
Chemical formula	CH ₃ OH	C ₂ H ₅ OH	C ₄ H ₉ OH	Various	C ₈ H ₁₈
Density (kg/L)	0.79	0.79	0.81	0.74	0.69
Viscosity (cP)	0.64	1.08	3.64	0.4–0.8	0.51
Lower heating value (MJ/kg)	19.9	26.8	37	42.7	44.3
Stoichiometric AFR	6.5	9	11.2	14.7	15.1
Specific energy (MJ/kg air)	3.06	2.98	3.30	2.90	2.93
Specific energy ratio	1.044	1.015	1.126	0.990	1.000
Volumetric energy content (MJ/L)	15.72	21.17	29.97	31.60	30.57
Research octane number	106	109	96	95	100
Motor octane number	92	98	78	85	100
Latent heat of vaporization (kJ/kg)	1170	930	430	180	270
Oxygen content by weight (%)	50	34.8	14.6	0	0
Mole ratio of products to reactants	1.065	1.061	1.067	0.937	1.058
Reid vapor pressure (bar)	0.17	0.16	0.02	0.56	0.14
Boiling point (°C)	64.7	78.5	117.2	30–190	99.8
Stoichiometric CO ₂ emissions, (g _{CO₂} /MJ _{fuel})	69	71.2	68.8	71.9	69.7

common choice for blending with gasoline is, however, ethanol. In fact, in today's fuel market, methanol and ethanol are the only commercially viable [28] alcohols used for blending. In comparison, butanol is still too expensive, although intensive research is under way to lower production costs, mainly because butanol offers some advantages concerning evaporative emissions (due to its low vapor pressure) and also heating value [29]. This is due to the longer carbon chain that makes butanol more like gasoline, though butanol loses some of the advantages of shorter carbon alcohols such as high latent heat of evaporation and high octane number.

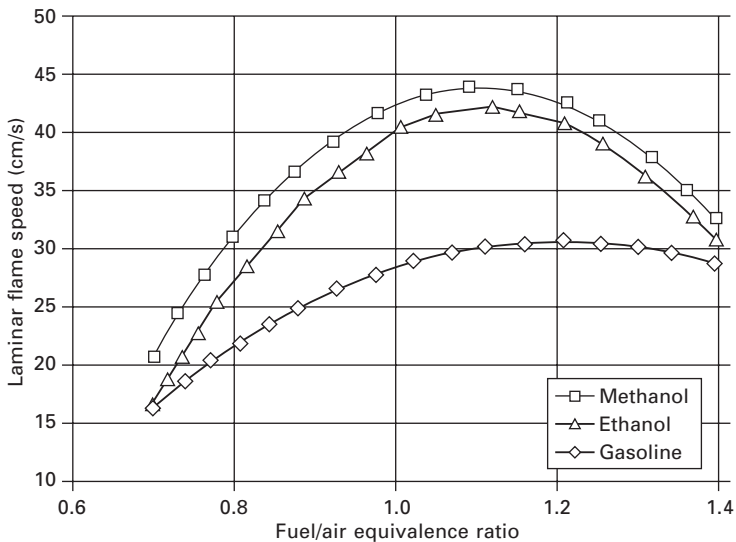
Alcohols, more specifically ethanol and methanol, have been used in pure form or as blends with gasolines, such as M85 or E85, where M and E stand for methanol and ethanol and the number following is their concentration by volume into gasoline. In countries like Brazil, for instance, hydrated ethanol with 6–7% water content is also used as fuel, and is often designated as E94h, although sometimes it is referred to as just E100.

Compared to gasoline, despite their lower calorific values (Table 9.4), short carbon chain alcohols tend to produce more power due to the following factors:

- *Lower stoichiometric air–fuel ratio.* Due to their intramolecular oxygen content, alcohols demand less oxygen for complete combustion. This leads to lower stoichiometric air–fuel ratios when compared to gasoline,

which means a higher specific energy, i.e., the amount of energy that can be generated per kg of inducted air.

- *Higher latent heat of vaporization.* Alcohols have a substantially higher latent heat of vaporization than gasoline. This enables a high evaporative charge cooling that increases volumetric efficiency. Also, by reducing the initial charge temperature, the knock limit can be expanded, allowing for further improvements in power. Furthermore, the reduction of charge temperature means that less compression work is needed, again benefiting, cycle efficiency and power.
- *Higher octane rating.* The higher octane rating of ethanol enables higher compression ratios to be used with optimum spark advance, a fact that improves both full-load performance and efficiency. In the case of ethanol, it is reported that increases in compression ratio of 2 to 4 units are possible [30]. It also benefits the exploitation of forced induction (turbocharging or supercharging) with higher boost pressures.
- *Higher laminar flame speed.* Alcohols offer significantly higher burning velocities than paraffins, Fig. 9.2, allowing more efficient power development [31–34] due to the reduction of negative work (less ignition advance is needed for the same angle of peak pressure). This fact also gives them the ability to burn at rich mixture strengths, which coupled with their high latent heat of vaporization yields further increase in volumetric efficiency.
- *Mole ratio of products to reactants.* The combustion of alcohols generates



9.2 Laminar flame speed of M100, E100 and gasoline as a function of fuel–air equivalence ratio (1 atm, 300 K), adapted from [32].

a larger volume of combustion products, which allows the development of higher cylinder pressures and potentially higher power output. In fact, despite the expansion promoted by the heat released by combustion, alcohols show a slight molar expansion during combustion, whereas gasolines, generally show a contraction (Table 9.4).

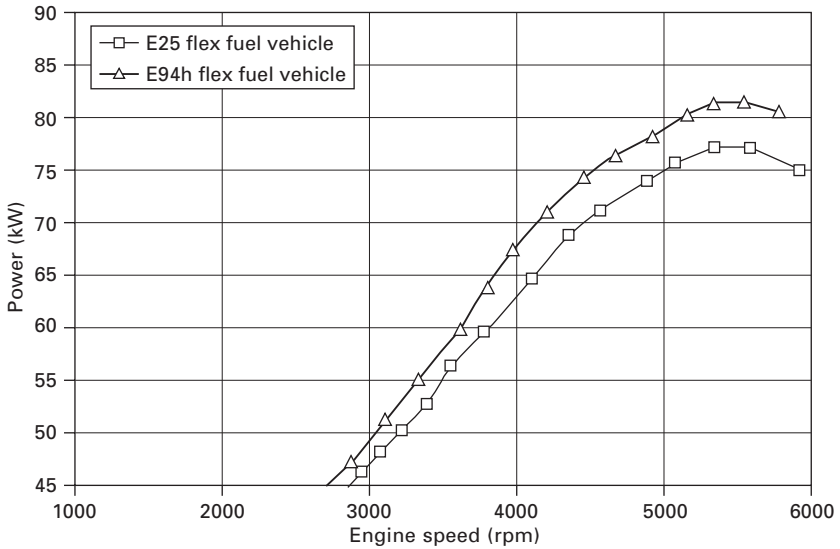
Fuel consumption, in itself is not an issue unless it severely limits vehicle range. The important points are the environmental and financial costs of running the vehicle. With ethanol, the range is not significantly affected. Everything else being the same, the range with ethanol is about 30% less than that with gasoline. However, the following points should be observed:

- Owing to the low volumetric energy content of alcohols, engines fueled with them tend to show higher volumetric fuel consumption.
- Alcohols have better anti-knock properties that allow the use of higher compression ratios and/or boost levels than gasoline, increasing efficiency and therefore benefiting fuel consumption.
- Alcohols burn with lower flame temperatures and luminosity, hence less heat is lost by convection and radiation to the cooling system, benefiting efficiency.
- Alcohol-fueled forced inducted engines are able to run with higher boost levels than with gasoline, enabling more aggressive downsizing concepts, which in turn, due to engine friction reduction and a decrease in total vehicle weight, lead to even lower vehicular fuel consumption.
- If forced induction is done by means of a turbocharger, alcohols offer even more benefits due to lower exhaust temperatures when compared to gasoline combustion, a fact that improves turbocharger life and increases efficiency by avoiding or reducing the need for full-load enrichment to cool down the turbine.
- Due to the anti-knock properties of alcohols, less enrichment at full load is needed to avoid knock and to lower exhaust temperatures.

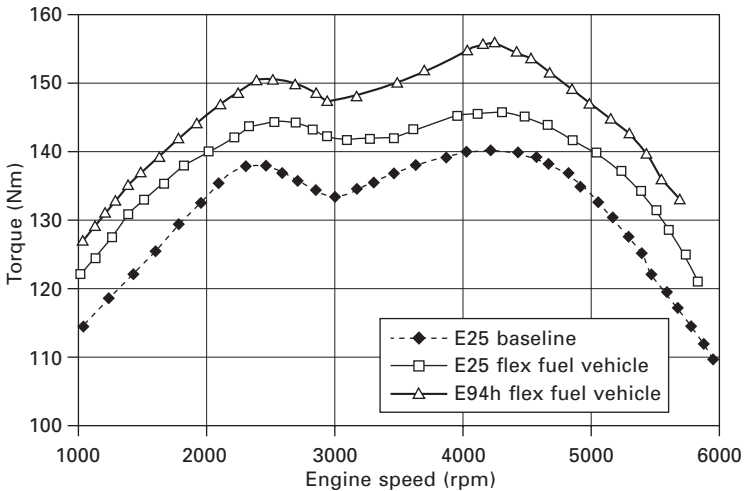
Improvements in thermal efficiency with alcohols that can go up to 16% have been reported in several publications [30–42].

However, to make appropriate use of some beneficial properties of alcohols and increase efficiency, engines must be specially designed or optimized for them [35]. These benefits, however, tend to be less noticeable when alcohols are used in blends with gasoline, whether to solve cold start issues for the former (E85, M85) or as anti-knock additives of the latter (E25).

Figure 9.3 shows power figures for a flex-fuel 1.6 litre engine supplied to the Brazilian market when fueled with E25 and E94h. There is an improvement up to 6% in power of with E94h. Figure 9.4 shows torque figures for the same engine in its flex-fuel version compared with the original, baseline gasoline (referred as E25) engine. Torque values are higher overall and also show a 6% maximum improvement [35].



9.3 Power comparison between alcohol (E94h) and gasoline (E25), 1.6 liter engine, 4 cylinder, spark-ignited, compression ratio = 12.3:1, adapted from [35].



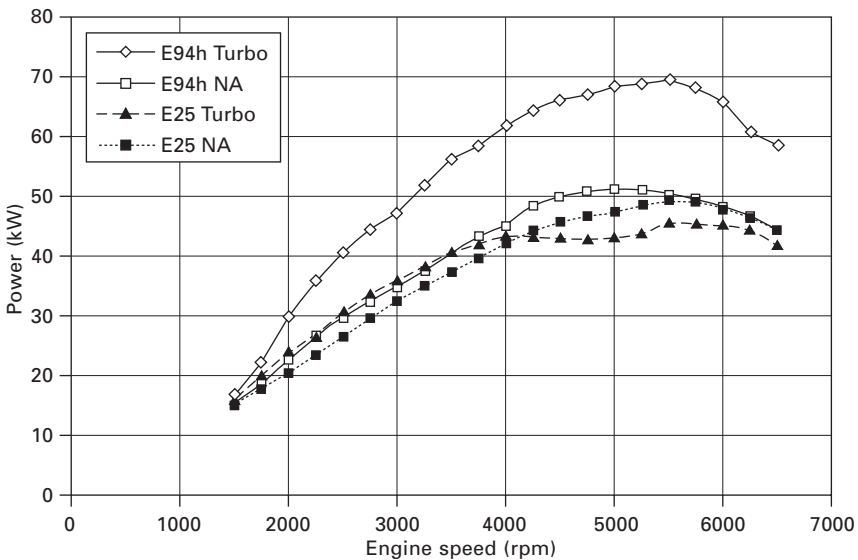
9.4 Torque comparison between alcohol (E94h) and gasoline (E25) flex fuel engines and gasoline (E25) dedicated engine, 1.6 liter engine, 4 cylinder, spark-ignited, compression ratio = 12.3:1, adapted from [35].

In terms of power, fuels with a high content of alcohols in gasoline offer significant benefits, as can be seen from Figs 9.4 and 9.5 which show test data from a 1.3L automotive engine, spark-ignited with an 11:1 compression ratio, tested with E25 and E94h [39,40]. If one compares the power of both naturally aspirated versions, it can be noticed that torque and power are substantially higher with E94h for the majority of the speed range (Fig. 9.5).

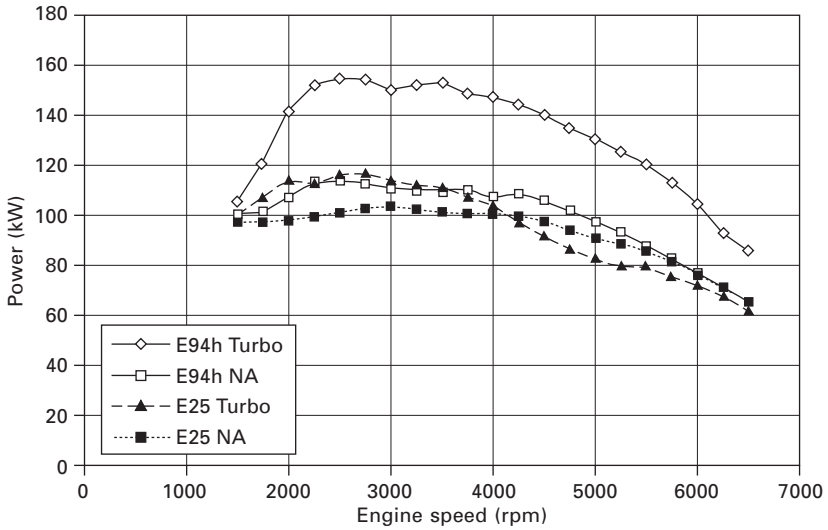
Forced inducted engines offer significant benefits when running with high ethanol content blends, as can also be seen from Fig. 9.5. The performance difference between the turbocharged versions with E25 and E94h is remarkable. Peak power is around 40% higher, whereas torque (Fig. 9.6) shows more than a 30% improvement for the majority of the speed range.

Looking again at the two E25 fueled engines, in comparison to the naturally aspirated version, it can be observed that the turbocharged version showed a lower power output at high speed, mainly due to the retarded ignition timings needed to avoid knock [39,40]. This obviously has an impact on efficiency and therefore fuel consumption, as is evident in Fig. 9.7 where a clear increase in BSFC happens above 4000 rpm, also due to the WOT enrichment needed.

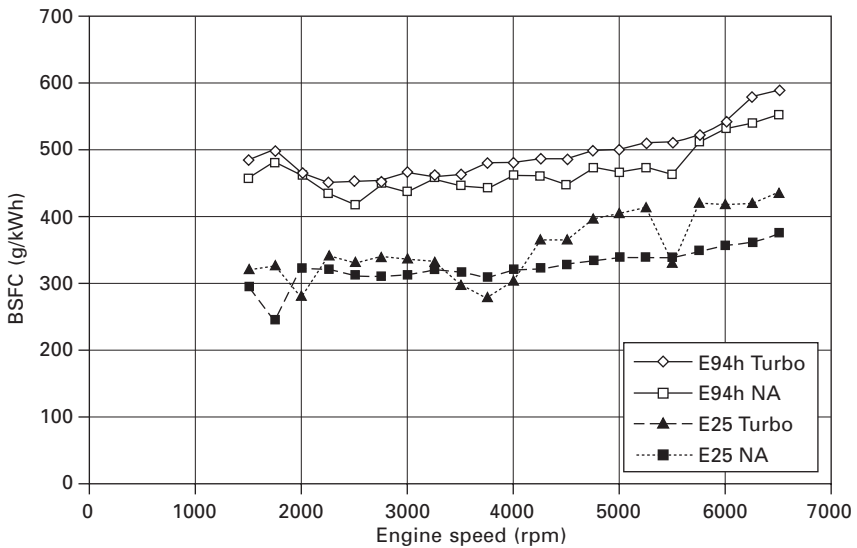
Figure 9.8 shows the efficiency increase of E94h over E25 for the engine in naturally aspirated operation, with an average improvement of 8%. It



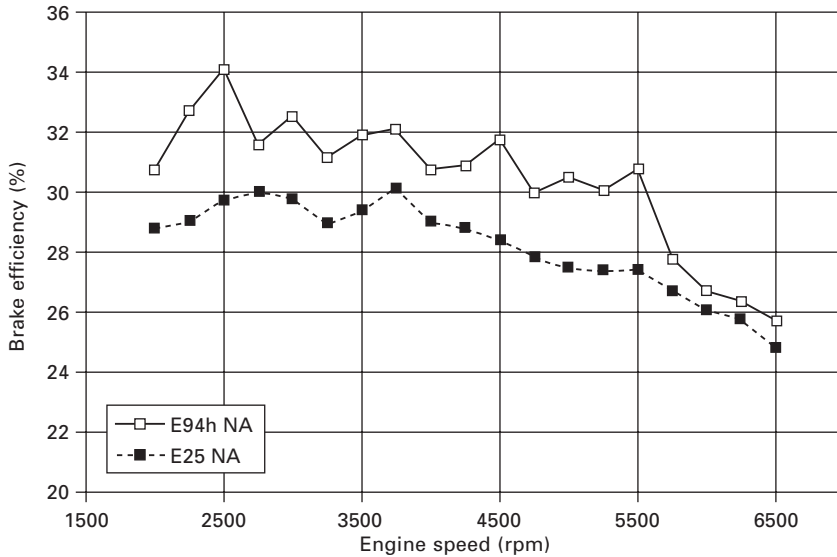
9.5 WOT power curves of a 1.3L engine, with compression ratio of 11:1, fueled with E25 and E94h, in naturally aspirated and boosted operation, adapted from [39,40].



9.6 WOT torque curves of a 1.3L engine, with compression ratio of 11:1, fueled with E25 and E94h, in naturally aspirated and boosted operation, adapted from [39,40].



9.7 Brake specific fuel consumption of a 1.3L engine, with compression ratio of 11:1, fueled with E25 and E94h, in naturally aspirated and boosted operation, adapted from [39,40].



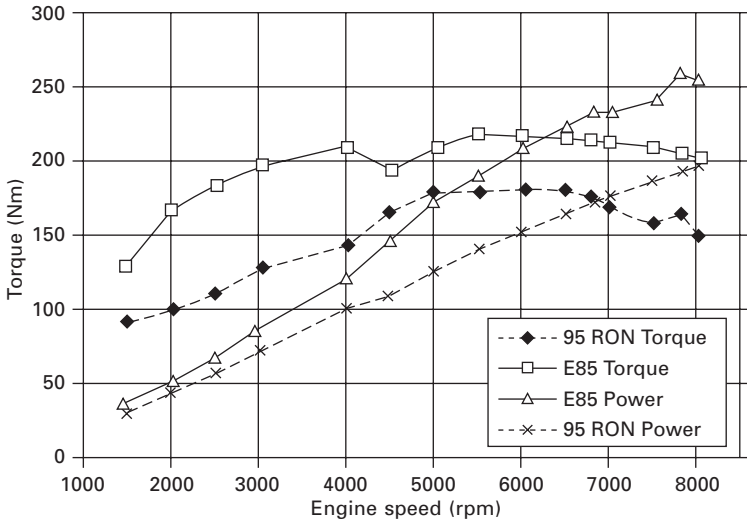
9.8 Brake efficiency of a 1.3L engine, with compression ratio of 11:1, fueled with E25 and E94h, in naturally aspirated operation, adapted from [39,40].

should be pointed out that the engine was essentially the same with only calibration changes for each fuel.

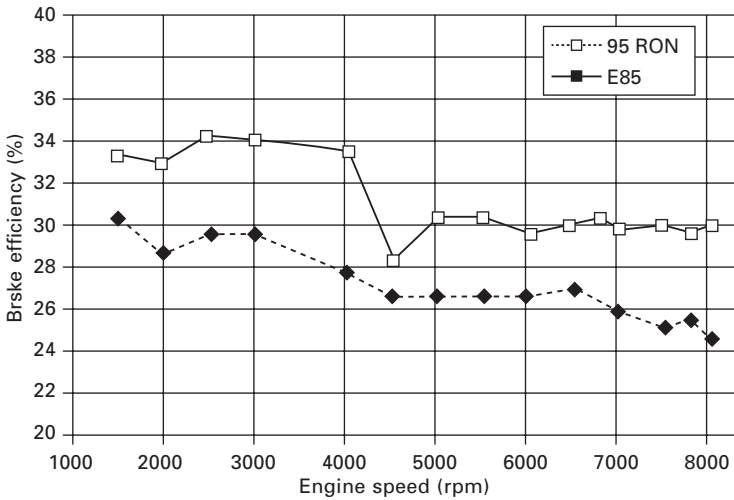
High alcohol content fuels are obviously very suitable for high performance sports car engines, as can be seen in Fig. 9.9, which shows performance data for a sports car engine fueled with E85 vs. 95 RON gasoline. A remarkable improvement in both torque and power is evident when using E85 fuel. Figure 9.10 shows, for the same engine, efficiency figures with both fuels. An efficiency increase of up to 9% is shown [41].

Vehicles running on alcohols, due to the better efficiency of their engines, can help to reduce CO₂ to an appreciable extent. This is further enhanced by the fact that alcohols such as methanol, ethanol and butanol have a higher H/C ratio than gasoline (4, 3, 2.5, and 1.8, respectively). Jeuland *et al.* [42] reported a reduction of 9% in CO₂ emissions, in comparison to gasoline, in the same engine, when using ethanol during the New European Drive Cycle. These figures do not take into account the fact that alcohols are often produced from growing biomass, which further lowers CO₂ emissions.

Biofuels such as ethanol have important potential in reducing well-to-tank CO₂ emissions. In fact, CO₂ emissions became a key parameter when designing new engines, especially after the commitment taken by ACEA with the European Union to decrease CO₂ emissions of the fleet down to 140 g/km in 2008 and to 120 g/km in 2012 [43], making alcohols and especially ethanol very desirable for new and more efficient engines.



9.9 Comparison of performance: E85 v 95 RON unleaded gasoline, adapted from [41] FTP75 test cycle.



9.10 Efficiency comparison: E85 v 95 RON unleaded gasoline, adapted from [41].

Alcohols offer, indeed, very good potential for engine downsizing by suitably exploring their properties. Furthermore, very high efficiency figures are claimed when more advanced combustion modes are used. Engines running with a very high compression ratio and EGR-diluted charge to

control knock, in stoichiometric operation, are able to achieve efficiencies exceeding those of similar diesel engines while still keeping emissions to appropriate levels.

The high EGR tolerance of alcohols is a key feature to make possible the operation with high compression ratios. In addition, the ability to sustain combustion with very high levels of EGR increases the ratio of specific heats (γ). Both parameters can increase cycle efficiency [44].

Brusstar *et al.* [32,33] reported that brake thermal efficiencies of 43% with methanol and 41% with ethanol could be achieved in a PFI spark-ignited engine with 19.5:1 compression ratio, with EGR amounts up to 50%, when the baseline diesel engine showed only up to 40% efficiency.

The benefits of alcohol-based fuels can be further enhanced if direct injection is used. Successful combustion is achieved, despite the little time available for proper mixing (due to the small time window between injection and firing) and the lower volatility of alcohols. Furthermore, direct injection allows the full potential of alcohol-based fuels to be explored when it comes to volumetric efficiency. Direct injection of alcohols also shows higher thermal efficiency and lower exhaust emissions than that of gasoline during part-load operation [45–47].

Concerning ethanol, efficiency gains are also possible with the use of air-assisted direct injection. This also enables the use of wet ethanol, which is desirable from the point of view of lifecycle inventory. Ethanol with several degrees of hydration can be successfully burnt due to the improved mixture offered by air-assistance [48–50].

Alcohols also offer great potential when it comes to even more advanced combustion modes such as CAI or HCCI. They lead to expansion in load range, increased efficiency and lower emissions when compared to gasoline in this combustion mode [51]. Also, due to the nature of CAI combustion, i.e. with no flame propagation, combustion can happen in situations otherwise impossible in a normal SI combustion mode. Thus, CAI also offers the potential to use highly hydrated alcohols while still showing good efficiency values [52].

9.4 Emissions

9.4.1 Alcohols and blends with gasoline

Biofuels have a wide range of properties regarding their impact on the environment and health. The two most common alcohols, methanol and ethanol, are good examples. Ethanol has little or no direct adverse effect; in fact, it is used in medical care and alcoholic beverages. The concern that being massively and cheaply produced for fuel it might encourage alcohol addiction, by direct use from the pump, in beverages, could be an

issue. To avoid such a danger, when sold at the pump, ethanol is usually denatured, i.e., mixed with a small amount of gasoline that prevents human consumption. Moreover, ethanol is biodegradable and so leakage from tanks is of minor concern. On the other hand, methanol may be lethal if ingested and contaminates the water table if it leaks from storage tanks. It was used as an oxygenating additive for gasoline in the United States.

In addition to their role as fuels, both ethanol and methanol have a beneficial environmental aspect as they can be used as anti-knocking additives to gasoline, so avoiding the use of tetraethyl lead, a poisonous compound, for the same purpose.

Due to the relatively new increase in alcohol-fueled vehicles, there is not a very large repository of information about them, especially in the case of butanol, which is why this section will concentrate on methanol and ethanol and their blends with gasoline. Furthermore, the information about such fuels is often related to prototype or modified engines, some of them rather old, lacking the modern engine control and aftertreatment systems that would surely provide better emission results. As a starting point, however, the following information might be useful.

The influence of alcohols in exhaust emissions can be summarized by the following factors [53]:

- Reduced stoichiometric air/fuel ratio, making the charge leaner if closed-loop mixture control is not used
- Changes in fuel distribution due to the different evaporative characteristics of alcohols
- Lower charge temperatures due to evaporative cooling
- Higher gas specific heat and charge mass when closed-loop air/fuel ratio control is applied, which gives reduced combustion temperatures
- Different combustion chemistry, changing composition, reactivity and toxicity of exhaust gases
- Changes in combustion rate, modifying pressure and temperature histories in the engine cycle
- Presence of oxygen in the alcohol molecule, and consequently in the core of the spray, improving combustion efficiency and lowering emissions.

The addition of alcohols to gasoline can lead to substantial reduction of regulated emissions. CO can be reduced by up to 75%, HC up to 40% and NO_x up to 50% [53].

Furthermore, gasoline blends with either methanol or ethanol can offer different behavior concerning evaporative emissions since they tend to form azeotropes, with significant changes in Reid vapor pressure when compared to reference gasoline (Table 9.5) and even higher when compared to gasoline with other compositions (Table 9.4). This may be an issue, concerning

Table 9.5 Reid vapor pressure comparison between M85, E85 and California Phase 2 reformulated gasoline (RFG)

Fuel blend	M85	E85	RFG
	85% methanol 15% RFG	85% ethanol 15% RFG	100% RFG
Reid vapor pressure (bar)	0.75	0.62	0.69

Source: adapted from [54].

Table 9.6 Fleet-averaged change in FTP emissions with M85 in FFV

Regulated tailpipe emission	Change with M85
CO	-17%
NO _x	+3%
NMHC	-30%

Source: adapted from [58].

evaporative emissions. Such behavior, however, is not exhibited by butanol, which has vapor pressures lower than that of gasoline.

The tendency to show lower NO_x emissions, due to lower flame temperatures, is less noticeable, however, if the engine is optimized for burning alcohols. This would normally mean increased compression ratios and higher cylinder temperatures, yielding a possible increase in NO_x emissions.

The intramolecular oxygen content of alcohols promotes cleaner and more complete combustion, leading to lower CO emissions. However, as mentioned previously, this is, sometimes more a consequence of a leaner charge, due to the lack of closed-loop mixture control, than of the oxygen content in the molecule. Reduced HC and increased aldehyde emissions are also reported [54–56].

The low temperature combustion of alcohols, added to the fact that engines designed for them can have higher compression ratios, tends to cause low exhaust temperatures, which can adversely affect the catalyst efficiency, mainly during start-up [57]. Thus, strategies to improve catalyst light-off strategies might be necessary.

9.4.2 Methanol

Methanol is often used as a blend with 15% gasoline, referred to commonly as M85. Pure methanol applications are very rare, mainly because they would impose cold-start challenges.

Tables 9.6 and 9.7 show FTP regulated and toxic emissions of fleet-averaged results for flexible fuel vehicles (model year 1992–93) running on

Table 9.7 Fleet-averaged toxic emissions with M85 in FFV

Toxic emission	California Phase 2 RFG (mg/mile)	M85 (mg/mile)
Benzene	6.0	3.0
Formaldehyde	1.6	17.1
Acetaldehyde	0.4	0.5
1,3-Butadiene	0.6	0.10
Total	8.6	20.7

Source: adapted from [58]

Table 9.8 Comparison of emission levels between E25 and E100 during FTP 75 test cycle

	Brazilian legal requirement	Gasohol (E25)	Alcohol (E100)
CO (g/km)	2	0.29	0.17
NO _x (g/km)	0.6	0.14	0.16
HC (g/km)	0.3	0.09	0.14
Aldehyde (g/km)	0.03	0.012	0.019
Evaporative emissions (g/km)	6	1.69	1.02

Source: adapted from [35].

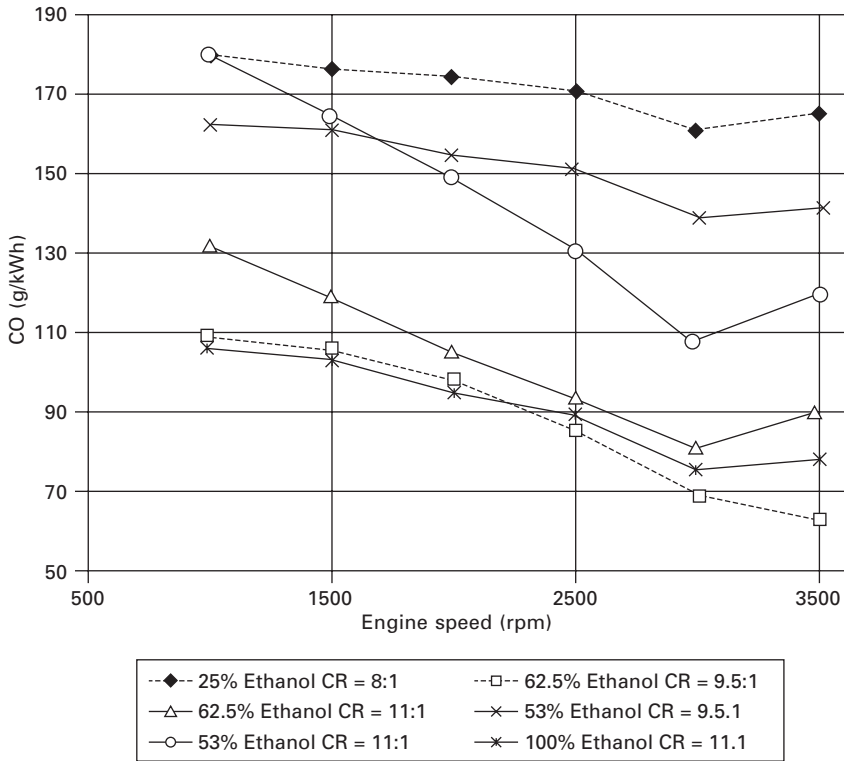
M85 and California Phase 2 reformulated gasoline (RFG). CO emissions showed a 17% reduction in comparison to gasoline, whereas NO_x showed a 3% increase and non-methane hydrocarbons were reduced by 30%.

Toxic emissions in general decreased, except from formaldehyde which showed a substantial increase. Evaporative emissions of M85 tend to be higher than from gasoline, due to higher vapor pressures, as explained above, with results showing up to 30% increase [54].

9.4.3 Ethanol

Due to the lower flame temperatures of ethanol, NO_x emissions can be 40% lower than from gasoline [59] in the same engine. However, if the engine is optimized for ethanol, with increased compression ratio, this advantage may no longer accrue. This is evident when looking at Table 9.8, which shows emission data from an engine with two configurations, each optimized for its respective fuel, in comparison to the legal requirements in Brazil.

Older, carbureted engines running on ethanol used to have much lower emissions of pollutants than their gasoline counterparts. Figure 9.11 shows carbon monoxide emissions for the same engine tuned for ethanol and E25,

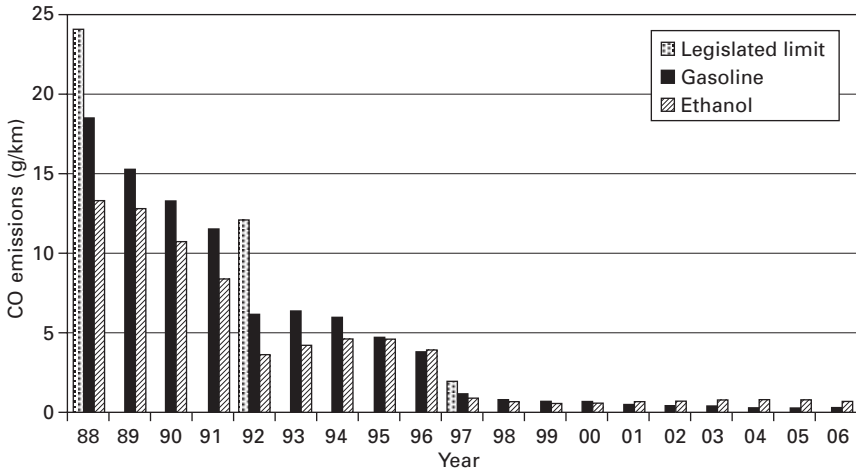


9.11 CO emissions with different compression ratios and ethanol concentrations, adapted from [60].

and adjusted for compression ratios of 8, 9.5 and 11. Carbon monoxide emissions produced by ethanol with 11:1 compression ratio were half that of gasoline with 8:1. Engine efficiency also benefited.

Figure 9.12 shows CO emissions from ethanol-fueled vehicles running on FTP 75 cycle between 1988 and 2006 in Brazil [61]; NO_x and evaporative emissions measured by the same source followed the same trend. Again, ethanol showed a clear advantage until 1996, when the situation was reversed, with gasoline producing slightly lower emissions. Perhaps this could be explained by the greater attention given to improving gasoline engines at that time, since ethanol vehicles were becoming rare.

Tables 9.9 and 9.10 show FTP regulated emissions and toxic emissions from the fleet-averaged results for flexible fuel vehicles (model year 1992–93) running on E85 and California Phase 2 reformulated gasoline (RFG). Different trends can be observed. With E85, the NO_x emissions were 29% lower, while CO increased by 8%. Non-methane hydrocarbons (NMHC) were 10% lower. The main toxic emission component was formaldehyde, with an almost



9.12 Fleet averaged CO emissions during FTP 75 cycle between 1988 and 2006 in Brazil, adapted from [61].

Table 9.9 Fleet-averaged change in FTP emissions with E85 in FFV

Regulated tailpipe emission	Change with E85
CO	+8%
NO _x	-29%
NMHC	0.3%

Source: adapted from [58].

Table 9.10 Fleet-averaged toxic emissions with E85 in FFV

Toxic emission	California Phase 2 RFG (mg/mile)	E85 (mg/mile)
Benzene	5.1	1.8
Formaldehyde	2.1	4.1
Acetaldehyde	0.5	24.8
1,3-Butadiene	0.7	0.2
Total	8.4	30.9

Source: adapted from [58].

100% increase with the use of E85. It should be noted, however, that this data was acquired from flexible fuel vehicles, which in general represent an optimization compromise between the two fuels when in full concentration. Moreover, the vehicles analyzed were 1992–93 models. Engines and EMS systems of today, together with modern calibration strategies, tend to be

more precise and lead to cleaner combustion. Therefore, it is likely that these figures will change in future studies, showing perhaps better results.

Evaporative emissions of gasoline–ethanol blends with small percentages of ethanol tend to be higher than those of pure gasoline due to the tendency of ethanol to form azeotropes. The addition of up to 40% ethanol into gasoline causes an increase in vapor pressure of the resultant blend [60], with the maximum vapor pressure occurring with 20% of ethanol. Higher concentrations start to show progressively lower values. For 100% ethanol, the Reid vapor pressure becomes more than 50% lower than that of gasoline [62]. This fact can be further illustrated when looking at Table 9.5, where evaporative emissions of E100 are shown to be lower than those of E25 and substantially less than the legislated limit.

9.4.4 Flex-fuel vehicles

A comparison has been made at CETESB [63] using a flex-fuel car running on a modified FTP 75 with hydrated ethanol (E94h) and pure gasoline. The car was a 2006 Volkswagen Fox, whose catalyst converter had been removed to deliver raw engine emissions. In total there were 10 cycles for each fuel. Table 9.11 summarizes the average emissions. Emissions of CO and HC were about the same, but NO_x for ethanol was 70% of the gasoline counterpart. NMHC showed a slight advantage for ethanol, whereas formaldehyde was twice as large for ethanol and acetaldehyde about eight times higher.

The low NO_x emission of ethanol clearly shows that the engine was not optimized for taking advantage of the properties of ethanol such as high octane number and spark ignition advance. Aldehydes, on the other hand, were at least an order of magnitude lower than HC and NMHC. It is worth saying that despite the very large number of ethanol vehicles in the São Paulo metropolitan area, by far the largest concentration of ethanol engines in the world, no air pollution episode has been reported by the environmental agency that has been attributed to the emission of aldehyde.

Twelve polycyclic aromatic hydrocarbons (PAHs) ranging from naphthalene to benzo(a)pyrene were also measured for both fuels. Gasoline showed a value of 206 mg/m^3 , concentrated on naphthalene (116 mg/m^3) and fluoranthene (81 mg/m^3), the remainder being negligible or not detected. Ethanol did not

Table 9.11 Emission data for a flex-fuel vehicle running on a modified FTP 75

Fuel	CO (g/km)	CO ₂ (g/km)	HC (g/km)	NO _x (g/km)	NMHC (g/km)	Formal- dehyde (g/km)	Acetal- dehyde (g/km)	Economy (L/100 km)
Ethanol 94%	6.0	161.7	0.85	1.64	0.84	0.045	0.131	12.2
Gasoline	6.1	166.8	0.88	2.32	0.91	0.023	0.016	7.4

produce detectable PAH emissions. Running with gasoline produced twice as much particulate matter as with ethanol.

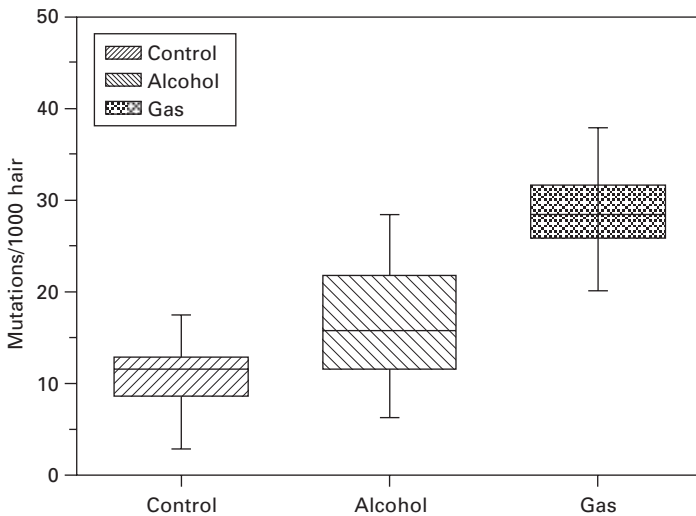
9.4.5 Biological assessment

Biological impacts of exhaust gases were assessed using *Tradescantia* KU 20, a biomonitor (plant) developed by Kyoto University. Figure 9.13 shows the results of the tests, from which it can be seen that the control group had a mutagenic index of 12, ethanol 16 and gasoline about 29. The same tests were repeated after an interval of a year, producing much the same result.

9.5 Operation

9.5.1 Cold start

Both ethanol and methanol suffer from low volatility compared to gasoline, as can be concluded from their respective vapor pressures (Table 9.4). Because of their high latent heats, alcohols also tend to drop the charge temperature via evaporative cooling, making cold start even more difficult. In addition, methanol and ethanol have flash points between 10°C and 15°C [64], which also brings difficulties when cold starting. Therefore, additional technology must be employed to provide acceptable cold start behavior. Several alternatives have been tested, in a variety of systems.



9.13 Biological assessment of mutagenic effects from exhaust gases of ethanol and gasoline, expressed as number of mutations per 1000 hair, *Tradescantia* KU 20.

Cold start improvements have been suggested by modifications in the ignition system, ranging from the use of multi-spark ignition strategies [65] to systems like plasma-jet ignition (shown to enable cold start in sub-zero conditions) [66]. Also, in engines with variable cam timing, optimizing the valve timing would provide increased compression temperatures and facilitate ignition of the cold charge [67]. This could be further improved by the use of direct injection with proper cold start strategies [68]. Some other researchers also report that cold start enrichment with E85 could be reduced by heating the intake air and/or the fuel rail and also by the use of air-assisted cold start injectors [69,70].

Nowadays, however, the most common way to cold start vehicles running on alcohols is to use a volatile primer, normally gasoline, either mixed with alcohol (E85 and M85) or injected separately, coming from a small onboard auxiliary tank. The former is the preferred solution in the USA and in Europe, while the latter has been extensively used in Brazil in the past 30 years. During 2009, at least some Brazilian vehicles have been able to start in 3 seconds at 8°C with no auxiliary fuel or heating and even quicker with ethanol heating.

9.5.2 Materials compatibility

Both methanol and ethanol are corrosive to some degree to some metals normally used in fuel systems of conventional vehicles, such as aluminum, copper, brass, magnesium and die-cast zinc. Special coating and protective layers are normally needed. Some alloys such as Zamac, commonly used in fuel systems, need protective coatings of nickel to overcome the problem.

Alcohols induce the swelling and weakening of rubber components such as rubber hoses, carburetor plastic floats and fiber gaskets that can be attacked. Compatible material such as highly fluorinated rubbers (Viton™) should be used. Nylons can be used if properly chosen. It is important to make the correct choice of materials. A number of studies and test programs have been performed to find the appropriate materials [34,42,57,64,71,72].

It should be emphasized, however, that most Brazilian cars of today can use ethanol with no corrosion problems even if they were manufactured for gasoline and later converted to ethanol. There are a large number of converted vehicles in the country that in most if not all cases had changes made only to the fuel control system. Experience with corrosion, from the early days of large-scale use of ethanol in cars, was mostly with mufflers and carburetors [73].

9.5.3 Engine wear

Piston rings and cylinder wear with alcohols has been reported [74]. However, it was attributed mainly to the long warm-up times with rich mixtures that

would dissolve the oil film in the cylinders. Nowadays, this would probably not be a concern, due to improved engine warm-up from modern engine management systems.

Some studies also report corrosive wear [58] that could be caused by combustion by-products, attacking mainly piston rings and cylinders [75]. This also is much less likely to be a problem nowadays due to improved engine management systems leading to cleaner and more complete combustion.

Nevertheless, another study states that no noticeable difference in wear was found when running with E85 in comparison to gasoline [76]. It is also reported that valve seats should be specially designed to operate with alcohol-based fuels since they have less lubricity than pure gasolines [36].

However, the experience of 30 years of ethanol-fueled vehicles in Brazil has shown no significant problems with engines. It is common knowledge that lubricants get less contamination and last longer, and engines are cleaner and less subject to sludge formation, when using ethanol.

9.6 Conclusions

Biofuels are a necessity that comes from aspects as diverse as climate change, fuel safety and local economic benefits. Competition with food production does not seem to be an issue provided the fraction of arable land used is small. Developing countries could benefit from producing biofuels and they have the potential to keep prices of fossil fuels low.

Economics is an important aspect that cannot be left aside. In places like Brazil ethanol is competitive and profitable even when environmental externalities are not taken into account. As the oil price rises, other processes will be competitive as well. Energy balance and carbon emissions are generally favorable.

Today the most used biofuel for SI engines is ethanol. Besides having good properties as a fuel, ethanol is good for the engine, relatively harmless, biodegradable and easily obtainable. Experience such as with the Brazilian fleet of ethanol vehicles that extends back for 30 years makes it crystal clear that biofuels are viable. New methods of obtaining SI biofuels are being developed in several stages and together with the traditional ones should bring benefits in the near future.

Concerns are often expressed about underground oil reserves but not so often about the atmospheric reservoir of carbon. There are many ways of relieving this problem and biofuels is one of them.

9.7 References

1. *Climate Change 2007 – Mitigation*, IPCC report, 2007.
2. UNICA (Sugar Cane Union Industry) <http://www.portalunica.com.br/>, accessed September 2008.
3. Waldheim, L., Morris, M., Verde Leal, M.R.L. 'Biomass power generation: sugar cane bagasse and trash', in *Progress in Thermochemical Biomass Conversion, VI*, Blackwell Science, 2001.
4. Shapouri, H., Duffield, J.A., Graboski, M.S. 'Estimating the net energy balance of corn ethanol', United States Department of Agriculture Agricultural Economic Report No. 721, July 1995.
5. Wang, L., Weller, C.L., Jones, D.D., Hanna, M.A. 'Contemporary issues in thermal gasification of biomass and its application to electricity and fuel production', *Biomass and Bioenergy*, (2008), doi: 10.1016/j.
6. Demirbas, A. 'Progress and recent trends in biofuels', *Progress in Energy and Combustion Science*, 33 (2007) 1–18.
7. Ouwens, C.D., den Uil, H., Boerrigter, H. 'Tri-generation from biomass and residues options for the co-production of Fischer–Tropsch liquids, electricity and heat', in *Progress in Thermochemical Biomass Conversion, VI*, Blackwell Science, 2001.
8. Bridgwater, A.V., Czernik, S., Piskorz, J. 'An overview of fast pyrolysis', in *Progress in Thermochemical Biomass Conversion*, ed. A.V. Bridgwater, Blackwell Science, 2001.
9. Guibet, J.C. *Fuels and Engines*, Volume 2, Editions Technip, Paris, 1999.
10. Knoef, H.A.M., ed. *Handbook of Biomass Gasification*, BTG Biomass Technology Group, 2005.
11. <http://www.revistapesquisa.fapesp.br/?art=3468&bd=1&pg=1&lg=>, accessed September 2008.
12. http://www.anfavea.com.br/tabelas2007/autoveiculos/tabela10_producao.pdf, accessed September 2008.
13. <http://www.bgtbiogasoline.com/>, accessed September 2008.
14. Fernando, S., Adhikari, S., Kota, K., Bandi, R., 'Glycerol based automotive fuels from future biorefineries', *Fuel*, 86 (2007) 2806–2809.
15. Tsuchida, T., Yoshioka, T., Sakuma, S., Takeguchi, T., Ueda, W. 'Synthesis of biogasoline from ethanol over hydroxyapatite catalyst', *Ind. Eng. Chem. Res.*, 47 (2008) 1443–1452.
16. Wang, L., Weller, C.L., Hanna, M.A., Jones, D.D. 'Contemporary issues in thermal gasification of biomass and its application to electricity and fuel production', *Biomass and Bioenergy*, 32 (2008) 573–581.
17. Dietenberger, M.A., Anderson, M. 'Vision of the US biofuel future: a case for hydrogen-enriched biomass gasification', *Ind. Eng. Chem. Res.*, 46, (2007) 8863–8874.
18. Macedo, I.C., Verde Leal, M.R.L., da Silva, J.E.A.R. *Assessment of Greenhouse Gas Emissions in the Production and Use of Fuel Ethanol in Brazil*, São Paulo State Secretariat of the environment, 2004.
19. Flowers, D.L., Aceves, S.M., Frias, J.M. 'Improving ethanol life cycle energy efficiency by direct utilization of wet ethanol in HCCI engines', SAE paper 2007-01-1867, 2007.
20. Dal Den, A.J. 'Análise de desempenho de um motor ciclo Otto alimentado com etanol 75% inpm', PhD thesis, University of São Paulo, Brazil, 2008.
21. Macedo, I.C. 'Situação atual e perspectivas do etanol', *Instituto de Estudos Avançados*, vol. 21 no. 59, São Paulo, January April 2007.

22. Dale, B. 'Biofuels: thinking clearly about the issues', *J. Agric. Food Chem.*, 56(11) (2008) 3885–3891.
23. Gnansounou, E., Panichelli, L., Villegas, J.D. 'Sustainable liquid biofuels development for transport', EPFL working paper 437.103, 2008.
24. http://www.sindipecas.org.br/paginas_NETCDM/modelo_detalhe_generico.asp?subtit=&ID_CANAL=17&id=567, accessed September 2008.
25. International Energy Agency (IEA) *World Energy Outlook 2006*, available at <http://www.iea.org/textbase/nppdf/free/2006/weo2006.pdf>.
26. Huttebraucker, D. 'The flexible fuel concept by Mercedes-Benz', SAE paper 921456, 1992.
27. Malça, J., Freire, F. 'Renewability and life-cycle energy efficiency of bioethanol and bio-ethyl tertiary butyl ether (bioETBE): Assessing the implications of allocation', *Energy*, 31 (2006) 3362–3380.
28. Minteer, S. *Alcoholic Fuels*, Taylor & Francis Group, Boca Raton, FL, 2006, p. 4.
29. Popuri, S., Bata, R. 'A performance study of iso-butanol-, methanol-, and ethanol-gasoline blends using a single cylinder engine', SAE paper 932953, 1993.
30. Pischinger, S., Rottmann, M., Fricke, F. 'Future of combustion engines', SAE paper 2006-21-0024, 2006.
31. Ferguson, C., Kirkpatrick, A. 'Internal combustion engines', in *Applied Thermosciences*, second edition, John Wiley & Sons, New York, 2001.
32. Brusstar, M., Bakenhus, M. 'Economical, high-efficiency engine technologies for alcohol fuels', US Environmental Protection Agency, National Vehicle and Fuel Emissions Laboratory, <http://epa.gov/otaq/presentations/epa-fev-isaf-no55.pdf>, accessed 14 September, 2008.
33. Brusstar, M., Stuhldreher, M., Swain, D., Pidgeon, W. 'High efficiency and low emissions from a port-injected engine with neat alcohol fuels', SAE paper 2002-01-2743, 2002.
34. Owen, K., Coley, T. *Automotive Fuels Reference Book*, Society of Automotive Engineers, Warrendale, PA, 1995, p. 598.
35. Clemente, R., Werninghaus, E., Coelho, E., Ferraz, L. 'Development of an internal combustion alcohol fueled engine', SAE paper 2001-01-3917, 2001.
36. Giroldo, M., Makant, W., Werninghaus, E., Coelho, E. 'Development of 1.6L flex fuel engine for Brazilian market', SAE paper 2005-01-4130, 2005.
37. Alcohol fuels review article, National Alternative Fuels Training Consortium, <http://www.naftc.wvu.edu/NAFTC/data/indepth/methanol/methanol.html>, accessed 14 September 2008.
38. American Petroleum Institute. *Alcohol and Ethers: A Technical Assessment of Their Application as Fuels and Fuel Components*, API Publication 4261, third edition, June 2001.
39. Baeta, J. *et al.* 'Optimization performance of multi-fuel spark ignition engine using a turbocharging system', SAE paper 2006-01-2641, 2006.
40. Baeta, J. *et al.* 'Metodologia experimental para a maximização do desempenho de um motor multicombustível turboalimentado sem prejuízo à eficiência energética global', PhD thesis, Universidade Federal de Minas Gerais, Brazil, September 2006.
41. Turner, G., Pearson, R., Holland, B., Peck, R. 'Alcohol-based fuels in high performance engines', SAE paper 2007-01-0056, 2007.
42. Jeuland, N., Montagne, X., Gautrot, X. 'Potentiality of ethanol as a fuel for dedicated engine', *Oil & Gas Science and Technology – Rev. IFP*, 59 (6) (2004), 559–570.

43. European Union, 'Commission proposal to limit the CO₂ emissions from cars to help fight climate change, reduce fuel costs and increase European competitiveness', press release IP/07/1965, Brussels, 19 December 2007.
44. Heywood, J.B. *Internal Combustion Engine Fundamentals*, McGraw-Hill, New York, 1988, 170.
45. Smith, J., Sick, V. 'The prospects of using alcohol-based fuels in stratified-charge spark-ignition engines', SAE paper 2007-01-4034, 2007.
46. Stone, R., Wyszynski, L., Kalghatgi, G. 'The volumetric efficiency of direct and port injection gasoline engines with different fuels', SAE paper 2008-01-0839, 2008.
47. Taniguchi, S., Yoshida, K., Tsukasaki, Y. 'Feasibility study of ethanol applications to a direct injection gasoline engine', SAE paper 2007-01-2037, 2007.
48. Li, Y., Zhao, H., Brouzos, N. 'CAI combustion with methanol and ethanol in an air assisted direct injection gasoline engine', SAE paper 2008-01-1673, 2008.
49. Brewster, S. 'Initial development of a turbo-charged direct injection E100 combustion system', SAE paper 2007-01-3625, 2007.
50. Brewster, S., Raiton, D., Maisey, M., Frew, R. 'The effect of E100 water content on high-load performance of a spray guide direct injection boosted engine', SAE paper 2007-01-2648, 2007.
51. Kamio, J., Kurotani, K., Kuzuoka, K., Kubo, Y., Taniguchi, H., Hashimoto, K. 'Study on HCCI-SI combustion using fuels containing ethanol', SAE paper 2007-01-4051, 2007.
52. Flowers, D., Aceves, S., Frias, J. 'Improving ethanol life cycle energy efficiency by direct utilization of wet ethanol in HCCI engines', SAE paper 2007-01-1867, 2007.
53. Taylor, A., Mocan, D., Bell, A., Hodgson, N., Myburgh, I., Botha, J. 'Gasoline/alcohol blends: exhaust emissions, performance and burn-rate in a multi-valve production engine', SAE paper 961988, 1996.
54. Kelly, K., Eudy, L., Coburn, T. 'Light-duty alternative fuel vehicles: federal test procedure emissions results', National Renewable Energy Laboratory, Technical Report NREL/TP-540-25818, September 1999.
55. Pouloupoulos, S., Samaras, D., Philippopoulos, C. 'Regulated and unregulated emissions from an internal combustion engine operating on ethanol-containing fuels', *Atmospheric Environment*, 35 (2001) 4399–4406.
56. Yuksel, F., Yuksel, B. 'The use of ethanol-gasoline blend as a fuel in an SI engine', *Renewable Energy*, 29 (2004) 1181–1191.
57. Cowart, J., Boruta, W., Dalton, J., Dona, R., Rivard, F., Furby, R., Piontkowski, J., Seiter, R., Takai, R. 'Powertrain development of the 1996 Ford flexible fuel taurus', SAE paper 952751, 1995.
58. Cadle, S., Groglicki, P., Gorse, R., Hood, J., Korduba-Sawicky, D., Sherman, M. 'A dynamometer study of off-cycle exhaust emissions – the auto/oil air quality improvement research program', SAE paper 971655, 1997.
59. Dai, W., Cheemalamar, S., Curtis, E., Boussarsar, R. 'Engine cycle simulation of ethanol and gasoline blends', SAE paper 2003-01-3093, 2003.
60. Sotto Pau *et al.* 'Análise experimental dos fenômenos da combustão e da emissão de gases em motores de combustão interna utilizando misturas de etanol e gasolina como combustível', PhD thesis, University of São Paulo, Brazil, 2003.
61. CETESB – Companhia de Tecnologia de Saneamento Ambiental, Qualidade do ar no Estado de São Paulo, 2007.

62. Kar, K., Last, T., Haywood, C., Raine, R. 'Measurement of vapor pressures and enthalpies of vaporization of gasoline and ethanol blends and their effects on mixture preparation in an SI engine', SAE paper 2008-01-0317, 2008.
63. CETESB – Companhia de Tecnologia de Saneamento Ambiental, internal report not yet published, 2008.
64. Nan, L., Best, G., Neto, C. 'Integrated energy systems in China – the cold Northeastern region experience', Food and Agriculture Organization of the United Nations, Rome, 1994, <http://www.fao.org/docrep/t4470E/t4470e00.htm>, accessed 28 September 2008.
65. Davis, G., Bouboulis, J., Heil, E. 'The effect of multiple spark discharge on the cold startability of an E85-fueled vehicle', SAE paper 1999-01-0609, 1999.
66. Gardiner, D.P. *et al.* 'Sub-zero cold starting of a port-injected M100 engine using plasma jet ignition and prompt EGR', SAE paper 930331, 1993.
67. Tsunooka, T. *et al.* 'High concentration ethanol effect on SI engine cold startability', SAE paper 2007-01-2036, 2007.
68. Kapus, P., Fuerhapter, A., Fuchs, H., Fraidl, G. 'Ethanol direct injection on turbocharged si engines – potential and challenges', SAE paper 2007-01-1408, 2007.
69. Huang, Y., Matthews, R., Hall, M. 'Conversion of a 1999 Silverado to dedicated E85 with emphasis on cold start and cold driveability', SAE paper 2000-01-0590, 2000.
70. Kane, E., Mehta, D., Frey, C. 'Refinement of a dedicated E85 1999 Silverado with emphasis on cold start and cold drivability', SAE paper 2001-01-0679, 2001.
71. Hammel-Smith, C., Fang, J., Powders, M., Aabakken, J. 'Issues associated with the use of higher ethanol blends (E17–E24)', National Renewable Energy Laboratory, Technical Report NREL/TP-510-32206, October 2002.
72. Ando, N. *et al.* 'The permeation effect of ethanol-containing fuels on fluoropolymers', SAE paper 2007-01-2035, 2007.
73. Clontz, R., Elum, M., McCrae, P., Williams, R. 'Effects of low-purge vehicle applications and ethanol-containing fuels on evaporative emissions canister performance', SAE paper 2007-01-1929, 2007.
74. Owens, E.C. *et al.* 'Effects of alcohol fuels on engine wear', SAE paper 800857, 1980.
75. Naegeli, D. 'Combustion-associated wear in alcohol-fueled spark ignition engines', SAE paper 891641, 1989.
76. Aakko, P., Nylund, N. 'Technical view on biofuels for transportation – Focus on ethanol end-use aspects', VTT Technical Research Centre of Finland, Research Report PRO3/5100/03, May 2004.

Optical diagnostics for direct injection gasoline engine research and development

V. SICK, The University of Michigan, USA

Abstract: The capabilities and applications of optical diagnostics for engine research and development have grown dramatically since early applications were reported in the 1930s. They have long become a crucial component that enables the development of ever better internal combustion engines, making the transition from being esoteric research tools to becoming mainstream tools. A growing interest in developing direct injection engines of all sorts (spark-ignition and compression ignition) has triggered a flurry of developments in optical diagnostics that in turn were crucial in developing and improving new engine concepts. Optimized multiphase flow, stratified charge, partially premixed combustion, spray impingement, soot formation, and other effects that were not important in carbureted and port-fuel-injection gasoline engines have become critical to the success of direct injection engines. Techniques and their applications for measurements of important parameters such as fuel concentration, flow, temperature, and pollutants are presented in this chapter.

Key words: laser induced fluorescence, particle image velocimetry, chemiluminescence, imaging diagnostics, high-speed imaging, direct injection engine.

10.1 Need for and merit of optical diagnostics

While the basic operating principles remain unchanged since the early days of internal combustion engines, many details have been modified to improve energy efficiency and to lower pollutant formation and release. Traditionally, fuel and air have been premixed prior to spark ignition. It is a fortunate coincidence that the turbulent flame speed of premixed flames scales approximately with turbulence intensity, and turbulence intensity scales with engine speed. This enables the operation of internal combustion engines that can run at variable speeds, a key feature for automotive applications. Fuel will burn faster with increasing engine speed and therefore will burn during the appropriate portion of the engine cycle to release energy when it is needed to propel the piston. However, upon closer inspection one finds that there is a need to adjust spark timing as engine speed is varied to ensure best performance. The immediate question is how can we learn about the origin of this by directly observing the chemical and physical processes inside the engine cylinder?

It is important to realize that mixing and combustion in the enclosure of

the engine cylinder will be significantly affected by the physical boundaries and therefore, since early on in the development of internal combustion engines, researchers have thought of ways to study internal combustion engine phenomena through the use of optical engines (Rassweiler and Withrow, 1938; Withrow and Boyd, 1931; Bowditch, 1960). The direct observation of flame initiation, growth and extinction, and correlation of these data with, e.g., pressure measurements, quickly gained in importance. The biggest boost for optical diagnostics in engines came after the invention of laser and digital cameras. This enabled the development of measurement tools that allowed researchers to measure multi-dimensional distributions of fuel, pollutants, temperature, and velocity with very high spatial and temporal resolution as well as high specificity. These measurement capabilities were crucial in the development of modern internal combustion engines. In the late 1980s and early 1990s laser imaging techniques (still often only qualitative in nature) became increasingly important to enable and assist the development of spark-ignition direct injection engines (Kuwahara and Ando, 2000; Hentschel, 2000; Drake and Haworth, 2007; Fansler *et al.*, 1995). In those engines, it is necessary to produce a highly stratified fuel/air mixture around the spark plug to ensure flammability of a globally lean mixture that would not burn if fully premixed (Zhao *et al.*, 1999). Imaging techniques that can visualize the distribution of the fuel have become the focus of optical diagnostics work for IC engines since that time (Zhao and Ladommatos, 1998).

As much as fuel/air mixing itself is different for direct injection engines compared to port fuel injected or carbureted engines, even when fuel is injected early in the intake stroke, the changes in ignition, combustion, and pollutant formation needed equal attention and specialized diagnostics equipment. The role of cycle-to-cycle variability has increased with combustion modes that take advantage of very lean and highly stratified operating conditions, since it is now more likely that mixtures occasionally exceed flammability limits and misfires occur. Homogeneous or partially premixed charge compression ignition strategies for gasoline fuels have been under investigation for a while now as well (Zhao *et al.*, 2003). Measurements of mixture and temperature distributions are especially critical for this engine concept where control of the onset of combustion is the biggest issue to be solved. Optical diagnostics again are useful to unravel local and temporal evolutions of chemical and physical properties that govern the HCCI process. Spark-assisted compression-ignition may be a way to address some of these issues and, again, optical diagnostics are crucial for progress towards better understanding and guidance for new engines (Alt *et al.*, 2007).

Improvements in internal combustion engines will require a fundamental understanding and exploration of the physical and chemical processes that govern internal combustion engine operation. However, it will be impossible to experimentally study and evaluate a very large number of engine concepts

and operating conditions. Not only is this too time-consuming and too expensive; this approach also bears the risk of missing the overall optimum. A key area for the use of optical diagnostics in internal combustion engine research is therefore to assist and guide the development and calibration of advanced engine simulation tools that include the transient phenomena that are so important for modern engines. As an example, optical experiments of sprays are used to acquire data that is then used to calibrate a spray model for those or at least very similar conditions. This is required since to date no fully predictive models are available for the early phase of spray development. Clearly, the development of fully predictive simulation tools for all engine-relevant processes will gain importance in the future.

A potentially significant drawback of optical engine research is the often substantial difference in thermal properties of transparent engines to their full-metal counterparts. Matching combustion characteristics of an optical engine to that of a full-metal engine is challenging (Fansler *et al.*, 1995). Fundamental studies are less affected by this, as the physics and chemistry of internal combustion engine processes are addressed and data for model development and validation are generated. These models can then be used to project to full-metal engines. However, engine development and optimization would benefit from direct application of optical diagnostics to realistic and production engines. More and more emphasis will have to be put on the development of optical sensors that will require only small-sized optical access, such as spark plug sensors and similar devices. In those, fiber-optical elements are used for illumination and signal collection.

10.2 Applications of optical diagnostics

A wide variety of optical measurement techniques for IC engine studies has been developed and applied over the past decades. The multi-phase nature and the importance of flow-wall interactions in engines with fuel direct injection often complicate the application of optical diagnostics. This chapter presents a selection of optical measurement techniques for key parameters of gasoline IC engine operation. A survey of the literature immediately shows that thousands of publications document the application of optical diagnostics to IC engine research and development. Optical diagnostics has made it into the mainstream of engine research and development, becoming an indispensable tool. Therefore, the contents of this chapter are not an attempt to give a comprehensive review of all techniques and applications but rather an illustration of the use of optical techniques to study specific properties in engines. Fuel direct-injection is a versatile approach to allow the realization of multiple engine combustion concepts with the same engine hardware. Namely, operation with homogeneous spark-ignition, stratified-charge spark-ignition, and homogeneous or partially premixed compression-ignition can

all be achieved by choosing injection timing, exhaust gas recirculation and spark properties accordingly. The examples discussed in this chapter reflect those different operating conditions.

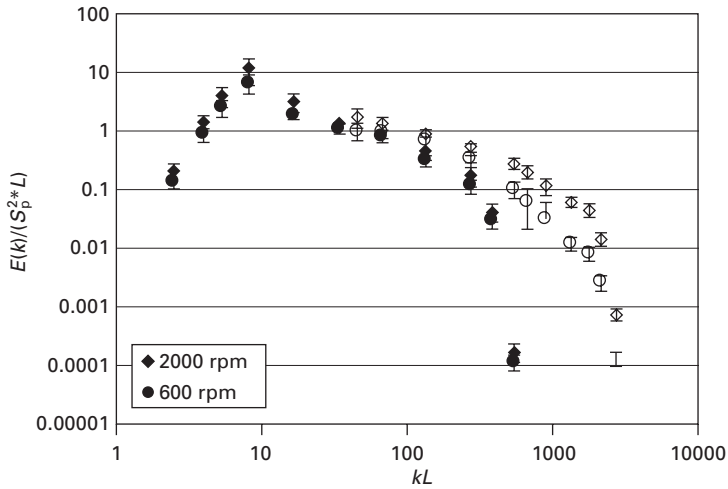
10.2.1 Flow in engines

Mixing of fuel, air and residual gases is dominated by the flow into, within, and out of the cylinder. Ignition is likely to be affected by the flow around the spark plug. Furthermore, the rate at which fuel is consumed depends on the level of turbulence during combustion. Heat transfer rates will also depend on flow conditions. Therefore, measurements of velocities and related quantities, such as kinetic energy, Reynolds stresses, strain rates, dissipation rates, etc., are essential for engine research and development. Engine flows are highly non-uniform in time and space and multi-dimensional, time-resolved measurements are especially important.

Laser Doppler Velocimetry (LDV) provides very high temporal resolution that is adequate to study engine flows (Rask, 1979; Arcoumanis *et al.*, 1990, 1994; Fansler, 1993; Corcione and Valentino, 1994). Even though the measurements typically provide velocities at one point, access is available to all three spatial components (Yoo *et al.*, 1995). Three-dimensional velocity measurements in engines were also demonstrated with Doppler Global Velocimetry (DGV) and yielded three spatial velocity components in a plane (Dingel *et al.*, 2004).

Since the first demonstration of Particle Image Velocimetry (PIV) in engines (Reuss *et al.*, 1989), PIV has become the most widely employed technique for flow measurements in engines. Mostly applied in a planar configuration, two or three velocity components can be measured (Raffel *et al.*, 1998). Vector fields can be used to extract important information for validation and development of CFD tools (Reuss *et al.*, 1995; Dugué *et al.*, 2006) and to directly analyze the impact of engine geometry on flow structures and cycle-to-cycle variability (Reuss, 2000). Energy and dissipation rate spectra that can be determined from PIV flow data are important factors towards a validation of commonly used turbulence models in engine simulations (Fajardo *et al.*, 2007). Figure 10.1 shows an example of energy spectra that were obtained at two engine speeds to illustrate how flow information can be non-dimensionalized.

The unsteadiness of in-cylinder flows combined with cycle-to-cycle fluctuations in velocities that produce apparent turbulent kinetic energy when using Reynolds decomposition in the analysis require investigation with high-speed PIV methods. This allows measurements of several velocity fields per cycle even at sub-crank angle resolution in numerous consecutive cycles (Towers and Towers, 2004; Gandhi *et al.*, 2005; Fajardo and Sick, 2007). The influence of the fuel spray on local turbulence levels near the



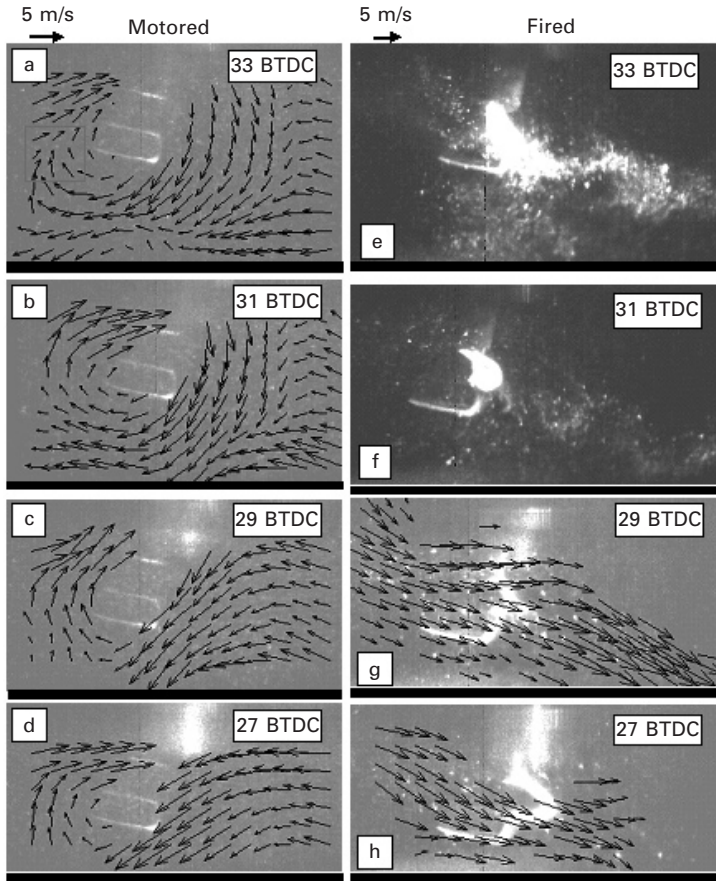
10.1 Kinetic energy spectra obtained from two-dimensional vector fields that were measured with PIV. Gaussian bandpass filtering was used to extract spectral energy densities from the original vector fields. Data shown in open symbols were obtained with high-resolution PIV for improved assessment of small-scale turbulence. S_p: mean piston speed, L: engine bore = 86 mm (Fajardo and Sick, The University of Michigan).

spark plug is significant and will have a leading role in ignition stability, especially for spray-guided spark-ignition direct injection engines (Sick and Fajardo, 2008). Figure 10.2 shows an example of a flow field sequence that was captured in a direct injection engine at a rate of 6 kHz. It is evident how much the spray affects the local flow velocity and direction.

Holographic PIV provides full three-dimensional information on velocities but its application to engines is very difficult given the sensitivity of holography to phase distortions and the large amount of data reduction (Coupland *et al.*, 2006).

10.2.2 Fuel/air/exhaust mixing

The most intense area of optical diagnostics development and application for engine research is seen in measurements of fuel, air and residual gas mixing in the intake system and even more so inside the cylinder. Those measurements are usually performed using laser-induced fluorescence imaging or absorption, mostly using diode lasers. The former is suitable for two- and three-dimensional measurements, while the latter yields line-of-sight information but typically can be performed at much higher data acquisition rates. Furthermore, infrared diode lasers allow direct measurements of



10.2 Instantaneous flow images between 33° BTDC and 27° BTDC for a single engine cycle in a spray-guided direct injection engine. Left column: motored engine; right column: fired engine. The spark luminosity is captured at 33° BTDC. The deformation of the plasma channel can be seen at 29° BTDC and 27° BTDC. ((Fajardo and Sick, 2008)) With kind permission from Springer Science+Business Media: *Experiments in Fluids*, DOI 10.1007/s00348-008-0535-z, Fig. 10.9).

hydrocarbons, water, carbon monoxide, and carbon dioxide. For practical purposes this is not really the case for LIF measurements. Standard gasoline is composed of hundreds of hydrocarbons, of which especially the aromatic compounds will absorb ultraviolet laser light and emit fluorescence. The varying composition of gasoline on the one hand and the species-specific fluorescence properties on the other make the use of LIF for quantitative fuel concentration measurements almost impossible. Mixing studies in engines that use LIF thus usually employ a non-fluorescing fuel, often iso-octane, and a fluorescing tracer is added to this fuel. The photophysical properties of these

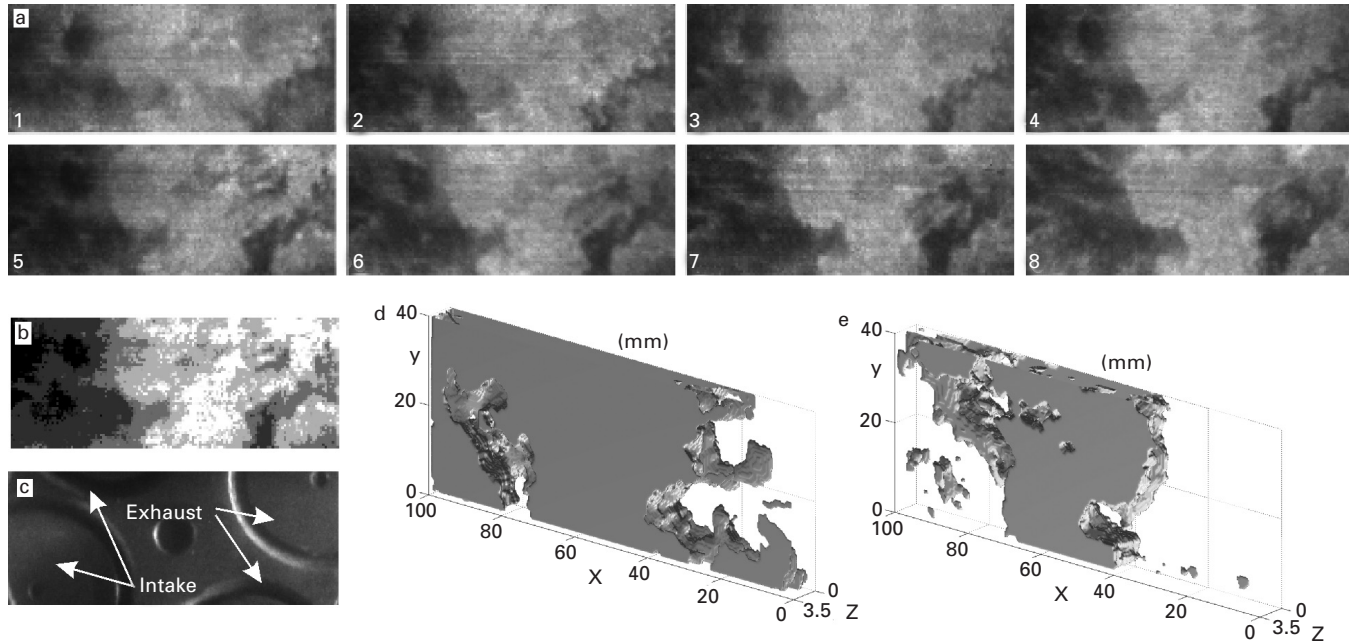
tracers can be characterized and quantitative measurements in engines can be performed. A comprehensive review of tracer-based engine measurements describes the fundamentals of tracer photophysics and applications for a variety of purposes in technical combustion devices (Schulz and Sick, 2005).

Adding a fluorescing tracer to a non-fluorescing fuel for LIF imaging is the most common approach for fuel distribution measurements. When calibrated this provides a measure of fuel concentration distributions or equivalence ratio (Arnold *et al.*, 1993; Reboux and Puechberty, 1994; Koban *et al.*, 2005; Schulz and Sick, 2005). Acetone, 3-pentanone, and toluene are the most widely used tracers for such measurements. LIF imaging using these tracers does not distinguish between liquid and gas phase fuel but can still be used to characterize the entire injection and mixing process (Frieden and Sick, 2003). Applications of LIF-based fuel detection using endoscopes that enable measurements in production or near-production engines have been demonstrated (Reichle *et al.*, 2006; Kallmeyer *et al.*, 2007). The use of a laser cluster allowed a near-instantaneous measurement of the three-dimensional fuel distribution (Nygren *et al.*, 2002) based on tracer-LIF imaging. Images obtained with eight parallel light sheets were used to render a three-dimensional fuel distribution map as shown in Fig. 10.3.

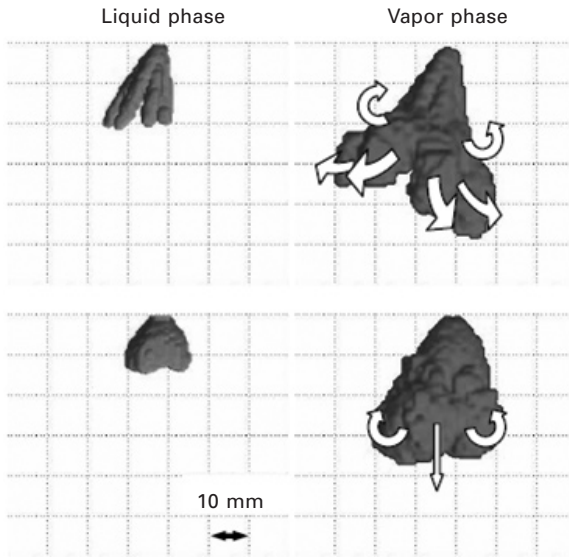
The characterization of sprays is difficult and reported results critically depend on definitions made. A new standard was recently developed to guide spray studies (Hung *et al.*, 2008). Simple time-resolved spray visualizations can be accomplished using Mie scattering and high-speed imaging (Smith and Sick, 2006b). Characterization of droplet sizes has been pursued with phase-Doppler measurements (Gold *et al.*, 2000) and planar techniques that use a combination of Mie scattering and laser-induced fluorescence (Jermy and Greenhalgh, 2000; Stojkovic and Sick, 2001; Düwel *et al.*, 2003).

An approach to separately measure the fuel amount in liquid and gas phase is based on exciplex laser-induced fluorescence. Laser excitation of a combination of tracers leads to the formation of an excited complex in the liquid but not the gas phase. This complex emits light at a longer wavelength than any of the tracers and therefore signals can be separated from each other (Knapp *et al.*, 1996; Rogler *et al.*, 2007). The major drawback of exciplex imaging is the sensitivity to oxygen quenching which makes quantitative measurements very challenging. The example shown in Fig. 10.4 illustrates the evaporation process from a spray emerging from a multi-hole nozzle into a well-characterized environment.

In some cases, the particular sensitivity of excited molecules to fluorescence quenching by molecular oxygen is actually helpful (Reboux and Puechberty, 1994; Schulz and Sick, 2005) to measure equivalence ratios. This also enabled the measurement of oxygen concentration distribution using a combination of 3-pentanone and toluene (Frieden *et al.*, 2002). The fluorescence of 3-pentanone is almost unaffected by collisions with oxygen at higher pressures whereas



10.3 (a) A three-dimensional fuel-tracer LIF sequence. Eight parallel and equidistant two-dimensional cuts of the fuel distribution in the engine are shown. The data were recorded at 2 CAD after TDC, when the engine was running at $\phi = 0.25$. (b) The five different gray scales corresponding to LIF intensities of <20%, 20–40%, 40–60%, 60–80%, and >80% of the maximum intensities in frame 5 in Fig. 10.3a. (c) Field of view for detection through the piston. (d) Three-dimensional fuel isoconcentration surface, corresponding to 50% of the maximum LIF intensity, calculated from the data presented in Fig. 10.3(a). $z = 0$ at the first frame. (e) Three-dimensional fuel isoconcentration surface corresponding to 70% of the maximum LIF intensity. Reproduced with permission of the Combustion Institute from Nygren, *et al.*, (2002), Fig. 3.



10.4 Exciplex imaging of two sprays from a multihole injector (top) and an annular orifice injector (bottom) at $p_{\text{amb}} = 0.94$ MPa and $T_{\text{amb}} = 220^\circ\text{C}$, $t = 800 \mu\text{s}$ after start of injection (Rogler *et al.*, 2007). Reprinted with permission from SAE Paper 2007-01-1827, © 2007 Society of Automotive Engineers of Japan, Inc. and © 2007 SAE International.

toluene is strongly quenched by oxygen. The ratio of LIF signals from the two tracers can therefore be calibrated to yield the oxygen concentration under suitable conditions.

Since gasoline is a multi-component blend of hundreds of hydrocarbons, some of which fluoresce, direct quantitative measurements of gasoline via LIF imaging are difficult to quantify. However, LIF measurements of gasoline have been demonstrated as a useful development approach (Fansler *et al.*, 1995). Tracer combinations have been used for measurements of fuel component distributions and their dependence on the evaporation rate of the components (Krämer *et al.*, 1998; Swindal *et al.*, 1995). It was experimentally observed that early injection strategies where fuel is injected into lower-pressure environments can lead to component-specific fuel stratification (Santavicca *et al.*, 2001), while for late injection into the high-pressure conditions of near-TDC timings, this is not the case, in agreement with internal transport processes in the fuel droplets (Zhang and Sick, 2007). Single-event measurements are possible if tracers are chosen where the fluorescence emissions can be spectrally separated from each other. This has also been demonstrated in combination with infrared absorption tomography. Infrared

absorption measurements can directly measure all hydrocarbons and even be tailored to distinguish aliphatic from aromatic hydrocarbons (Krämer *et al.*, 1998). Other tomographic applications for IC engine work have been summarized elsewhere (Sick and McCann, 2005). However, with the line-of-sight arrangement for absorption measurements the spatial resolution that is provided with LIF measurements is lost. The absorption of hydrocarbons in the infrared region is strong and therefore even short absorption pathlengths yield good signal strength. This allowed the integration of absorption setups into spark plugs (Koenig and Hall, 1998; Nishiyama *et al.*, 2004; Itoh *et al.*, 2006; Berg *et al.*, 2006; Kawahara *et al.*, 2007). Some of these devices can also be used to measure carbon dioxide and/or water to monitor residual gases (Cundy *et al.*, 2008; Berg *et al.*, 2006). Infrared absorption was also applied to measure the cylinder-specific EGR rate in the exhaust manifold of a diesel engine (Green, 2000) to demonstrate the capability of such measurements.

A key feature of direct injection engines is their inherent sensitivity to fuel/air mixing, especially when light-load late injection strategies are pursued that lead to highly stratified fuel distributions. Even though the fuel spray enters the cylinder with a very high momentum, the in-cylinder flow and cycle-to-cycle variations in the spray evolution lead to significant fluctuations in the local equivalence ratio at a given crank angle position. Related to ignition and combustion, such variations can have a significant impact on performance and pollutant formation. Time-resolved imaging of the fuel distribution is therefore important in understanding the relationship between fuel concentration and observed engine performance. Traditional LIF imaging systems are capable of capturing a single image per engine cycle. High-speed LIF for gas phase fuel concentration imaging was developed to enable measurements that yield at least one image every crank angle degree for many consecutive cycles (Smith and Sick, 2005a, b). High repetition rate laser pulses at 355 nm are used to excite biacetyl that was added to iso-octane fuel as a fluorescence tracer. Data obtained at 12 kHz (= one image per crank angle at 2000 rpm) illustrate how much variation the fuel concentration shows in comparison to the ensemble average distribution (see Plate XI (between pages 172 and 173)). In particular, this is important in the assessment of misfires as the local fuel concentration at the spark plasma channel can vary dramatically during the duration of the plasma discharge (1–2 ms) (Smith and Sick, 2006a, b). The same technique, in combination with chemiluminescence imaging, was used to investigate details of spark-ignition direct injection engine operation using ethanol and butanol as fuels (Smith and Sick, 2007).

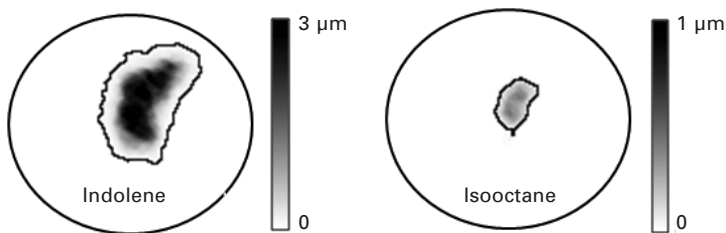
As mentioned before, the direct measurement of residual gases or EGR with imaging techniques is not practical because the main constituents, water and carbon dioxide, cannot be measured with linear LIF techniques in an engine. An indirect approach was proposed by using a sulfur dioxide

that is being formed during combustion from a precursor molecule that does not fluoresce (Sick, 2002). The application to a direct injection engine has recently been demonstrated (Fujikawa *et al.*, 2007).

Fuel films can lead to delayed vaporization of the fuel and to pool fires. Unburned hydrocarbon and soot emissions can be the result. Thus, fuel films are of particular importance for direct injection engines that use wall-guided strategies to stratify the fuel cloud around the spark plug. A range of optical methods has been developed and used for engine measurements (LeCoz *et al.*, 1994; Almkvist *et al.*, 1995; Johnen and Haug, 1995; Hentschel *et al.*, 1997; Witze and Green, 1997; Drake *et al.*, 2002; Lin and Sick, 2004). The refractive index matching approach of Drake *et al.* (2002, 2003) was combined with high-speed recording and allowed investigations of the instantaneous formation and evaporation of the liquid fuel film on the surface of the piston. Correlations of liquid deposits with engine emissions were investigated and linked fuel film mass with smoke emissions. Figure 10.5 shows an example of a fuel film in a DI engine for two fuels with different evaporation characteristics. Optical techniques have also been used to measure the thickness of lubricant films in engines, including bearings (Arcoumanis *et al.*, 1998; Nakayama *et al.*, 2003; Tian *et al.*, 1996) and with a combined LIF/PIV technique the oil film was measured at the piston (Baba *et al.*, 2007).

10.2.3 Temperature measurements

Temperature is one of the governing parameters in combustion and there is a strong need for its measurement. In engines this is mostly pursued using line-of-sight diode laser absorption or tracer-LIF; more rarely Coherent anti-stokes Raman Scattering (CARS), Rayleigh scattering, or soot luminosity have been employed. Absorption spectroscopy of water was used for temperature measurements in HCCI engines (Ghandhi *et al.*, 2003), Rayleigh scattering



10.5 Fuel film thickness measurement (μm) on the piston top of a direct injection engine using a refractive index matching approach (Drake *et al.*, 2002).

imaging has been used for studies on nitric oxide formation (Bräumer *et al.*, 1995; Schulz *et al.*, 1996), and flame propagation (Orth *et al.*, 1994) has been used in research engines that were designed to minimize reflections. To suppress such reflections and Mie scattering from fuel droplets in direct injection engines, filtered Rayleigh techniques could in principle be used (Yalin and Miles, 1999).

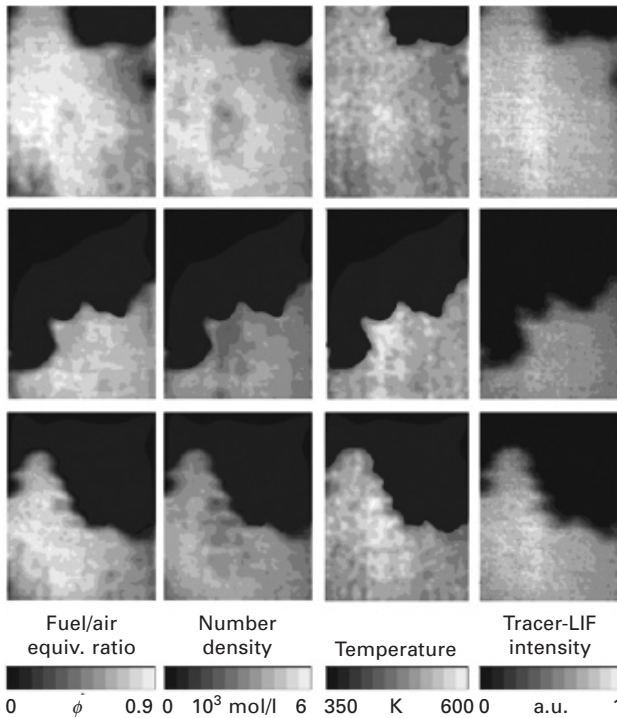
Fluorescence-based temperature imaging measurements were pursued in several different ways. Characteristic to all of them is that the temperature in either the burnt or the unburnt areas can be measured. A convenient indicator molecule that is found in either domain has not yet been identified. Nitric oxide may be such a candidate but may have to be added in quantities that could affect ignition and combustion properties. Indium atoms that are released at higher temperature from indium salts produce a very strong fluorescence signal and have been used to demonstrate a temperature imaging technique in an engine (Kaminski *et al.*, 1998). The drawback, as with the use of hydroxyl radical LIF (Meier *et al.*, 2000), is that temperature information is only available in burning or burned areas. Thermal radiation from soot that forms during rich combustion areas in direct injection engines was also used to determine temperature distributions (Stojkovic *et al.*, 2005). The measurement was based on a two-color measurement approach using Planck's law and yielded temperature, soot and hydroxyl radical data at 9 kHz (see Plate XII (between pages 172 and 173)).

A major drawback of tracer-based LIF fuel concentration imaging can be the temperature sensitivity of the signals when using a particular excitation wavelength (Schulz and Sick, 2005). This apparent disadvantage, however, has been used successfully to develop temperature imaging techniques for engine research (Großmann *et al.*, 1996; Einecke *et al.*, 2000; Rothamer *et al.*, 2008). The techniques that are based on ketones produce strong signals but need two excitation wavelengths. The associated need for energy and laser sheet corrections is eliminated when using toluene for temperature measurements. A single excitation wavelength is sufficient and beam and energy corrections are not required (Luong *et al.*, 2008). Figure 10.6 shows measurements based on 3-pentanone LIF imaging.

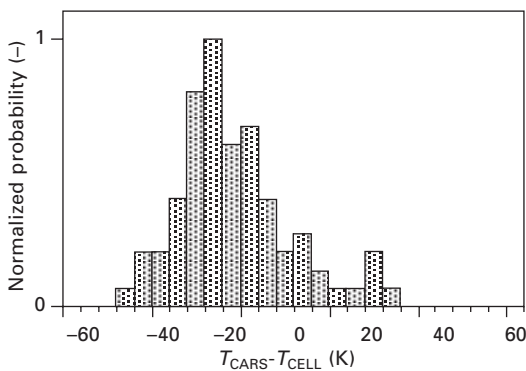
Evaporative cooling is critically important in direct injection engines and has been experimentally studied using coherent anti-Stokes Raman scattering (CARS) in automotive sprays (Beyrau *et al.*, 2004) as shown in Fig. 10.7.

The difficulty of applying LIF-based imaging techniques for temperature measurements under late injection conditions is based on the presence of liquid fuel/tracer. The temperature dependence of LIF signals for liquids has not been well characterized and dynamic range issues with the cameras may also be a limiting factor at this time.

Very recently, an approach that uses laser excitation of a phosphor powder that is added to the intake air has been demonstrated for temperature imaging



10.6 Temperature and fuel measurements based on 3-pentanone LIF imaging in an engine. Excitation at 248 and 308 nm was used for these measurements (Einecke *et al.*, 2000). With kind permission from Springer Science+Business Media: *Appl. Phys. B* 71, 2000, 717–723, Fig. 10.9.



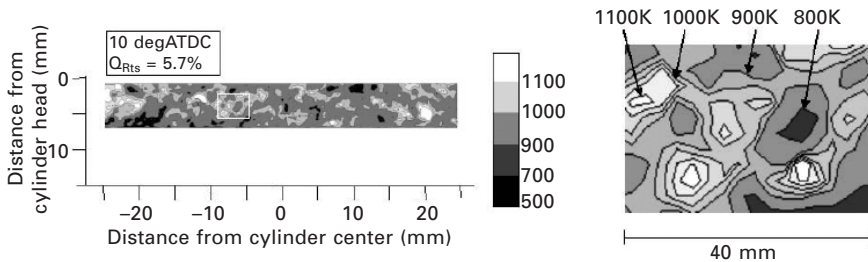
10.7 Probability density of the temperature results 4 ms after the SOI when the spray has reached the measurement location. Local cooling due to the evaporation is evident. The mean temperature is 408 K with a standard deviation of 18 K. Reproduced with permission from the Optical Society of America (Beyrau *et al.*, 2004).

in engines. Significant improvements in potential temperature measurement accuracy and precision appear feasible with this technique (Hasegawa *et al.*, 2007). Figure 10.8 shows an example taken in an HCCI engine.

10.2.4 Ignition and combustion

Optical studies of ignition and combustion in direct injection engines were performed with a range of techniques. These include emission spectroscopy, chemiluminescence, PIV, and LIF to detect properties of the plasma, unburned fuel, oxygen, residual gas, and the flame. In gasoline direct injection engine operation with early fuel injection, homogeneous fuel/air mixtures are present at the spark plug at the time of ignition. Ignition and combustion processes are as observed in carbureted and port fuel injection engines (Maly, 1984; Heywood, 1988). In late injection operation highly stratified fuel/air mixtures will be present around the spark plug at the time of the ignition. This stratification can lead to mixture conditions that cannot be ignited because they are too lean or too rich. In combination with highly turbulent flow conditions, reliable ignition is not always achieved and ignition stability is an important research topic. Combustion will not proceed as a pure premixed flame as in the case of homogeneous charge operation; rather flames can burn as premixed, partially premixed, or even non-premixed flames. Flames can extinguish, can burn too rich and form soot and will travel at varying speeds based on local mixture and flow conditions. Mixture and flow conditions change rapidly in time and space and thus studies of stratified engine operation greatly benefit from the use of high-speed imaging techniques.

The electric plasma of the spark discharge ionizes and electronically excites molecules in its path and light emissions from those molecules provide a means to relate this back to the initial fuel air mixture. Spectrally

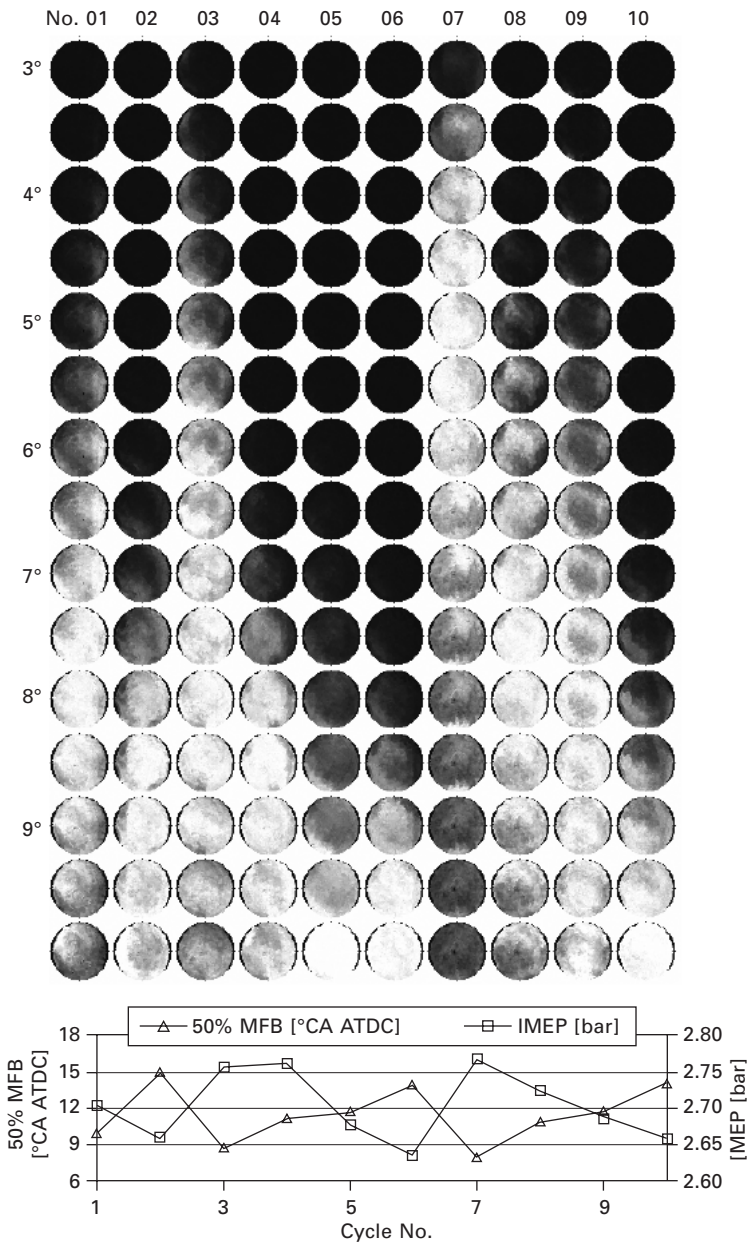


10.8 Contour images of single-shot temperature distribution at -10° ATDC in HCCI combustion. The white rectangular area in the left figure is enlarged in the right figure. (Hasegawa *et al.*, 2007) Reprinted with permission from SAE Paper 2007-01-1883, © 2007 Society of Automotive Engineers of Japan, Inc. and © 2007 SAE International.

resolved emissions to specifically detect excited CN and CH radicals have been used to measure the fuel/air ratio at the spark location (Fansler *et al.*, 2002) in a direct injection engine. A combination of back illumination to visualize the fuel spray, high-speed plasma emission imaging, and pressure-based combustion analysis was used to characterize the ignition process in a homogeneous-charge compression-ignition engine that uses spark-assistance to enable control of combustion phasing (Reuss *et al.*, 2008). High-speed imaging of Mie scattering from the fuel droplets, detection of the plasma luminosity, and measurements of electric properties of the spark discharge enabled studies of the impact of the spray momentum on the plasma motion and on ignition stability in a spray-guided direct injection engine (Smith and Sick, 2006b); see Plate XIII (between pages 172 and 173). The spark motion and influence of the flow field at the spark was examined with high-speed ultraviolet PIV (Fajardo and Sick, 2007). A high-speed fuel measurement technique was developed that uses LIF of biacetyl and enabled studies of the role of local fuel concentration on ignition stability in direct injection engines (Smith and Sick, 2005a, 2006a). Plasma emissions and flame luminosity can also be recorded during those measurements to enable multi-variable investigations with minimized experimental effort.

Combustion in a spray-guided direct injection engine was investigated with spectrally isolated bands to follow the evolution of combustion by monitoring OH* (chemiluminescence) and soot (thermal radiation) (Drake *et al.*, 2005). OH* imaging is a convenient diagnostic tool that provides useful information on combustion start and propagation. While the signals are integrated over the third dimension, sufficient spatial and especially temporal information is retained to enable studies of the impact of operating conditions or fuels, e.g. hydrocarbons vs. alcohols (Smith and Sick, 2007), on combustion progress. Correlations of OH* with heat release rate (Aleiferis *et al.*, 2004; Fissenewert *et al.*, 2005) and NO formation (Chin *et al.*, 2008) have been observed. Optical fiber bundles have also been used to collect OH* signals from a direct injection engine (see Fig. 10.9). A deconvolution algorithm allowed the reconstruction of the three-dimensional flame structure and its growth over time (Sauter *et al.*, 2006; Han *et al.*, 2006). Global combustion progress under varying swirl conditions was investigated with quasi-3D LIF measurements of toluene (Frieden and Sick, 2003) where the flame growth was marked by the disappearance of the fuel signal.

The combined measurement of multiple parameters is especially valuable for stratified combustion conditions. Combined measurements of fuel via tracer-LIF and OH-LIF detection allowed the study of the relationship between local fuel concentration near the flame front and combustion in a direct injection engine (Rothamer and Ghandhi, 2003). Toluene LIF, spark emission, and OH* chemiluminescence high-speed imaging can be coupled in a single camera setup to address the relationship between local and temporal



10.9 Auto-ignition and combustion progress are visualized with high spatial and temporal resolution by recording OH* chemiluminescence with a fiber optical bundle system (Sauter *et al.*, 2006). Reproduced with permission of IOP Publishing Ltd.

variations in fuel concentration, the plasma discharge and the developing and propagating flame (Smith and Sick, 2005b, c).

10.2.5 Pollutant formation

Nitric oxide, carbon monoxide, and unburned hydrocarbons are the most prominent pollutants that are formed and released during internal combustion engine operation. Some work has been done to measure carbon monoxide in internal combustion engines using laser-induced fluorescence (Kim *et al.*, 2008). However, the need to employ two-photon excitation makes this technique difficult to apply in engines, particularly if quantitative results are required. In-cylinder measurements were reported (Kim *et al.*, 2008) but most laser applications related to carbon monoxide measurements focus on measurements in the exhaust gas using diode laser absorption spectroscopy (Wang *et al.*, 2000). Unburned hydrocarbons can be qualitatively imaged, and work has been done to address the release of unburned hydrocarbons from crevices during the expansion stroke (Maly, 1994; Drake *et al.*, 1995; Franqueville, 2007).

Research addressing the formation of nitric oxide using in-cylinder optical techniques has been pursued primarily with the use of laser-induced fluorescence imaging. Two-atomic molecules, such as nitric oxide, have fairly simple absorption and emission spectra and therefore lend themselves to very specific detection by tuning the excitation wavelength and selecting the detection band-pass to effectively suppress the detection of other species. The spectroscopy of nitric oxide for engine conditions has been extensively studied and led to the development of photophysical models that can be used to quantify measurements (Bessler *et al.*, 2003a; Daily *et al.*, 2005; Schulz *et al.*, 1995, 1997, 1999) assisted by a web-based simulation tool (Bessler *et al.*, 2003b)

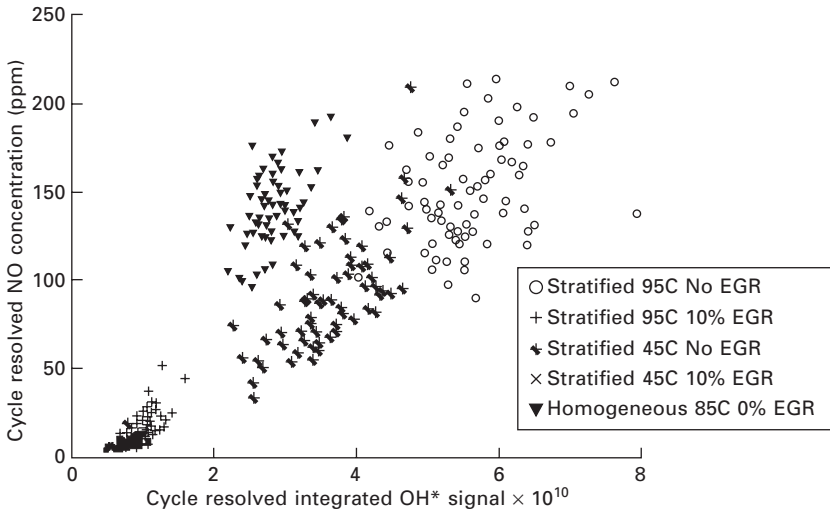
The formation of nitric oxide in a propane-fueled square-piston engine was studied with a combination of laser-induced fluorescence and Rayleigh scattering (Bräumer *et al.*, 1995). The spatial and temporal evolution of nitric oxide was measured for a range of engine loads and equivalence ratios. From a comparison of temperature and nitric oxide profiles the importance of prompt NO formation under engine conditions was assessed and an upper limit for prompt NO concentrations was estimated at 150 ppm. In similar work, iso-octane combustion was investigated with laser imaging techniques and a numerical analysis of prompt vs. thermal nitric oxide formation was conducted (Schulz *et al.*, 1998). The ability to determine spatially and temporally resolved nitric oxide concentrations was important in enabling detailed comparisons with modeling efforts to describe nitric oxide formation (Josefsson *et al.*, 1998). All of the above studies were conducted for premixed combustion and model fuels that themselves do

not produce fluorescence signals. This simplifies the experimental approach significantly.

Investigations of nitric oxide formation in engines with more complex geometries, standard fuels, and stratified combustion strategies can be carried out with the same laser-induced fluorescence approaches. The influence of mixture stratification and exhaust gas recirculation on NO formation in a gasoline-operated direct injection engine was studied with a combination of in-cylinder LIF measurements and sampling techniques (Bessler *et al.*, 2005), and Plate XIV (between pages 172 and 173) shows an example of the results. This work also highlights the difficulty of correlating planar measurements (LIF), volumetric measurements obtained with a fast gas sampling valve, and cycle-average exhaust gas measurements. Fast, cycle-resolved, exhaust NO detection and in-cylinder LIF measurements (Fissenewert and Sick, 2005) show similar features.

OH chemiluminescence was shown to be linked to heat release rate (Aleiferis *et al.*, 2004). The addition of simultaneous detection of hydroxyl chemiluminescence to the NO LIF measurement provided opportunities to correlate inhomogeneities in local NO concentrations with those in combustion intensity (Fissenewert *et al.*, 2005). It has to be kept in mind, though, that the chemiluminescence images represent the two-dimensional integration of a three-dimensional signal representation. Furthermore, the comparison of crank angle history of NO concentrations and chemiluminescence intensities that were obtained by phase-averaging images from many engine cycles with cycle-resolved NO exhaust measurements does not allow an evaluation of how these data are correlated instantaneously. NO formation is a highly non-linear process with temperature and therefore data obtained from the same cycle are required. To date, there is no laser source available that would enable NO measurements at engine speeds that would provide, e.g., one NO image per degree crank angle. However, high-speed imaging of OH chemiluminescence is feasible. A combination of OH chemiluminescence using an intensified high-speed camera and fast, cycle-resolved, NO exhaust gas detection demonstrated that there is a significant correlation between the cycle-integrated OH chemiluminescence and the total NO that is produced in that particular cycle (Chin *et al.*, 2008). However, the correlation is not universal and appears to depend on the combustion mode, potentially caused by signal quenching (see Fig. 10.10).

Soot formation is typically connected with diesel engines but under some operating conditions soot can be formed in direct injection gasoline engines. Laser-induced incandescence imaging can be used to measure the presence and distribution of soot in engines (Block *et al.*, 2000). Recording of thermal radiation in a two-color, high-speed measurement setup was also applied to study the formation and oxidation of soot in direct injection engines (Stojkovic *et al.*, 2005).



10.10 A correlation between cycle-specific engine-out nitric oxide concentration and cycle-integrated OH* chemiluminescence for that particular cycle was observed for similar engine operating conditions. The correlation is not maintained if combustion conditions are very different (Chin *et al.*, 2008). Reprinted with permission from SAE Paper 2008-01-1072, © 2008 SAE International.

10.3 Future trends

Optical diagnostics is now well established as a research and development tool for internal combustion engines. Future needs include smaller, more robust, and cheaper laser devices and cameras. High-speed imaging capability will play a central role in future research and development work to enable studies of coupled non-linear processes and to provide data for model validation, in particular large eddy simulations. Furthermore, the demand to acquire and link many additional signals such as pressure data, thermocouple signals, etc., synchronously to images and other data from optical measurements will increase. Simultaneous optical measurements of several parameters are needed to understand complex relationships that cannot be revealed with separate measurements (Sick, 2007). There is increased need to develop techniques that can deliver time-resolved three-dimensional data. Image processing routines will have to become more powerful to allow handling of the enormous amount of data that is acquired with high-speed imaging diagnostics. Multi-phase flow measurement capabilities have to be improved to enable a better characterization of spray–flow interaction and the formation and consumption of soot.

Fundamental spectroscopic work at high pressure and temperature is required to enable the development of additional quantitative measurement

techniques for molecules such as peroxides and carbon monoxide among others. In-situ particle measurements under high temperature and pressure conditions need improvement. The accuracy and precision of temperature measurements needs to be improved.

Studies of gas–liquid–surface interaction require improvements in high-resolution measurement techniques that will work in engines. This will include velocity and concentration profiles. Surface properties, namely temperature, must be measured.

Especially for applications in development rather than research, the availability of endoscopic techniques will gain increased interest as this will allow measurements in production or near-production engines.

10.4 Conclusions

The capabilities and applications of optical diagnostics for engine research and development have grown dramatically since early applications were reported in the 1930s. They have long become a crucial component that enables the development of ever better internal combustion engines, making the transition from being esoteric research tools to becoming mainstream tools. A growing interest in developing direct injection engines of all sorts (spark-ignition and compression ignition) has triggered a flurry of developments in optical diagnostics that in turn were crucial in developing and improving new engine concepts. Optimized multiphase flow, stratified charge, partially premixed combustion, spray impingement, soot formation, and other effects that were not important in carbureted and port-fuel-injection gasoline engines have become critical to the success of direct injection engines. Important parameters such as fuel concentration, flow, temperature, and pollutants can be measured with optical diagnostics, often quantitatively. Work remains to improve the ease of use, reliability, cost, parameters that can be captured, and application to production engines.

10.5 References

- Aleiferis P, Hardalupas Y, Taylor A M K P, Ishii K and Urata Y 2004 Flame chemiluminescence studies of cyclic combustion variations and air-to-fuel ratio of the reacting mixture in a lean-burn stratified-charge spark-ignition engine *Combustion and Flame* **136** 72–90
- Almkvist G, Denbratt I, Josefsson G and Magnusson I 1995 Measurements of fuel film thickness in the intake port of an S. I. engine by laser induced fluorescence *SAE Paper 952483*
- Alt M, Grebe U, Najt P, Wermuth N, Huebler M and Reuss D 2007 Gasoline HCCI – from thermodynamic potential to real world fuel economy – Results from multi-cylinder testing. In: *11th Conference ‘The Operating Process of Internal Combustion Engines’*, Graz, Austria

- Arcoumanis C, Hu Z, Vafidis C and Whitelaw C H 1990 Tumbling motion – a mechanism for turbulence enhancement in spark ignition engines *SAE Paper 900060*
- Arcoumanis C, Bae C S and Hu Z 1994 Flow and combustion in a four-valve, spark-ignition optical engine *SAE Paper 940475*
- Arcoumanis C, Duszynski M, Lindenkamp H and Preston H 1998 Measurements of the lubricant film thickness in the cylinder of a firing diesel engine using LIF *SAE Paper 982435*
- Arnold A, Buschmann A, Cousyn B, Decker M, Sick V, Vannobel F and Wolfrum J 1993 Simultaneous imaging of fuel and hydroxyl radicals in an in-line four cylinder SI engine *SAE Transactions* **102** 1–9
- Baba Y, Suzuki H, Sakai Y, Wei D L T, Ishima T and Obokata T 2007 PIV/LIF measurements of oil film behavior on the piston in I. C. engine *SAE Paper 2007-24-0001*
- Berg T, Beushausen V, Thiele O and Voges H 2006 Fibre optics spark plug sensor for the optimisation of engine combustion processes *Motortechnische Zeitschrift* **67** 2–6
- Bessler W G, Schulz C, Lee T, Jeffries J B and Hanson R K 2003a Strategies for laser-induced fluorescence detection of nitric oxide in high-pressure flames: III. Comparison of A-X strategies *Applied Optics* **42** 2922–36
- Bessler W G, Schulz C, Sick V and Daily J W 2003b LIFSIM. <http://www.lifsim.com>)
- Bessler W G, Hofmann M, Zimmermann F, Suck G, Jakobs J, Nicklitzsch S, Lee T, Wolfrum J and Schulz C 2005 Quantitative in-cylinder NO–LIF imaging in a realistic gasoline engine with spray-guided direct injection *Proc. Combust. Inst.* **30** 2667–74
- Beyrau F, Bräuer A, Seeger T and Leipertz A 2004 Gas-phase temperature measurement in the vaporizing spray of a gasoline direct-injection injector by use of pure rotational coherent anti-Stokes Raman scattering *Optics Letters* **29** 247–9
- Block B, Oppermann W and Budack R 2000 Luminosity and laser-induced incandescence investigations on a DI gasoline engine *SAE Paper 2000-01-2903*
- Bowditch F W 1960 A new tool for combustion research: a quartz engine. In: *SAE National Automobile Week*, Detroit, MI: SAE International
- Bräumer A, Sick V, Wolfrum J, Drewes V, Zahn M and Maly R 1995 Quantitative two-dimensional measurements of nitric oxide and temperature distributions in a transparent square piston SI engine *SAE Paper 952462*
- Chin M K, Smith J D and Sick V 2008 Cycle-resolved NO measurements in a spray-guided SIDI engine using fast exhaust measurements and high-speed OH* chemiluminescence imaging *SAE Paper 2008-01-1072*
- Corcione F E and Valentino G 1994 Analysis of in-cylinder turbulent air motion dependence on engine speed *SAE Paper 940284*
- Coupland J M, Garner C P, Alcock R D and Halliwell N A 2006 Holographic particle image velocimetry and its application in engine development *Journal of Physics: Conference Series* **45** 29–37
- Cundy M E, Schucht T, Thiele O and Sick V 2009 High-speed laser-induced fluorescence and spark plug absorption sensor diagnostics for mixing and combustion studies in engines *Applied Optics* **48** (4) B94–B104
- Daily J W, Bessler W G, Schulz C, Sick V and Settersten T B 2005 Role of non-stationary collisional dynamics in determining nitric oxide laser induced fluorescence spectra *AIAA Journal* **43** 458–64
- Dingel O, Kahrstedt J, Behnk K and Zuelch S 2004 Measurement of 3-D in-cylinder flow fields using Doppler global velocimetry *SAE Paper 2004-01-1409*
- Drake M C and Haworth D C 2007 Advanced gasoline engine development using optical diagnostics and numerical modeling *Proc. Combust. Inst.* **31** 99–124

- Drake M C, Fansler T D and French D T 1995 Crevice flow and combustion visualization in a direct- injection spark-ignition engine using laser imaging techniques *SAE Paper* 952454
- Drake M, Fansler T and Rosalik M 2002 Quantitative high speed imaging of piston fuel films in direct-injection engines using a refractive-index-matching technique. In: *15th Annual Conference on Liquid Atomization and Spray Systems*, Madison, WI
- Drake M C, Fansler T D, Solomon A S and Szekely J G A 2003 Piston fuel films as a source of smoke and hydrocarbon emissions from a wall-controlled spark-ignited direct-injection engine *SAE Paper* 2003-01-0547
- Drake M C, Fansler T D and Lippert A 2005 Stratified charge combustion: Modeling and imaging of a spray-guided direct-injection spark-ignition engine *Proc. Comb. Inst.* **30** 2683–91
- Dugué V, Gauchet N and Veynante D 2006 Applicability of large eddy simulation to the fluid mechanics in a real engine configuration by means of an industrial code *SAE Paper* 2006-01-1194
- Düwel I, Kunzelmann T, Schorr J, Schulz C and Wolfrum J 2003 Application of fuel tracers with different volatilities for planar LIF/Mie drop sizing in evaporating systems. In: *Proceedings of the 9th International Conference on Liquid Atomization and Spray Systems ICLASS 2003*, Sorrento, Italy, paper 9–3
- Einecke S, Schulz C and Sick V 2000 Measurement of temperature, fuel concentration and equivalence ratio fields using tracer LIF in IC engine combustion *Applied Physics B* **71** 717–23
- Fajardo C M and Sick V 2007 Flow field assessment in a fired spray-guided spark-ignition direct-injection engine based on UV particle image velocimetry with sub crank angle resolution *Proc. Combust. Inst.* **31** 3023–31
- Fajardo C M and Sick V 2009 Development of a high-speed UV particle image velocimetry technique and application for measurements in internal combustion engines *Experiments in Fluids* **46** (1) 43–53
- Fajardo C M, Sick V and Reuss D L 2007 Engine in-cylinder turbulence assessment using sub-millimeter resolution PIV. In: *PIV 2007*, Rome, Italy
- Fansler T, French D and Drake M C 1995 Fuel distributions in a firing direct-injection spark-ignition engine using laser-induced fluorescence imaging *SAE Paper* 950110
- Fansler T D 1993 Turbulence production and relaxation in bowl-in-piston engines *SAE Paper* 930479
- Fansler T D, Drake M C, Stojkovic B D and Rosalik M E 2002 Local fuel concentration, ignition and combustion in a stratified charge spark ignited direct injection engine: Spectroscopic, imaging and pressure-based measurements *International Journal of Engine Research* **4** 61–87
- Fissenewert U and Sick V 2005 Cycle-resolved investigation of in-cylinder and exhaust NO in a spray-guided gasoline direct-injection engine: Effect of intake temperature and simulated exhaust gas recirculation *SAE Transactions Journal of Fuels and Lubricants* 1213–28
- Fissenewert U, Sick V and Pucher H 2005 Characterization of combustion and NO formation in a spray-guided gasoline direct-injection engine using chemiluminescence imaging, NO–PLIF, and fast NO exhaust gas analysis *SAE Transactions Journal of Fuels and Lubricants* 786–803
- Franqueville L 2007 Investigating Unburned Hydrocarbon (UHC) Emissions in a GDI engine (homogeneous and stratified modes) using formaldehyde LIF and fast-FID measurements in the exhaust port *SAE Paper* 2007-01-4029

- Frieden D and Sick V 2003 Investigation of the fuel injection, mixing and combustion processes in an SIDI engine using quasi-3D LIF imaging *SAE Transactions Journal of Engines* 270–81
- Frieden D, Sick V, Gronki J and Schulz C 2002 Quantitative oxygen imaging in an engine *Applied Physics B: Lasers and Optics* **74** 137–41
- Fujikawa T, Fukui K, Tohyama M, Hattori Y and Akihama K 2007 A study of internal EGR distribution measurements in an engine cylinder. 1st Report: Fundamental Examination of a New Approach, 'Tracer Producing LIF Technique' *JSAE Paper 20075121*
- Ghandhi J B, Sanders S T and Kim T 2003 Gas temperature measurements during ignition in an HCCI engine *SAE Paper 2003-01-0744*
- Ghandhi J B, Herold R E, Shakal J S and Strand T E 2005 Time-resolved particle image velocimetry measurements in an internal combustion engine *SAE Paper 2005-01-3868*
- Gold M, Li G, Sapsford S and Stokes J 2000 Application of optical techniques to the study of mixture preparation in direct injection gasoline engines and validation of a CFD model *SAE Paper 2000-01-0538*
- Green R M 2000 Measuring the cylinder-to-cylinder EGR distribution in the intake of a diesel engine during transient operation *SAE Paper 2000-01-2866*
- Großmann F, Monkhouse P B, Ridder M, Sick V and Wolfrum J 1996 Temperature and pressure dependences of the laser-induced fluorescence of gas-phase acetone and 3-pentanone *Applied Physics B* **62** 249–53
- Han K-M, Velji A and Spicher U 2006 A new approach for three-dimensional, high-speed combustion diagnostics in internal combustion engines *SAE Paper 2006-01-3315*
- Hasegawa R, Sakata I, Yanagihara H, Samrner G, Richter M, Alden M and Johansson B 2007 Two-dimensional temperature measurements in engine combustion using phosphor thermometry *SAE Paper 2007-01-1883*
- Hentschel W 2000 Optical diagnostics for combustion process development of direct-injection gasoline engines *Proc. Combust. Inst.* **28** 1119–36
- Hentschel W, Grote A and Langer O 1997 Measurement of wall film thickness in the intake manifold of a standard production SI engine by a spectroscopic technique *SAE Paper 972832*
- Heywood J B 1988 *Internal Combustion Engine Fundamentals* New York: McGraw-Hill
- Hung D L S, Harrington D L, Gandhi A H, Markle L E, Parrish S E, Shakal J S, Sayar H, Cummings S D and Kramer J L 2008 Gasoline fuel injector spray measurement and characterization – a new SAE J2715 recommended practice *SAE Paper 2008-01-1068*
- Itoh T, Kakuho A, Hiraya K, Takahashi E and Urushihara T 2006 A study of mixture formation processes in direct injection stratified charge gasoline engines by quantitative laser-induced fluorescence imaging and the infrared absorption method *International Journal of Engine Research* **7** 423–34
- Jermy M C and Greenhalgh D 2000 Planar dropsizing by elastic and fluorescence scattering in sprays too dense for phase Doppler measurement *Applied Physics B* **71** 703–10
- Johnen T and Haug M 1995 Spray formation observation and fuel film development measurement in the intake of a spark ignition engine *SAE Paper 950511*
- Josefsson G, Magnusson I, Hildenbrand F, Schulz C and Sick V 1998 Multidimensional laser diagnostic and numerical analysis of NO formation in a gasoline engine *Proc. Combust. Inst.* **27** 2085–92

- Kallmeyer F, Dankers S, Hentschel W, Grosse G, Thiele O and Schulz C 2007 *Motorische Verbrennung*, ed A Leipertz, Munich: VDI, Haus der Technik
- Kaminski C F, Engström J and Aldén M 1998 Quasi-instantaneous two-dimensional temperature measurements in a spark ignition engine using 2-line atomic fluorescence *Proc. Combust. Inst.* **27** 85–93
- Kawahara N, Tomita E and Tanaka Y 2007 Residual gas fraction measurement inside engine cylinder using infrared absorption method with spark plug sensor *SAE Paper 2007-01-1849*
- Kim D, Ekoto I, Colban W F and Miles P C 2008 In-cylinder CO and UHC imaging in a light-duty diesel engine during PPCI low-temperature combustion *SAE Paper 2008-01-1602*
- Knapp M, Luczak A, Beushausen V, Hentschel W and Andresen P 1996 Vapor/liquid visualization with laser-induced exciplex fluorescence in an SI-engine for different fuel injection timings *SAE Paper 961122*
- Koban W, Koch J D, Sick V, Wermuth N, Hanson R K and Schulz C 2005 Predicting LIF signal strength for toluene and 3-pentanone under engine-related temperature and pressure conditions *Proc. Combust. Inst.* **30** 1545–53
- Koenig M and Hall M J 1998 Cycle-resolved measurements of precombustion fuel concentration near the spark plug in a gasoline SI engine *SAE Paper 981053*
- Krämer H, Einecke S, Schulz C, Sick V, Natras S R and Kitching J S 1998 Simultaneous mapping of the distribution of different volatility classes using tracer LIF and NIR tomography in an IC engine *SAE Transactions* **107** 1048–59
- Kuwahara K and Ando H 2000 Diagnostics of in-cylinder flow, mixing and combustion in gasoline engines *Meas. Sci. Technol.* **11** R95–R111
- LeCoz J, Catalano C and Baritaud T 1994 Application of laser induced fluorescence for measuring the thickness of liquid films on transparent wall. In: *7th International Symposium of Laser Techniques to Fluid Mechanics*, Lisbon, Portugal, pp 29.3.1–8
- Lin M-T and Sick V 2004 Is toluene a suitable LIF tracer for fuel film measurements? *SAE Paper 2004-01-1355*
- Luong M Y, Zhang R, Schulz C and Sick V 2008 Toluene laser-induced fluorescence for in-cylinder temperature imaging in internal combustion engines *Applied Physics B* **91** 669–75
- Maly R 1984 *Fuel Economy in Road Vehicles Powered by Spark Ignition Engines*, ed J C Hilliard and G S Springer, New York and London: Plenum Press, p 453
- Maly R R 1994 State of the art and future needs in S. I. engine combustion *Proc. Combust. Inst.* **25** 111–24
- Meier U E, Wolff-Gaßmann D and Stricker W 2000 LIF imaging and 2D temperature mapping in a model combustor at elevated pressure *Aerospace Science Technology* **4** 403–14
- Nakayama K, Morio I, Katagiri T and Okamoto Y 2003 A study for measurement of oil film thickness on engine bearing by using laser-induced fluorescence (LIF) method *SAE Paper 2003-01-0243*
- Nishiyama A, Kawahara N, Tomita E, Fujiwara M, Ishikawa N, Kamei K and Nagashima K 2004 In-situ fuel concentration measurement near spark plug by 3.392 μm infrared absorption method – Application to a port-injected, lean-burn engine *SAE Paper 2004-01-1353*
- Nygren J, Hult J, Richter M, Aldén M, Christensen M, Hultqvist A and Johansson B 2002 Three-dimensional laser induced fluorescence of fuel distributions in an HCCI engine *Proc. Combust. Inst.* **29** 679–85

- Orth A, Sick V, Wolfrum J, Maly R R and Zahn M 1994 Simultaneous 2D-single shot imaging of OH concentrations and temperature fields in a SI engine simulator *Proc. Combust. Inst.* **25** 143–50
- Raffel M, Willert C E and Kompenhans J 1998 *Particle Image Velocimetry: a Practical Guide*, Berlin: Springer Verlag
- Rask R B 1979 Laser Doppler anemometer measurements in an internal combustion engine *SAE Paper 790094*
- Rassweiler G M and Withrow L L 1938 Motion pictures of engine flames correlated with pressure cards *SAE Journal (Trans.)* **42** 185
- Reboux J and Puechberty D 1994 A new approach of PLIF applied to fuel/air ratio measurement in the compressive stroke of an optical SI engine *SAE Paper 941988*
- Reichle R, Pruss C, Osten W, Tiziani H, Zimmermann F and Schulz C 2006 Hybrid excitation and imaging optics for minimal invasive multiple-band UV-LIF-measurements in engines. In: *VDI-Berichte*, pp 223–35
- Reuss D, Kuo T-W, Silvas G, Natarajan V and Sick V 2008 Experimental metrics for identifying origins of combustion variability during spark assisted compression ignition *International Journal of Engine Research* **9** (5) 409–434
- Reuss D L 2000 Cyclic variability of large-scale turbulent structures in directed and undirected IC engine flows *SAE Paper 2000-01-0246*
- Reuss D L, Adrian R J, Landreth C C, French D T and Fansler T D 1989 Instantaneous planar measurements of velocity and large-scale vorticity and strain rate in an engine using particle-image velocimetry *SAE Paper 890616*
- Reuss D L, Kuo T, Khalighi B, Haworth D and Rosalik M 1995 Particle image velocimetry measurements in a high-swirl engine used for evaluation of computational fluid dynamics calculations *SAE Paper 952381*
- Rogler P, Grzeszik R, Arndt S and Aigner M 2007 3D Analysis of vapor and liquid phase of GDI injectors using laser-induced exciplex fluorescence tomography in a high-pressure/high-temperature spray chamber *SAE Paper 2007-01-1827*
- Rothamer D, Snyder J, Hanson R and Steeper R 2008 Two-wavelength PLIF diagnostic for temperature and composition *SAE Paper 2008-01-1067*
- Rothamer D A and Ghandhi J B 2003 Determination of flame-front equivalence ratio during stratified combustion *SAE Paper 2003-01-0069*
- Santavicca D A, Tong K, Quay B D and Zello J V 2001 Fuel volatility effects on mixture preparation and performance in a GDI engine during cold start *SAE Paper 2001-01-3650*
- Sauter W, Nauwerck A, Han K-M, Pfeil J, Velji A and Spicher U 2006 High-speed visualisation of combustion in modern gasoline engines *Journal of Physics: Conference Series* **45** 120–32
- Schulz C and Sick V 2005 Tracer-LIF diagnostics: Quantitative measurement of fuel concentration, temperature and fuel/air ratio in practical combustion systems *Prog. Energy Combust. Sci.* **31** 75–121
- Schulz C, Yip B, Sick V and Wolfrum J 1995 A laser-induced fluorescence scheme for imaging nitric oxide in engines *Chem. Phys. Lett.* **242** 259–64
- Schulz C, Sick V, Wolfrum J, Drewes V, Zahn M and Maly R 1996 Quantitative 2D single-shot imaging of NO concentrations and temperatures in a transparent SI engine *Proc. Combust. Inst.* **26** 2597–604
- Schulz C, Sick V, Heinze J and Stricker W 1997 Laser-induced fluorescence detection of nitric oxide in high-pressure flames using A-X(0,2) excitation *Applied Optics* **36** 3227–32

- Schulz C, Wolfrum J and Sick V 1998 Comparative study of experimental and numerical NO profiles in SI combustion *Proc. Combust. Inst.* **27** 2077–84
- Schulz C, Sick V, Meier U, Heinze J and Stricker W 1999 Quantification of NO A-X(0,2) LIF: Investigation of calibration and collisional influences in high-pressure flames *Applied Optics* **38** 434–443
- Sick V 2002 Exhaust-gas imaging via planar laser-induced fluorescence of sulfur dioxide *Applied Physics B* **74** 461–3
- Sick V 2007 Towards 4D⁺ imaging. In: *Frontiers in Optics 2007/Laser Science XXIII*, San Jose, CA: OSA
- Sick V and Fajardo C M 2008 Development and application of high-speed imaging diagnostics for spray-guided spark-ignition direct-injection engines. In: *8th International Symposium on Internal Combustion Diagnostics*, Baden-Baden, Germany: AVL
- Sick V and McCann H 2005 *Process Imaging for Automatic Control*, ed H McCann and D Scott, Boca Raton, FL CRC Press, Taylor & Francis Group, pp 263–97
- Smith J D and Sick V 2005a Crank-angle resolved imaging of biacetyl laser-induced fluorescence in an optical internal combustion engine *Applied Physics B* **81** 579–84
- Smith J D and Sick V 2005b Crank-angle resolved imaging of fuel distribution, ignition and combustion in a direct-injection spark-ignition engine *SAE Transactions Journal of Engines* 1575–85
- Smith J D and Sick V 2005c High-speed fuel tracer fluorescence and OH radical chemiluminescence imaging in a spark-ignition direct-injection engine *Applied Optics* **44** 6682–91
- Smith J D and Sick V 2006a A multi-variable high-speed optical study of ignition instabilities in a spray-guided direct-injected spark-ignition engine *SAE Paper 2006-01-1264*
- Smith J D and Sick V 2006b Real-time imaging of fuel injection, ignition and combustion in a direct-injected spark-ignition engine. In: *ILASS 2006*, Toronto: ILASS
- Smith J D and Sick V 2007 The prospects of using alcohol-based fuels in stratified-charge spark-ignition engines *SAE Paper 2007-01-4034*
- Stojkovic B D and Sick V 2001 Evolution and impingement of an automotive fuel spray investigated with simultaneous Mie/LIF techniques *Applied Physics B: Lasers and Optics* **73** 75–83
- Stojkovic B D, Todd D, Fansler T D, Drake M C and Sick V 2005 High-speed imaging of OH* and soot temperature and concentration in a stratified-charge direct-injection gasoline engine *Proc. Combust. Inst.* **30** 2657–65
- Swindal J C, Dragonetti D P, Hahn R T, Furman P A and Acker W P 1995 In-cylinder charge homogeneity during cold-start studied with fluorescent tracers simulating different fuel distillation temperatures *SAE Paper 950106*
- Tian T, Wong V W and Heywood J B 1996 A piston ring-pack film thickness and friction model for multigrade oils and rough surfaces *SAE Paper 962032*
- Towers D P and Towers C E 2004 Cyclic variability measurements of in-cylinder engine flows using high-speed particle image velocimetry *Meas. Sci. Technol.* **15** 1917–25
- Wang J, Maiorov M, Jeffries J B, Garbuzov D Z, Connolly J C and Hanson R K 2000 A potential remote sensor of CO in vehicle exhausts using 2.3 μm diode lasers *Meas. Sci. Technol.* **11** 1576–84
- Withrow L L and Boyd T A 1931 Photographic flame studies in the gasoline engine *Ind. Eng. Chem.* **23** 539
- Witze P O and Green R M 1997 LIF and flame-emission imaging of liquid fuel films and pool fire in an SI engine during a simulated cold start *SAE Paper 970886*

- Yalin A P and Miles R B 1999 Ultraviolet filtered Rayleigh scattering temperature measurements with a mercury filter *Optics Letters* **24** 590–2
- Yoo S-C, Lee K, Novak M, Schock H and Keller P 1995 3-D LDV measurement of in-cylinder air flow in a 3.5l four- valve SI engine *SAE Paper 950648*
- Zhang R and Sick V 2007 Multi-component fuel imaging in a spray-guided spark-ignition direct-injection engine *JSAE Paper 20077146*
- Zhao F, Lai M-C and Harrington D L 1999 Automotive spark-ignited direct-injection gasoline engines *Prog. Energy Combust. Sci.* **25** 437–562
- Zhao F, Asmus T W, Assanis D N, Dec J E, Eng J A and Najt P M eds 2003 *Homogeneous Charge Compression Ignition (HCCI) Engines: Key Research and Development Issues*, Pittsburgh, PA: Society of Automotive Engineers
- Zhao H and Ladommatos N 1998 Optical diagnostics for in-cylinder mixture formation measurement in IC engines *Prog. Energy Combust. Sci.* **24** 297–336

-
- abnormal combustion phenomenon, 135
 - absorption spectroscopy, 270
 - accumulator, 211–12
 - ACEA target, 92
 - acetone, 266
 - aftercooler, 53, 82
 - aftertreatment system, xiii
 - air-assisted direct injection, 171, 246
 - air-fuel ratio distribution, Plate II
 - superimposed spray and gas velocity vector fields, Plate IX
 - air-guided combustion systems, 26–7, 189, 190
 - air-to-fuel ratio, 106, 112, 124, 125
 - distribution, 188
 - and exhaust-to-inlet manifold pressure ratio, 125
 - for typical turbocharged gasoline engine, 106
 - air-fuel mixing, 72
 - alcohols, and blends with gasoline, 246–8
 - aldehydes, 252
 - aluminium, 209, 210
 - ammonia, 101, 102
 - Arrhenius rate equation, 58
 - Atkinson cycle, 6
 - Audi 2.0 FSI engine, 39, 177
 - autoignition combustion, 106
 - approaches to CAI in gasoline engine, 137–46
 - internal EGR, 139–42
 - residual gas trapping, 142–6
 - thermal management, 137–9
 - development of gasoline engines with autoignition and SI combustion, 158–61
 - CPS device with coaxial bucket tappet, 160
 - successful CAI–SI and SI–CAI transitions, 162
 - valve lift profiles adopted by electromechanical camless system, 158–61
- direct injection gasoline engines, 133–63
 - BSFC improvement achieved with AVL-CSI engine, 141
 - effect of injection timing on heat release process, 153
 - energy balance analysis of different engine operations, 143
 - fast thermal management system adopted in OKP engine, 138
 - in-cylinder high speed chemiluminescence measurements, 154
 - in-cylinder pressure diagram with negative overlap, 144
 - negative valve overlap achieved by camless and mechanical actuation, 144
 - NO_x emission reduction achieved with AVL-CSI engine, 142
 - operational region of autoignition combustion reported in literature, 145
 - relationship between BMEP values and percentage of trapped residual gas, 149
 - summary of fuel injection timing effects, 152
 - variable intake and exhaust valve

- lifts of mechanical VVA system, 146
- future trends, 161–3
- gasoline engine requirements to operate with CAI, 137
- hybrid combustion of flame and autoignition
 - first combustion image, 156
 - without spark ignition, 156
- operation and control, 146–58
 - brake mean effective pressure, 148
 - brake specific fuel consumption, 150
 - brake specific hydrocarbon emissions, 150
 - concentration of residual gas concentration, 149
 - contour of the position of 10% mass fraction burned, 151
 - effects of injection strategy, 152–5
 - effects of spark discharge, 155–7
 - extending operational range, 157–8
 - operation of gasoline engines with autoignition combustion, 147–9, 151–2
- principle, 135–7
 - ideal heat release models of SI and autoignition combustion, 136
 - spark ignition and autoignition combustion, 135
- valve timing diagram
 - autoignition combustion in AVL-CSI engine, 140
 - OKP engine concept, 138
- AVL-CSI engine
 - autoignition combustion, 140
 - BSFC improvement achieved, 141
 - NO_x emission reduction achieved, 142
- AVL415 smoke meter, 186
- azeotropes, 247, 252
- bagasse, 234
- bio-oil, 231
- biofuels
 - approximate composition of typical syngas, 232
- CO emissions with different
 - compression ratios and ethanol concentrations, 250
- comparison of emission levels
 - between E25 and E100 during FTP 75 test cycle, 249
- E85 vs 95 RON unleaded gasoline
 - comparison of performance, 245
 - efficiency comparison, 245
- emissions, 246–53
 - alcohols and blends with gasoline, 246–8
 - biological assessment, 253
 - ethanol, 249–52
 - flex-fuel vehicles, 252–3
 - methanol, 248–9
- factors affecting power production of
 - short chain alcohols, 238–40
 - higher laminar flame speed, 239
 - higher latent heat of vaporisation, 239
 - higher octane rating, 239
 - lower stoichiometric air–fuel ratio, 238–9
 - mole ratio of products to reactants, 239–40
- 1.3L engine
 - brake efficiency, 244
 - brake specific fuel consumption, 243
 - WOT power curves, 242
 - WOT torque curves, 243
- operation, 253–5
 - cold start, 253–4
 - engine wear, 254–5
 - materials compatibility, 254
- performance, 237–46
 - fuel economy, torque and power, 237–46
 - laminar flame speed of M100, E100 and gasoline, 239
 - power comparison between alcohol and gasoline, 241
 - properties of alcohol fuels, gasoline and iso-octane, 238
 - torque comparison between alcohol and gasoline, 241
- ratio of bioenergy output to fossil energy, 236
- Reid Vapour Pressure comparison

- between M85, E85, and California Phase 2 reformulated gasoline, 248
- for spark-ignition engines, 229–55
- types and sources, 231–7
 - fast pyrolysis, 231
 - fermentation and distillation, 232–7
 - gasification, 231–2
- biogasoline, 229, 231
- BMEP, *see* brake mean effective pressure
- BMW 2002 tii turbo engine, 49
- BMW Valvetronic device, 145
- Bosch six-hole injector, 171
- brake mean effective pressure, 7–8, 51–2, 107, 147, 148, 149
- brake specific fuel consumption, 112, 141
- BSFC, *see* brake specific fuel consumption
- butanol, 237, 269
- butyric acid, 230

- CAI, *see* controlled autoignition
- California Phase 2 reformulated gasoline, 248, 249, 250, 251
- cam profile switching, 159, 160
- carbon dioxide, 101
- carbon monoxide, 14, 107, 265, 276, 279
- carbon steel, 210
- central direct-injection system, 161
- centrifuge separators, 234
- cetane number, 219
- CFD, *see* computational fluid dynamics
- CFD modelling
 - dual-fan-shape spray vs conventional spray, Plate IV
 - fuel spray, air-fuel ratio distribution and gas vector field, Plate VIII
 - oval piston cavity vs shell-shaped cavity, Plate VII
 - velocity field and spray distribution, Plate X
- chargecooler, *see* aftercooler
- chemiluminescence, 153, 156
- chemiluminescence imaging, 269, 273, 274, 277
- Chevrolet Corvair Monza Spyder, 48
- coherent anti-stokes Raman scattering, 270, 271
- cold start, 204, 240, 248, 253–4
- combustion, 220
- compressed natural gas, 208
- compression ignition, 163
- compression ratio, 93, 207, 208
- computational fluid dynamics
 - use in direct injection gasoline engine design and optimisation, 166–95
 - DISI injector technologies, 169–73
 - Ford Duratec 3.5L v6 PFI engine combustion system, 167
 - future trends, 194–5
 - homogeneous charge DI system, 173–89
 - stratified-charge DI combustion system, 189–92
 - turbo-charged or super-charged DI combustion system, 192–4
- controlled autoignition, 9–10
 - see also* autoignition combustion
- cooperative fuels research, 57
- COV of IMEP, 110, 111, 114, 115, 119, 126, 127
- CPS, *see* cam profile switching
- cylinder pressure, 206, 207

- DCVCP system, 67–8
- deep Miller strategies, 104
- deflagration, 106
- DeNOx catalyst, 15–16
- detonation, 106
- Dies-Otto engine, 162
- diesel engines, 56
- diode laser absorption spectroscopy, 276
- direct injection combustion engines, xi–xiii
- direct injection Formula 1 engine, 66
- direct injection gasoline engine, 1–18
 - advantages over existing PFI engines, 168
 - with autoignition combustion, 133–63
 - approaches to CAI in gasoline engine, 137–46
 - development of gasoline engines with autoignition and SI combustion, 158–61
 - future trends, 161–3
 - operation and control, 146–58
 - principle, 135–7

- boosted by exhaust gas recirculation, 105–31
 - EGR circuit design, 115–24
 - EGR operating maps, 124–7
 - fundamentals of WOT-EGR operation, 108–15
 - future trends, 130–1
 - in-vehicle requirements, 127–9
- design and optimisation using
 - computational fluid dynamics, 166–95
 - DISI injector technologies, 169–73
 - future trends, 194–5
 - homogeneous charge DI system, 173–89
 - stratified-charge DI combustion system, 189–92
 - turbo-charged or super-charged DI combustion system, 192–4
- exhaust emissions and aftertreatment
 - devices, 14–17
 - lean-NO_x trap, 16
 - urea-based SCR NO_x aftertreatment, 17
- high-pressure fuel injection system, 11, 13–14
 - gasoline injector comparison, 14
 - production of gasoline injector, 12
- optical diagnostics research and development, 260–79
 - applications, 262–77
 - future trends, 278–9
 - need for and merit of optical diagnostics, 260–2
- overview, 2–5
 - main features of a typical engine, 4
 - operating modes, 3
- potential and technologies for
 - high-efficiency, 5–11
 - engine downsizing principle, 7
 - gasoline engine fuel economy analysis, 5
 - spray-guided vs wall-guided combustion systems, 9
 - stratified charge combustion systems, 9
- direct injection natural gas engine, 199–227
- building an engine, 201–8
 - compression ratio, 204–8
 - converting from a diesel engine, 203
 - converting from a petrol engine, 202
 - designing a new engine, 201–2
 - options, 201
- combustion, 220
- emission control, 220–1
- fuel injection, 212–17
 - hole size vs hole number, 216–17
 - injection pressure, 214–16
 - injectors, 212–14
- fuel storage and supply, 208–12
 - fuel compressors/pumps and heat exchangers, 210–11
 - fuel filters, 212
 - fuel tanks, 209–10
 - reservoirs and accumulators, 211–12
- future trends, 225–7
- ignition, 217–19
 - glow plug ignition, 218
 - pilot fuel ignition, 218–19
 - spark plug ignition, 217–18
- potential applications, 221–2
 - buses, 222
 - heavy duty trucks, 221
 - light duty trucks and passenger cars, 222
- strengths and weaknesses, 222–5
 - cost of fuel systems, 225
 - emissions, 223
 - fuel energy densities, 225
 - fuel resources, 224
 - operation cost, 223–4
- technologies, 200–21
 - brake efficiency vs compression ratio, 205
 - compression ratio limit vs cylinder pressure limit, 207
 - fuel injection pressure and maximum cylinder pressure, 215
 - fuel supply system, 209
 - maximum cylinder pressure vs compression ratio, 206
- direct injection spark-ignition (DISI) injector technologies, 169–73

- Bosch 6-hole injector and
 - corresponding spray image, 173
- droplet distribution for typical low load fuelling event, 172
- major types of injectors, 169–73
 - air-assisted injector, 171
 - multi-hole injector, 171–3
 - outwardly opening piezo injector, 173
 - slit injector, 173
 - swirl injector, 170–1
- orbital air-assisted direct fuel injection system, 172
- Siemens piezo injector, 174
- spray images of Siemens swirl injector
 - 2 ms after start of injection, 170
 - 4 ms after start of injection, 169
- swirl injector spray characteristics, 171
- typical combustion system for DISI engine with side-mounted swirl injector, 168
- direct injection spark-ignition engine
 - advantages, 65–73
 - effect on knock and abnormal combustion, 70–2
 - effect on mechanical loading, 67–9
 - effect on pollutant emissions, 73
 - effect on thermal loading, 69–70
 - effect on turbo lag, 70
 - VW-Audi 2.0 litre T-FSI engine, 68
 - challenges, 74–5
 - future trends, 75–83
 - 3-cylinder ‘Sabre’ research engine, 79
 - BMW 3-litre in-line 6-cylinder twin-turbocharged engine, 78
 - effect of exhaust period on BMEP, 77
 - full-load BMEP and BSFC for ‘Sabre’ turbocharged DISI engine, 80
 - General Motors ‘LNF’ 2.0 litre 4-cylinder DISI engine, 76
 - problems and challenges, 51–65
 - knock and abnormal combustion, 57–64
 - mechanical loading, 51–2
 - thermal loading, 52–4
 - turbocharger lag, 54–7
 - turbocharging impact on pollutant emissions, 64–5
 - turbocharging, 45–84
 - divided exhaust period, 61–2
 - for turbocharged engines, 61
 - valve events, 62
 - Doppler Global Velocimetry, 263
 - downsizing, 103
 - dual-fuel-single-injectors, 219
 - dual-fuel-two-injectors, 219
 - dynamometer, 182, 188, 191
 - E100, 252
 - E85 gasoline, 244, 250
 - Ecotec engine, 161
 - EGR, *see* exhaust gas recirculation
 - EGR-boosted direct injection, 8
 - EGR pressure ratio, 115
 - electro-hydraulic valve actuation system, 141
 - electrohydraulic actuation, 143
 - electromechanical actuation, 143
 - electromechanical camless valve actuation system, 158
 - electronic control module, 202
 - emission control, 220–1
 - emission spectroscopy, 273
 - emissions, 223
 - engine brake efficiency, 204
 - engine building, 201–8
 - engine cycle model, 205
 - engine downsizing, 6–7
 - principle, 7
 - engine knock, 57
 - engine simulation code Ricardo WAVE, 96
 - enzymatic hydrolysis, 230, 236
 - EPA 2004, 203
 - epoxy, 210
 - ethanol, 230, 232, 237, 244, 246, 249–52, 269
 - biological assessment of mutagenic effects from exhaust gasses, 253
 - CO₂ emissions and avoided emissions in production and use, 235
 - fleet averaged CO emissions during

- FTP 78 cycle between 1988 and 2006, 251
- simplified flow diagram for sugarcane based production in Brazil, 233
- EURO IV, 203
 - emissions, 104
- EURO V, 14
- Euro VI, 101
- exciplex laser-induced fluorescence imaging, 266
- exhaust back-pressure, 53
- exhaust blowdown method, 157
- exhaust gas recirculation, xii, 15, 92
 - boosted direct injection gasoline engines, 105–31
- circuit design, 115–24
 - advantages and disadvantages of different layouts, 116
 - circuit layout, 115–17
 - exhaust plenum crack angle resolved measurements, 123
 - high-pressure, low-pressure and hybrid EGR circuits, 116
 - loci of operation superimposed on turbocharger compressor map, 120
 - low-speed torque curves, 123
 - original and modified exhaust plenum, 118
 - pre-vs post-compressor EGR feed, 117–21
 - schematic of high-pressure EGR circuit, 118
 - valve location effects, 121–4
 - valve locations for high- and low-pressure circuit layout, 122
- fundamentals of WOT-EGR operation, 108–15
 - details of the research engine used for fundamental studies, 109
 - engine speed effects, 113–15
 - knock suppression effects, 108–13
 - schematic of hybrid EGR circuit, 109
 - torque and plenum pressures for four-cylinder turbocharged gasoline engine, 113
- future trends, 130–1
- in-vehicle requirements, 127–9
 - boost pressure, intercooler heat rejection and EGR cooler heat rejection, 128
 - potential solution for WOT-EGR vehicle coolant circuit, 129
- key parameters during excess fuel, excess air and cooled EGR sweeps at 4000 rpm, 300 Nm and 19 bar BMEP, 111
- sweeps at 5500 rpm, 250 Nm, 114
- key parameters during pre- and post-compressor, 119
- operating maps, 124–7
 - maps of percentage reduction in engine-out emissions, 126
 - modified production engine details, 124
- relative air-to-fuel ratio and exhaust-to-inlet manifold pressure ratio, 125
- for typical turbocharged gasoline engine, 106
- exhaust valve closing, 147
- fan spray injector, 191, 192
- fast pyrolysis, 229
- fermentation, 229
 - and distillation, 232–7
- ferti-irrigation, 234
- FFV, *see* flex-fuel vehicles
- fibreglass, 210
- filter smoke number, 186
- filtration elements, 212
- Fischer–Tropsch synthesis, 229, 231
- flex-fuel vehicles, 233, 252–3
 - emission data for FFV running on modified FTP 75, 252
 - fleet-averaged change in FTP emission with E85, 251
 - emissions with M85, 248
 - fleet-averaged toxic emission with E85, 251
 - with M85 in FFV, 249
- flow field evolution process, 191
- fluorescing tracer, 266
- Ford Eco-Boost engine, 5
- Ford Motor Company, 177
- fossil fuels, 235

- four-valved pent-roofed design, 108
- FSI system, *see* fuel stratified injection system
- FTP 75, 250, 252
- fuel
 - consumption, 240
 - injection, 212–17
 - hole size vs hole number, 216–17
 - injection pressure, 214–16
 - injectors, 212–14
 - categories, 214
 - dual-fuel-single-injector, 219
 - dual-fuel-two-injectors, 219
 - resources
 - potential reserves, 224
 - proven reserves, 224
 - storage and supply, 208–12
 - fuel compressors/pumps and heat exchangers, 210–11
 - fuel filters, 212
 - fuel tanks, 209–10
 - reservoirs and accumulators, 211–12
- fuel direct-injection, 262
- fuel distribution
 - spray-guided direct injection engine, Plate XI
- fuel pressure activated injector, 212, 213
- fuel reforming, xii–xiii
- fuel stratified injection system, 66–7
- fuel–air mixing
 - effect of intake cam phasing on velocity, Plate VI
 - homogeneity, Plate III
 - modelling prediction and optical engine measurement, Plate V
 - process, 177, 186, 188, 190
- Galant/Legnum's 1.8 L straight-4, 3
- gasification, 231–2, 236
- gasoline engine
 - direct injection, 1–18
 - exhaust emissions and aftertreatment devices, 14–17
 - high-pressure fuel injection system, 11, 13–14
 - overview, 2–5
 - potential and technologies for high-efficiency, 5–11
 - Goliath GP700 E, 2
 - 2GR-FSE V6, 4
 - greenhouse effect, 91
 - greenhouse gas emission, 199, 234–5
 - GT Power model, 112, 205
 - Gutbrod Superior 600, 2
 - Halford Special engine, 47–8
 - turbocharged racing car engine, 47
 - HCCI combustion engines, *see* homogeneous charge compression ignition
 - hollow-cone injector, 170
 - homogeneous charge compression ignition, 57, 134, 163, 236, 246, 270
 - see also* autoignition combustion; controlled autoignition
 - homogeneous charge DI system
 - design and optimisation, 173–89
 - mini-map points and associated design objectives, 175
 - intake port optimisation, 175–7
 - Audi FSI combustion system with valve in intake port, 179
 - CFD-based port optimisation process, 178
 - typical trade-off between port flow capacity and tumble ratio, 176
 - mixing homogeneity improvement, 177, 179–89
 - CFD predicted intake valve fuel wetting and engine-out soot emissions, 185
 - engine soot emission measurements vs engine speed, 180
 - experimentally measured engine-out emission, 188
 - in-cylinder gas evaluation process, 187
 - liner wetting with end of injection of 180° bTDC, 183
 - Toyota D-4S combustion system, 184
 - velocity and fuel spray distribution at BDC, 181
 - hybrid EGR circuit, 117
 - hydrate natural gas, 224

- hydrocarbons, 14–15, 107
- ignition, 217–19
 - autoignition, *see* autoignition
 - combustion
 - glow plug ignition, 218
 - pilot fuel ignition, 218–19
 - spark plug ignition, 217–18
- IMEP, *see* indicated mean effective pressure
- indicated mean effective pressure, 94, 110, 174, 192
 - fluctuations, 162
 - values, 157
- Indium, 271
- infrared absorption tomography, 268
- infrared diode laser, 264
- injection pressure surplus, 215
- intake cam phasing effect, 188
- intake charged engine, 206
- intake valve opening, 147, 186
- integrated exhaust manifold, 79–80
- inter-cylinder exhaust, 158
- intercooler, *see* aftercooler
- intern EGR, 139
- iso-octane, 265

- KIVA codes, 168
- knock phenomenon, 195

- Laser Doppler Velocimetry, 263
- laser-induced fluorescence (LIF) imaging, 265, 266, 268, 269, 270, 271, 273, 274, 276, 277
- lean boost direct injection combustion system
 - concept, 93–9
 - characteristics, 94
 - combustion stability characteristics, 97
 - cumulative CO₂ emissions over the NEDC drive cycle, 99
 - NEDC drive-cycle CO₂ and fuel consumption results, 98
 - power curves for baseline engine and LBDI concept, 95
 - transient performance comparison, 98
 - turbine-out temperature, 97
 - vehicle acceleration times for
 - 1500-3000 rev/min, 95
 - vehicle installation of LBDI engine, 98
 - vehicle tractive effort, 96
- downsizing strategies, 93
- exhaust emissions control, 99–101
 - drive-cycle emissions, 99
 - LBDI concept fuel consumption benefit, 101
 - off-cycle emissions, 99–101
 - regeneration of fuel consumption penalty, 100
 - Tailpipe NO_x emissions, 102
- future trends, 104
- for improved fuel economy, 91–104
- pressures on gasoline engine, 91–3
- SCR NO_x control as an alternative to LNT, 101–3
- lean-boosted direct injection technology, 8
- lean NO_x catalyst, 15–16
- lean NO_x trap (LNT), 99, 101–3
 - principle, 16
- Leidenfrost effect, 182
- LIF, *see* laser-induced fluorescence (LIF)
 - imaging
- life cycle assessment, 235
- light-duty diesel engines, xi
- line-of-sight diode laser absorption, 270
- liquefied natural gas, 208
- liquified urea, 16
- Livengood–Wu integral equation, 58
- Lotus 97T, 50

- M85, 248
- magnetostrictive device, 213
- maximum opening position, 110, 186, 187
- mechanical supercharger, 158
- Mercedes-Benz CLS 350 CGI, 40
 - cylinder head BMW, 41
 - second generation direct injection, 42
 - stratified charge range of BMW engine, 42
- Mercedes-Benz 300SL, 2
- methane, 232
- methanol, 237, 246, 248–9
- Mie scattering, 266, 271, 274, Plate XIII
- Miller cycle, 6, 140

- Mitsubishi GDI, 37–8
 multi-hole injector, 171–3, 192, 216
 multi-spark ignition, 254
- natural gas, 199–200
 near-valve flow structure, Plate I
 net indicated mean effective pressure, 139
 New European Driving Cycle, 35, 91, 98, 99, 101, 104, 244
 nickel, 254
 Nippon Clean Engine, 135
 nitric oxide, 271, 276
 concentration distribution in direct-injection engine, Plate XIV
 nitrogen oxide, 14–16
 nitrous oxide, 107
 non-methane hydrocarbons, 250, 252
 NO_x adsorber catalysts, 36
 nylons, 254
- octane fuel, 6
 OKP engine
 adopted fast thermal management system, 138
 concept, 137–8
 valve timing diagram, 138
 Oldsmobile Cutlass Jetfire, 48
 Opel Vectra, 161
 operation cost, 223–4
 optical diagnostics
 applications, 262–77
 flow in engines, 263–4
 fuel/air/exhaust mixing, 264–6, 268–70
 ignition and combustion, 273–4, 276
 pollutant formation, 276–7
 temperature measurements, 270–1, 273
 for DI gasoline engine research and development, 260–79
 auto-ignition and combustion progress visualised with high spatial and temporal resolution, 275
 contour images of single-shot temperature distribution, 268
 cycle-specific engine-out nitric oxide concentration and cycle integrated OH* chemiluminescence, 278
 flow field sequence captured in direct injection engine, 265
 fuel film thickness measurement, 270
 kinetic energy spectra obtained at two engine speeds, 264
 probability density of temperature, 272
 single-shot temperature distribution, 273
 sprays from multihole injector and annular orifice injector, 268
 temperature and fuel measurement based on 3-pentanone LIF imaging, 272
 three-dimensional fuel distribution map, 267
 future trends, 278–9
 need for and merit of optical diagnostics, 260–2
- Otto cycle, 21–2
 outwardly opening piezo injector, 173
 overfuelling, 63
- particle image velocimetry, 273, 274
 particulate matter, 221, 223
 particulate matter emissions, 17
 3-pentanone, 266
 peroxides, 279
 PFI, *see* port fuel injection
 phosphor powder, 271
 piezo-electric actuation, 13–14
 piezo injector, 190
 piezo-resistive pressure transducer, 155
 piezoelectric device, 213
 piezoelectrically activated injector, 213
 pilot diesel, 204
 pilot fuel, 218
 pilot fuel ignition method, 218
 Planck's law, 271
 plasma-jet ignition, 254
 platinum, 104
 pneumatic device, 213
 pneumatically activated injector, 213
 pollutant emissions, 64–5, 73
 polycyclic aromatic hydrocarbons, 252–3
 Porsche 917, 48

- port fuel injection, 107
 - analysis of losses, 33
 - vs gasoline direct injection,
 - comparison of combustion process, 34
- potential reserves, 224
- premixed combustion, 202
- pressure atomisation, 13
- pressure charging, 46
- ProCo system, 2
- production engine
 - stratified gasoline direct injection, 36–42
 - first-generation gasoline direct injection engines, 37–9
 - second-generation gasoline direct injection engines, 39–42
- production ignition system, 96
- propane-fueled square-piston engine, 276
- proven reserves, 224
- pulse-divided turbocharger, 62–3
 - concept in turbocharged engines, 63
- pushback process, 188
- pyrometry, Plate XII

- Rayleigh scattering, 270–1, 276
- Reid vapour pressure, 247, 248, 252
- Renault turbocharged V6 Formula 1 engine, 50
- reservoirs, 211–12
- residual gas trapping method, 152
- reverse-mode thermodynamic analysis, 112
- reverse tumble concept, 189
- Reynolds decomposition, 263
- Reynolds stresses, 263
- rhodium, 103, 104
- Rolls-Royce Crecy, 2
- RON gasoline, 83, 244
- Royal Aircraft Establishment, 47

- Saturn Aura, 161
- SCR, *see* selective catalytic reduction
- selective catalytic reduction, 16, 101–3
- SI combustion mode, 246
- Siemens piezo injector, 173
- Siemens swirl injector, 170
- simple pressure-modulating solenoid valve, 160

- single-cylinder testing, 188
- slit injector, 173
- Smart Idling Stop System, 10–11
- solenoid actuators, 213
- soot formation, 184
- soot luminosity, 270
- spark-assisted autoignition combustion, 157
- spark-assisted compression-ignition, 261
- spark ignition gasoline engines, xi
- spark-ignition (SI) engines
 - biofuels, 229–55
 - emissions, 246–53
 - operation, 253–5
 - performance, 237–46
 - types and sources of biofuels, 231–7
 - combustion
 - development of gasoline engines with autoignition and SI combustion, 158–61
 - successful CAI–SI and SI–CAI transitions, 162
 - valve lift profiles adopted by electromechanical camless system, 159
- split injection, 73
- spray-guided combustion systems, 27–32, 35–6, 189, 190, 192, 264, 265, 274
 - exhaust gas treatment, 35–6
 - fuel consumption, 32, 35
 - fuel economy in first- and second-generation DI vs port fuel injection, 36
 - nozzle types comparison, 29–31
 - spray profiles, 30
 - theoretical efficiency, 28
 - thermodynamic analysis, 31–2
- spray-guided direct injection engine, 274
- spray-guided spark-ignition direct injection engines, 264
- spray nozzle, 29–31
- stainless steel, 210
- stillage, 234
- stratified charge combustion
 - direct injection gasoline engines, 20–43
 - future trends, 42–3

- production engines with stratified gasoline direct injection, 36–42
 - thermodynamic and combustion process, 21–32, 35–6
- stratified-charge DI combustion system, 189–92
 - cross-section through the spark gap at 25° bTDC for idle operation, 193
 - effect of spray cone angle for swirl injector, 191
 - Toyota stratified-charge combustion system, 190
- sugar cane, 233–4
- sugarcane bagasse, 232
- sulfur dioxide, 269
- supercharged DI combustion system, 192–4
- supercharged engine, 206
- swirl, 175, 188
 - control valve, 182, 184
 - injector, 191
 - ratio, 175
- syngas, 230
 - approximate composition, 232
- temperature control valve, 138
- thermal energy, 59
- thermal radiation, 271, 274.
- thermodynamics, 21–36
 - air-guided combustion systems, 26–7
 - comparison of wall-, air-, and spray-guided combustion, 25
 - constant-volume processes for port fuel injection and direct injection, 23
 - engine operation maps, 25
 - operating modes for gasoline direct injection engines, 24
 - principles, 108
 - spray-guided combustion systems, 27–32, 35–6
 - exhaust gas treatment, 35–6
 - fuel consumption, 32, 35
 - nozzle types comparison, 29–31
 - thermodynamic analysis, 31–2
 - thermal efficiency of the constant-volume process, 22
 - wall-guided combustion systems, 25–6
- thermosyphon, 53
- three-way catalyst, 112, 127, 130
- titanium, 210
- toluene, 266, 271, 274
- Top Dead Centre (TDC), 142
- Toyota's 3GR-FSE engine, 182
- tracer-LIF, 270
- Tradescantia KU 20, 253
- TSI 1.4 litre DI gasoline engine, 4
- tumble, 175, 188
- tumble ratio, 175
- turbo-charged DI combustion system, 192–4
 - engine design with less flow capacity for higher tumble ratio, 195
- turbocharged engine, 206
- turbocharged gasoline direct fuel injection engine, 106
- turbocharger lag, 48, 54–7
 - BMW diesel configuration, 56
 - turbocharged engine transient and steady-state torque curves, 55
- turbocharging
 - direct injection spark-ignition engine, 45–84
 - advantages of combining with direct injection engines, 65–73
 - challenges in direct injection application, 74–5
 - future trends and possibilities, 75–83
 - historical background, 46–51
 - problems and challenges, 51–65
- turboexpansion, 60–1
 - system in a turbocharged engine, 60
 - temperature-entropy, 61
- turbulence intensity, 188
- typical tumble port concept, 181
- unburned hydrocarbon, 14–15, 64–5
- urea, 101
- US06 cycle driving, 102
- US Tier 2 Bin 5, 101
- validated system simulation, 95
- valve event timing, *see* variable cam timing
- vaporisation, 71–2
- variable cam timing, 138, 186
 - devices, 159

- variable compression ratio, 139
- variable nozzle turbine, 94
- variable valve actuation camless system, 143
- variable valve train, 81
- vinasse, 234
- Viton, 254
- Volkswagen Fox, 252
- vortex induced stratified combustion concept, 190
- VVA, *see* variable valve actuation camless system
- VW Lupo FSI, 38–9
- wall-guided combustion system, 11, 13, 25–6, 189, 190, 270
- wastegate, 48–9
- Wave model, 205
- wet ethanol, 246
- wide open throttle EGR (WOT-EGR), 108–15, 127, 129
- Wiebe function, 112
- Woschni correlation, 112
- WOT-EGR, *see* wide open throttle EGR
- Zamac, 254

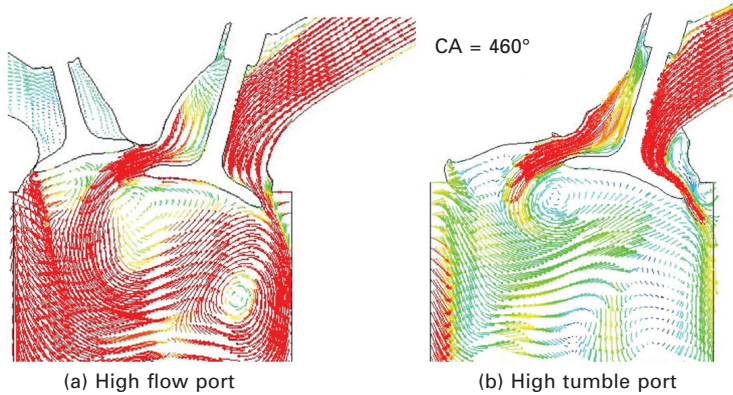


Plate I Comparison of near-valve flow structure between high flow port (left) and high tumble port (right). The high flow port has a more uniform velocity flow field around the valve seat area, while the high tumble port shows a more biased flow structure with flow separation on the short side of the port. The operating condition is full load at 5000 rpm (Iyer and Yi, 2008).

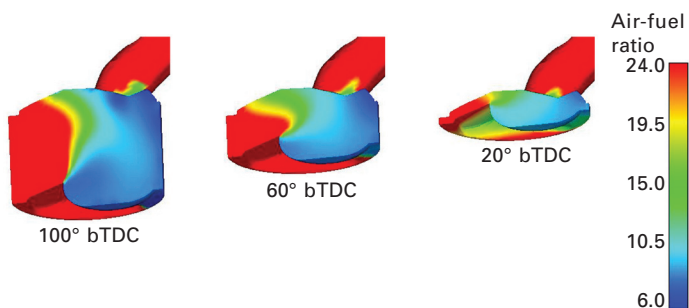


Plate II Air-fuel ratio distribution at 6000 rpm full load in the initial combustion system design. The start of injection is 10° After Top Dead Center (aTDC) in the intake stroke. The injection duration is about 188° and the average air-fuel ratio is about 13:1. (Yi *et al.*, 2002).

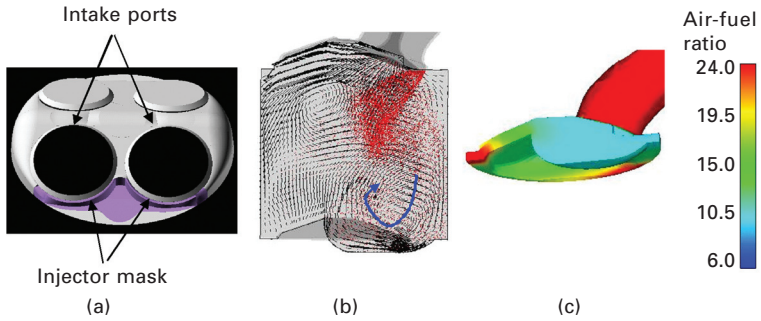


Plate III Fuel–air mixing homogeneity is greatly improved as compared with Plate II and Fig. 7.16 by an injector mask that alleviates the interaction between intake flow and fuel spray: (a) the mask design to shield the fuel spray from the intake flow; (b) the resulting flow field at BDC with the mask design. The fuel droplets penetrate further toward the exhaust side (left side). (c) The improved fuel–air mixing homogeneity at 20° bTDC. The operating condition is the same as in Plate II (Yi *et al.*, 2002).

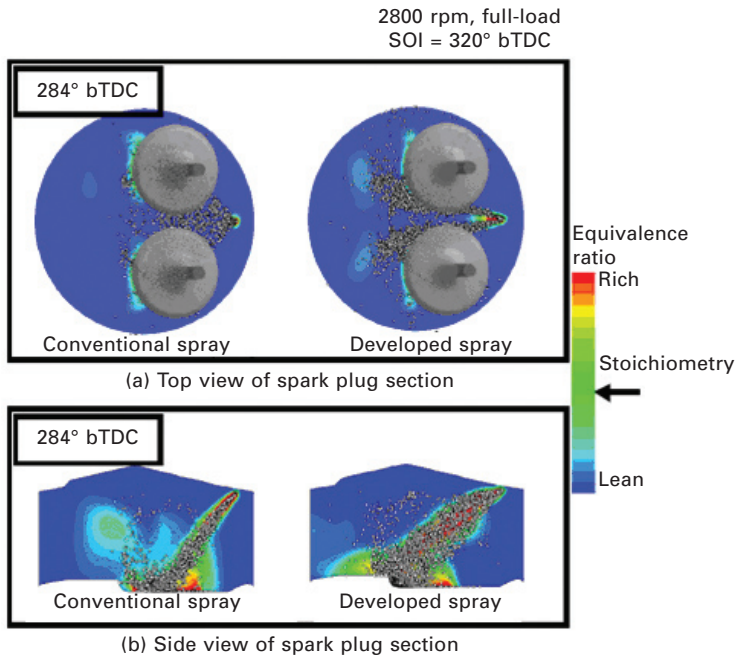


Plate IV CFD modeling predicted more evenly distributed fuel spray dispersion and better mixing with the dual-fan-shape spray as compared with a conventional spray (Ikoma *et al.*, 2006).

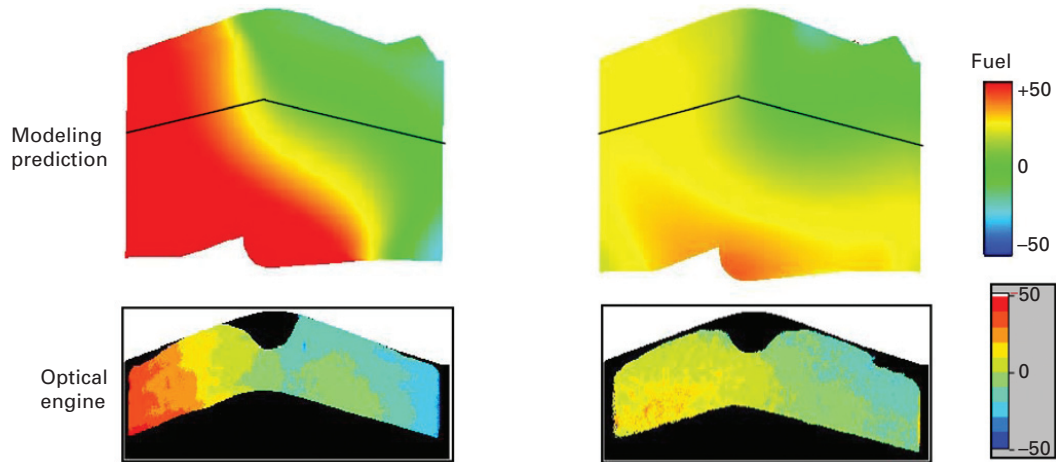


Plate V Correlation between modeling prediction and optical engine measurement of fuel-air mixing at 630° (90° bTDC compression). The modeling is with constant MAP of 62 kPa. The experiment is at an operating condition of 1500 rpm, 2.62 bar BMEP. The injector has a 60° spray cone angle and the EOI is 280° bTDC (Yi *et al.*, 2004b).

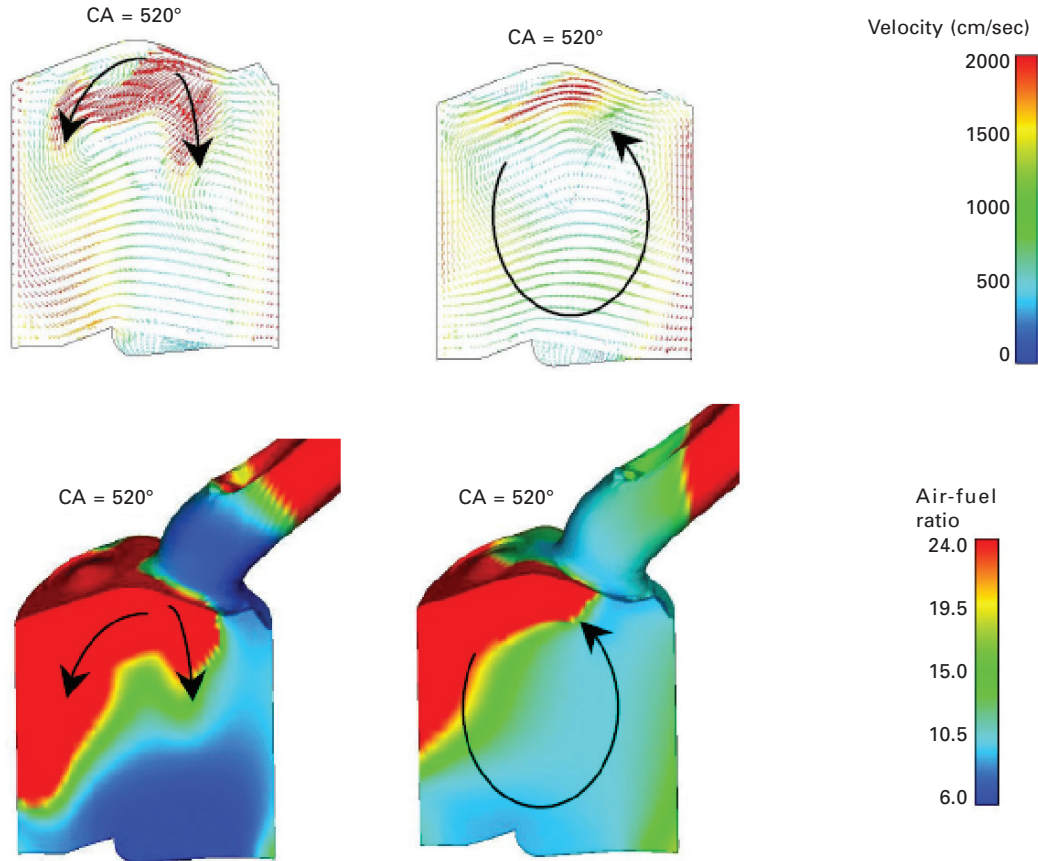


Plate VI Effect of intake cam phasing on velocity and fuel–air mixture distribution. Velocity (top) and air fuel ratio (bottom) for an operating condition of 1500 rpm, 2.62 bar BMEP. In the case of MOP of 512° after TDC, the tumble flow structure moves the fuel cloud upward and to the exhaust port side. The downward motion in the case of MOP = 472° is likely to be responsible for keeping the richer mixture from moving to the upper left, i.e., toward the exhaust side. The injector has a 60° spray cone angle and the EOI is 280° bTDC (Yi *et al.*, 2004b).

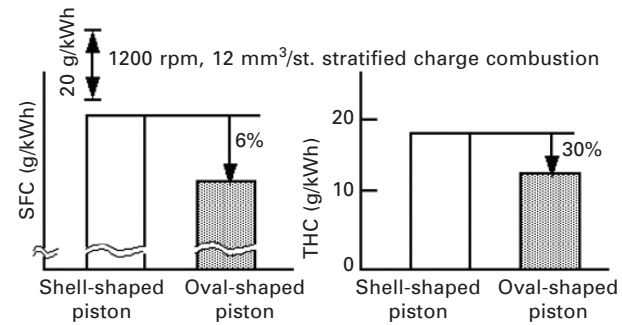
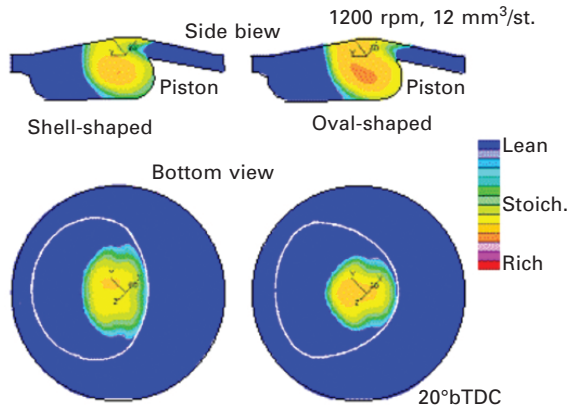


Plate VII CFD modeling predicted that mixture formation with an oval piston cavity is better located than in the case of a shell-shaped cavity (left), which agrees with the experimental results showing improvement in fuel economy and UHC emissions, (Abe *et al.*, 2001).

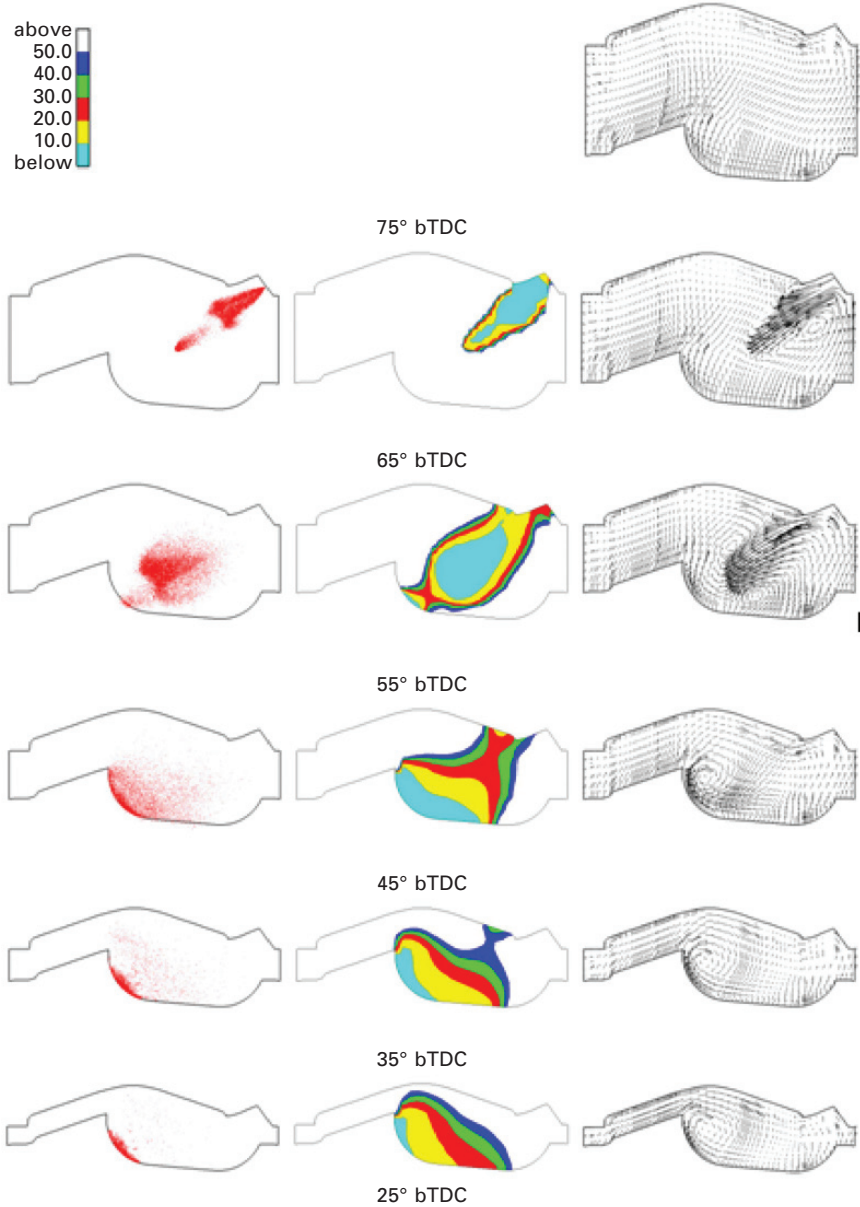
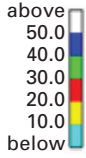


Plate VIII CFD-predicted evolution of the fuel spray, air–fuel ratio distribution, and gas vector field in the central plane of the combustion chamber. The simulated engine conditions are 1500 rpm, 10 mg injected fuel mass and 1.0 bar intake manifold pressure. The nominal spray cone angle is 60°, the start of injection (SOI) is 70° bTDC, the injection duration is about 8.7 crank angle degrees, and the injection pressure is 100 bar. (Han *et al.*, 2002).

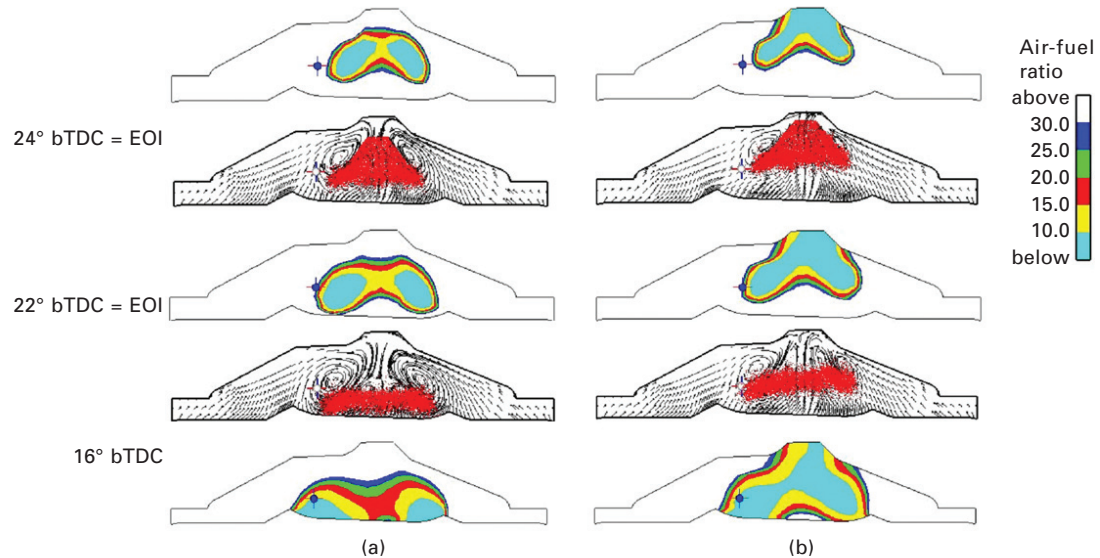


Plate IX Computed air-fuel ratio distribution and superimposed spray and gas velocity vector fields in the central cutting plane with (a) initial injector position, and (b) injector position raised up 4 mm along the injector axis. The cross with the blue dot in the middle corresponds to the location of the spark plug. Simulation conditions: 1500 rpm, 2.62 bar BMEP, EOI = 24° bTDC, SCV closed, MAP = 95 kPa, 80° cone piezo injector (Iyer *et al.*, 2004).

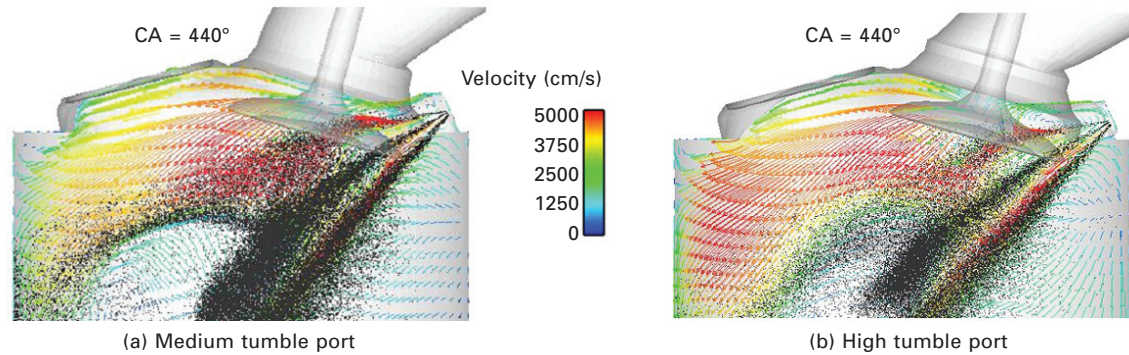


Plate X CFD-predicted velocity field and spray distribution for medium tumble (left) and high tumble (right) intake port designs in a turbo-charged DISI engine equipped with a multi-hole injector mounted beneath the intake ports. The operating conditions are 2000 rpm, 19 bar BMEP, split injection with 80/20 ratio between the first and second injection with start of injection of 400° and 500° aTDC, (Iyer and Yi, 2008).

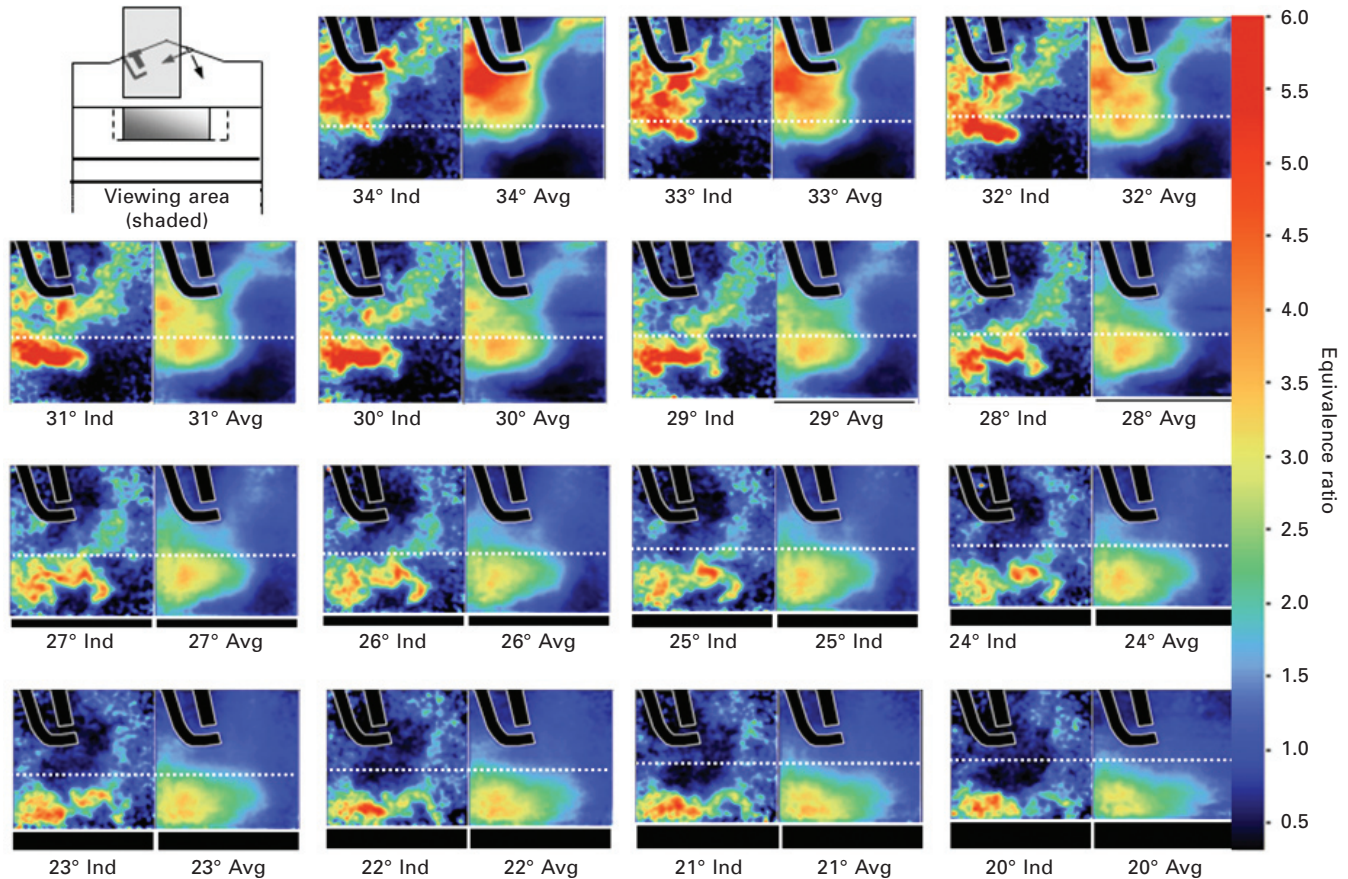


Plate XI The evolution of the fuel distribution near the spark plug in a spray-guided direct injection engine is not well represented by the average fuel distribution. This is evident in the comparison of a sequence of fuel images that were captured with high-speed LIF in a single cycle and the average from hundreds of cycles. Spatial gradients that critically determined ignitability get smeared out in the ensemble-average and thus imply favorable combustion conditions when in an individual cycle this might not be the case. (J. D. Smith, PhD Dissertation, The University of Michigan, 2006).

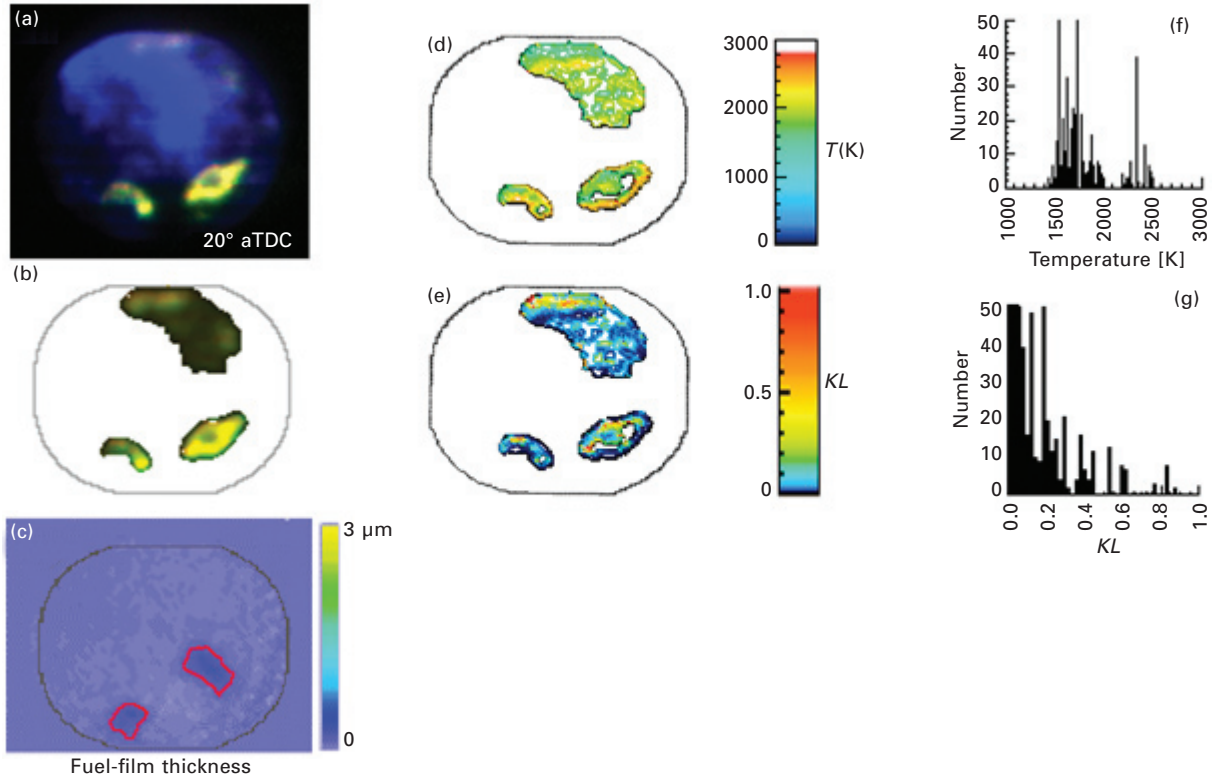


Plate XII Two-color pyrometry data and analysis: (a) one frame from a spectrally resolved high-speed video shown in false color; (b) soot emission (650, 750 nm) components from (a) with the OH* contribution removed; (c) quantitative image of liquid fuel film on the piston recorded in a separate experiment under similar conditions (Drake *et al.*, 2003); (d) line-of-sight-averaged temperature map evaluated from (b); (e) map of KL factor (relative line-of-sight integrated soot concentration); (f) and (g) histograms of soot temperature and KL factor from (d) and (e). Reproduced with permission of the Combustion Institute from Stojkovic, *et al.* (2005), Fig. 2.

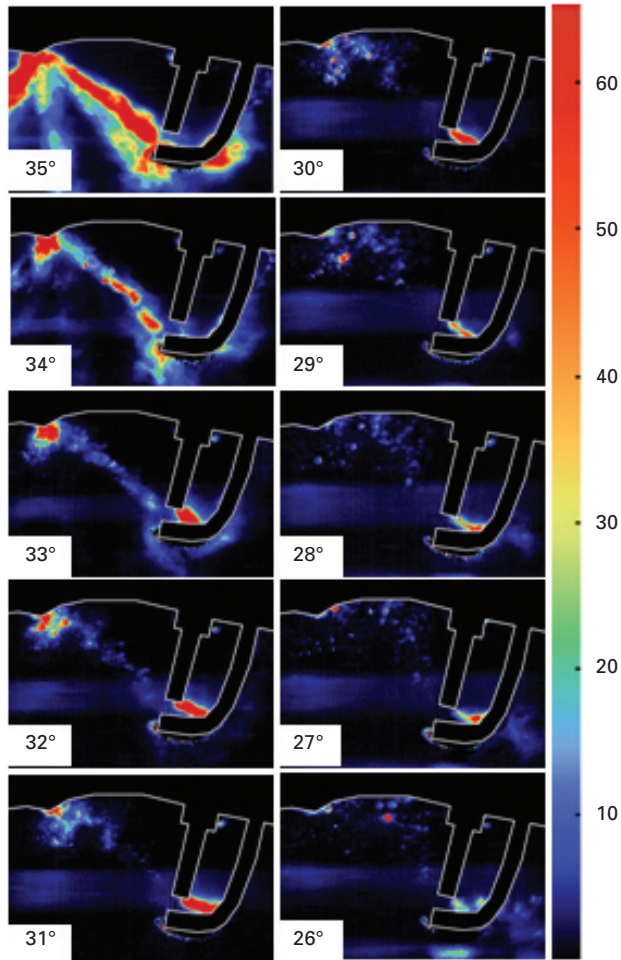


Plate XIII Single cycle sequence of Mie scattering images that were acquired at 12 kHz in a spray-guided direct-injection engine. The arc follows the original spray trajectory, showing the impact of the spray momentum of the development of the spark (Smith and Sick, 2006b).

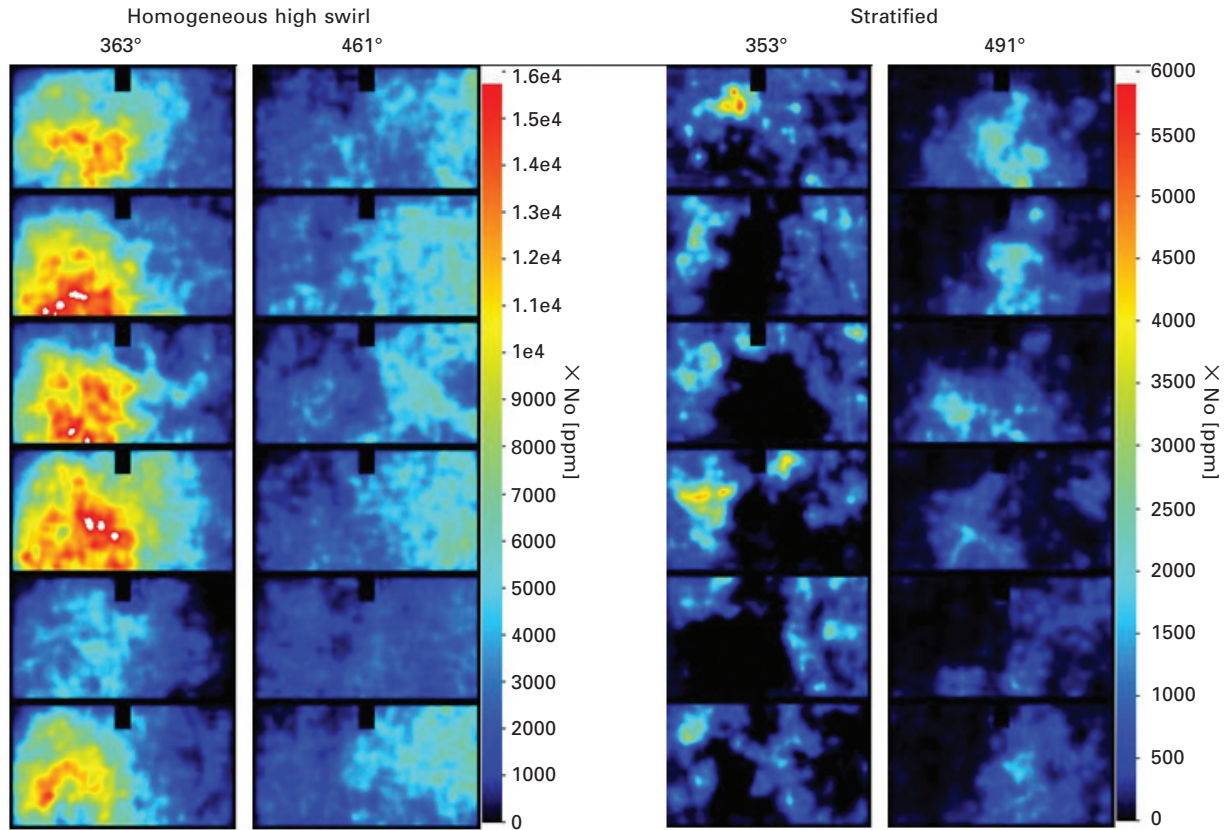


Plate XIV The instantaneous concentration distribution of nitric oxide in a direct-injection engine shows the strong impact of mixture preparation on nitric oxide formation. Measurements were performed with laser-induced fluorescence. (Fissenwert *et al.*, 2005). Reprinted with permission from SAE Paper 2005-01-2089, © 2005 SAE International.